ULTRAMAFIC ROCKS SW OF THE MANITOBA NICKEL BELT

RESUME

Des dunites et harzburgites serpentinisées sous-affleurement sous les roches paléozoïques de la région "I",a l'extrémité sud-ouest du Manitoba Nickel Belt.Ces roches se composent de lizardite,de spinelle chromifère avec bordures de magnétite,et de sulphures de nickel.La composition des chromites dépasse le domaine des chromites magmatiques,ce qui indique un épisode de métamorphisme avant la serpentinisation.Ces roches ressemblant aux serpentinites de la région exposée du Manitoba Nickel Belt.

Les dunites serpentinisées de la région "III" voisine sont entourées de roches volcaniques mafiques et de roches sedimentaires argileuses. métamorphisées dans le faciès épidote-amphibolite.La serpentinite,composée de lizardite-clinochrysotile,y est partiellememt remplacée par l'antogorite, de la chromite,et de la millerite.Les grains de chromite sont enrobés de ferritchromit,qui change sans interruption vers le composition de magnétite. On attribue cette bordure de ferritchromit à un metamorphisme qui suit la serpentinisation,quand la chromite a réagi avec la magnétite produit lors des épisodes de serpentinisation anterieures.

Il semble que la chromite soit un indice pétrogénétique de métamorphisme précieux,surtout quand un metamorphisme tardif a embrouillé la minéralogie originelle des roches ignées serpentinisées.

A COMPARATIVE STUDY OF TWO ULTRAMAFIC BODIES AT THE SW END OF THE MANITOBA NICKEL BELT: with special reference to the chromite mineralogy

by
N.W. Bliss

A thesis submitted to the Faculty of Graduate Studies and Research of McGill University in partial fulfilment of the requirements for the degree of Doctor of Philosophy in Geological Sciences.

Montreal, P.Q.
1972

N.W.Bliss-A Comparative Study of Two Ultramafic Bodies at the SW End of the Manitoba Nickel Belt:with special reference to the chromite mineralogy-Department of Geological Sciences-Doctor of Philosophy.

ABSTRACT

Serpentinised dunite and harzburgite in Area I sub-outcrops beneath the Palaeozoic rocks at the SW end of the Manitoba Nickel Belt and consist of lizardite,chromite with magnetite rims and nickel sulphides. The chromite composition falls outside the normal range of magmatic chromite indicating metamorphism prior to serpentinisation.These serpentinites resemble those from the exposed portion of the Manitoba Nickel Belt.

Serpentinised dunite in the adjacent Area III is enclosed by mafic volcanics and pelitic sediments of the epidote-amphibolite facies.The serpentinite consists of lizardite-clinochrysotile,partly replaced by antigorite,chromite and millerite.The chromite is surrounded by alteration rims of ferritchromit which varies continuously in composition towards magnetite.The ferritchromit is interpreted as resulting from post-serpentinisation metamorphism when the chromite reacted with a magnetite rim formed during serpentinisation.

It is concluded that chromite is a metamorphic petrogenetic indicator,important where post-metamorphism serpentinisation has obscured the silicate mineralogy.

TABLE OF CONTENTS

LIST OF FIGURES

LIST OF TABLES

INTRODUCTION

Amax Exploration Inc. has had title to a group of claims and mineral reservations between Wabowden and Grand Rapids, Manitoba. These properties, many of which have now lapsed, covered ground at the SW end of the Manitoba Nickel Belt in rocks of Precambrian age and their extension beneath the cover of Palaeozoic rocks.

During mineral exploration it became apparent that two types of serpentinized ultramafic body occurred on these properties and that both types sub-outcropped beneath Reservation 34. This thesis records the results and conclusions of an investigation into the apparent differences between the two types from Reservation 34. The Reservation is entirely underlain by Palaeozoic rocks and the samples used in this investigation have been obtained from extensive diamond drilling by Amax Exploration Inc. through the Palaeozoic cover into the underlying Precambrian rocks.

The first part of the thesis is a description of the two types of serpentinite and their regional setting. Contrasting silicate, sulphide and oxide mineralogy indicate differences in both the nature of the original ultramafic rocks and their geological history subsequent to emplacement. This leads to conclusions concerning regional geology at the SW end of the Nickel Belt.

In the second part of the thesis, zoning in chrome spinels from both types of serpentinites is examined in detail and

compared with zoning previously described from chromite. It is concluded that chrome spinel can be used as a metamorphic petrogenetic indicator for the serpentinites in Reservation 34. This conclusion should be generally applicable.

I THE MANITOBA NICKEL BELT

A REGIONAL GEOLOGY

The Manitoba Nickel Belt lies within the Churchill Province of the Canadian Shield very close to its boundary with the Superior Province (Fig.I.1). Recently the granulites of the Superior Province adjacent to the Churchill Province have been redefined as the Pikwitonei Province (Bell, 1971, p.12).

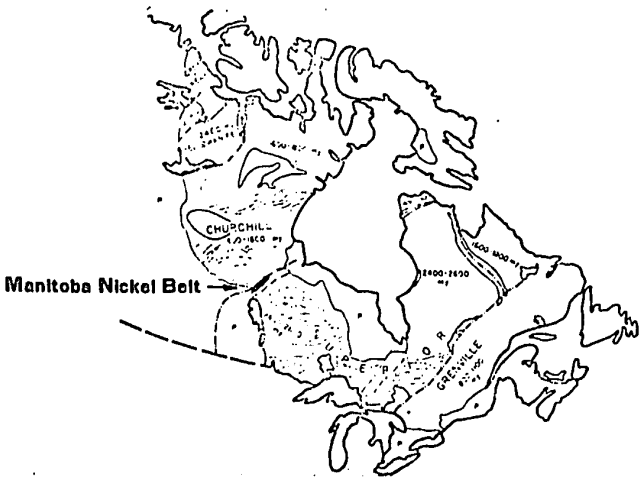

Fig. I.1 Position of the Manitoba Nickel Belt, (after Wilson and Brisbin, 1962, Fig.1).

The Nickel Belt is a tract of country 120 miles long and 15 miles wide characterized by numerous serpentinized ultramafic bodies most of which contain some nickel sulphides and a few sufficient to be economically exploitable. The emplacement of the ultramafic rocks is related to a major fracture zone, the Setting Lake Lineament, which cuts the SE margin of the Churchill Province.

The regional geology may be described in terms of five units (Fig.I.2) - (1) Granite and Kisseynew-type gneiss forming an unnamed sub-province of the Churchill Province; (2) the Setting Lake Lineament; (3) granodiorite and paragneiss comprising the Wabowden sub-Province of the Churchill Province; (4) the granulite and associated rocks of the Pikwitonei Province and (5) a granite-greenstone complex comprising the Cross Lake sub-Province of the Superior Province.

A sixth unit comprises the ultramafic rocks emplaced adjacent to the Setting Lake Lineament (Fig.I.3). These units are all unconformably overlain to the SW by flat-lying Palaeozoic sediments (Fig.I.2).

The Cross Lake sub-Province of the Superior Province is a typical Archaean granite-greenstone complex. The Cross Lake group of rocks, comprising the schist belt at Cross Lake (Fig.I.2), consists of basalt, overlain by conglomerate, arkose and sub-greywacke, metamorphosed to the amphibolite facies and folded into a WNW-trending syncline. These supracrustal rocks rest unconformably on biotite-granodiorite gneiss, but are enclosed laterally by younger granodiorite gneisses (Bell, 1971; Rousell, 1965). Radiometric age determinations, 1830 m.y. to 2435 ± 170 m.y. (Wanless et al., 1967) are slightly younger than normal for the Superior Province (Fig.I.1).

The granulites and amphibolites outcropping along the NE margin of the Cross Lake sub-Province were originally classified as a sub-Province of the Superior Province (Bell, 1966). Bell (1971) states that the pre-metamorphism sites of the schist belts

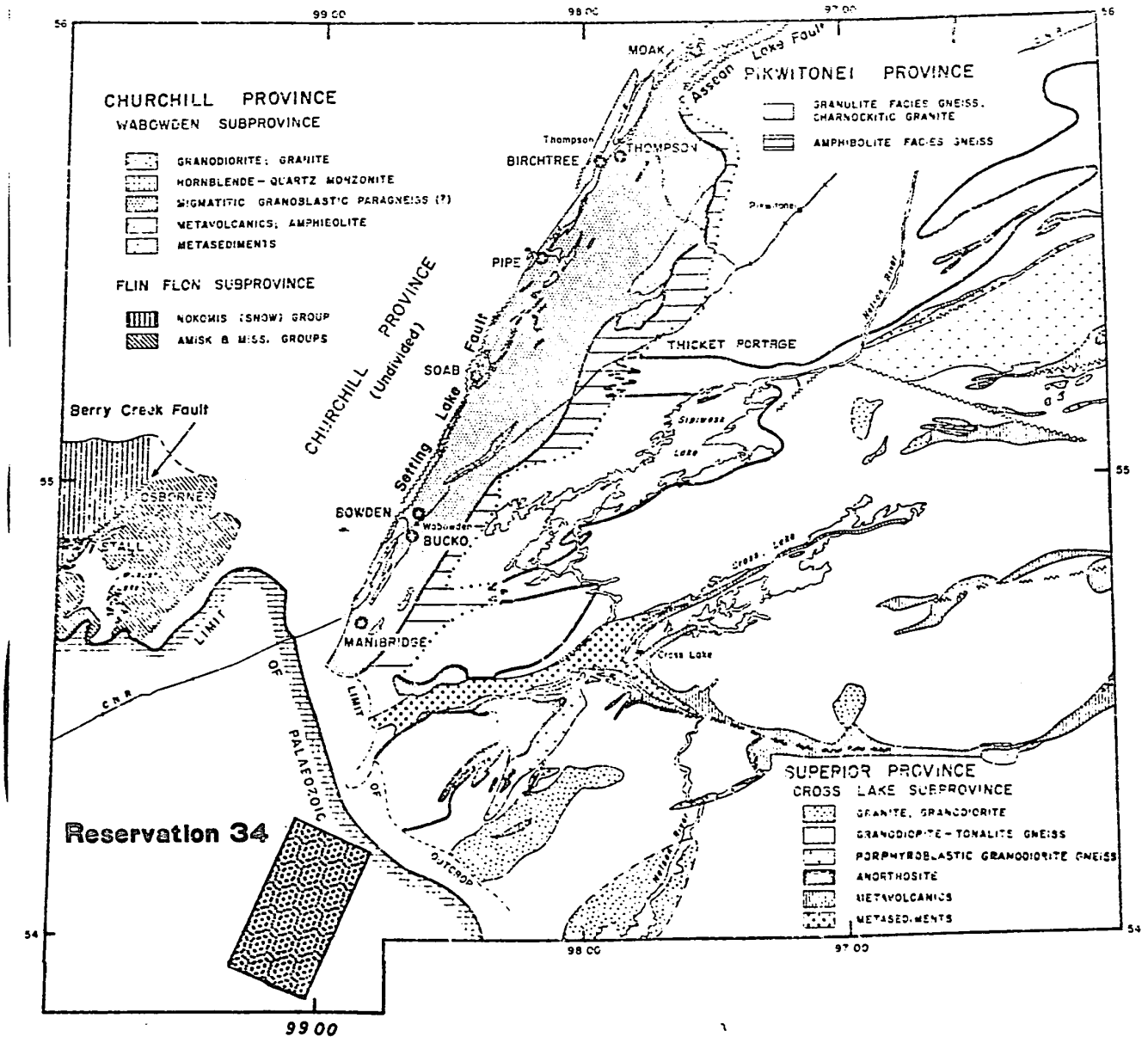

GEOLOGICAL MAP OF THE MANITOBA NICKEL BELT

Adapted from Bell, 1971, fig. 1, with the position of Reservation 34 added

SYMBOLS

- Faults known, assumed
- Metamorphic facies boundary
- Geological Province boundary
- Nickel deposits, copper–zinc deposits

MILES 0 8 16 24 32

Fig. I.2

can be traced across the granulites and concludes that the latter are the older; accordingly he redefines the Pikwitonei as a separate geological province. The rocks are charnockites (s.l.), principally enderbite and retrogressively metamorphosed equivalents, together with garnetiferous gneisses and granodiorites (Rance, 1966, p.65; Rousell, 1965, p.28; Patterson, 1963, p.11). The eastern margin of the granulites is occupied by gneiss retrograde after charnockite and garnetiferous-pyroxene-granulite (Rance, 1966, p.66; Patterson, 1963, p.13). This gneiss is similar in lithology to the granodiorite gneiss of the Wabowden sub-Province except for occasional occurrences of secondary biotite and magnetite after pyroxene. Radiometric ages vary between 2375 ± 165 m.y. to 2715 ± 80 m.y. indicating that the Province has not been affected by the Hudsonian orogeny.

The Wabowden sub-Province of the Churchill Province outcrops between the Setting Lake Lineament and the Pikwitonei Province (Bell, 1971), (Fig.I.2), and consists of ortho- and paragranodiorite gneiss intruded by granite and monzonite. The gneiss contains mineralogical features which led Rance (1966, p.70) to suggest that it resulted from retrogressive metamorphism of granulites of the Pikwitonei Province. Rocks of lower metamorphic grade occur sporadically; magnetite-bearing iron formation and quartz-rich sediments form scattered outcrops in the vicinity of Halfway Lake (Godard, 1968, p.5).

The Churchill Province consists of Aphebian and Archaean rocks both of which have been involved in the Hudsonian orogeny between 1600 and 1800 m.y. (Fig.I.1).

Garnet-sillimanite paragneiss and gneissic biotite granite outcrop in the Churchill Province immediately to the north of the Setting Lake Lineament (Cranstone and Toogood, 1969; Godard, 1966; Rance, 1966; Patterson, 1963). West of Thompson the garnet-sillimanite paragneiss is uniform in composition, well-banded and intricately folded; towards the SW the gneiss is less uniform and extensively invaded by pegmatite (Cranstone and Toogood, 1969a). The pink, lightly foliated, gneissic biotite granite occurs in sheet-like bodies intruded along zones of dislocation parallel to the overall structural trend.

There is a major structural break between the Pikwitonei Province and the Wabowden sub-Province separating the predominantly NE-trending structures of the Churchill Province from the east to west structures of the Pikwitonei and Superior Provinces (Bell, 1971; Patterson, 1963; Wilson and Brisbin, 1962).

The Setting Lake Lineament is the surface trace of a major fault zone striking SSW between Thompson and the Palaeozoic sediments (Fig.I.2). Northward from Thompson the Lineament is less well-defined and appears to split, some branches having an easterly strike, others continuing the original strike (Bell, 1971, Fig.2). The SE continuation beneath the Palaeozoic rocks, that is, beneath the area considered in this thesis, is obscure.

The trace of the fault zone on the surface is not well exposed, although it can be followed through a series of elongate lakes, Setting, Ospwagen, Mystery and Moak. However, since the strike of the Lineament is parallel to the steeply SE-dipping regional foliation it may be difficult to locate even in areas

where it is exposed. Patterson (1963, p.46) suggests that drag folds NE of Thompson indicate right hand movement on the fault.

Rocks intersected by the Lineament are extensively sheared, and ultramylonites, mylonites and cataclasites occur in zones up to $\frac{1}{2}$ mile wide.

The discontinuity of structure across the Setting Lake Lineament is not marked. The trends in the Kisseynew gneiss are parallel to the Lineament while those in the Wabowden sub-Province tend to intersect the Lineament at a low angle (Wilson and Brisbin, 1962, Fig. 3).

The nature of the Lineament has not been determined. It has been interpreted as the trace of a Benioff zone (Wilson and Brisbin, 1962; 1961) and as an unconformity between rocks of Archaean age to the SE and Aphebian age to the NW (Rance, 1966).

Sediments and volcanics of metamorphic grade lower than normal in the Churchill Province occur close to the Lineament. The Assean Lake group, fine-grained micaceous quartzite and phyllite, outcrops on either side of the Setting Lake Lineament in the vicinity of Thompson and at the north end of Ospwagen Lake (Patterson, 1963, p.14). Quartzose greywackes and fine-grained schistose metavolcanics, with a lithology similar to the Assean Lake group, have been intersected in drill holes beneath Setting Lake north of Wabowden (Coats, 1966, p.144).

B ULTRAMAFIC ROCKS

Numerous ultramafic bodies outcrop in the vicinity of the Manitoba Nickel Belt (Scoates, 1971; 1969).

1 Discrete Ultramafic Bodies of the Manitoba Nickel Belt

These ultramafic bodies are virtually confined to the Wabowden sub-Province and are spatially related to the Setting Lake Lineament (Fig.I.3). Very few are exposed at the surface, being obscured by overburden or water (Kilburn et al., 1969, p.277).

The ultramafics, originally dunite and peridotite, are almost entirely serpentinized. The forsterite content of relict olivine is in the range Fo_{84} to Fo_{90} while relict orthopyroxene has a composition En_{77} to En_{85} (Coats, 1966, pp. 37 and 41). Chromite is an accessory mineral only and no chromitite segregations are known. Cumulus textures are common, but the proportion of cumulus and intercumulus material varies considerably. The Bucko and Bowden Lake bodies were intruded as a crystal mush with a negligible amount of intercumulus liquid (Wilson et al., 1969, p.306). Phlogopite, tremolite-actinolite, magnetite, spinel and carbonate minerals all occur in response to later metamorphism.

The serpentine mineralogy of the Manitoba Nickel Belt has been described by Coats (1968; 1966) who demonstrated that lizardite-chrysotile mesh textures predominate. Antigorite is rare and is known only from one locality in an ultramafic rock adjacent to granite. Wicks (1969, p.424) has recognized a

sequence of serpentine mineralogy and textures in the Manitoba Nickel Belt (Fig.I.3), which are from NE to SW as follows: (1) In the vicinity of Pipe Lake; lizardite mesh textures replaced by lizardite-chrysotile interlocking textures in turn replaced by chrysotile to form chrysotile mesh texture with lizardite-chrysotile mesh centres; (2) In the vicinity of Joey Lake; lizardite hourglass textures; (3) In the vicinity of Wabowden; secondary lizardite interlocking textures associated with lizardite interlocking veins; (4) In the vicinity of Manibridge; lizardite mesh textures.

Most of the ultramafic bodies contain accessory nickel sulphide mineralization consisting of pentlandite associated with pyrrhotite and minor chalcopyrite, pyrite, marcasite and violarite (Coats, 1966, p.129; Godard, 1966; Zurbrigg, 1963). Massive and disseminated nickel sulphides of economic interest, occur within, and adjacent to, many of the ultramafics (Coats and Brummer, 1971; Godard, 1968, 1966; Patterson, 1963; Quirke et al., 1970). Pyrrhotite, pentlandite and pyrite with minor chalcopyrite, marcasite and gersdorffite, occur as disseminations in serpentinite and as massive and disseminated sulphides in the adjacent gneissic wall-rocks.

The age of the ultramafic rocks is uncertain, and conflicting statements have been made as to whether they are older or younger than the group of monzonite stocks (1785±60 m.y.) intruded into the Wabowden sub-Province (Bell, in Wanless et al., 1966, p.56 and 1965, p.78). Fragments of pegmatite, similar to those associated with the late Hudsonian granites,

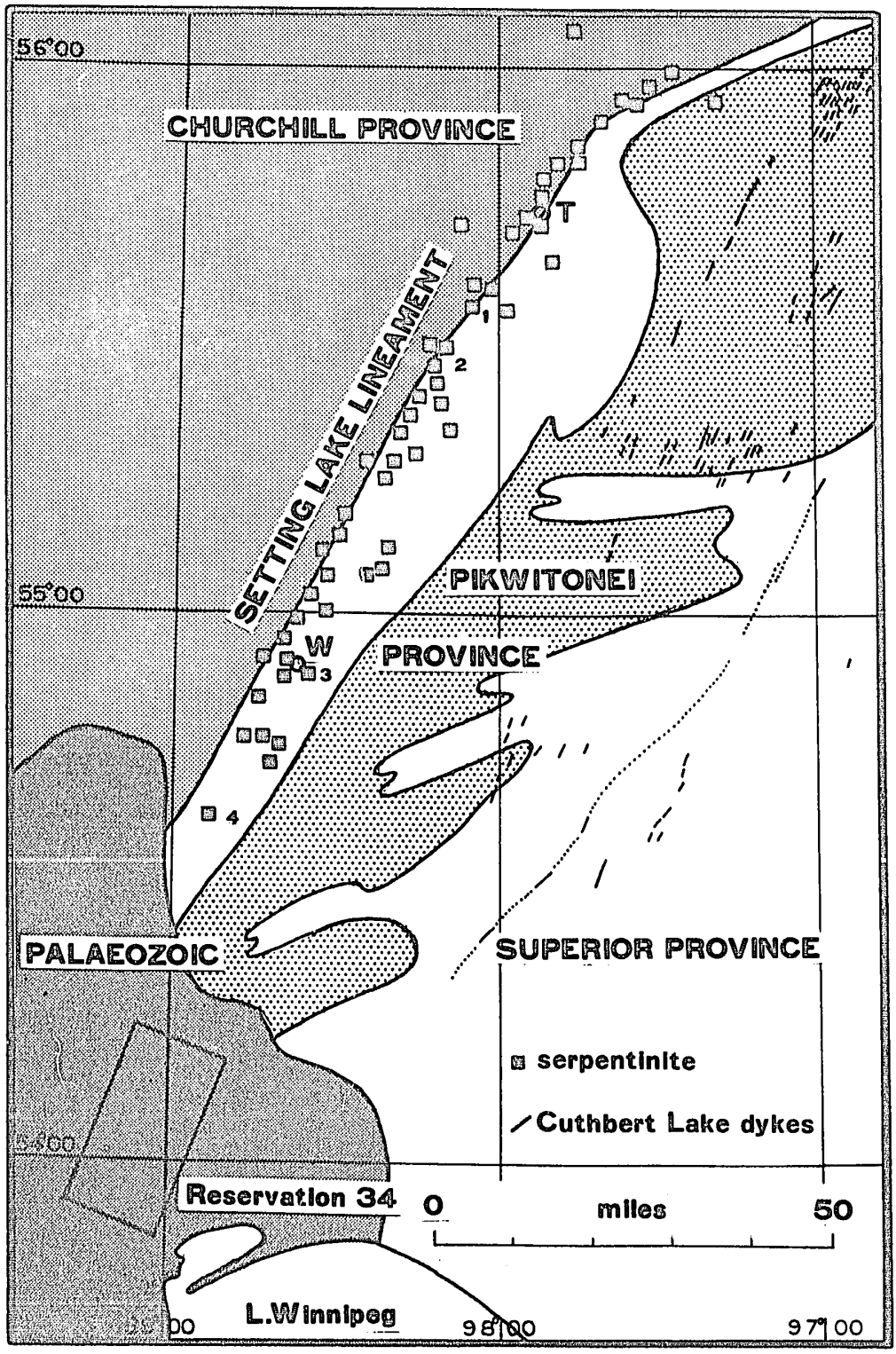

Fig. I.3 Ultramafic and mafic rocks in the vicinity of the Manitoba Nickel Belt. Data from Collett and Bell (1971) and Scoates (1971; 1969). 1, 2, 3 and 4 refer to the sequence of serpentine textures described on p.9. T-Thompson, W-Wabowden.

are found in breccia ore at Thompson. This indicates that movement of the sulphides occurred towards the end of, or after, the Hudsonian orogeny.

2 Discrete Ultramafic Bodies of the Superior Province

Ultramafic bodies have been emplaced in the schist belts to the east of Cross Lake (Davies et al., 1962) and in the Island Lake schist belt (Scoates, 1971). In the Oxford and Knee Lake areas, ultramafic rocks are completely serpentinized but relict primary magmatic textures are apparent (Barry, 1959, p.25). Accessory sulphides are known from these ultramafics but no deposits of economic importance have been found. These ultramafic bodies have been deformed and metamorphosed with the schist belts, and some are now being considered extrusive (Bell, 1971, p.18).

3 Cuthbert Lake-Type Intrusives

The Cuthbert Lake swarm of partially serpentinized, composite, ultramafic and mafic dykes has been mapped in a broad band from Cross Lake NNE towards Kelsey (Fig.I.2), (Scoates, 1971, Fig.6; Patterson, 1963; Macdonald, 1960). The strike is very nearly parallel to that of the Setting Lake Lineament. Individual dykes are not continuous over long distances but tend to an *en echelon* arrangement. They are generally less than 80 feet in width, but exceptionally may reach 200 feet. Nickel sulphides are not found associated with the Cuthbert Lake intrusives.

4 Ultramafic Rocks Forming Portions of Layered Intrusions

Ultramafic rocks forming the basal portions of layered intrusions are common in the Churchill Province although the majority outcrop over 40 miles to the west and NW of the Manitoba Nickel Belt (Scoates, 1971, Fig.1). Layered intrusions also outcrop in the schist belts of the Superior Province (Barry, 1959, p.25), and may pre- or post-date the deformation of the schist belts. Minor amounts of nickel sulphides are associated with these layered intrusions.

C REGIONAL GEOPHYSICS

The Bouguer gravity anomalies in the vicinity of the Manitoba Nickel Belt show a linear zone of very low gravity values symmetrically flanked by zones of comparatively high values, the Burntwood River high to the NW and the Nelson River high to the SE (Gibb, 1968, Fig.2). The central zone of low gravity values coincides with the Setting Lake Lineament; the eastern margin of the zone is closely coincident with the boundary between the Wabowden sub-Province and the Pikwitonei Province, and the Nelson River high with the high density rocks of the Pikwitonei Province (Gibb, 1968, Fig.5).

The SW extension of these features beneath the Palaeozoic rocks, as depicted by the gravity anomalies, is not well-defined. The gravity low that coincides with the Manitoba Nickel Belt widens and swings to the north, causing it to pass to the north of Reservation 34, which is underlain by the SW continuation of the Nelson River high.

In the vicinity of the Manitoba Nickel Belt distinctive aeromagnetic patterns can be correlated with the surface geology. Kornik's (1969) aeromagnetic divisions are shown in Figure I.4. Area A corresponds to the Cross Lake sub-Province, while sub-areas A,A' and A", with their distinctive 'bird's-eye maple' pattern, correspond to the granulites of the Pikwitonei Province. Area B corresponds to the zone of retrogressively metamorphosed granulites on the NW margin of the Pikwitonei Province. The eastern area of the Moak Lake-Setting Lake structure corresponds to the Wabowden sub-Province, whereas the western area corresponds in part to the Kisseynew-type gneisses of the Churchill Province.

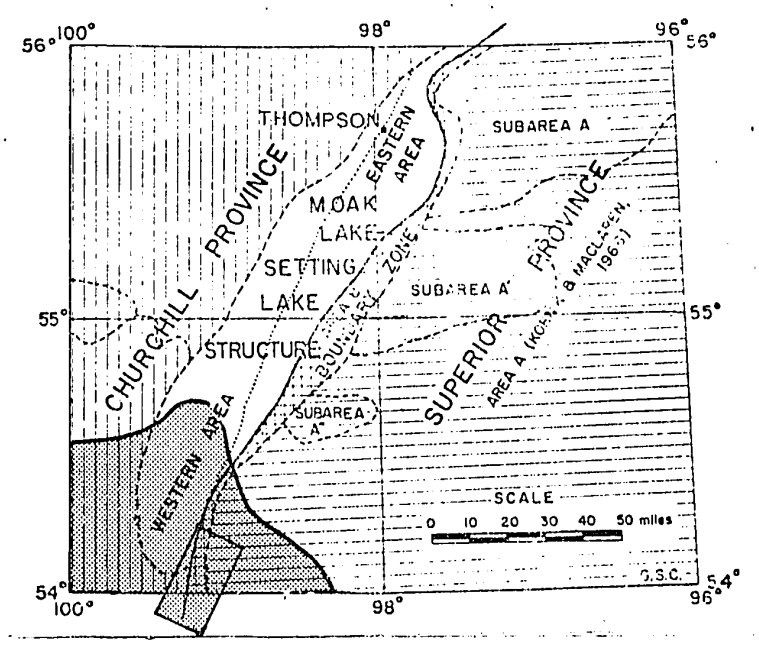

Fig. I.4 Aeromagnetic divisions in the vicinity of the Manitoba Nickel Belt (Kornik, 1969, Fig.2). Palaeozoic sediments and the position of Reservation 34 have been added. The Setting Lake Lineament is shown as a dotted line.

The patterns become less distinct when traced beneath the Palaeozoic cover, possibly a result of major changes in the Precambrian beneath the Palaeozoic. Interpretation of the aeromagnetic divisions indicates that the Wabowden sub-Province may not be present, the continuation of the Setting Lake Lineament bringing Kisseynew-type gneisses into contact with the Superior or Pikwitonei Province rocks.

D SUMMARY

The Manitoba Nickel Belt comprises a series of serpentinized nickeliferous dunites and peridotites spatially related to the Setting Lake Lineament, a major fault zone which cuts the SE margin of the Churchill Province. Kisseynew-type gneisses of Aphebian age outcrop to the NW of the Lineament and mixed ortho- and paragneisses derived from both Archaean and Aphebian rocks outcrop to the SE. Both suites of gneisses have been intruded by later granites. Granulites of the Pikwitonei Province outcrop on the SE margin of the Churchill Province; until recently the Pikwitonei Province was regarded as part of the Superior Province. A zone of retrogressively metamorphosed granulites outcrops around the margin of the Pikwitonei Province where it adjoins the mixed gneisses of the Wabowden sub-Province. An Archaean granite-greenstone complex outcrops further to the SE forming the Cross Lake sub-Province of the Superior Province.

Each of these units is characterized by its own structure, lithology and absolute age but the major break occurs between

the Churchill and Pikwitonei Provinces. The east-trending structural elements in the Superior and Pikwitonei Provinces, resulting from the Kenoran orogeny at 2400 to 2600 m.y., are cut obliquely by NE structures at the margin of the Churchill Province resulting from the Hudsonian orogeny between 1600 and 1800 m.y.. The structural trends in the Wabowden sub-Province are intersected at an acute angle by the Setting Lake Lineament whereas those in the Kisseynew-type gneisses to the NW are more nearly parallel to the Lineament.

The Setting Lake Lineament is the locus of a zone of low Bouguer gravity anomalies which is flanked on either side by zones of high values which can be related to the known surface geology. The regional aeromagnetic maps show areas of distinct magnetic pattern which can also be related to surface geology. Extrapolation of the Precambrian geology beneath the Palaeozoic rocks at the SW end of the Nickel Belt indicates that the geology is not a simple linear extension of that in the Nickel Belt.

The serpentinized ultramafic rocks were emplaced in fracture zones associated with the Setting Lake Lineament. Sulphide minerals present are pyrrhotite, pentlandite, chalcopyrite, pyrite, violarite, marcasite, millerite and gersdorffite. Mineralization of ore grade occurs in three ways:- (1) as massive segregations or breccia matrix in biotite schist; (2) as stringers and veins in serpentinite; and (3) as disseminated and semi-massive segregations in serpentinite. Both serpentinite and country rock are mineralized and economic sulphide deposits may occur in wall-rock adjacent to serpentinites containing only accessory sulphides.

II GEOLOGY OF RESERVATION 34

A INTRODUCTION

Reservation 34 is underlain by Palaeozoic sediments to a depth of about 300 feet; there are no exposures of the underlying Precambrian basement and sub-surface geology (Fig.II.1) is inferred from diamond drilling supplemented by ground and aeromagnetic surveys.

A narrow linear belt of supracrustal rocks, metamorphosed to the epidote-amphibolite facies, strikes almost due north through the western portion of the Reservation and comprises an eastern metasedimentary unit and a western metavolcanic unit. There is virtually no information on the sub-surface geology to the east of this. A NW-striking spur of the meta-volcanic unit divides the western portion of the Reservation into two areas of granite and gneiss. Ultramafic rocks occur predominantly in Areas I, II and III, Areas I and III being the subject of more detailed investigation in this thesis.

B METASEDIMENTARY UNIT

The metasedimentary unit consists predominantly of argillaceous rocks with minor intercalated mafic volcanics. The argillaceous rocks consist of almandine, biotite, quartz and muscovite with minor tourmaline, graphite, apatite, carbonate and opaque oxide.

Argillite is a fine grained, dark rock, massive to lightly laminated, consisting of coarse porphyroblastic garnet in a fine matrix of brown biotite and quartz. The rock has a prominent

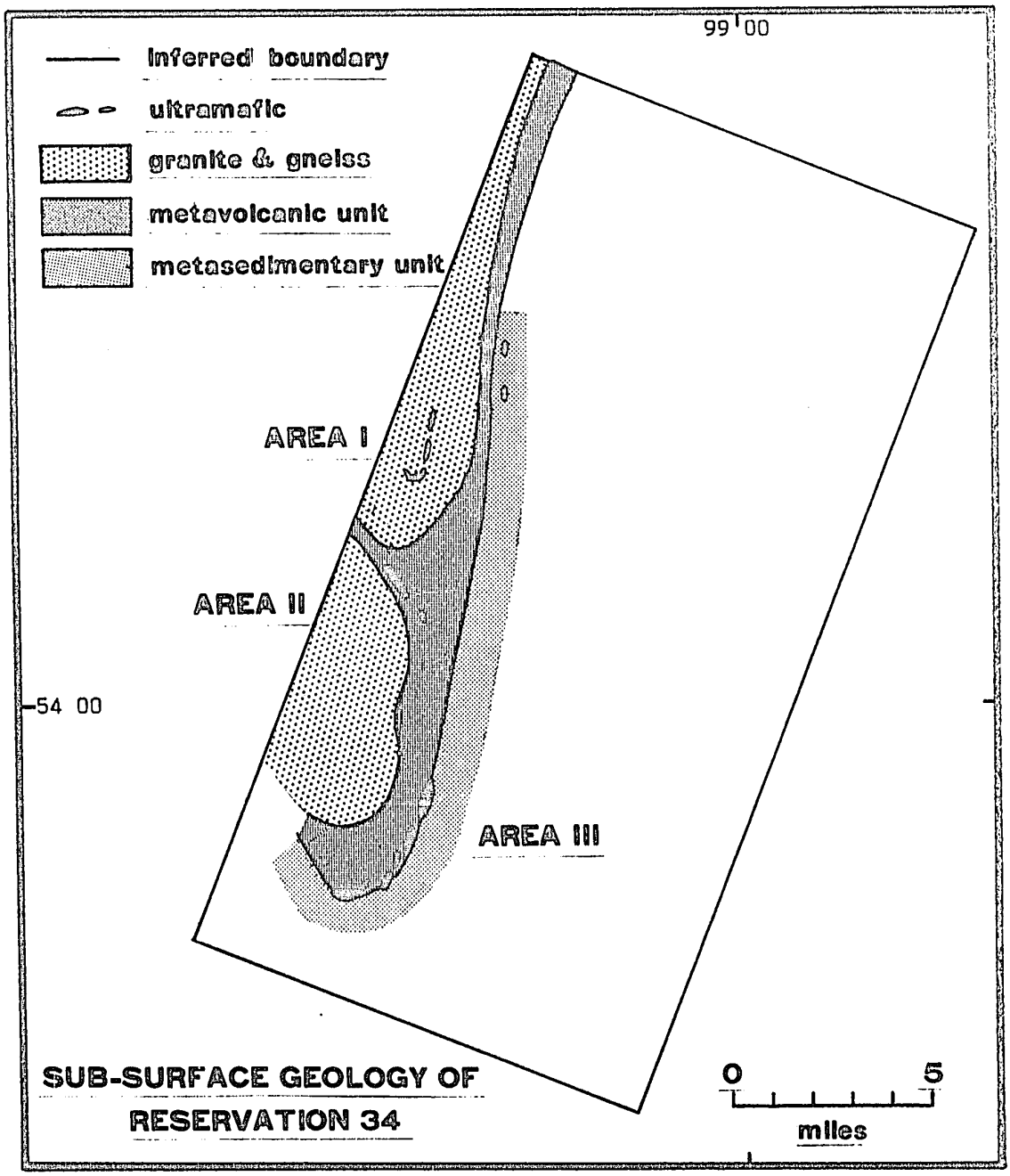

Fig. II.1 Sketch map of the inferred sub-surface geology of Reservation 34. Areas I, II and III refer to major sub-outcrops of ultramafic rocks.

pervasive foliation due to the parallel orientation of biotite flakes. Faint and irregular compositional banding due to slight variation in quartz content may reflect original bedding laminations.

Quartz-bearing argillite is dark grey and finely laminated and banded due to alternation of layers of dark argillaceous and white arenaceous material. This banding is generally 1 inch or less in thickness, but individual bands may be sub-divided by laminations. Prominent pervasive foliation is parallel to the lithological banding and is intersected by a less prominent non-pervasive cleavage.

Thinly-banded and laminated quartz-magnetite schist consists of alternations of light grey quartzite with dark magnetite-biotite-garnet layers, giving rise to a prominent 'zebra stripe' texture.

Garnet in the argillaceous rocks is normally euhedral with a sieve-textured core containing randomly orientated inclusions of quartz, magnetite and biotite. The enveloping foliation is deformed around the garnet, resulting in the formation of pressure shadows in the plane of foliation. Euhedral garnet may truncate the enveloping foliation. Less commonly the garnet contains inclusions arranged in a linear fashion, the direction of which lies at a small angle to the foliation in the groundmass. Anhedral garnet with fragmented margins occurs in the coarser, quartz-rich argillites, where it distorts, but does not truncate, the foliation. Quartz tends to occur in streaks and lenticles except in the well-defined monomineralic bands of quartz-magnetite schist. The grains, along with magnetite and biotite,

where present, develop a dimensional orientation, parallel or at a small angle to, the lithologic banding. In extreme cases this defines a ribbon texture. In a few cases the coarser quartz grains are reorientated parallel to the later, non-pervasive, cleavage. They have lost any clastic appearance they may have had, each grain being sutured against its neighbours. Undulose extinction is developed.

Biotite is brown and uniformly distributed throughout the finer portions of the argillites. In quartz-magnetite schist green biotite occurs in the argillaceous bands together with magnetite and apatite. Biotite and magnetite tend to be antipathetic, resulting in mineralogical lamination within the banding.

Two garnets from an argillaceous quartzite have been analyzed by electron microprobe (Table II.1). They were found to consist principally of almandine together with approximately equal proportions of spessartine, pyrope and grossular. The cores are slightly enriched in spessartine and grossular and depleted in almandine and pyrope compared to the margins.

Criteria have been enumerated by Spry (1969, p.250) for recognizing the time of crystallization of a mineral relative to the tectonic event that produced the major pervasive foliation in the rock. Pre-tectonic crystallization of garnet in the metasedimentary unit is indicated by the following:- (1) Inclusions in the core are randomly orientated in contrast to the preferred orientation of quartz, magnetite and biotite in the matrix; (2) the foliation due to the parallel alignment of

Table II.1 Electron microprobe analyses of garnet from argillaceous quartzite, Reservation 34.

	W 226 #1			W 226 #2		
	margin	centre	margin	margin	centre	margin
SiO_2	35.62	36.46	35.35	35.86	35.58	35.30
Al_2O_3	21.02	20.71	20.78	20.48	20.64	20.92
MgO	1.66	1.58	1.67	1.67	1.72	1.69
FeO	32.53	31.66	33.58	34.30	32.39	32.16
MnO	2.65	3.52	2.82	2.69	3.75	3.11
CaO	1.75	3.47	1.88	1.77	2.57	1.72
Total	95.23	96.90	96.08	96.77	96.65	94.90
	Number of ions on basis of 12 (O)					
Si	3.01	3.02	2.98	3.00	2.98	2.99
Al	- } 3.01	- } 3.02	0.02 } 3.00	- } 3.00	0.02 } 3.00	0.01 } 3.00
Al	2.09	2.03	2.04	2.02	2.02	2.08
Ca	0.16	0.30	0.17	0.16	0.23	0.16
Fe^2	2.30 } 2.86	2.16 } 2.90	2.37 } 2.95	2.40 } 2.96	2.27 } 2.98	2.28 } 2.87
Mg	0.21	0.19	0.21	0.21	0.21	0.21
Mn	0.19	0.25	0.20	0.19	0.27	0.22
	End members in molecular %					
Almandine	80.42	74.48	80.34	81.08	76.17	79.44
Spessartine	6.64	8.62	6.78	6.42	9.06	7.67
Pyrope	7.34	6.55	7.12	7.09	7.05	7.32
Grossular	5.59	10.34	5.76	5.41	7.72	5.57
	End members in weight %					
Almandine	82.02	76.21	81.92	82.64	77.82	81.02
Spessartine	6.74	8.77	6.88	6.51	9.21	7.78
Pyrope	6.08	5.44	5.89	5.87	5.84	6.06
Grossular	5.16	9.58	5.32	4.99	7.14	5.15

quartz, magnetite and biotite is deformed around the garnet; and (3) mechanical fragmentation of the rims of anhedral garnet. Continued post-tectonic growth of garnet is indicated by the idioblastic, inclusion-free rims that frequently truncate the foliation. The faint alignment of some inclusions in garnet also indicates growth subsequent to the imposition of the foliation. The line of these inclusions may make a slight angle with the foliation in the matrix, indicating that they have been rotated out of the plane of foliation. This rotation is believed due to the same event that caused the non-pervasive cleavage, as such garnets have edges parallel to this cleavage.

C METAVOLCANIC UNIT

The metavolcanic unit consists predominantly of plagioclase amphibolite and tremolite-chlorite schist with subordinate bands of quartz- and biotite-bearing amphibolite, possibly derived from sediments.

Plagioclase amphibolite is speckled, dark green and white, massive to lightly foliated rock consisting of amphibole and plagioclase with minor epidote, leucoxene, opaque oxide and quartz. It corresponds to basalt in composition (Table II.2) and compares closely to the average Canadian Archaean basalt (Wilson et al., 1965, p.167).

The amphibole, a member of the tremolite-actinolite series, (Table II.5), occurs in large, ragged sieve-textured plates, pale green, but more intense at the margin than in the core. The plagioclase determined by electron probe is andesine, An_{27}.

Table II.2 Analysis of plagioclase amphibolite from Reservation 34.

wt.%		cipw norm	
SiO_2	50.50	or	1.52
Al_2O_3	14.60	ab	20.94
FeO	9.18	an	24.15
MgO	10.10	en	.59
CaO	11.20	fs	16.80
K_2O	.25	di	25.65
Na_2O	2.68	hd	0.00
H_2O^+	.67	fo	9.45
H_2O^-	.06	fa	0.00
CO_2	.10	il	.84
TiO_2	.43	ap	.07
P_2O_5	.03		
MnO	.08		
NiO	.01		
Cr_2O_3	.07		
S	.06		
	100.02		

Analytical methods are described in Appendix VI.

Epidote occurs as fine granular aggregates and larger subhedral crystals comprising about 5% of the thin section. Leucoxene, opaque oxide and quartz are all minor constituents.

Tremolite-chlorite schist is fine-grained, well-foliated, and contains occasional olivine relics. The chlorite has the optical properties of clinochlore: colourless to very pale green, clear, euhedral crystals with low birefingence, small positive 2V and a maximum extinction angle in longitudinal sections of 9°. Twinning is prominent and some crystals are curved. Tremolite occurs in small, discrete, grains, colourless to light green, with low birefringence. Opaque oxide is the only other constituent. Shearing causes fragmentation of the tremolite along the cleavage and conversion of clinochlore to irregular wispy, green penninite, with straight extinction and anomalous blue interference colours.

Analyses of clinochlore from an unsheared tremolite-chlorite schist (Table II.3) cluster in the clinochlore and sheridanite fields of Hey (1954). (See also, Deer, Howie and Zussman, 1962, v.3, p.137).

The tremolite-chlorite schist is interpreted as metamorphosed olivine basalt. The average of the four analyses from Reservation 34 (Table II.4) resembles analyses of metamorphosed picritic basalt from the Cape Smith-Wakeham Bay area (Wilson et al., 1969, Table 7), and very olivine-rich basalt (Rittmann, 1962, p.105). Rocks of very similar composition have been described from the Rhodesian Archaean (Bliss and Stidolph, 1971).

Table II.3 Electron microprobe analyses of chlorite in tremolite-chlorite schist from Reservation 34.

weight percent			No. of ions on basis of 36 (O,OH)				
SiO_2	28.17	30.13	Si	5.53	8.00	5.84	8.00
Al_2O_3	16.33	14.58	Al	2.47		2.16	
MgO	38.89	34.17	Al	1.31	12.58	1.17	12.49
FeO	8.12	8.83	Fe^2	1.33		1.43	
MnO	.09	.09	Mn	.02		.01	
CaO	.00	.01	Mg	9.92		9.88	
(H_2O)	(12.23)	(12.36)	Ca	0.00		0.00	
	98.83	98.21	(OH)		(16.02)		(15.99)

Water has been calculated on the basis of 8 molecules for every 28 oxygen atoms.

Table II.4 Chemical analyses and CIPW norms of tremolite-chlorite schist from Reservation 34.

	weight percent				
	1	2	3	4	average
SiO_2	41.50	44.60	47.00	44.80	44.48
Al_2O_3	9.60	12.80	8.20	7.00	9.40
FeO	13.14	9.36	9.90	9.54	10.49
CaO	5.00	7.20	7.10	8.60	6.98
MgO	22.50	19.00	20.50	20.50	20.63
K_2O	0.00	.05	.05	.05	.03
Na_2O	.13	.70	.65	.35	.46
MnO	.07	.07	.06	.11	.08
Cr_2O_3	.39	.29	.32	.31	.33
TiO_2	.20	.20	.16	.16	.18
P_2O_5	.04	.00	.00	.00	.01
H_2O^+	6.06	3.61	4.04	4.54	4.56
H_2O^-	.14	.11	.09	.05	.10
S	.02	.09	.10	.07	.07
CO_2	.10	.30	.10	3.20	.93
Total	98.89	98.38	98.27	99.28	98.73
S.G.	2.97	3.02	2.98	2.97	2.99

CIPW norms

C	.42	-	-	-	-
or	.00	.31	.32	.32	.19
ab	1.19	6.29	5.86	3.24	4.19
an	26.56	33.58	20.57	19.03	25.27
di	.00	2.67	10.49	17.24	7.28
he	.00 } 0.00	.80 } 3.47	3.10 } 13.59	4.94 } 22.18	2.27 } 9.55
en	22.25	21.02	29.23	22.76	23.71
fs	9.22 } 31.47	7.24 } 28.26	9.88 } 39.11	7.48 } 30.24	8.49 } 32.20
fo	26.90	19.60	14.22	17.62	19.74
fa	12.28 } 39.18	7.44 } 27.04	5.30 } 19.52	6.38 } 24.00	7.79 } 27.53
il	.41	.40	.32	.33	.37
cr	.62	.45	.50	.50	.52
ap	.10	-	-	-	.03
Py	.05	.20	.22	.16	.16

Table II.5 Electron microprobe analyses of amphibole from Reservation 34.

	plagioclase amphibolite		tremolite chlorite schist	
	1	2	3	4
SiO_2	52.40	51.98	52.97	53.94
TiO_2	.08	.06	n.d.	n.d.
Al_2O_3	3.69	4.76	6.04	3.43
FeO	13.82	14.27	7.47	7.32
MnO	.33	.33	.18	.23
MgO	14.36	13.32	21.40	22.49
NiO	.01	.00	n.d.	n.d.
CaO	12.22	11.85	8.60	8.85
Na_2O	n.d.	.58	.88	1.11
K_2O	n.d.	.13	.10	.04
(H_2O^+)	2.05	2.06	2.14	2.13
Total	98.96	99.33	99.78	99.65

Water is calculated on a basis of 1 molecule of H_2O for every 23 oxygen atoms.

No of ions on basis of 23 O

Si	7.640 } 8.00	7.573 } 8.00	7.383 } 8.00	7.550 } 8.00
Al	.360 }	.427 }	.617 }	.450 }
Al	.274	.390	.375	.116
Ti	.009	.007	-	-
Fe^2	1.685	1.739	.871	.857
Mg	3.121 } 7.04	2.892 } 7.00	4.446 } 7.00	4.691 } 7.02
Mn	.041	.041	.021	.027
Ni	.001	.000	-	-
Ca	1.909	1.850	1.284	1.327
Na	-	.080	.010	-
Na	- } 0.00	.084 } 0.11	.228 } 0.25	.301 } 0.31
K	-	.024	.018	.007
(OH)	1.994	2.002	1.990	1.990

total iron content reported as FeO

Following Stout (1972) the cations have been allocated as follows:-
8 tetrahedral (T) sites occupied by Si and Al
5 small octahedral (M) sites occupied by Mg, Fe, Al_2, Mn and Ti } combined
2 large octahedral (M) sites occupied by Ca, Na, Fe^2, Mg and Mn }
1 A-site occupied by Na and K

Biotite-bearing plagioclase amphibolite consists of fine, generally acicular, green pleochroic actinolite and brown biotite in a matrix of quartz and plagioclase. The plagioclase is andesine with a composition An_{38}, determined optically. Where aggregates of quartz are developed, straight boundaries and triple-point junctions approaching 120° indicate recrystallization. Undulose extinction is slightly developed. Actinolite occurs in small acicular crystals pleochroic in pale green with colourless cores. Deep brown biotite is distributed in streaks suggestive of original compositional variations.

Quartz-bearing amphibolite is rare and consists almost entirely of hornblende and quartz.

D METAMORPHISM

In the most recent metamorphic facies nomenclature of Turner (1968, p.307) the almandine-amphibolite facies is renamed the amphibolite facies and the epidote-amphibolite facies is considered a transition between the greenschist and amphibolite facies. An examination of the mineral assemblages present in pelitic, quartzo-felspathic and basic rocks in the greenschist, epidote amphibolite and amphibolite facies (Turner, 1968, Chap.7), suggests that in ambiguous examples an analysis of both plagioclase and amphibole is necessary to decide the metamorphic grade. The compositional differences are summarized in Table II.6.

The mineral assemblage in the metasediments is quartz-biotite-garnet-muscovite. Neither plagioclase* not amphibole

---

* The very fine-grained nature of the argillites makes optical identification difficult and these were examined for plagioclase by electron microprobe.

is present so there is no way to determine unequivocally the metamorphic facies.

Table II.6. Some mineralogical characteristics by which to distinguish low- and medium-grade metamorphic facies.

mineral	greenschist facies	epidote-amphibolite facies	amphibolite facies
plagioclase	albite	albite & oligoclase with up to An_{25}	An_{25-60}
amphibole	non-aluminous actinolite	low aluminous hornblende or actinolite with up to 8% Al_2O_3	hornblende

The plagioclase in the plagioclase amphibolites is andesine (An_{27}) and the amphibole is a low-alumina hornblende close to actinolite in composition (Table II.5). Thus the plagioclase amphibolite is of a metamorphic grade transitional between the greenschist and amphibolite facies, the epidote amphibolite facies. The presence of chlorite in the tremolite-chlorite schist would apparently place the rocks in the greenschist facies of metamorphism but chlorite is recorded from basic assemblages in the epidote-amphibolite facies (Turner, 1968, p.303) and in magnesian assemblages in the amphibolite facies (Lyons, 1955, p.118).

Garnets from the metasedimentary unit analyzed by electron microprobe (Table II.1) are principally almandine together with approximately equal proportions of spessartine, pyrope and grossular. The cores are slightly enriched in spessartine and grossular and depleted in almandine and pyrope compared to the margins. Almandine in the greenschist facies tends to be

enriched in the spessartine molecule compared to almandine in the amphibolite facies, but Miyashiro (1953) has shown that this enrichment is relative and dependent upon original bulk composition of the rock. Hence the MnO content of isolated specimens from a regionally metamorphosed terrain cannot be used to estimate the metamorphic grade.

Miyashiro (1953, fig.5,6 and 7) and Brown (1967, fig.23) have demonstrated that garnet in rocks from the amphibolite and epidote-amphibolite facies tend to fall in the almandine apex of a spessartine-pyrope-almandine compositional triangle: the composition of both the core and the rim of the garnets in Reservation 34 plot towards the almandine apex. Thus it is not possible to use garnet composition to distinguish between the amphibolite and epidote-amphibolite facies of metamorphism.

It is concluded that the metavolcanic and metasedimentary units have been metamorphosed to the epidote-amphibolite facies, transitional between the amphibolite and greenschist facies.

E GRANITES AND GNEISSES

The supracrustal rocks in Area II are separated by a fault from granodiorite gneiss to the SW. The granodiorite gneiss is grey to grey-green, depending on mafic mineral content, coarse-grained, foliated, and with a tendency to a granoblastic texture. It consists of quartz, plagioclase, biotite, hornblende, garnet and occasional microcline with accessory apatite, sphene, opaque oxide and sericite. The plagioclase is andesine with a composition An_{40} determined optically; microcline is not normally present.

Biotite occurs in deep brown pleochroic crystals when hornblende is present and in deep olive-green crystals when hornblende is absent. Hornblende is green pleochroic and anhedral. Epidote is a late mineral, as either large euhedral crystals transecting biotite or as minute granules in small shear zones with granular quartz and plagioclase. Garnet is extremely poikiloblastic and occurs as round grains or fragments which deform the pervasive foliation in the rock.

The country rocks of Area I are granite and gneissic granite with minor amphibolite. The granitic rocks are predominantly pink in colour, massive to lightly foliated, consisting of quartz, lightly sericitised oligoclase, microcline, olive-green biotite, sericite, opaque oxide, apatite and zircon. The more gneissic varieties are darker in colour and have biotite and hornblende strewn throughout the rock. The amphibolite is altered; hornblende is fragmented along the cleavage and partly replaced by chlorite and the biotite has been replaced by a fine opaque aggregate of hematite. In the far northern portion of the Reservation unaltered amphibolite occurs with gneissic granite similar to that in Area I. The plagioclase amphibolites are well banded, fine-grained assemblages of hornblende, oligoclase and quartz with minor leucoxene and sphene.

F CONCLUSIONS

The wall-rocks to the ultramafics in Area III, the meta-volcanic and metasedimentary units show evidence of two deformations, one producing a pervasive foliation and the other

a non-pervasive cleavage. They have been metamorphosed to the epidote-amphibolite facies a lower grade than normal for the Wabowden sub-Province. Lithologically they resemble either the low grade rocks which outcrop sporadically in the Wabowden sub-Province or volcanics and sediments characteristic of Archaean schist belts.

The wall-rocks to the ultramafics in Area I are granite and gneissic granite with minor amphibolite. The metamorphic grade is in the amphibolite facies, and lithologically they resemble granites and gneisses in the Wabowden sub-Province.

III CONCLUSIONS REGARDING THE POSITION OF RESERVATION 34

It is clear from Figures I.2, I.3 and I.4 that Reservation 34 lies south of a direct continuation of both the Setting Lake Lineament and the Wabowden sub-Province so that it could be underlain by Pikwitonei or Superior Province rocks.

The Setting Lake Lineament has been mapped by Rance (1966) to within 3 miles of the edge of the Palaeozoic. The aeromagnetic pattern of the Kisseynew gneisses to the NW and the granodiorite gneiss to the SE of the Lineament are quite distinct (Kornik, 1969); both can be traced for a few miles under the Palaeozoic cover where they are interrupted by a north to south lineament (Fig. III.1). West of this lineament the aeromagnetic pattern is complicated and does not indicate a simple continuation of the geology of the Nickel Belt beneath the Palaeozoic rocks. The Setting Lake Lineament bifurcates and alters strike to the NE of Thompson (Bell, 1971, Fig.2) and it may behave in a similar fashion beneath the Palaeozoic. One possible continuation passes to the west of Reservation 34, but it is also possible that one of the two lineaments beneath Reservation 34 is a continuation.

Reservation 34 may be divided into four regions of differing magnetic* relief and pattern (Fig. III.1). Region 1 has high

---

* The following aeromagnetic maps published jointly by the Dept. of Mines and Technical Surveys, Ottawa and the Dept. of Mines and Natural Resources, Manitoba, have been used:- 7135 G Sipiwesk; 7740 G Grand Rapids; 7132 G Wekusko Lake; 7136 G Nelson House, published between 1965 and 1969 at a scale of one inch to four miles.

and irregular magnetic relief with contours elongated in a WSW direction. This region lies SW of the granulites of the Pikwitonei Province although the magnetic pattern in the granulites is distinct in both pattern and direction. The region may be an area of retrograde granulites but there is no diamond drill information by which to verify this. Region 2 has medium and irregular relief in which the magnetic contours are elongated in a north to south direction. The region is sharply demarcated from region 1 and may represent an extension of the Archaean rocks of the Cross Lake sub-Province where a structural discontinuity is known to occur between them and the granulite of the Pikwitonei Province to the north (Wilson and Brisbin, 1962, Fig.3). Region 3 is a linear zone of irregular and high magnetic relief underlain by mafic volcanics and pelitic schists metamorphosed to the epidote-amphibolite grade (Chapter II). Region 4 consists of smooth and low magnetic relief. The SW corner of the Reservation, Area 4', is underlain by garnetiferous granodiorite-gneiss without cordierite or sillimanite. These rocks resemble gneisses collected from parts of the Wabowden sub-Province and closely match Rance's (1966, p.67) description of garnetiferous granodiorite gneiss from the Wabowden sub-Province. The more massive granites of region 4" are not distinctive and similar granites may be found on either side of the Setting Lake Lineament. No diamond drilling has been undertaken in region 5, which has an aeromagnetic pattern resembling that in Region 4.

No unequivocal conclusion can be made regarding the classification of rocks beneath Reservation 34. The extreme

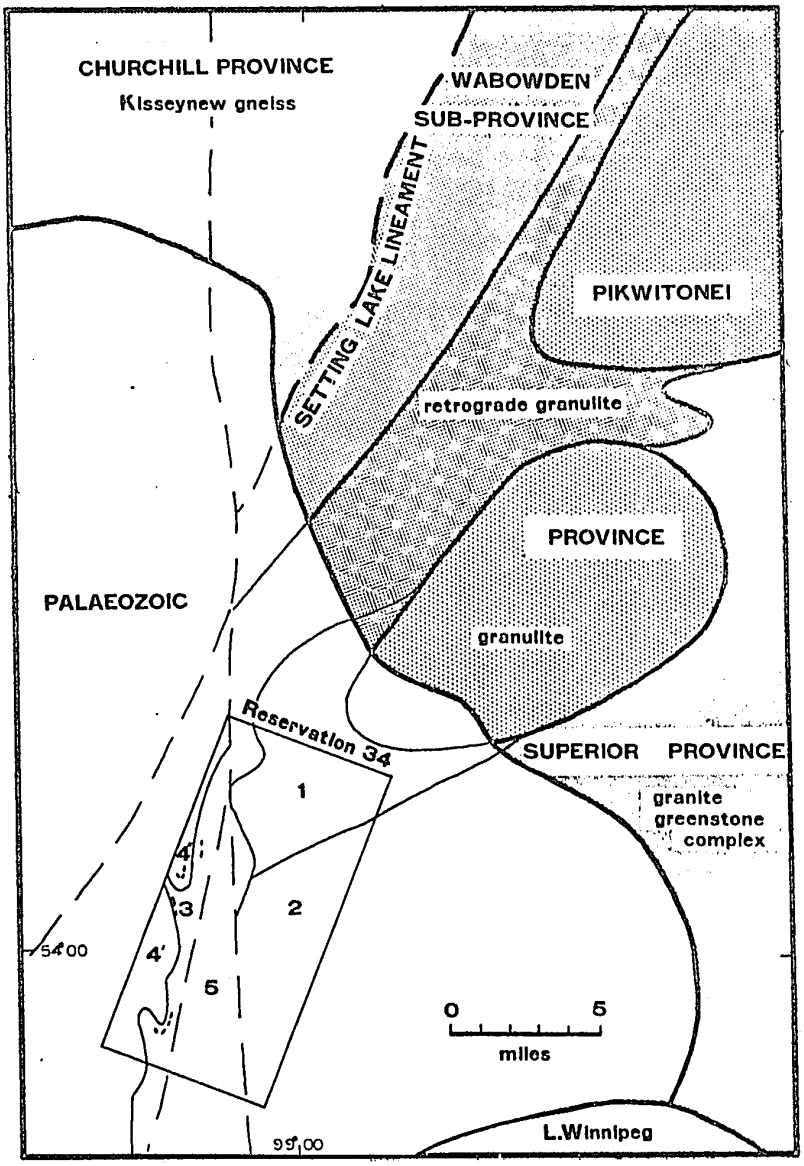

Fig.III.1 Interpretation of the sub-surface geology of Reservation 34 in the context of the known regional geology.

To the NE of the Palaeozoic cover the aeromagnetic patterns can be related to surface geology and the sub-divisions are indicated by heavy lines. Aeromagnetic sub-divisions beneath the Palaeozoic rocks are faintly outlined and their relation to geology is inferred. Dashed lines are faults and lineaments. Aeromagnetic data from Federal-Provincial aeromagnetic map series, Wekusko Lake 7132 and Grand Rapids 7740. The numbers represent areas of characteristic relief described in Chapter III.

western portion is underlain by rocks resembling those found in the Wabowden sub-Province. The metamorphic grade of the Wabowden sub-Province is predominantly in the amphibolite facies but rocks of lower metamorphic grade are known (see p.8). Godard (1968, p.5) has described magnetite-bearing iron formation and quartzose sedimentary rocks, metamorphosed to the epidote-amphibolite facies only, which are similar to those of the metasedimentary unit. Thus the metavolcanic and metasedimentary units may belong to the Wabowden sub-Province. However, these rocks are also lithologically similar to volcanics and sediments in Archaean greenstone belts; indicating that rocks of the Cross Lake sub-Province may sub-outcrop beneath part of Reservation 34.

Ultramafic bodies forming a SW continuation of the Manitoba Nickel Belt might sub-outcrop in the extreme west of Reservation 34. If, as country rock lithology suggests, Archaean rocks of the Superior Province extend beneath the Reservation, then Archaean ultramafic rocks might also occur.

IV ULTRAMAFIC ROCKS OF AREA III

A COMPOSITION OF THE SERPENTINITES

The ultramafic rocks of Area III were emplaced in the vicinity of the contact between the metavolcanic and metasedimentary units (Fig.II.1).

They are completely serpentinized dunite; containing lizardite, clinochrysotile, antigorite, magnetite and chrome spinel, with minor chlorite, dolomite and tremolite developed subsequent to serpentinization. The details of the mineralogy are described in the following sections.

An average of 5 analyses of serpentinized dunite are shown in Table IV.1, together with an average analysis of the Moak Lake serpentinite (Macdonald, 1960), and an average of 24 serpentinites from the Manitoba Nickel Belt (Coats, 1966). The analyses show the Area III serpentinites to be richer in SiO_2 and poorer in MgO than the Manitoba Nickel Belt analyses previously published.

B PRIMARY NATURE OF THE ULTRAMAFIC ROCK

1 Introduction

The diversity in origin, mode of emplacement and tectonic history of ultramafic rocks has been documented by Wyllie (1970, 1967) and Naldrett and Gasparrini (1971) who show in effect that any ultramafic body has to be considered in terms of three parameters:- (1) the petrogenesis; (2) the tectonic environment during rise, emplacement and cooling and (3) the

Table IV.1 Analyses of serpentinites from Area III and the Manitoba Nickel Belt.

	1.	2.	3.
SiO_2	38.42	35.73	36.46
Al_2O_3	1.68	1.95	3.00
FeO	8.63	8.48	9.43
CaO	.70	.29	.76
MgO	33.68	39.10	35.65
K_2O	.01	.00	.02
Na_2O	.01	nd	.03
H_2O^+	12.26	12.11	10.92
H_2O^-	.54	nd	.28
Co_2	.90	.60	.80
MnO	.07	.05	.09
Cr_2O_3	.44	.54	.44
TiO_2	.07	.10	.15
NiO	.31	.34	.91
P_2O_5	nd	nd	.05
S	.06	.63	.50
CoO	nd	.02	nd
	97.78	99.94	100.23

1. Average of 5 serpentinites from Area III. 2. Average of 5 Manitoba Nickel Belt serpentinites (Coats, 1966). 3. Moak Lake serpentinites (Macdonald, 1960). Analytical methods are described in Appendix VI.

subsequent tectonic and metamorphic history. The first two parameters are closely interrelated; the petrogenesis will determine the characteristic chemical and mineralogical features according to whether fusion or crystallization occurs; the tectonic environment, orogenic or anorogenic, will imprint distinctive textural and structural features on the ultramafic body. Tectonic and metamorphic activity subsequent to initial emplacement may modify or destroy primary mineralogical and textural features.

It is reasonable to refer all ultramafic rocks, other than those produced solely by metasomatic activity, to a mantle origin, but the process of derivation varies. Complete fusion of the mantle would result in the production of an ultrabasic magma which, if introduced as such, would form a high-temperature peridotite. This magma is capable of fractional crystallization and if placed in a tectonic environment in which it cools slowly will form a stratiform complex of ultramafic and mafic rocks, which may remain near the mantle or be intruded, in whole or in part, at various levels in the crust. Partial fusion of the mantle would produce a basic magma and a peridotitic residue, the relative proportions of which will depend on the degree of partial fusion. The basic magma can be separated from the residue and intruded as a magma, or migrate and fractionally crystallize to produce a stratiform intrusion. The peridotitic residue, whose characteristics are determined by the partial fusion process, could itself by moved tectonically and emplaced as a solid, or if sufficient interstitial liquid is present, as a

crystalline mush. Finally ultramafic rocks may be derived directly from the mantle by thrusting, to be exposed in deep ocean trenches or suitable continental environments. While these ultramafic show characteristics of solid intrusion, they also show characteristics of their mantle origin.

The tectonic environment may be considered as orogenic or anorogenic. In an anorogenic environment magma has time and space to fractionally crystallize to produce stratiform intrusions, dominated by cumulus textures. These bodies remain associated with their primary, thermal, metamorphic aureole. In orogenic environments liquid magma may be forced to migrate, as soon as it forms, to higher levels and thus become separated from the increasingly ultramafic residue. The residual material may be emplaced, as either a solid or a crystal mush, so that flow structures and deformation textures characterize the resulting ultramafic rock. Such ultramafic rocks are not associated with a thermal metamorphic aureole.

Subsequent tectonic and metamorphic events may modify the primary features of an ultramafic body, superimposing structural, textural and possibly chemical features that were not characteristic of the environment in which it originally formed. It is not necessary for stratiform intrusions, for example, to form only in the stable crustal regions where they are so often preserved intact. Thayer (1969) believes that most Alpine-type peridotites are disrupted fragments of deep stratiform or cumulate bodies. Challis (1965) and Cotterill (1969) have described ultramafic bodies from New Zealand and Rhodesia

respectively, normally thought of as Alpine-type, which have some features of cumulates. Conversely, ultramafic bodies consisting predominantly of dunite and harzburgite should not necessarily be classed as Alpine-type, especially if they occur away from readily recognizable orogenic belts. Ultramafic rocks whose emplacement is controlled by major crustal fractures could simulate Alpine-type ultramafics but have a different origin. "Thus the term Alpine peridotite is considered to have significance in designating a peridotite occurring in an orogenic environment but which generally may have one of several quite distinct origins" (Green, 1964, p.185).

Metamorphism can severely modify the chemical characteristics of ultramafic rocks, but at least in the lower grades of metamorphism sufficient textural and structural features by which to identify the origin may be preserved (e.g., Allard, 1970). Serpentinization may modify the bulk composition, as well as textural and structural features if accompanied by deformation. Na, Mn, Cr, Sc, Co (Stueber and Goles, 1967) and Ni contents (Goles, 1967, p.358; Faust et al., 1956) are static during serpentinization, and chemical characteristics dependent upon these elements could be used to identify the pre-serpentinization origin of an ultramafic.

Thus it is not valid to envisage ultramafic rocks as belonging to one of two or three distinct types, of which Alpine and stratiform intrusions are predominant. There are physical, chemical and mineralogical differences between various types of ultramafic bodies (Irvine and Findlay, 1972; Jackson and Thayer, 1972; Thayer, 1960; Green, 1964) which depend on the petrogenesis,

(fusion or crystallization) and tectonic environment of emplacement (orogenic or anorogenic). These distinctive structural and mineralogical features may be used to interpret the origin and history of ultramafic bodies in environments atypical of those normally associated with one or other of the major types.

It must be concluded that an empirical approach is necessary in interpreting the origin of ultramafic bodies. This is especially true of ultramafic bodies like those in the Manitoba Nickel Belt, whose form and environment are not typical of either Alpine or stratiform types.

2 Mineralogy and Petrology

The ultramafic rocks in Area III are completely serpentinized, the only primary mineral being the chromite cores of some secondarily zoned spinels. The serpentinites are, for the most part, completely unsheared, so that igneous textures are well preserved.

Serpentine after olivine is prominent in thin section and hand specimen, where it appears as dark, euhedral to subhedral, pseudomorphs in a light green antigorite matrix. These pseudomorphs are interpreted as derived from olivine for the following reasons:- (1) the shape, typically eight-sided, somewhat rounded and frequently elongated (Plates 1, 2, 3 etc.), is characteristic of primary magmatic olivine crystals and shows to advantage where small areas of interstitial serpentine (Plate 3) or magnetite (Plate 2) outline the pseudomorphs; (2) the pseudomorphs display true mesh texture, which develops

only from olivine, in contrast to pseudomesh texture which develops from pyroxene (Wicks, 1969). The shape of the pseudomorphs (Plate 3) corresponds to the shape of similar pseudomorphs from Area I in which relict olivine is found.

Bastite pseudomorphs after pyroxene are very rare and not distinguishable in hand specimen. They are interpreted as pseudomorphs after pyroxene for the following reasons:- (1) the more euhedral resemble longitudinal or transverse sections of pyroxene. Longitudinal sections display a single cleavage parallel to the length of the crystal, while cross-sections frequently show a relict intersecting (110) cleavage. The subhedral pseudomorphs are interstitial to the olivine pseudomorphs (Plate 16), sometimes in a manner suggestive of a relict poikilitic texture; (2) they do not show true mesh texture but consist either of a felted mesh of serpentine or randomly oriented, isotropic, serpentine.

Bladed pseudomorphs that resemble serpentinized amphibole have been observed in one thin section (Plate 14) from the centre of a serpentinite body.

Small interstitial patches of unknown primary composition occur throughout the serpentinite (Plates 2 and 16) and are interpreted as crystallized interstitial material in an olivine cumulate. The interstices, now occupied by a mixture of serpentine, magnetite and carbonate, have in some cases been enlarged by growth of the carbonate.

Accessory chrome spinel comprises about 1% to 2% of the rock and no banded or segregated chromitites are known. Chrome

spinel is interstitial to olivine pseudomorphs and is zoned from chromite in the core through ferritchromit to magnetite at the rim. Electron microprobe analyses of the cores (Table IV.3) show that they fall within the compositional field of chromite from layered intrusions (Fig.VIII.1) partly overlapping the field of Alpine-type intrusions (Fig.VIII.2). The ferritchromit rims are considered of secondary origin. The details of spinel petrology are discussed in Chapter VIII.

Original magmatic sulphide has not been recognized.

3 Texture and Structure

The serpentinites in Area III are characterized by the ready recognition of pseudomorphs of the primary ultramafic minerals and textures. These indicate that the rocks were originally olivine cumulates with 1% to 2% of accessory chrome spinel, and less than 5% interstitial material (Plates 1, 2, etc.). In a few samples bastite pseudomorphs suggestive of an intercumulus origin (Plate 16) indicate that harzburgite was a very minor rock type. Elongate olivine similar to that illustrated in Plate 1 is also found in some ultramafic extrusives (Wicks, personal communication, 1972), but the thickness of the Area III ultramafics and the absence of spinifex, or quench, textures would mitigate against their being extrusive.

Textures that result from the protoclastic deformation of ultramafics consequent upon the intrusion of an essentially crystalline material have been described by various authors, for example, Raleigh (1967); Lipman (1964) and Ragan (1963)

and include:- (1) strain lamellae parallel to (100) in olivine, resulting from sub-parallel kink bands; (2) rounding and granulation of olivine (Plate 17); (3) large porphyroblasts of olivine in a matrix of finer grains; (4) clusters of small olivine grains differing only slightly in crystallographic orientation which result from the disruption of larger grains; and (5) ragged appearance of pyroxene crystals that may also be bent or otherwise deformed (Plate 18). Interdigitated and interlocking grain boundaries and the absence of fine-grained olivine indicate that recrystallization has accompanied deformation.

Serpentinization will destroy any optical irregularity resulting from deformation; but the morphological textures will survive provided that deformation does not accompany, or follow, serpentinization. Wicks (1969) interprets the distinctly inequigranular,'bimodal' serpentine texture illustrated in Plate 17 as resulting from the serpentinization of a deformed dunite consisting of porphyroblastic olivine in a matrix of fine olivine (Plate 18). No serpentine textures suggestive of this mode of origin have been recognized in Area III.

The available textural evidence indicates that Area III ultramafics formed from a liquid crystallizing olivine, spinel and minor pyroxene. The lack of textures suggestive of protoclastic deformation resulting from intrusion in a crystalline state suggests crystallization in situ, or very thorough lubrication at the tectonic contact with country rock if emplaced as a solid.

Ground and air magnetic surveys indicate that the ultramafic bodies are lensoid in shape, varying between 2000 and 4000 feet in length. The maximum drill hole intersection is about 1000 feet; the dip is uncertain but steep and probably to the SE, indicating a true thickness of about 750 feet. The form and structure of the bodies within these gross dimensions is not known, but the complete lack of internal deformation suggests that they are unlikely to be highly folded and that this indicated thickness is true. Only minor amounts of country rock are intersected within the masses; this together with the thickness of the bodies suggests that they are not extrusive in origin. Spinifex textures have not been observed.

4 Summary and Conclusions

(a) The ultramafic rocks of Area III were originally dunite containing accessory chrome spinel. Harzburgite was a very minor rock type.

(b) Primary magmatic sulphide has not been recognized.

(c) Relict primary textures indicate an original olivine cumulate. Relict deformation textures consequent upon the solid intrusion of a crystalline mass have not been observed. This suggests that the ultramafic body crystallized in situ, or, if intruded as a crystalline mass, was sufficiently well lubricated at the tectonic contacts to preclude internal deformation.

(d) The ultramafic bodies vary between about 2000 to 4000 feet in length and are about 750 feet thick; these dimensions suggest that the ultramafics were not extrusive.

(e) The composition of the chromite cores to zoned spinels, the only primary minerals remaining, straddle the compositional fields of chromite from layered intrusions and from Alpine-type bodies.

C SERPENTINE MINERALOGY

1 Introduction

The serpentinized dunite is characterized by lizardite-chrysotile mesh textures. Individual olivine pseudomorphs displaying mesh textures are fringed and veined by later antigorite intermixed with small amounts of chlorite. Opaque iron oxide, largely magnetite formed during serpentinization, is more prevalent near mesh-textured serpentine than near antigorite. Brucite has neither been observed nor identified in X-ray microbeam photographs.

2 Mesh-Textured Serpentine

Two types of serpentine fibre differing in optical orientation are known; α-serpentine with length fast fibres (negative elongation) and γ-serpentine with length slow fibres (positive elongation). Optical orientation of the fibres forming the mesh rims provides a convenient means of describing the mesh structures. Lizardite may be α-serpentine or γ-serpentine; antigorite and chrysotile are γ-serpentine.

The mesh textures in Area III serpentinites consist of rims of α-serpentine separating sub-rectangular mesh centres of an isotropic serpentine, frequently referred to as serpophite.

The geometry of mesh textures varies and is generally irregular. No attempt has been made to determine the symmetry of the texture as described by Wicks (1969), but most can be described as typical sub-rectangular mesh patterns (Plates 3 and 4). Mesh texture may look extremely irregular in plane-polarized light, but under crossed nicols, the mesh directions are parallel to faces of the original olivine crystal. The mesh texture in which the individual olivine pseudomorphs are clearly visible (Plate 4) is very typical of Area III.

Ribbon structure, in which one mesh rim direction is preferentially developed, is less common and results in a series of parallel cross-fibre veinlets with or without intervening mesh centres. Francis (1956, p.220) has suggested that ribbon structure is promoted by shearing, whereas Hess, Smith and Dengo (1952) have suggested that the formation of antigorite is promoted by shearing. The development of ribbon texture and antigorite are not complementary in the Area III serpentinites.

The mesh rims are bipartite, consisting of a thin central zone of either structureless or randomly orientated serpentine separating marginal zones of α-serpentine fibres radiating normal to the vein wall (Plates 7 and 8). Very fine grains of opaque oxide may occur along the central parting. The median may be more than just a parting; it sometimes approaches the marginal fibre zones in width (Plate 8). When this occurs the serpentine becomes orientated normal to the length of the vein as a mixture of α- and γ-serpentine. In these cases the vein is strictly tripartite but the original terminology of

Francis (1956), subsequently followed by Coats (1966) in describing serpentine from the Manitoba Nickel Belt, will be followed here.

External mesh rims to serpentinized olivine are rare (Plate 10). This may be due to later development of antigorite around the margins of the serpentinized olivine, although serpentinized olivine with neither feature is common (Plate 4). The shape of mesh centers on opposite sides of a mesh rim occasionally indicates displacement across the mesh rim.

The mesh centres are either colourless or pale shades of red-brown, with a dusty or cloudy appearance (Plate 3), and isotropic (Plate 4). This material has been named serpophite in the past, although its mineralogical nature remained in doubt. Deer, Howie and Zussmann (1962, v.3, p.183) suggested it could be amorphous serpentine, olivine or enstatite, while other writers have suggested it to be randomly orientated, fibrous, crystalline serpentine. Electron microprobe analyses (Table IV.2) show that Area III mesh centres have the composition of serpentine. X-ray powder diffraction patterns taken with a Debye-Scherrer camera, could not be conclusively interpreted due to the small number of reflections. This probably results from the small amount of material that could be removed from a thin section.

X-ray microbeam studies* were undertaken at the Royal Ontario Museum by Dr. F. Wicks; these showed the mesh centres

---

*Details of the microbeam studies are presented in Appendix II.

Table IV.2 Partial electron microprobe analyses of serpentine species (W89, Area III).

	1	2	3	4	5	6	7	8	9	10	11
	Mesh centres-lizardite & clinochrysotile				Mesh rims-lizardite				Antigorite		
	#1	#2	#3	Av.#1 to #3	#1	#2	#3	Av.#1 to #3	#1	#2	Av.#1 & #2
SiO_2	44.19	42.49	42.46	43.05	42.24	41.21	40.17	41.21	40.97	40.23	40.60
Al_2O_3	.65	.57	.45	.56	.09	.02	.17	.09	3.48	3.18	3.33
MgO	38.60	37.76	37.72	38.03	41.31	43.51	42.77	42.53	40.81	40.62	40.72
NiO	.23	.41	.40	.35	.36	.18	.20	.25	.28	.31	.30
MnO	.11	.14	.27	.17	.00	.00	.00	.00	n.d.	n.d.	n.d.
CaO	.36	.67	.77	.60	.00	.00	.00	.00	.00	.00	.00
FeO	4.03	5.42	6.56	5.34	3.94	4.39	3.58	3.97	2.89	3.13	3.01
(H_2O)	12.93	12.66	12.73	12.77	12.82	12.93	12.63	12.79	12.97	12.79	12.88
	101.10	100.14	100.36	100.87	100.76	102.29	99.53	100.94	101.41	100.26	100.84
	Number of ions on basis of 9(O,OH)										
Si	2.05	2.01	2.00	2.02	1.98	1.91	1.91	1.94	2.00	2.00	2.00
Al	.00	.00	.00	.00	.01	.00	.01	.01	.11	.12	.11
Al	.04	.03	.02	.03	.00	.00	.00	.00	.08	.06	.07
Mg	2.66	2.66	2.64	2.66	2.88	3.00	3.00	2.97	2.81	2.83	2.82
Ni	.01	.01	.02	.01	.01	.01	.01	.01	.01	.01	.01
Mn	.00	.01	.01	.01	.00	.00	.00	.00	-	-	-
Ca	.02	.03	.04	.03	.00	.00	.00	.00	.00	.00	.00
Fe	.16	.21	.26	.21	.15	.17	.14	.16	.11	.12	.11
OH	4.00	4.00	4.00	4.00	4.00	4.00	4.00	4.00	4.00	4.00	4.00
O	5.00	5.00	5.00	5.00	5.00	5.00	5.00	5.00	5.00	5.00	5.00

The weight percentage of H_2O has been calculated on the basis of two molecules of H_2O for every 7(O)
Details of the analytical procedure and standards for electron microprobe analyses are given in Appendix III

to consist predominantly of randomly orientated clinochrysotile with subordinate lizardite in some centres. The random orientation would explain the isotropic nature of the centres. More rarely the centres are fibrous and slightly birefringent, the fibres being orientated parallel to the long axis of the pseudomorph (Plate 9). The fibrous serpentine may surround featureless isotropic serpentine. X-ray microbeam studies again indicate that the centres consist of a mixture of lizardite and clinochrysotile but could not demonstrate whether or not either mineral was restricted to the fibrous or isotropic zone. When the mesh centres are fibrous there is a tendency for one direction of mesh rims to predominate. These form cross-fibre veinlets of α-serpentine (lizardite) alternating with intervening fibrous mesh centres of γ-serpentine (clinochrysotile). In extreme development the cross-fibre veins may completely replace the intervening γ-serpentine.

Microbeam studies show that the mesh rims consist of lizardite in type 1 orientation (Appendix II).

Electron probe analyses of lizardite from the mesh rims (Table IV.2, cols.5-8) were recalculated in terms of (1) $MgO-SiO_2-H_2O$; (2) $MgO-FeO-SiO_2$; (3) $MgO-Al_2O_3-SiO_2$ and (4) $MgO-FeO-H_2O$, (where FeO is total iron). They fall at the margin of the compositional field of lizardite as demonstrated by Whittaker and Wicks (1970, p.1035).

3 Bastite Pseudomorphs

Bastite pseudomorphs after pyroxene are very rare but were found in a heavily carbonated serpentinite at the base of one drill hole. The olivine has been entirely replaced by antigorite. The bastite pseudomorphs are green, anhedral, somewhat cuspate masses, between the serpentine pseudomorphs after olivine or more rarely as euhedral pseudomorphs after longitudinal or transverse sections of pyroxene.

The cross-sections consist of felted fibro-lammellar γ-serpentine in a right-angled decussate texture suggestive of the serpentinization being controlled by the (110) cleavage in pyroxene. Longitudinal and interstitial bastites are sometimes isotropic with a few fibro-lamellar flakes and occasionally an irregular assemblage of α- and γ-serpentine.

Much magnetite, and some hematite, are associated with the bastite, but it is unlikely that all of this results from the serpentinization of pyroxene. Magnetite is not associated with antigorite in Area III serpentinites, and it tends to accumulate in fractures and in mesh-textured serpentine remnants. Thus the magnetite associated with bastite pseudomorphs has possibly migrated from the mesh-textured serpentine on replacement by antigorite. Only minor replacement of bastite by antigorite has occurred.

4 Serpentine Pseudomorphs after Amphibole

Pseudomorphs resembling serpentinized amphibole have been observed only once in Area III (Plate 14). The pseudomorphs are

bladed with a distinct cross-parting and lack the true mesh texture of the serpentinite in which they occur. Irregular fringes of α-serpentine develop from the cross-partings enclosing pseudomesh centres of γ-serpentine together with some isotropic serpentine. The outer edges of the pseudomorphs are irregularly rimmed by α-serpentine developing normal to the edge.

5 Antigorite

Antigorite is colourless, but with occasional pale green, pleochroic patches in the coarser crystals. The birefringence has a slight, but consistent and characteristic, anomalous blue tinge. Textural evidence indicates that the antigorite developed subsequent to the mesh-textured serpentine, initially as coarse fibro-lamellar fringes around, and normal to the margins of the mesh-textured olivine pseudomorphs, so that individual relicts become clearly outlined (Plate 3). This texture is readily apparent in both thin section and hand specimen, the green antigorite matrix enclosing grey olivine pseudomorphs. Coarse fibro-lamellar crystals of antigorite also develop from fractures across the mesh-textured relics, forming 'curtains' of antigorite along the fractures (Plate 6). The coarse antigorite is confined to the margins and later fractures; the interior of the olivine pseudomorphs is subsequently replaced by finer and randomly orientated antigorite with a felted texture. When this replacement is incomplete, the mesh rims of the remaining mesh-textured serpentine are still parallel to each other, indicating a lack

of deformation during the crystallization of the antigorite (Plate 5). When the mesh-textured serpentine is entirely replaced by antigorite the margins of the olivine relics may become obscure unless the fringe of coarse antigorite, or an outline of secondary magnetite, remains.

X-ray microbeam photographs (Appendix II) confirm the optical identification of antigorite. Electron microprobe analyses (Table IV.2) show the high Al_2O_3 content characteristic of antigorite. It was difficult to obtain consistent analytical results for antigorite, far more so than with lizardite and clinochrysotile.

6 Summary

The serpentinized dunites of Area III are characterized by the development of mesh-textured serpentine which pseudomorphs the original olivine so as to leave the outlines clearly visible. The mesh texture consists of mesh rims of bipartite cross-fibre veinlets of α-serpentine or lizardite enclosing mesh centres consisting of mixtures of lizardite and clinochrysotile. The lizardite and clinochrysotile in the mesh centres is normally randomly orientated resulting in isotropism under crossed nicols.

Antigorite replaces the mesh-textured serpentine, initially as coarse fibro-lamellar crystals around the margin of, and along fractures through, the olivine pseudomorphs. These fringes of antigorite emphasize the outline of the olivine pseudomorphs. Subsequently the centres of the pseudomorphs are replaced by a felted mass of finer-grained antigorite, which obscures the

pseudomorph outlines ultimately.

Bastite pseudomorphs are very rare and consist of intergrown α- and γ-serpentine. Antigorite replacement of bastite is minimal.

Serpentine after amphibole is rare and consists of γ-serpentine enclosed by fringes of α-serpentine developing from the edge of the pseudomorph and from cross fractures through the pseudomorph.

7 Discussion

a General

In a detailed study of serpentine, Wicks (1969) has concluded that the production of pervasive lizardite mesh textures is the normal early event of serpentinization. The mesh textures may be replaced by various secondary textures characterized by chrysotile and antigorite.

Antigorite has not been synthesized in the laboratory. Experiments with natural antigorite indicate that it is stable to higher pressures and temperatures than either chrysotile or lizardite. D.T.A. curves show that antigorite breaks down between 782° and 802° C, whereas chrysotile and lizardite break down between 637° and 715° C (Faust and Fahey, 1962, p.77; Nagy and Faust, 1956, Fig.5; Hess, Smith and Dengo, 1952, Fig.1). Raleigh and Patterson (1965) experimentally deformed serpentine at temperatures up to 700°C and pressures up to 5 kbars. Serpentinites composed of antigorite and chrysotile weakened as a result of dehydration and reaction to forsterite

and talc above 500°-600°C; lizardite-chrysotile serpentinites weakened between 300° and 350°C. Nelson and Roy (1958, p.78) found antigorite reacted to chlorite, forsterite and talc at 605°C and 20,000 psi (1.36Kb). However, in this case chrysotile-bearing serpentine also breaks down at the same pressure and temperature.

The formation of antigorite in natural serpentinites has been variously ascribed to the effects of thermal, regional or dynamic metamorphism. Wolfe (1967) has shown that antigorite replaces mesh-textured serpentine in the contact aureole of an intrusive granite. Coats (1968, p.333) records the only occurrence of antigorite in the Manitoba Nickel Belt as one half mile from an intrusive granite.

Wilkinson (1953, p.314) has found that antigorite in some Queensland ultramafic bodies formed from chrysotile when the mafic wall-rocks had been metamorphosed to the albite-epidote-amphibolite facies. He concluded that formation of antigorite is mainly dependent upon temperature, and shearing stress is not important. Thayer (1956, p.693) correlates serpentine textures containing antigorite with regional or thermal metamorphism. Cerny (1968) equates the formation of antigorite with 'high' dynamothermal metamorphism. Coleman (1966, p.17 and p.67) states that antigorite-bearing serpentinites from New Zealand are restricted mainly to metamorphic terrains.

Hess, Smith and Dengo (1952, p.74) conclude that in addition to heat, shearing stress, promotes the development of antigorite. They point out that thermal metamorphism has, in some cases,

failed to generate antigorite up to a temperature where re-generated olivine appears (Leech, 1953). They present evidence for the development of antigorite at the albite-epidote-amphibolite facies of metamorphism. Leech (1953) described the development of antigorite from mesh-textured serpentine as a result of intense shearing, and Francis (1956, p.220) the possible development of antigorite resulting from shearing. Wicks (1969, Table VIII.1) found regional metamorphism to be the most common agent of antigorite development.

Green (1961) describes antigorite replacing mesh-textured serpentines in ultramafic breccias that have been subjected to high intensity brecciation but not in those subjected to 'low intensity brecciation'. Directed stress played no part in the brecciation, temperature and fluid pressure being the main variables.

Antigorite is chemically slightly different from chrysotile and lizardite having a higher range of Al_2O_3 content (Nagy and Faust, 1956), higher SiO_2, lower MgO and H_2O (Whittaker and Wicks, 1970; Faust and Fahey, 1962). The range of substitution of Fe and Al is nearly the maximum possible (Whittaker and Wicks, 1970). The compositional variations support Green's (1961, p.10) suggestion that Al and Fe in the rock are necessary constituents for the formation of antigorite. Coleman (1966) has suggested that the lower H_2O and MgO content result from shearing stress and that Al replaces Si in tetrahedral co-ordination. As a result of metamorphism, a substitution denied by Whittaker and Wicks (1970).

There is no unanimity on the paragenesis of antigorite and it cannot be unequivocally correlated with any particular type of metamorphism. It is chemically distinct from lizardite and chrysotile; an additional factor, higher temperature, or pressure, or both, is required for its formation. Texturally, it replaces both chrysotile and lizardite. Evidence indicates that regional metamorphism will aid in the formation of antigorite.

The present author is not aware of experimental work indicating differences in the stability fields of chrysotile and lizardite. The conditions of formation of lizardite-chrysotile interlocking textures are not understood. Lizardite-chrysotile interlocking textures may replace lizardite mesh textures, to be in turn replaced by chrysotile. This relation suggests a progressive alteration, but the cause of the alteration is unknown (Wicks, 1969, p.419-423). It is possible that chrysotile and antigorite develop from lizardite as the result of progressive metamorphism, but the paragenetic relation between antigorite and chrysotile is not clear.

b Area III

The mesh-textured serpentine consists of lizardite mesh rims enclosing isotropic, randomly orientated lizardite-clinochrysotile mesh centres. Antigorite partly replaces the mesh-textured serpentine. The presence of clinochrysotile and antigorite in addition to mesh-textured serpentine indicate a complex history of serpentinization. Antigorite shows that the serpentinites have been regionally metamorphosed to at least the epidote-amphibolite facies. The clinochrysotile is

too fine to observe optically, so the textural relations between lizardite and clinochrysotile are not known. It is uncertain therefore whether they are contemporary or sequential.

Wicks (1969) has demonstrated a sequence of increasing complexity of serpentinization in the Manitoba Nickel Belt ultramafics from Manibridge NE towards Thompson (Fig.I.3), in which the serpentine changes from lizardite mesh-texture to lizardite-chrysotile interlocking textures and chrysotile textures. The next stage of complexity in this sequence would be the presence of antigorite, which might be expected from beyond Thompson to the NE. In Area III the serpentine assemblage is lizardite-chrysotile-antigorite; this is only 40 miles SW of Manibridge, where lizardite mesh-textures occur, and is thus at variance with the sequence of serpentine mineralogy in the Manitoba Nickel Belt. It is concluded that, either (1) the Area III ultramafics are part of the Manitoba Nickel Belt but have been involved in regional metamorphism, the effects of which are hidden by the Palaeozoic rocks, or (2) they are not part of the Manitoba Nickel Belt sequence of ultramafics.

D SPINEL MINERALOGY

1 Introduction

The spinels in Area III serpentinites consist of altered zoned chromite and secondary magnetite, which has formed from the iron released from the primary silicates upon serpentinization.

The chrome spinels are concentrically zoned. When the zoning is visible on polished sections due to reflectivity differences it is termed optical zoning; when no such differences exist, or

are difficult to observe, cryptic zoning. Simply zoned spinels consist entirely of spinel phases of varying composition and may be optically or cryptically zoned (Plates 22 and 25 respectively). Multiply zoned spinels include zones of minerals other than spinel within the grain boundary (Plate 24).

Magnetite occurs in two forms: as small, discrete, homogeneous crystals throughout the serpentinite (Plate 2) and occasionally as the extreme outer portion of the zoned spinels.

2 Simply Zoned Spinels

a Morphology

When a complete sequence of zoning is present, a simply and optically zoned spinel consists of a homogeneous grey, chromite core, surrounded by ferritchromit* with low reflectivity which varies continuously and regularly in composition and reflectivity towards magnetite at the margin of the grain of very much higher reflectivity (Plates 22 and 23). The composition of the rim may not always reach magnetite. Simply and cryptically zoned spinels are formed when the original chromite core has been eliminated (Plate 25); other cases of this zoning are apparent only and result from the plane of the section passing through the ferritchromit rim.

The rounded shape of the chromite cores is characteristic; it may vary from nearly spherical (Plate 23) to rectangular, but the corners of the non-spherical cores are always rounded (Plate 22). Sharp angular corners of the type illustrated in Plate 32 are absent.

---

* Defined on p.143

The contact between ferritchromit and chromite or magnetite is not marked either by a physical break or by a zone of silicate or sulphide inclusions.

b Composition

Chromite cores to zoned spinels vary in reflectivity; dark grey (Plate 22) and light grey (Plate 23) cores are recognized. Electron microprobe analyses (Table IV.3) show that light grey chromite cores contain slightly less MgO and more FeO than dark grey cores; both are virtually homogeneous in composition.

The complete compositional variation across a simply and optically zoned spinel is shown in Figure IV.1. There is a sharp compositional change across the contact between core and margin; Cr_2O_3, Al_2O_3 and MgO all decrease; FeO, Fe_2O_3, TiO_2 and Fe_2O_3/FeO increase. The most abrupt decrease is the Al_2O_3 content which drops from 15% to 1% within 15 microns of the contact after which it drops further to almost nil. MgO drops abruptly across the contact but then more slowly towards the margin. Cr_2O_3 is little affected until it reaches the zonal position at which the Al_2O_3 content has dropped to 1% where it too decreases abruptly and then more slowly towards the margin. Fe_2O_3 increases rapidly and FeO less so, both ultimately tending to level out. NiO and TiO_2 both initially increase and subsequently decrease toward the margin.

Compositional changes can also be expressed in terms of four spinel end members, Fe_3O_4, $MgCr_2O_4$, $FeCr_2O_4$ and $MgAl_2O_4$ calculated by the method of Stevens (1944). The compositional change from core to rim is represented by a complete and abrupt

Table IV.3 Electron microprobe analyses of grey chromite cores to zoned spinels in Area III.

	1	2	3	4	5	6	7	8	9	10	11	12
	269 #4	269	264	264	264 #3	269 #1	269 #3	89	91	89	89	84
	Core	Av. 6/80μ	Core	Core	Av. 3/30μ	Core	Core	Core	Av. 7/60μ	Av. 4/10μ	Core	Av. 4/20μ
Al_2O_3	14.88	15.27	16.11	14.99	15.56	15.46	15.47	17.32	16.02	15.43	15.50	13.53
Cr_2O_3	48.78	48.32	47.68	47.55	47.47	46.44	45.91	47.96	46.41	45.61	45.21	44.90
TiO_2	0.00	.29	.20	.29	.23	.20	.12	.19	.69	.22	.28	.82
Fe_2O_3	7.76	7.47	7.68	8.86	8.33	9.56	10.29	3.08	6.09	7.86	8.19	9.82
FeO	17.50	17.57	16.38	16.68	16.62	16.69	16.32	24.86	23.41	23.95	23.69	24.67
MgO	11.08	11.07	11.95	11.60	11.62	11.65	11.89	6.59	7.36	6.91	7.06	6.19
NiO	0.00	.01	0.00	.03	.16	0.00	0.00	0.00	.02	.02	.07	.07
Spinel	21.60	22.23	20.90	23.08	22.49	22.28	22.10	26.88	25.02	23.97	24.06	21.18
Magnesio-Chromite	28.74	28.08	27.61	33.25	30.19	30.33	31.62	0.00	5.48	4.25	4.87	4.53
Ferro-Chromite	38.22	38.66	31.31	29.85	35.06	33.35	31.27	68.22	59.81	59.33	58.16	58.60
Magnetite	11.46	11.09	10.09	13.82	12.27	14.04	15.02	4.90	9.69	12.44	12.91	15.68
$Fe^3/Fe^3\text{-}Cr\text{-}Al$	.10	.09	.10	.12	.11	.13	.13	.04	.08	.11	.11	.14
$Cr/Cr\text{-}Al$	.73	.73	.71	.73	.72	.72	.71	.70	.71	.71	.72	.74
$Mg/Mg\text{-}Fe^2$	.46	.46	.50	.49	.49	.49	.50	.27	.30	.28	.29	.26
$\frac{\text{mol.\% } Al_2O_3}{Al_2O_3+Fe_2O_3+Cr_2O_3}$	.29	.30	.31	.29	.30	.30	.30	.34	.32	.31	.30	.27
total iron as Fe	19.02	18.88	18.10	19.16	18.74	19.65	19.87	21.47	22.45	24.10	24.13	26.03

Columns 1 to 7 are analyses of dark grey cores and 8 to 12 of light grey cores. The analyses have been recalculated into an ideal spinel formula $R^{2+}R_2^{3+}O_4$ assuming no cation deficiencies so that all the Fe can be divided between the $R^{2+}$and R^{3+}groups. Core:- single analysis at centre of core. Av/30μ:- 3 analyses across a width of 30μ.

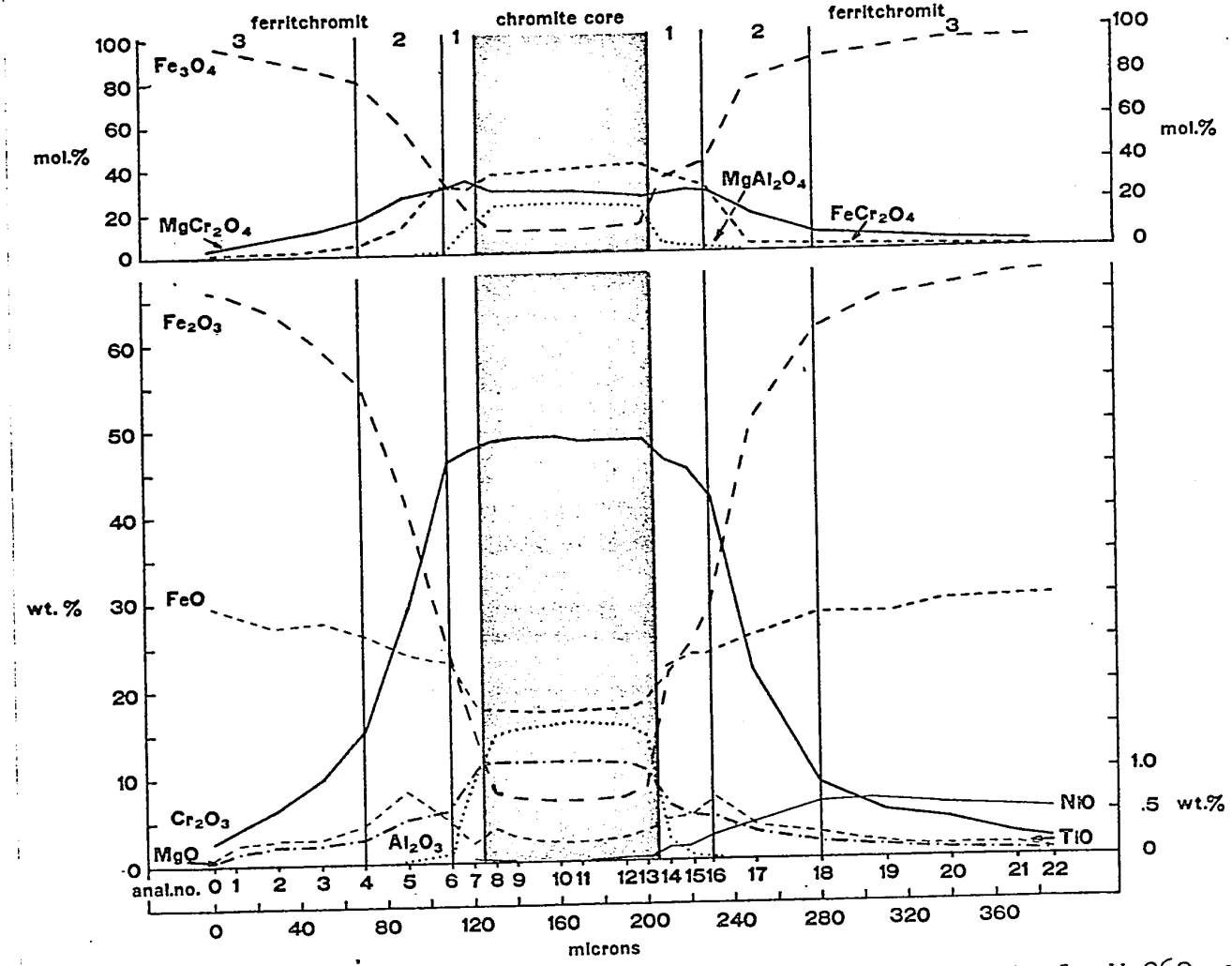

Fig.IV.1. Compositional variation across a simply zoned spinel, W 269, with a dark grey chromite core. The upper portion of the diagram shows the analyses recalculated into four spinel end members. The numbers refer to analyses listed in Appendix V, Table I. The microprobe traverse is across the spinel from rim to rim.

loss of $MgAl_2O_4$, followed by $MgCr_2O_4$ and $FeCr_2O_4$, which are compensated by an increase in Fe_3O_4 (Fig.IV.1).

The compositional changes induce varying reflectivities in the spinel. The inner portion of the altered rim (zone 1 of Figure IV.1), is distinctly grey, but lighter than the core. The outer portion of the rim has a much higher reflectivity, appearing whitish in reflected light. There is a continuous increase in reflectivity across zones 2 and 3, but it is slight and may be difficult to observe. Cryptic zoning is thus characteristic of zones 2 and 3.

The compositional variation in a cryptically zoned spinel (Fig.IV.2) is very similar to the outer portions of optically zoned spinels. When the variation curves are compared the fit is found to be close (Fig.IV.3); the important point is not an exact fit, which is determined by the weight percentage of any oxide relative to its distance from the centre, but by the similarity in the sequence of inflexions for both sets of curves. This means that, at least within the scale of a hand specimen, a uniform process operated to give rise to the ferritchromit rims.

Zoned spinels with light grey chromite cores, which are not clearly distinguishable from the rims of ferritchromit (Plate 23) have a similar compositional zoning to spinels with dark cores (Figs.IV.4, IV.5 and IV.6). There is a sharp compositional change across the boundary between core and ferritchromit margins in which the sequence of changes is similar to that already described.

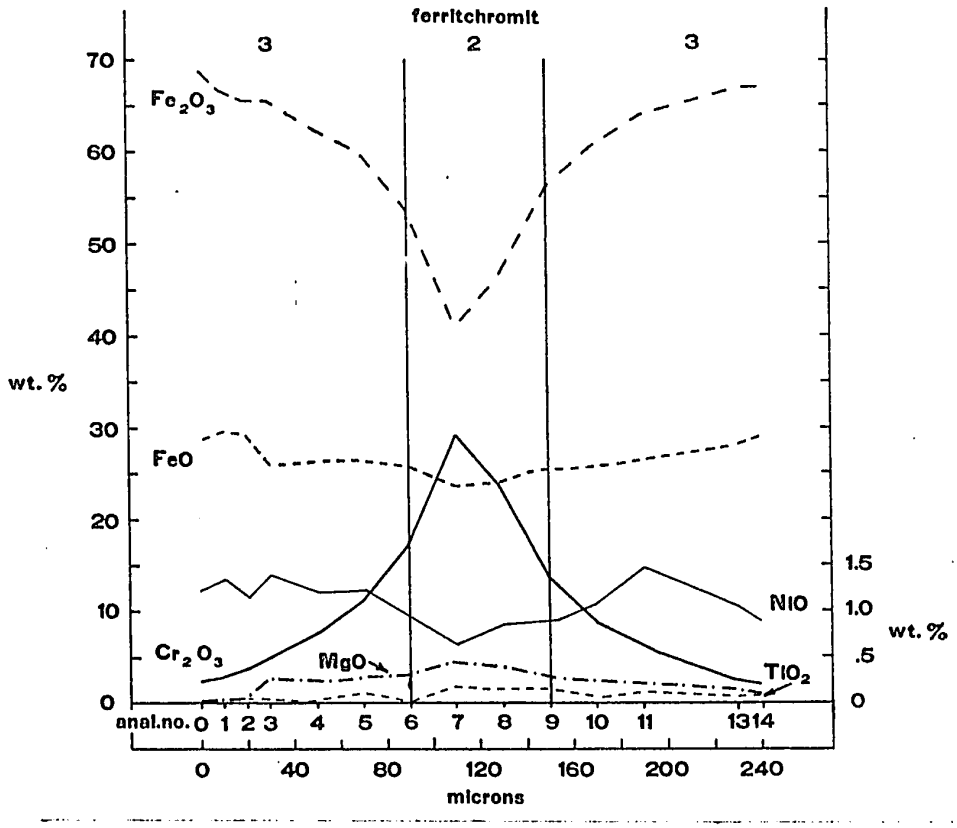

Fig.IV.2. Compositional variation across a cryptically zoned spinel with no chromite core. The analyses numbers refer to analyses listed in Appendix V, Table II. The microprobe traverse is across the spinel from rim to rim.

The alteration in any specimen may not be symmetrical; the extreme right margin of W 91 (Fig.IV.4) is much nearer magnetite in composition than is the left hand margin which has the composition of an Fe-rich ferritchromit.

The main difference between these spinels and those with dark grey cores is that the inner zone (zone 1) is of a similar reflectivity to zones 2 and 3, resulting in negligible reflectivity differences in the ferritchromit rim.

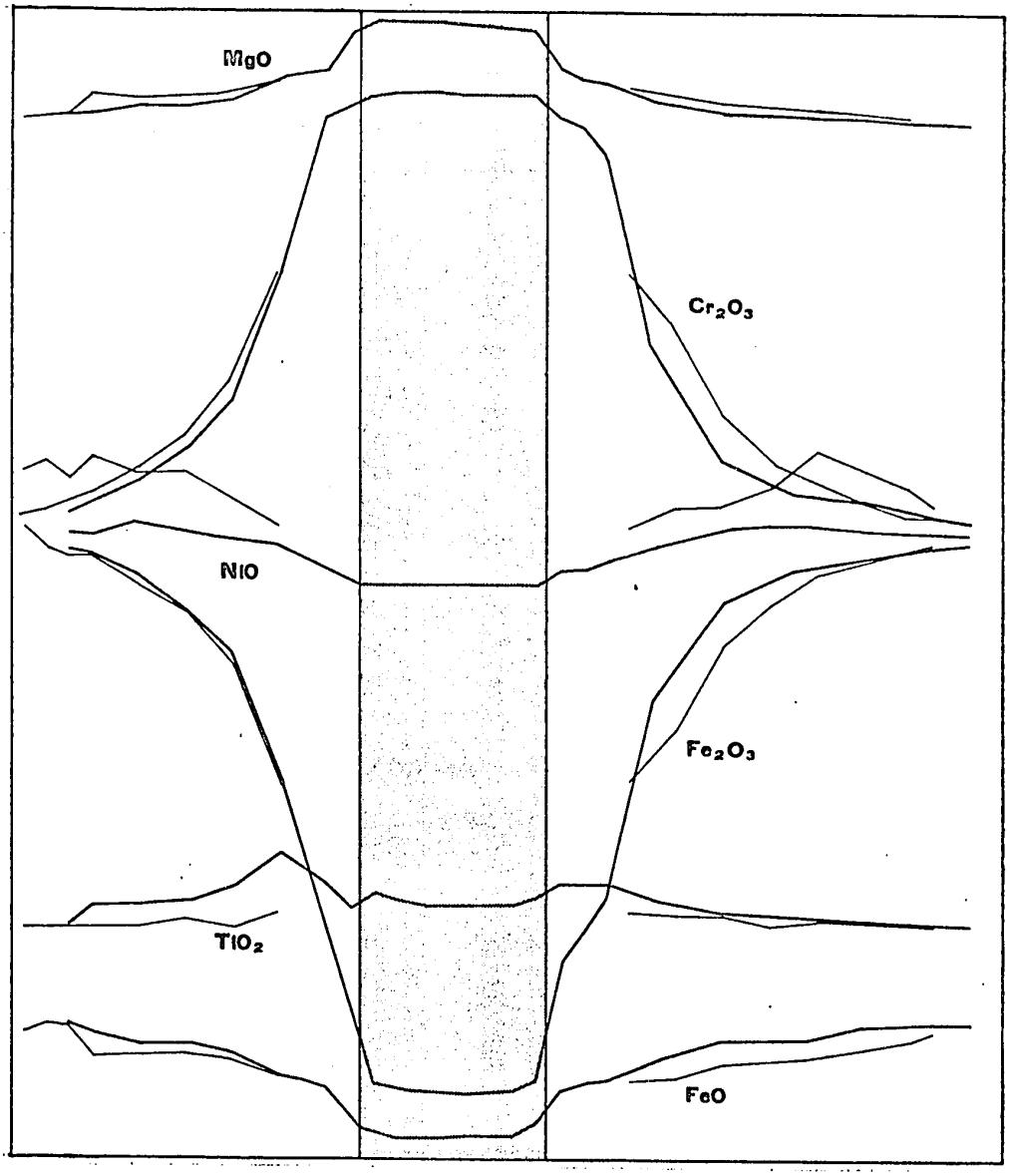

Fig.IV.3. Comparison of the variation in composition between a cryptically and optically zoned spinel. The compositional curves for the optically zoned spinel W269 are plotted as they appear in Fig.IV.1 (heavy lines). Each curve has been moved relative to each other for clarity. The curves for the cryptically zoned spinel illustrated in Fig.IV.2 (light lines) have been split at the point of inflection at 110 microns. The split Fe_2O_3 curves are then moved laterally outwards so that the end of each at the 42.5% lies on the optically zoned spinel at the 42.5% level. The remaining split curves are then plotted in the same relative position. For further description see text p.65.

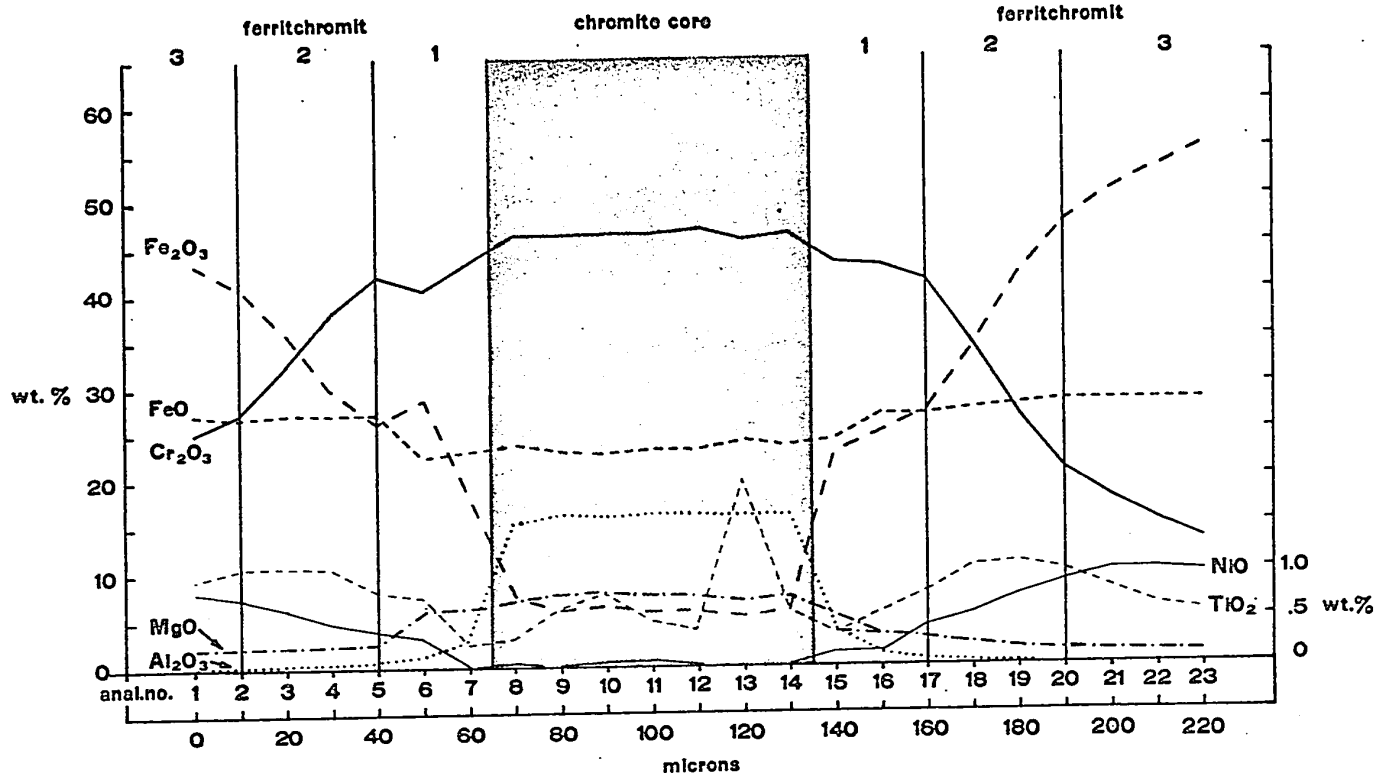

Fig.IV.4. Compositional variation across a zoned spinel with a light grey chromite core, W 91. The numbers refer to analyses listed in Appendix V, Table III. The microprobe traverse is across the spinel from rim to rim.

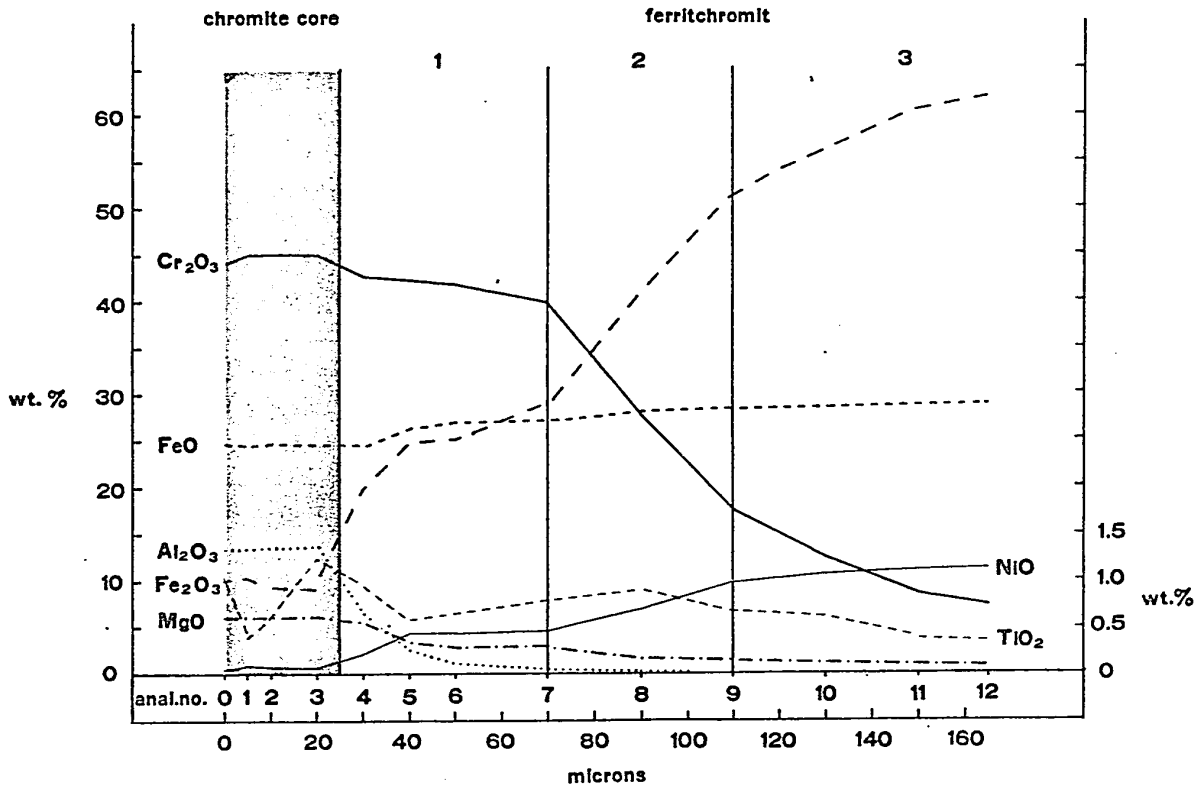

Fig.IV.5. Compositional variation across a zoned spinel with a light grey chromite core, W 84. The numbers refer to analyses listed in Appendix V, Table IV. The microprobe traverse is from the centre of the chromite core outwards to one margin.

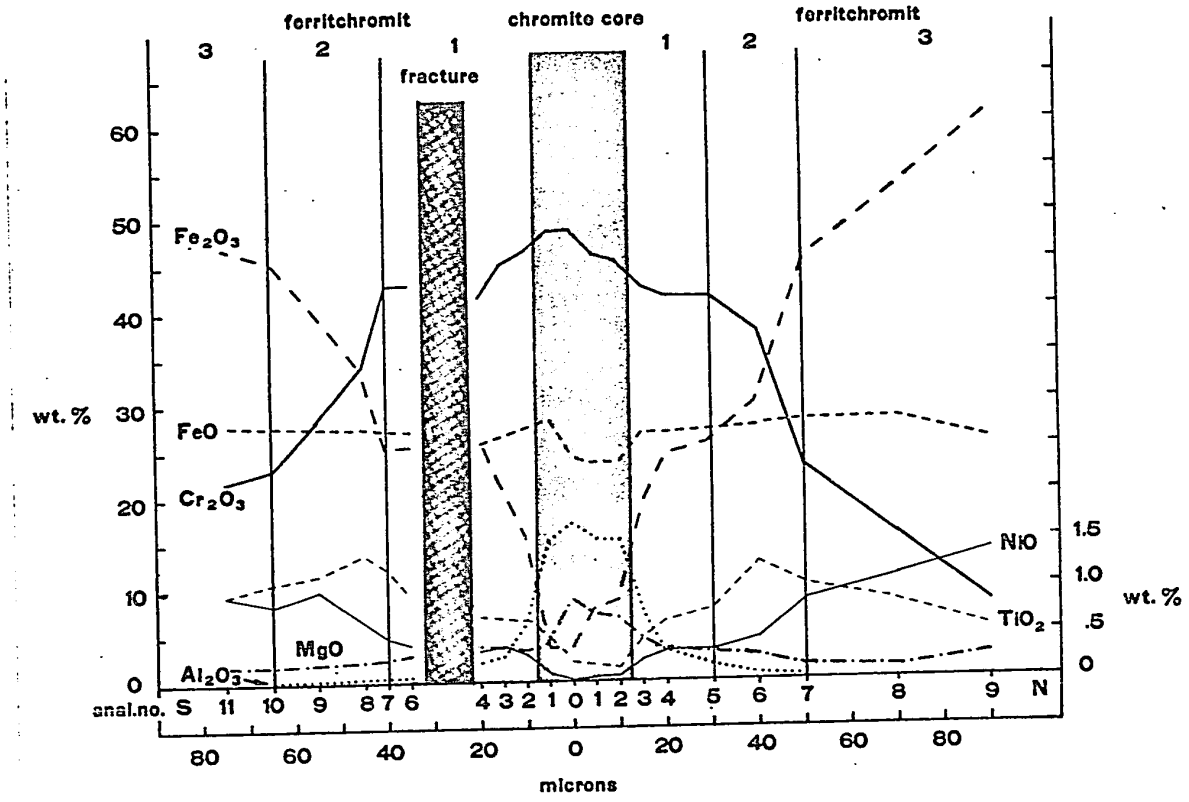

Fig.IV.6 Compositional variation across a zoned spinel with a light grey chromite core W 89, which is cut by a serpentine filled fracture. The numbers refer to analyses listed in Appendix V, Table V. The microprobe traverse is across the spinel from rim to rim, but the analyses are numbered outward from the centre in each direction.

When the data for the compositional variation across these zoned spinels are plotted on a variation diagram (Fig.IV.7) as described for Figure IV.3, a similar sequence of alteration is apparent between the four examples. Moreover, this sequence is similar to that for the zoned spinels with dark grey cores. This similarity suggests that the process responsible for the compositional zoning was pervasive and able to effect similar changes over wide areas.

The sequence of alterations in the ferritchromit rim is summarized as follows (Fig.IV.8):-

Zone 1 (inner zone). The inner portion of this zone represents the large compositional gap between the chromite core and the ferritchromit rim. The initial sharp loss of Al_2O_3 and minor loss of Cr_2O_3 is compensated by a sharp increase in Fe_2O_3; the initial loss of MgO is compensated by an increase in FeO. The outer portion of the zone shows less change in composition, with gradually increasing Fe_2O_3 replacing Cr_2O_3 and FeO replacing MgO.

Zone 2 (intermediate zone). This is a zone of abrupt compositional change in the trivalent oxides with Fe_2O_3 replacing Cr_2O_3; MgO diminishes gradually and FeO increases gradually although both tend to level out. Al_2O_3 has fallen to zero.

Zone 3 (outer zone). Fe_2O_3 continues to increase and Cr_2O_3 to decrease although less abruptly than in zone 2; the remaining oxide contents have stabilized. This zone may be either magnetite or ferritchromit.

Chromium is the only element not immediately affected by the change from chromite to ferritchromit and it does not start

Fig.IV.7. Comparison of compositional variation between three optically zoned spinels with light grey chromite cores and one cryptically zoned spinel. The method of constructing the diagram is the same as for Fig.IV.3.

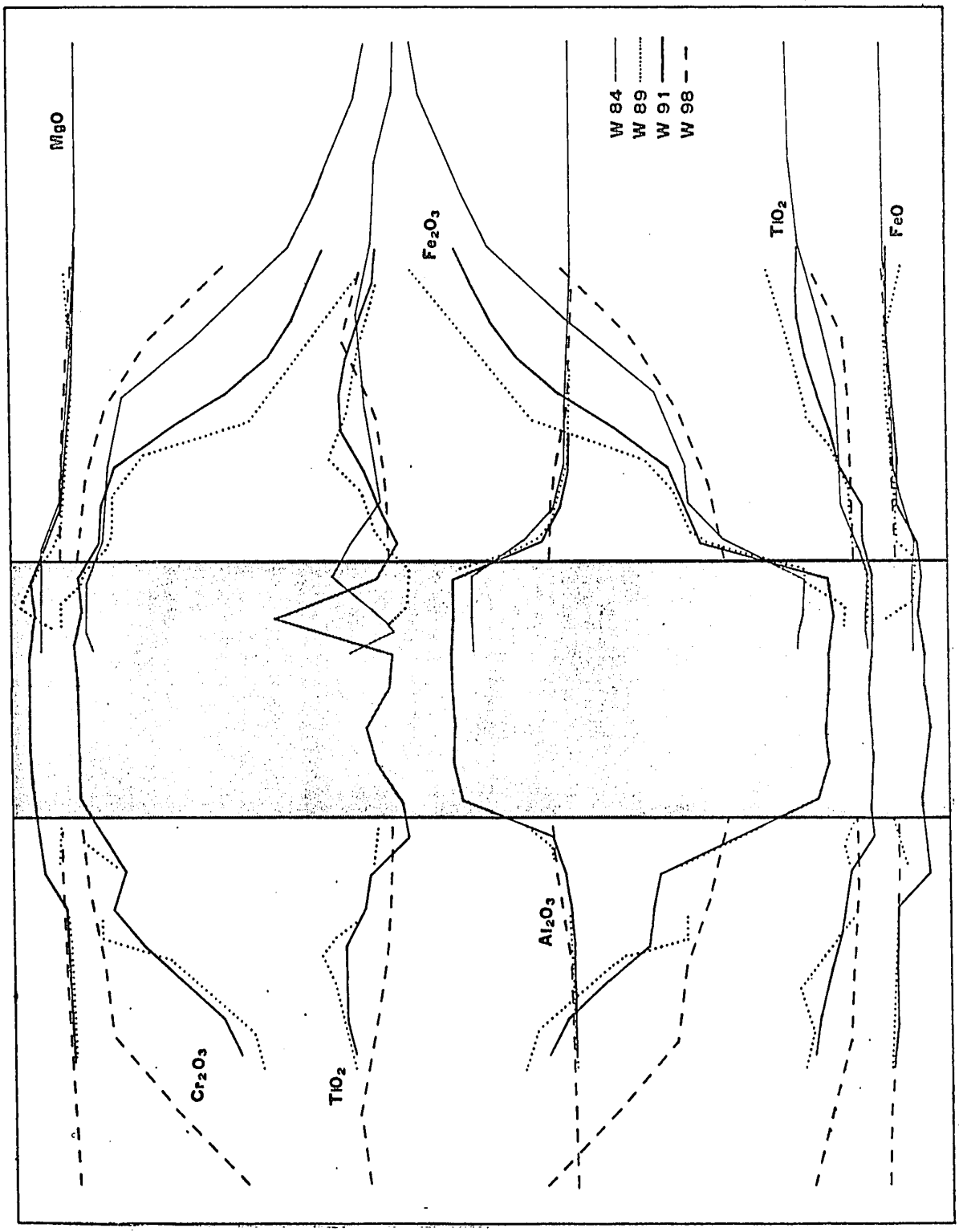
MgO
Cr2O3
TiO2
Fe2O3
Al2O3
TiO2
FeO
W 84
W 89
W 91
W 98

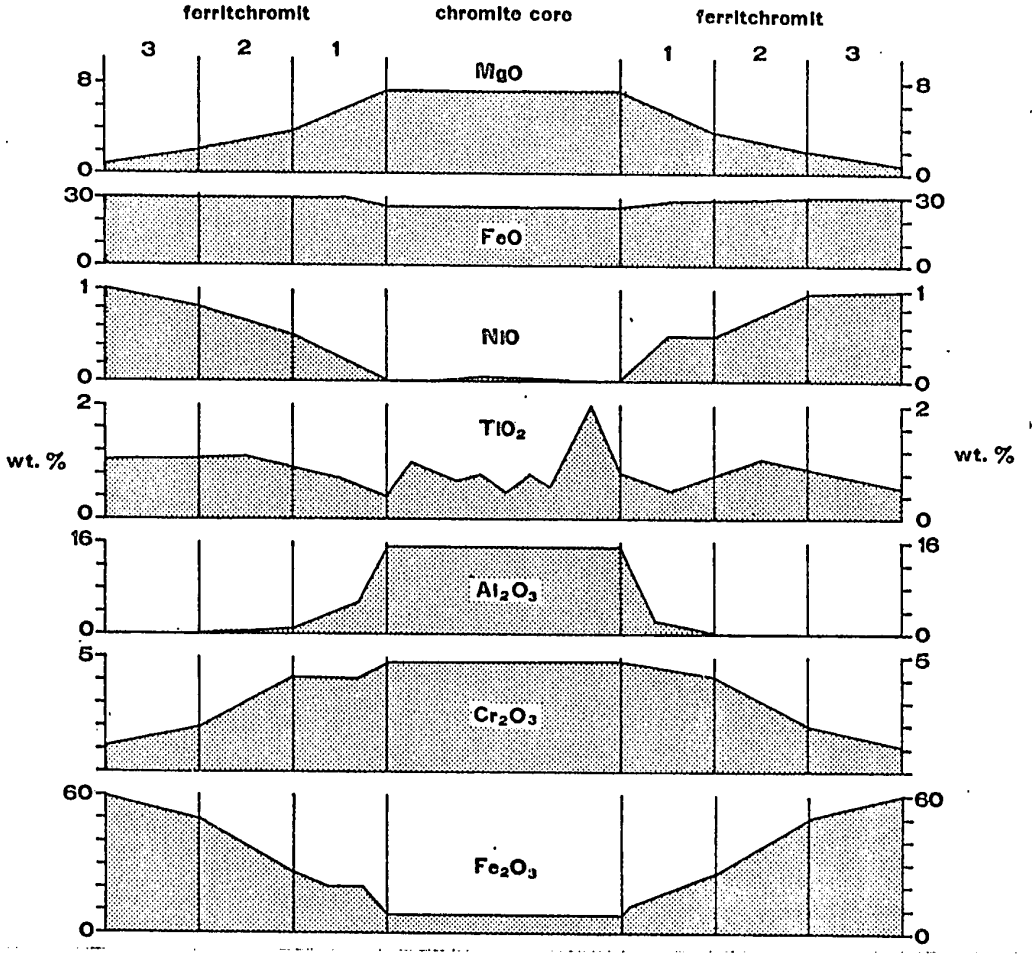

Fig.IV.8 Summary of compositional variation between core and rim in zoned spinels from Area III. The changes in either margin may not be symmetrical. The ordinate scale varies, and the abcissa scale is arbitrary, but represents the width of a spinel grain.

to diminish abruptly until the Fe_2O_3/FeO ratio reaches 1. NiO is very low in the core, and increases steadily across the rim of ferritchromit. TiO_2 is erratic in the core and continues to behave erratically in the ferritchromit; it may decrease sharply before rising to a maximum in zone 2 then to level out or decrease.

Typical analyses of ferritchromit and magnetite from Area III are given in Table IV.4, and may be compared to some previously published analyses of ferritchromit in Table VII.2.

It has been suggested that the compositional changes between core and rim as measured with the electron microprobe are more apparent than real, and result from secondary X-ray fluorescence of elements in the core. This is refuted on two grounds; firstly, the cryptically zoned spinels lacking a chromite core also show compositional variations (Fig.IV.2); secondly, in Area I chromite is surrounded by magnetite without spinel of intermediate composition between the two (Fig.V.1). This indicates that within a scale of 10-15 microns, a spot electron probe analysis is not distorted by excitation of elements in adjacent phases.

3 Multiply Zoned Spinels

a Morphology

In multiply zoned spinels parts of the ferritchromit may be replaced by a member of the pyroaurite-group of minerals, which is in turn mantled by a thin, discontinuous, rim of magnetite. There is normally one, or less frequently two or three 'necks' of ferritchromit linking the magnetite rim to

Table IV.4 Electron microprobe analyses of typical aluminous-ferritchromit, ferritchromit and magnetite from zoned spinels in Area III.

	1.	2.	3.	4.	5.	6.	7.	8.
Al_2O_3	9.24	2.96	.46	.63	.17	.00	.11	.00
Cr_2O_3	47.24	45.07	34.37	41.34	8.90	7.23	2.07	1.99
TiO_2	.21	.70	1.40	.79	.55	.33	.00	.10
MgO	9.89	3.51	2.44	2.98	2.57	.70	.80	.53
NiO	.06	.37	.65	.42	1.38	1.12	1.20	.56
FeO	18.21	26.55	27.32	26.83	25.91	28.89	28.69	29.70
Fe_2O_3	15.14	20.85	33.36	27.01	60.51	61.63	67.13	67.11

1. Aluminous ferritchromit W 269 Anal.7, Fig.IV.1, Table I, Appendix V.
2. Aluminous ferritchromit W 89 Anal.3S, Fig.IV.6, Table V, Appendix V.
3. Non-aluminous ferritchromit W 89 Anal.8S, Fig.IV.6, Table V, Appendix V.
4. Non-aluminous ferritchromit W 91 Anal.17, Fig.IV.4, Table III, Appendix V.
5. Ferritchromit near magnetite W 89 Anal.9, Fig.IV.6, Table V, Appendix V.
6. Ferritchromit near magnetite W 84 Anal.12, Fig.IV.5, Table IV, Appendix V.
7. Magnetite W 269(2) Anal.0, Fig.IV.2, Table II, Appendix V.
8. Magnetite W 269(1) Anal.22, Fig.IV.1, Table I, Appendix V.

the main body of the spinel which results in an "atoll-type" structure (Plates 20 and 21). Multiply zoned spinels are always optically zoned and the ferritchromit is cryptically zoned. The chromite core is always rounded and frequently spherical.

A typical multiply zoned spinel is illustrated in Plate 24. A rounded, dark grey chromite core is surrounded by an inner zone of ferritchromit which grades continuously to magnetite at the rim. The spinel phases are similar to those in simply zoned spinels. The pyroaurite-group mineral forms a zone towards the outer portion of the ferritchromit and separates it from the discontinuous magnetite rim; there is no evidence of alteration at the interface. The spinel boundaries on either side of the pyroaurite-group mineral do not 'fit', which suggests either that it has replaced the ferritchromit on a volume for volume basis or that both crystallized simultaneously. Radial dilation cracks cutting both the spinel and the pyroaurite-group mineral are filled by serpentine. These veins, with associated spongey magnetite (Plate 21) are late-stage features and post-date the serpentinization in the main body of the rock.

b Composition

The compositional variation in the spinel phases of the multiply zoned spinels is similar to that in the simply zoned spinels. The homogeneous chromite core is separated from the surrounding ferritchromit by a sharp boundary. The ferritchromit varies continuously in composition towards magnetite; MgO, Cr_2O_3, Al_2O_3 and TiO_2 decrease towards the outer margin, while NiO, FeO and Fe_2O_3 increase (Fig.IV.9). Scanning electron-beam

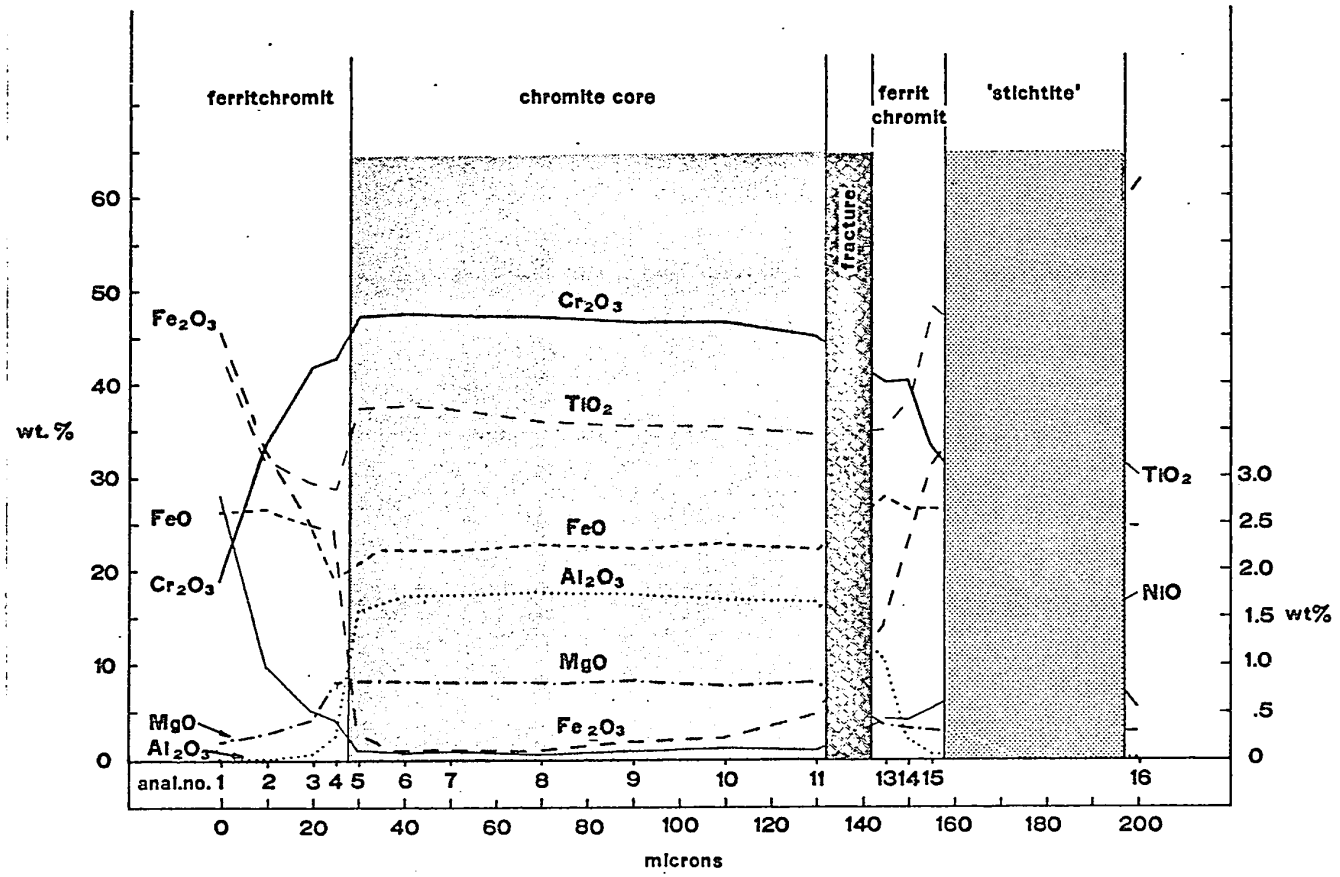

Fig.IV.9. Compositional variation across a multiply zoned spinel, W 264. The numbers refer to analyses listed in Appendix V, Table VIII. The microprobe traverse is from rim to rim across the spinel (see Plate 24).

photographs (Plate 43) illustrate these changes.

The non-spinel phase was identified by X-ray microbeam diffraction patterns as a member of the pyroaurite-group of minerals (Appendix II). The pyroaurite-group has the general formula $Mg_6R_2(OH)_{16}CO_3.4H_2O$. The individual mineral is pyroaurite, stichtite or hydrotalcite, when R = Fe, Cr or Al respectively (Frondel, 1941). They are variously regarded as alteration products of serpentine and spinel (E.g. Winchell, 1951; Dana, 1932). Electron microprobe analyses gave inconsistent results, but showed it to consist of Mg, Fe and Cr but no Al, suggesting that it is a mixture of pyroaurite and stichtite (Frondel, 1941).

4 Magnetite

Magnetite occurs in three forms throughout the serpentinites: (1) as rims to multiply zoned spinels; (2) as grains, discrete or aggregated, scattered throughout the serpentinite, and (3) as linings to small, serpentine-filled fractures in spinel.

Magnetite occurs as an outer rim to zoned spinels although in many examples the outer rim is an Fe-rich ferritchromit (Fig.IV.1 and IV.9). There is an optical distinction between the ferritchromit and magnetite but no physical break. The magnetite contains small amounts of Cr_2O_3, MgO and TiO_2; Al_2O_3 is absent but NiO content is high (Table IV.5).

Magnetite occurs as small discrete grains throughout the serpentinized ultramafic body (Plates 1 and 2), as stringers or trains of crystals outlining olivine pseudomorphs, or as dense aggregates within mesh centres. These grains contain fewer

impurities than magnetite rimming the zoned chromite, although the MgO content is of the same magnitude.

Magnetite occurs rarely with serpentine in late fractures in zoned spinels (Plates 21 and 24). Microprobe analyses of this magnetite show that it is very variable in composition (Table IV.5) but with no obvious characteristics by which to distinguish it from the magnetite around the rim of the zoned spinels except the unusually high Ni content.

5 Hematite*

Hematite is rare and known from only one thin section. Here it occurs either as rims to angular grains of ferritchromit (Plate 22), or as somewhat rounded and sieve-textured crystals. It is markedly anisotropic on polished sections and electron microprobe analyses show it to be comparatively pure.

6 Summary

Compositionally zoned chrome spinels occur in the ultramafic rocks of Area III. Simply zoned spinels range from chromite at the core through ferritchromit to magnetite at the rim. The zones are optically visible due to reflectivity differences. These differences may be very slight so that spinels in which there is no chromite core are cryptically zoned. The rim of the spinel is frequently an Fe-rich ferritchromit.Multiply zoned spinels contain a concentric zone of a pyroaurite-group mineral

---

*Hematite is not a spinel but it is convenient to describe it in this section.

Table IV.5 Electron microprobe analyses of magnetite from Area III.

	(1) Magnetite associated with ferritchromit							
	1	2	3	4	5	6	7	8
Al_2O_3	.15	.00	.11	.06	.07	.03	.00	.00
Cr_2O_3	2.93	1.99	2.07	2.36	2.95	.18	7.23	5.61
TiO_2	.14	.10	.00	.07	.56	.00	.33	3.00
MgO	.69	.53	.80	.93	1.12	.67	.70	2.95
NiO	.61	.56	1.20	.94	1.05	.15	1.12	1.76
FeO	29.46	29.70	28.69	28.73	28.36	29.85	28.99	24.97
Fe_2O_3	66.02	67.11	67.13	66.90	65.89	69.11	61.63	61.71

	(11) Magnetite as veins or in discrete grains			(111) Magnetite associated with late fracturing of spinel					
	9	10	11	12	13	14	15	16	17
Al_2O_3	.02	.00	.00	.03	.00	.04	.88	-	.67- 1.30
Cr_2O_3	.04	.03	.01	7.79	2.04	.06	9.00	-	.50- 5.00
TiO_2	.14	.02	.01	.17	.23	.26	.12	-	.20- 4.20
MgO	.90	.74	.93	2.34	2.57	1.52	2.42	-	2.85-15.10
NiO	.00	.00	.00	1.64	1.99	4.69	4.95	-	.09- 8.14
FeO	29.66	29.89	29.59	25.96	25.19	24.15	22.80	31.03	-
Fe_2O_3	69.24	69.32	69.45	62.07	68.00	69.29	59.83	68.97	-

1. W269(1) Anal.0, Fig.IV.1, Table I, Appendix V.
2. W269(1) Anal.22, Fig.IV.1, Table I, Appendix V.
3. W269(2) Anal.0, Fig.IV.2, Table II, Appendix V.
4. W269(2) Anal.14, Fig.Iv.2, Table II, Appendix V.
5. W162, Table VII, Anal.0, Appendix V.
6. W141, Table VI, Anal.7, Appendix V.
7. W84, Table IV, Anal.12, Appendix V.
8. W264, Table VIII, Fig.IV.9, Anal.16, Appendix V.
9. W162 discrete magnetite grain.
10. W141 discrete magnetite grain.
11. W141 discrete magnetite grain.
12. W264, discrete grain, Plate 21.
13. W264, magnetite in vein, Anal.7, Plate 21, Table IX.
14. W264, magnetite outside spinel, Anal.9, Plate 21, Table IX.
15. W264, magnetite in vein, Anal.10, Plate 21, Table IX.
16. Theoretical composition of magnetite.
17. Range of trace element content of magnetite from ultramafic rocks (Frietsch, 1970, Table 17).

in addition to the normal sequence of spinel zones.

The compositional changes between the core and rim involve a loss of MgO, Al_2O_3 and Cr_2O_3 and a gain of FeO, NiO, TiO_2 and Fe_2O_3. The loss of Al_2O_3, and to a lesser extent, of MgO, is abrupt so that the composition changes abruptly to ferritchromit and then more gradually towards magnetite. These changes follow a similar pattern in different grains of both the simply and multiply zoned spinels and are divided into three zones in which the sequence of changes is similar.

Both the simply and multiply zoned spinels may contain fractures filled by late serpentine and, less frequently, sulphide.

Magnetite occurs as discrete grains and irregular patches in the serpentinites as well as rims on some of the zoned spinels.

E DISTRIBUTION OF NICKEL AND SULPHUR

1 Country Rocks

The tremolite-chlorite schists, interpreted as metamorphosed olivine basalt (Chapter II), contain 0.16% to 0.19% Ni and 0.02% to .10% S, with an average of 0.07% S*. The Ni content is slightly higher than that of other olivine or picritic basalts for which analyses are available (Table IV.6).

An arithmetic mean of .13% is obtained from 13 analyses of plagioclase amphibolite adjacent to serpentinites in Area III. The Ni values to the north of Area III vary between .12 and .15%

---

*Methods of analysis are outlined in Appendix VI.

Table IV.6 Ni and S content of some mafic extrusive rocks (in wt.%).

Archaean meta-basalt		Basalt		Olivine basalt		Remarks	Reference
Ni	S	Ni	S	Ni	S		
		.15	.025				Krauskopf, 1967
		.16	.200			mafic rocks	Hawks & Webb, 1962
		.16	.03				Vinogradov, 1962
		.13	.03				Turekian & Wederpohl, 1961
		.09	-				Prinz, 1967
				.05-.15	-	picritic	Wager & Mitchell, 1953
				.008	-	olivine bas.	Wager & Mitchell, 1953
				.074	.16		Wilson et al., 1969
.13-.15	-						Viljoen et al., 1969
		.13	-	.16-.19	.02-.10	metamorphosed	This study

Table IV.7 Nickel content of ultramafic rocks (in wt.%).

Rock type	1	2	3	4	5	6	7	8	9
Ultramafic (general)		.10-.40	.12	.20	.20	.14			
Dunite							.18-.30		
Harzburgite/peridotite	.21						.10-.42	.30	
Pyroxenite	.07					.08	.11		
Serpentinite	.24						.16		
Serpentinized dunite	.29								.15-.30

References:- 1. Abdullaev et al., 1967; 2. Goles, 1967; 3. Hawkes and Webb, 1962; 4. Turekian and Wedepohl, 1961; 5. Vinogradov, 1962; 6. Vogt, 1923, 7. Williams, 1965; 8. Wilson, 1953; 9. This study.

although in the extreme north of the Reservation (Fig.II.1) they drop to .09%. These figures are of the same order of magnitude as those quoted for the Ni content of fresh basalts (Table IV.6).

Assays of 13 diamond drill hole intersections from the pelitic garnetiferous biotite schist gave an average Ni content of .006%. Shaw (1954) gives an average value of .006% Ni for schists of medium metamorphic grade containing two micas, quartz and feldspar, with or without garnet.

2 Serpentinites

a Whole Rock Data

The total Ni content of 95% of the serpentinites analysed lies between .15% and .30% (Fig.IV.10), corresponding to normal Ni values for ultramafic rocks and in particular for dunites and peridotites (Table IV.7). It is generally accepted that serpentinization of an ultramafic rock does not affect the

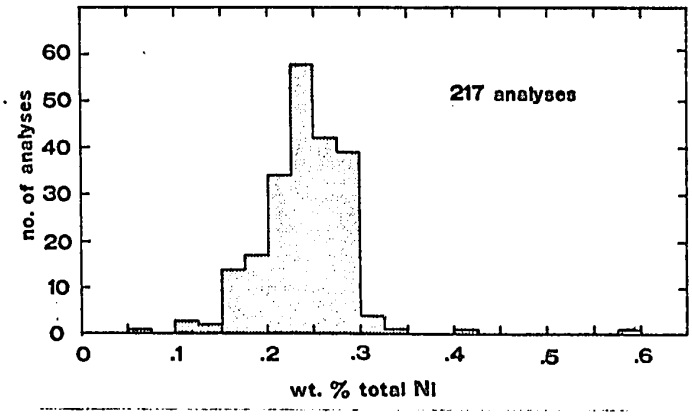

Fig.IV.10. Distribution of total Ni in Area III serpentinites.The values are taken from routine analyses,the procedure for which is described in Appendix VI.

total Ni content (Goles, 1967, p.358), although it may alter the proportion of sulphide and silicate Ni (Grudnin and Letnikov, 1969).

Sulphide and silicate Ni values are available for some samples from Area III in addition to the total Ni values. Sulphide and silicate Ni have an inverse relation (Fig.IV.12) with the analyses distributed along a linear zone corresponding to a total Ni value between .225% and .250%. This interval corresponds to the modal interval of the total Ni values (Fig.IV. 10). The inverse relation between sulphide and silicate Ni is clearly shown in diamond drill hole assays (Fig.IV.14).

Numerous intersections of talc-tremolite schist have been assayed giving an average Ni value of .17%.

The S content of the serpentinized ultramafic rocks lies predominantly in the range 0.00-0.10% with an unweighted average of 0.06% (Fig.IV.11).

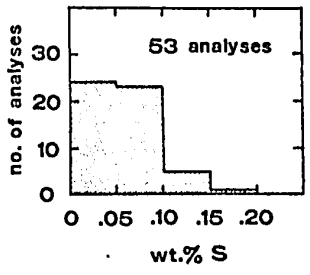

Fig.IV.11. Distribution of S in Area III serpentinites.

These analyses compare well with average S content of other ultramafic rocks: Turekian and Wedepohl (1961), 0.03%; Vinogradov, (1962), 0.01%, and Hawkes and Webb, (1962), 0.03%.

Sulphide-bearing peridotite from New Caledonia contains between .008% and .025% S (Guillon and Lawrence, 1971, p.425).

The values for S and total Ni plotted in Figure IV.13 give an intercept on the Y axis of .205% for S = 0 wt. %, a low figure as some S occurs in Ni-free sulphides. The value for total Ni should correspond to that obtained from Figure IV.12, between .225% and .250%.

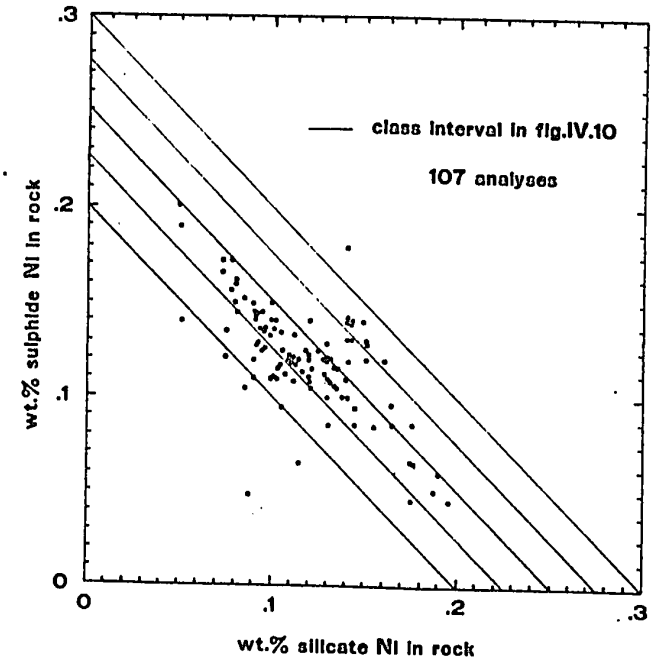

Fig.IV.12. Relation between silicate and sulphide nickel in Area III serpentinites.

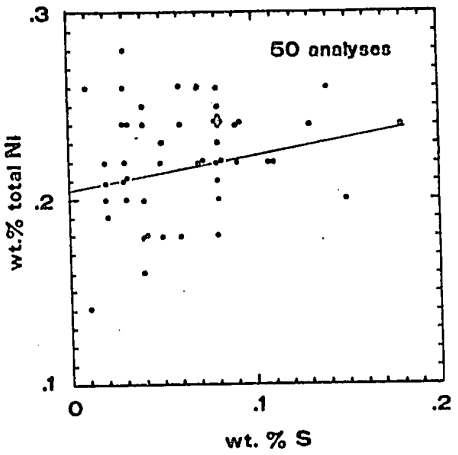

Fig.IV.13. Relation between total Ni and S content in Area III serpentinites.

The tendency for the total Ni value in the ultramafic rocks to be constant (Figs.IV.12 and IV.13) is illustrated when total Ni is plotted against depth in diamond drill hole intersections (Fig.IV.14). Furthermore, the sulphide and silicate Ni values

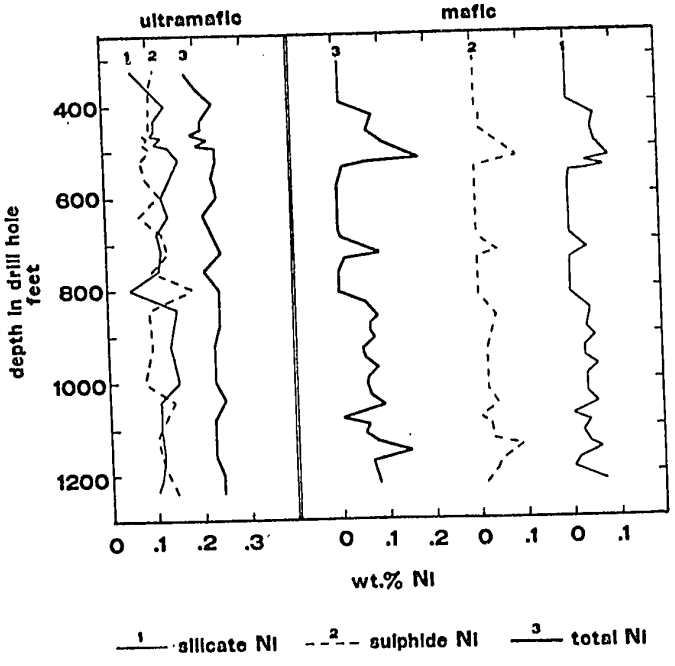

Fig.IV.14. Variation of silicate, sulphide and total Ni contentin Area III serpentinites. The data for the ultramafic is taken from a single drill hole and for the mafic rock from a single hole intersecting plagioclase amphibolite and tremolite-chlorite schist.

tend to vary inversely, in contrast to the direct variation in the mafic wall-rocks. This means that the Ni in the ultramafic rock was originally in the silicates and at some stage S was either introduced from outside or redistributed within the ultramafic body to combine with some of the Ni.

b Serpentine

Electron microprobe analyses of serpentine in Area III show small NiO contents (Table IV.2). Further partial analyses have been made and all the available values for NiO in serpentine have been tabulated in Table IV.8.

The mesh centres have the greatest range in NiO; this may reflect varying Ni content of the original olivine or an erratic behaviour of Ni upon serpentinization. The mesh rims have a more restricted range of NiO content, although the median value is similar to that of the mesh centres. There are far too few antigorite analyses for any interpretation.

There are few comparative values of NiO for serpentine minerals in the literature. Deer, Howie and Zusmann, (1962, v.3, p.177) quote .16% NiO in an antigorite. The NiO content of serpentine minerals from sulphide-poor serpentinites at Barberton, Transvaal, are summarized in Table IV.9. The limited petrographic description of these serpentinites suggest that they are similar to those in Area III. It is tentatively concluded that the NiO content of the serpentine minerals in Area III is somewhat higher than normal.

Table IV.8 NiO content in wt.% of serpentine from Area III.

	Mesh centres Lizardite & clinochrysotile	Mesh rims Lizardite	Antigorite
Wt.% NiO	.79, .76 .60 .41, .40 .34, .31 .28, .27, .23 .19, .16, .16, .15	.37, .36, .36, .32, .31 .20 .19, .18, .18	.31 .28, .26, .25
Median	.30	.31	.27
Arithmetic average	.36	.27	.28

Table IV.9 NiO content in wt.% of serpentine minerals from Barberton, Transvaal. Data from Mihalik and Hiemstra, 1966 and de Waal and Hiemstra, 1966.

	"serpentine"	clinochrysotile	antigorite
Wt.% NiO	.76 .39 .29, .28, .25, .27, .23 .19, .19, .19, .15, .14, .14, .14	.29 .20, .19	.15
Median	.21	.20	
Arithmetic average	.26	.23	

c Spinel

Electron microprobe analyses across zoned spinels from Area III are summarized in Figure IV.8 and clearly show that the Ni content of the chromite cores is negligible and that it increases through the ferritchromit towards magnetite at the rim. NiO values of the chromite cores are all below 0.03%, except for that in Table IV.3, column 5, which is from a spinel whose core is fractured and filled by a Ni-rich late magnetite (Plate 21). The NiO content of magnetite and ferritchromit vary considerably and reach about 2.0% by weight. Nickel was not detected in some discrete magnetite grains (Table IV.5), although NiO content of magnetite in vein-like segregations may reach over 2.0%. Late magnetite associated with fractured spinel contains up to 7.5% NiO.

Electron microprobe traverses for Ni on ferritchromit and adjacent serpentine grains indicate a slight impoverishment of NiO in serpentine adjacent to spinel; the depletion is inconsistent and may result from X-ray fluorescence.

d Discussion of Results

The higher Ni content of ferritchromit and magnetite rims compared to chromite cores is well established (Tables IV.3, VII.2 and Fig.IV.8). The NiO content of chromite is fairly consistent and low. Further confirmation is found in published NiO values of chromite: 0.9% to .17% for the Great Dyke (Bichan, 1969, p.109) and .06% to .19% for the Kempirsai pluton (Pavlov and Chuprynina, 1967). Erratic and variable NiO values are characteristic of secondary magnetite, for example, the Mwahanza

Hill serpentinite (Tanganyika), contains magnetite with between .59% and 8.14% Ni (Fawley, 1959).

The NiO content of magnetite associated with mafic igneous rocks is about .05%; it is less for magnetite from metamorphic and sedimentary rock (Frietsch, 1970, Fig.2). Thus there is clear evidence that magnetite formed during serpentinization is rich in NiO.

The distribution of Ni in constituent minerals of serpentinites from the Barberton area, Transvaal, has been investigated by Mihalik and Hiemstra (1966) and de Waal and Hiemstra (1966). On the basis of only a few analyses, they proposed a correlation between the Ni in the chromite and in the magnetite rim of the zoned spinels. There was no impoverishment of Ni in the silicates adjacent to the spinel; they concluded that the Ni zoning resulted from Ni redistribution in chromite as it was being replaced by magnetite at a late stage of serpentinization. There is no evidence in the Area III spinels that the Ni in the magnetite was derived from the chromite cores. On the contrary, the NiO content gradient from rim to core (Fig.IV.8) suggests that Ni moved inwards through the spinel. Nor is there evidence that Ni in the magnetite rims was derived from the adjacent serpentine minerals; rather, both serpentine and magnetite formed simultaneously as a result of serpentinization. During this event Ni from the original silicates was redistributed with a significant amount entering magnetite. Subsequent metamorphism caused a distribution of the Ni down a compositional gradient from the magnetite rim to the chromite core. (This is discussed more fully

Table IV.10 NiO content in wt.% of chromite cores, magnetite rims and associated discrete grains of magnetite in zoned spinels from serpentinites.

reference	NiO in chromite core	NiO in magnetite rim	NiO in discrete magnetite	ferritchromit present
de Waal & Hiemstra, 1966	.00-.13	.15- .61	.17-2.93	no
Mihalik & Hiemstra, 1966	.04	.45- .60	-	no
Golding and Bayliss, 1968	.00	c 1.27	-	yes
Bliss (unpub.)	.03-.10	.38	.47- .93	no
This thesis	.00-.03	.56-2.80	.00-2.18	yes

in Chapter VIII, in connection with the origin of the zoning in the spinels).

The Area III ultramafic body is sulphide-poor; and the magnetite has a high Ni content (Table IV.10). This relationship has been noted by Simpson and Chamberlain (1967) where the Ni content of magnetite rimming chromite grains was greater in sulphur-deficient than in sulphur-rich rock (Table IV.11).

Table IV.11 Ni content of spinels from the Puddy Lake ultramafic body.

Spinel	sulphur deficient rock	sulphur rich rock
Rim-% Ni(average)	.58	.14
Core-% Ni(average)	n.d.	n.d.

3 Conclusions

The ultramafic rocks of Area III have Ni contents comparable to the calculated average for dunite and peridotite. They are slightly richer in sulphur.

The Ni contents of the metamorphosed mafic volcanics and the sediments in the wall-rocks are also commensurate with average values for the respective rock types.

The sulphide and silicate Ni contents of the ultramafic rocks vary inversely; it is concluded that S was added to, or redistributed within, the ultramafic body. This probably occurred during serpentinization.

The sulphide and silicate Ni content of the mafic wall-rocks varies directly suggesting a partition of Ni between silicate and sulphide phases.

F SULPHIDES

Sulphides are rare in Area III; most occurrences are millerite. Pyrite was noted in one thin section.

Millerite occurs as small rounded, lozenge-shaped or skeletal grains between 2.0 and 10 microns in diameter. They occur (a) totally enclosed in the mesh centres of serpentinized olivine, (b) with stringers of magnetite serparating serpentinized olivines (Plate 2), and (c) occupying fractures in zoned spinels; the fractures post-date the formation of the zoning and so must the emplacement of the sulphide.

Electron microprobe analyses of millerite are given in Table IV.12 and histograms illustrating the range in composition in Fig.IV.15. Iron is present in nearly all analyses; Cu and Co were analysed for in some specimens and are present in small amounts only. The Co content is higher in analyses which plot to the S-rich side of the NiS-FeS join.

Two analyses of pyrite are given in Table IV.13.

G METAMORPHISM AND METASOMATISM

The contact between the serpentinite and the country rock is marked by widespread alteration zones. The sequence and detail of the alteration varies between drill holes and are probably due to the irregularity of the alteration zones, shown elsewhere (Phillips and Hess, 1936, p.339) to be dependent upon irregularities in the contact providing solution channelways. The sequence below is a compilation from all holes in Area III.

Table IV.12 Electron microprobe analyses of millerite from Area III

	W84	W84	W82	W82	W82	W82	W82
Ni	61.99	60.91	60.13	59.62	59.53	59.42	51.30
Fe	.41	.66	2.67	3.60	1.33	1.33	3.28
S	36.60	36.45	36.52	36.45	36.00	36.31	37.92
Cu	.04	.07	.00	-	-	-	.00
Co	.95	1.91	.62	.33	3.15	2.94	7.43
As	.00	.00	.06	-	-	-	.07
	100.00	100.00	100.00	100.00	100.00	100.00	100.00
	97.51	97.51	98.68	98.21	98.23	99.24	97.95

All analyses have been recalculated to 100% but the analytical total is shown below.

Table IV.13 Electron microprobe analyses of pyrite from Area III

	W61	W61
Ni	.31	.54
Fe	43.97	42.19
S	55.47	56.85
Cu	.20	.20
Co	.05	.23
	100.00	100.00

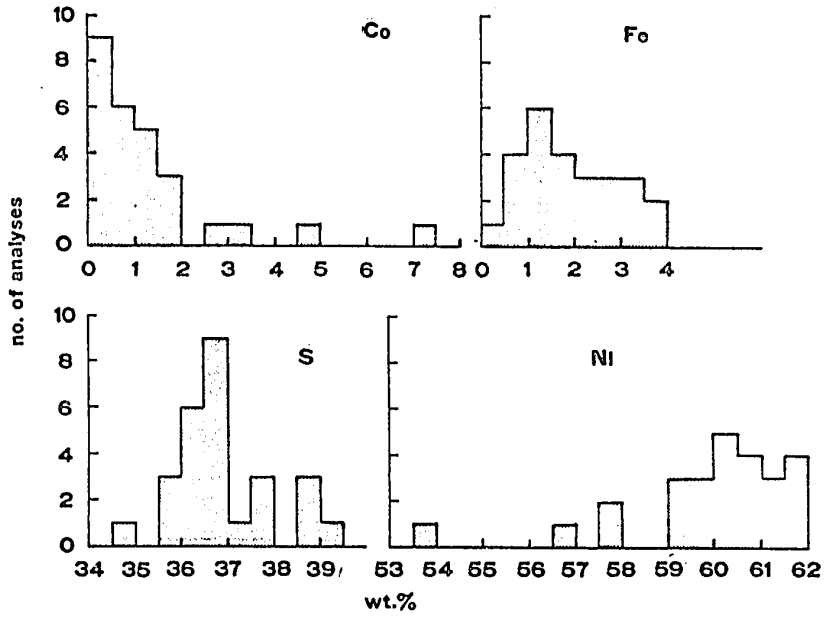

Fig.IV.15. The composition of millerite in Area III;electron microprobe analyses on 27 samples.

1 Wall-rock Alteration

Wall-rock alteration in Area III involves the production of chlorite, and more rarely nephrite*, in the rocks of the metavolcanic unit. The plagioclase amphibolite consists of hornblende with abundant epidote, some plagioclase and minor quartz. Hornblende occurs as large, bladed, feathery crystals, more intensely coloured at the margin than in the centre, and

*Nephrite is a variety of tremolite characteristically occurring as finely intergrown felted aggregates and in metasomatically altered wall-rocks adjacent to serpentinite (e.g. Coleman, 1966).

pleochroic according to the following scheme:-

	X	Y	Z
centre	light green	green	olivine green
margin	colourless	very light green	light green

Plagioclase, quartz and some epidote occurs in fine aggregates in interstitial spaces. The plagioclase is andesine, rarely twinned but frequently zoned, characterized by 120° triple junctions. Epidote also occurs as coarse euhedral crystals and aggregates of anhedral grains in the hornblende.

About 50 feet from the serpentinite, secondary green chlorite appears, largely as a network enclosing plagioclase grains, but also replacing the epidote. The hornblende becomes ragged as a result of fragmentation along the cleavage and is less highly coloured, suggesting that it is richer in MgO.

Closer to the ultramafic body hornblende is completely replaced by nephrite and the remainder of the rock by chlorite; minor idocrase is present. The original texture is undisturbed; the original hornblende outlines preserved, and the 120° triple junctions are apparent in the chlorite pseudomorphs after plagioclase. This gives rise to an interstitial polygonal mosaic of chlorite between the nephrite crystals. The cores of some chlorite polygons contain a distinctive, but unidentified mineral assemblage consisting of a brown spotted outer zone with an inner colourless mosaic. This perfect pseudomorph indicates that alteration has occurred without deformation.

2 Talc-Carbonate Alteration

A zone of talc-carbonate rock separates the serpentinites from the altered wall-rocks. The talc-carbonate rocks are buff to grey with prominent carbonate augen.

An early stage of alteration is represented by talc-tremolite-anthophyllite schist. Large tremolite crystals, marginally replaced by anthophyllite, are enclosed in a groundmass of fine talc and dolomite with some epidote. At a later stage anthophyllite entirely replaces tremolite resulting in sheaves and bundles of radiating anthophyllite crystals set in a talc carbonate matrix. In both rock types minor chlorite is present as intergrown mosaics and as discrete crystals. In the latest stage dolomite replaces anthophyllite forming radiating sheaves of dolomite crystals. Once the rock consists entirely of talc and dolomite a strong foliation is apparent.

3 Serpentinite Alteration

Much of the serpentinite contains small patches of carbonate irregularly distributed throughout. It has been identified as dolomite by X-ray diffraction (Table IV.14) and spot tests using Alizarin red (Friedman, 1959).

Near the contact with the talc-carbonate schist the patches of dolomite become more numerous and veins and stringers of dolomite traverse the serpentinite. Ultimately these coalesce to form a matrix of dolomite in which fragments of the serpentinite are enclosed. Areas interstitial to serpentinized olivine appear to have expanded when occupied by dolomite. Dolomite-filled

Table IV.14 X-ray powder diffraction data for dolomite.

1.		2.	
4.03	(3)		
3.69	(5)		
2.89	(100)	2.87	(100)
2.67	(10)		
2.54	(8)	2.51	(5)
2.41	(10)	2.40	(1)
2.19	(30)	2.18	(30)
2.07	(6)		
2.02	(15)	2.01	(10)
1.85	(5)		
1.80	(20)		
1.79	(30)		
1.78		1.78	(10)
1.57	(8)		
1.55	(10)	1.54	(5)
1.50	(1)		
1.47	(5)		
1.45	(4)		
1.43	(10)		
1.41	(4)		
1.39	(15)	1.39	(1)
1.34	(8)		
etc.			

1. DOLOMITE-ASTM 5/0586
2. DOLOMITE-W89 Area III, Reservation 34

The X-ray powder diffraction photograph No.2 was taken by J.M. Brown of McGill University, (fine focus tube, 35 KV, 15 ma, CuK radiation, 9½ hours exposure) and read by the author.

fractures across olivine pseudomorphs show clear evidence of dilation.

The carbonated serpentinites are not sheared; the dolomite matrix is massive and the olivine pseudomorphs remain euhedral.

Unserpentinized tremolite is sporadically developed in veins and patches towards the margin of some serpentinites in Area III: It occurs in both antigorite, serpentine, and in mesh-textured serpentine as euhedral, bladed crystals with characteristic rhombic cross-sections or longitudinal bladed sections. It is colourless, optically negative and has an extinction angle of 20°. Where talc-carbonate and carbonate alteration is present, the tremolite shows incipient alteration, becoming ragged, with very low birefringence around the margin of the crystals and with carbonate and talc penetrating along cross-fractures and developing in patches within crystals. These textural relations indicate that the tremolite pre-dates the talc-carbonate alteration, but post-dates the original serpentinization and the subsequent formation of antigorite.

Chlorite is seen occasionally interstitial to olivine in the serpentinites. It is unaffected by serpentinization. It occurs in euhedral crystals with characteristic olive-buff and deep ultramarine polarization colours. The buff-polarizing chlorite predominates and is optically positive; the blue-polarizing chlorite appears to be an alteration product of the buff, is subordinate in amount and is optically negative. Much of the chlorite in the talc-carbonate schist is also buff.

4 DISCUSSION

a General

The contact between any ultramafic body and its wall-rock may show superimposed metamorphic and metasomatic effects resulting from distinct geological events. There are basically three types of metamorphic effect and these are in order of appearance:- (1) thermal metamorphism of country rock consequent upon intrusion of the ultramafic body; (2) metasomatic effects resulting from contact equilibration between the ultramafic rock and its wall-rocks; and (3) the development of talc-carbonate schist as a result of CO_2 metasomatism.

Thermal metamorphic aureoles surrounding ultramafic intrusions are normally in the pyroxene hornfels facies (Haughton, 1969, p.181; Wolfe, 1967; Worst, 1960, p.125). The apparent lack of thermal aureoles around many non-stratiform ultramafic intrusions may be a result of tectonic intrusion, whereby the ultramafic rock is emplaced in a solid or semi-solid state.

Metasomatic alteration of both wall-rock and ultramafic body may occur as a result of tectonic emplacement of serpentinite (Fig.IV.16, a and b). The mineralogy of the alteration is dependent upon the nature of the wall-rocks (Coleman, 1966, 1963). Regional metamorphism of an ultramafic rock also produces contact metasomatism, the nature depending on whether the ultramafic rock is serpentinized or not (Fig.IV.16, c and d) (Philips and Hess, 1936; Read, 1934). The two-way transfer of material is the result of contact equilibration between rocks of vastly different chemical composition.

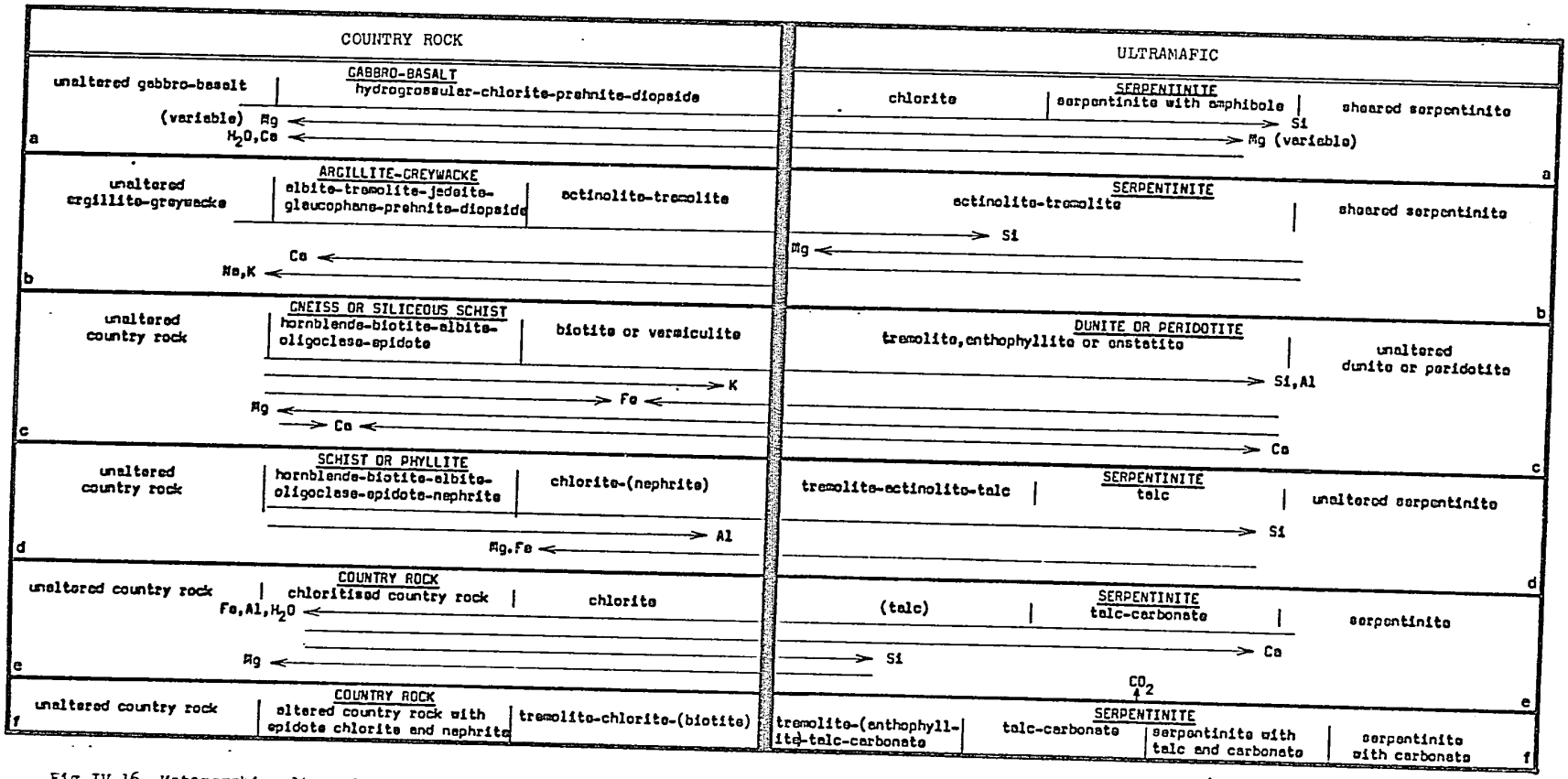

Fig.IV.16. Metamorphic alteration at contacts between ultramafic bodies and country rock.
a and b - Metamorphic effects, predominantly Ca metasomatism, which occur at the time of emplacement of the serpentine (Coleman, 1966;1963).
c and d - Contact equilibration effects across contact between ultramafic rock and country rock which have been subjected to metamorphism at comparatively high and low temperatures, respectively (Phillips and Hess, 1936).
e - CO_2 metasomatism resulting in talc-carbonate alteration (Jahns, 1967).
f - Mineral zones at contact between serpentinite and country rock in Area I.

The development of talc-carbonate schist as a result of CO_2 metasomatism (Jahns, 1967; Naldrett, 1966) may obscure previous contact relations.

b Area III

Mineralogy indicative of contact thermal metamorphism in the pyroxene-hornfels facies (Schwellnus, 1970; Turner, 1968; Worst, 1960) has not been observed in Area III. If such an aureole was present it has been entirely destroyed; alternatively the ultramafic rocks have been emplaced tectonically. Their disrupted nature and position along the contact between the metavolcanic and metasedimentary unit (Fig.II.1) suggest the latter alternative..Their lack of deformation and shearing is consistent with tectonic emplacement only if they were thoroughly lubricated at the contact. It may be that marginal talcose zones, now obscured by CO_2 metasomatism, provided the necessary lubrication.

Epidote is the first metamorphic mineral to develop in the country rock greenstone, with chlorite and nephrite abundant near the contact. Talc-tremolite schist developed at the serpentinite margin, but was altered by later CO_2-metasomatism which formed dolomite and replaced tremolite by anthophyllite. The anthophyllite was itself subsequently replaced by carbonate. Anthophyllite is stable between 510°C and 560°C at total fluid pressure of 2000 bars, in presence of high concentrations of CO_2 (Johannes, 1969). These temperatures will drop with decreasing pressure, hence it is theoretically possible to produce anthophyllite within a temperature range at which serpentinite is stable.

Thus the mineralogy on either side of the contact is consistent with contact equilibration between serpentinite and country rock resulting from a low to medium grade of regional metamorphism (Fig.IV.16 e). Subsequent CO_2 metasomatism has occurred.

H SUMMARY

The ultramafic rocks of Area III have been emplaced in the vicinity of the contact between the metavolcanic and the metasedimentary units (Fig.II.1).

The ultramafic rocks, originally dunite, are now completely serpentinized and consist of mesh-textured pseudomorphs of lizardite and subordinate clinochrysotile after olivine. Antigorite, and rarely tremolite, replace the mesh-textured serpentine. Chromite and secondary magnetite are minor but consistent constituents, while millerite and pyrite are rare. The mineralogy is almost entirely secondary and consequent upon serpentinization and subsequent regional metamorphism. The chrome spinels are zoned; a chromite core is surrounded by ferritchromit which varies continuously toward, but not always reaching, magnetite in composition. The chromite cores are believed to be the only relic of the primary igneous mineralogy. The mesh-textured serpentine has a relict cumulus texture.

The serpentinite contains about .22% Ni, an average Ni content for ultramafic rocks. Sulphides are rare; fine-grained millerite, formed during serpentinization, and pyrite have been observed.

Talc-carbonate alteration post-dates serpentinization and obscures any previous metamorphic and metasomatic effects that may have existed at the contact between ultramafic and country rock. A primary, thermal metamorphic aureole, resulting from the intrusion of the ultramafic body has not been recognized, which suggests that it may have been emplaced tectonically. The mineralogy of the country rock adjacent to the serpentinites indicates equilibration between the two under conditions of low to medium grade of regional metamorphism.

The serpentinites are lensoid in shape, with lengths up to 4000 feet and widths to 750 feet. Intercalations of country rock are rare and no pseudomorphed quench textures have been observed. These features suggest that the ultramafic rocks are not extrusive.

V ULTRAMAFIC ROCKS OF AREA I

A COMPOSITION OF THE SERPENTINITE

Area I ultramafic rocks are enclosed by gneissic granite west of the metavolcanic and metasedimentary units (Fig.II.1). The ultramafic rocks, originally dunite and harzburgite, are almost completely serpentinized; olivine is pseudomorphed by lizardite mesh textures and pyroxene by lizardite bastite. Magnetite and chrome spinel are accessory constituents. Phlogopite and chlorite developed subsequent to serpentinization. Analyses of typical serpentinites are shown in Table V.1.

B PRIMARY MINERALOGY AND PETROLOGY

1 Olivine

Fresh olivine, Fo_{90}, (Table V.2) remains in some mesh centres (Plate 11) and rarely constitutes about 25% of a serpentinized olivine. It is always colourless and unzoned.

2 Petrology of the Original Ultramafic Rocks

a Dunite

The most readily identifiable relict dunite is a dense black serpentinite in which the olivine pseudomorphs are easily recognized in thin section (Plate29), and on cut surfaces of hand specimens. The euhedral olivine pseudomorphs form a completely interlocking texture which has the appearance either of an orthocumulate with very minor intercumulus material or of an ultramafic rock which has recrystallized to an interlocking mosaic during metamorphism. Minor amounts of sulphide remain

Table V.1 Analyses of ultramafic rocks from Area I.

	1	2	3	4
SiO_2	33.50	38.10	37.30	38.40
Al_2O_3	.22	.67	.94	1.65
Fe_2O_3	6.70	4.30	4.40	4.15
FeO	1.13	3.63	.88	3.60
MgO	39.78	36.70	38.50	33.70
CaO	.45	.18	1.10	2.90
Na_2O	.10	.10	.23	.15
K_2O	.04	.05	.35	.76
H_2O^-	1.76	.53	.73	.24
H_2O^+	13.00	12.86	13.59	11.96
TiO_2	.02	.21	.25	.28
MnO	.11	.03	.06	.06
F	.05	.05	.08	.20
S	.56	.13	.21	.40
Cr_2O_3	.21	.28	.31	.19
NiO	.55	.41	.40	.54
CoO	.02	.02	.01	.01
CuO	.04	.00	.02	.00
ZnO	.00	.00	.01	.01
	98.24	98.15	99.37	99.20

1. Average of 4 dunites
2. Average of 2 harzburgites
3. Average of 2 phlogopite-bearing dunites
4. Average of 2 phlogopite-bearing harzburgites

Table V.2 Electron probe analyses of olivine from Area I.

	Wt.% oxides			cations on basis of 4(O)							
	1	2	3		1		2		3		
SiO_2	43.46	40.82	42.32	Si		1.06		1.03		1.02	
Al_2O_3	0.00	0.00	0.03	Mg	1.69		1.78		1.76		
MgO	46.23	47.37	48.83	Fe	.17	1.87	.16	1.95	.19	1.96	
FeO	8.20	7.37	9.38	Ni	.01		.01		.01		
NiO	.57	.54	.51	O		4.00		4.00		4.00	
CaO	-	-	.05								
CuO	-	-	.01	mol % Fo							
CoO	-	-	.03	$\frac{100 \times Mg}{Mg + Fe}$		90.86		91.75		90.26	
	98.46	96.10	101.16								

1. W31; 2. 2217; 3. 2238

along grain boundaries (Plate 29). Very small grains of serpentine with no mesh texture may be bastite after interstitial pyroxene (Plate 26).

b Harzburgite

The harzburgite in Area I contains up to 30% of totally serpentinized pyroxene. Pyroxene was more euhedral when the content was high; smaller amounts of pyroxene formed interstitially to olivine. The harzburgites with about 30% pyroxene have a granular texture in hand specimen and are readily distinguishable from serpentinized dunite.

c Amphibole-bearing Peridotite

Serpentinite with serpentine pseudomorphs after amphibole are locally abundant. In the protolith the amphibole formed later than the olivine and pyroxene through which it cuts. No textures indicative of an intergrowth of olivine and amphibole have been observed. The development of amphibole does not appear to have been restricted to contacts with late granite dykes. It is tentatively concluded that the amphibole results from a pre-serpentinization metamorphic event.

3 Size and Shape of Original Ultramafic Bodies

Ground and air magnetic surveys, coupled with diamond drilling, indicate that the serpentinites in Area I are a series of lenses in the form of a J (Fig.II.1). The thickness of the lenses varies up to 1000 feet. A large amount of country rock, predominantly granite, occurs within the serpentinite. Many of the contacts are faulted but others are not and are marked by

biotite, anthophyllite and talc selvedges. Extreme brecciation and faulting has resulted in the mechanical mixing of serpentinite and country rock. This is similar to that illustrated for the Roxbury District, Vermont, by Jahns (1967, Fig.5.4), except that the country rock in Area I is granite and not greenstone.

C SERPENTINE MINERALOGY

1 Mesh-Textured Serpentine

Mesh-textured serpentine is well developed in Area I, but lacks the regularity that characterizes the Area III serpentinites (Plate 26). Clearly outlined olivine pseudomorphs are far less common in Area I than in Area III. This type of mesh texture closely resembles the sub-rectangular mesh texture common in the Manitoba Nickel Belt (Coats, 1968, p.324).

The lack of clearly outlined olivine pseudomorphs in Area I is due to two factors. Firstly, there is very little interstitial material remaining, (Plate 29) indicating that olivine crystals were in close contact in the protolith. Secondly, antigorite is absent; its presence in Area III emphasizes pseudomorph outlines (Plates 1 and 3).

The mesh-textured serpentine consists of short lengths of mesh rims of α-serpentine enclosing irregular mesh centres of isotropic or nearly isotropic fibro-lamellar serpentine (Plate 26). There is evidence of fragmentation of pre-existing mesh texture; many of the mesh rims appear to be curved and fractured when examined in detail. Ribbon mesh texture is common in Area I where mesh rims extend in sub-parallel fashion through the rock crossing

the boundaries of the olivine pseudomorphs. The veins comprising the ribbon meshes may be bipartite or more strictly tripartite. The bipartite veins consist of two strips of fibro-lamellar α-serpentine fibres, orientated normal to the vein walls. The tripartite veins contain a central, discontinuous, strip of more fibrous α-serpentine with occasional sections of γ-serpentine. The mesh centres are isotropic with occasional γ-serpentine fibres.

In other textures sharp and clear-cut veins of α-serpentine are rimmed by irregular fringes of α-serpentine. An irregular parting of magnetite and isotropic serpentine separates the γ-serpentine fringes from the γ-serpentine fringe of the next set (Plate 27). These ribbon mesh textures compare closely with the close-packed parallel cross-fibre veinlets illustrated by Coats (1968, Fig.3).

X-ray microbeam determinations have identified the α-serpentine of the mesh centres as lizardite with varying degrees of orientation. No clinochrysotile has been identified.

2 Bastite Pseudomorphs

The presence of bastite after pyroxene indicates that serpentinized harzburgites are fairly common in Area I. The pseudomorphs have three characteristic shapes:- (a) cross sections showing prism outline and possibly relict (110) cleavage (Plate 13); (b) longitudinal sections showing prism terminations and the trace of the (110) cleavage (Plate 15); and (c) irregular grains with rounded outlines (Plate 26).

The bastite pseudomorphs are clear, generally free of magnetite grains and colourless to very light green. Under crossed nicols they are seen to consist of fibrous patches of α- and γ-serpentine orientated parallel to the long axis of the pseudomorph and with comparatively low and high birefringence respectively. In elongate sections the γ-serpentine developed along, and parallel to the longitudinal cleavage and also from irregular partings across the crystal. The γ-serpentine encloses irregular patches of α-serpentine together with the occasional patch of isotropic serpentine. In cross-sections the arrangement of α- and γ-serpentine is far less regular. The α-serpentine was determined by X-ray microbeam studies to consist of lizardite in type II orientation. (Appendix II)

In mesh-textured serpentine where the mesh centres have been replaced by carbonate, bastite is not affected.

An electron microprobe analysis of the serpentine in the bastite in Plate 13 is shown in Table V.3.

Table V.3. Electron microprobe analysis of bastite serpentine (see Plate 13).

SiO_2	40.86	Si	2.00	2.00
Al_2O_3	.18	Al	.01	
MgO	37.60	Mg	2.74	
NiO	.32	Ni	.01	
FeO	5.48	Fe	.22	2.99
CaO	.12	Ca	.01	
CoO	.02	Co	.00	
CuO	.02	Cu	.00	
S	.05	S	.00	
(H_2O)	12.25	OH		4.00
	96.90	H		4.00

H_2O has been calculated on the basis of two molecules for every 7 oxygen atoms

3 Amphibole Pseudomorphs

Bladed serpentine with feathery terminations, exhibiting longitudinal cleavage and a cross-parting, is interpreted as replacing amphibole (Plate 12). These pseudomorphs cross-cut all other serpentinized constituents and the original amphibole presumably formed late in the pre-serpentinization history of the ultramafic body, possibly as the result of metamorphism.

The optical orientation of the serpentine minerals varies considerably. Gamma-serpentine develops on the outside of the grains, along the longitudinal cleavage and at right angles to the cross-parting, enclosing centres of α-serpentine and occasional patches of isotropic serpentine. X-ray microbeam studies show that the α-serpentine is lizardite in type I orientation. Isotropic centres are rare, but where they do occur they are replaced by α-serpentine developing outward from the γ-serpentine rims. Rarely the whole width of the crystal consists of γ-serpentine; from the appearance of these pseudomorphs γ-serpentine is replacing α-serpentine.

4 Summary and Discussion

The ultramafic rocks in Area I are serpentinized dunite and harzburgite, with lizardite mesh texture after olivine and lizardite bastite after pyroxene. Neither antigorite nor clinochrysotile have been observed optically or identified by X-ray microbeam studies.

The relations between the serpentine minerals lizardite, chrysotile and antigorite have been discussed on p.56 . The

absence of chrysotile and antigorite indicates that the serpentinization history has been simple, producing only lizardite mesh textures. There has been no subsequent event to cause the replacement of the mesh-textured lizardite by antigorite or chrysotile.

Wicks (1969) has recognized a sequence of serpentine mineralogy and textures from the Manitoba Nickel Belt indicating an increase in the complexity of the serpentinization history from Manibridge in the SW toward Thompson in the NE. This sequence involves a change from lizardite mesh texture to lizardite-chrysotile interlocking textures and chrysotile textures from SW to NE (Fig.I.3). The Area I serpentinites, which outcrop 40 miles to the SW of Manibridge (Fig.I.3) consist of lizardite mesh textures only and clearly fit into the sequence of serpentine textures developed in the Manitoba Nickel Belt ultramafic rocks.

D SPINEL MINERALOGY

1 Introduction

Chrome spinels are not common in Area I serpentinites; those observed show evidence of fragmentation and replacement. The spinels are both simply and multiply zoned, consisting of a homogeneous magnetite rim around a homogeneous chromite or ferritchromit core or around an exsolved, two phase, chromite core. The contact between the chromite and magnetite is sharp whether the chromite is euhedral (Plates 37 and 19) or rounded (Plates 34 and 38). Pentlandite frequently occur adjacent to zoned spinels and may totally enclose them (Plate 37). In some cases the spinel is replaced by an intergrowth of pentlandite,

serpentine and magnetite (Plates 40 and 42). The magnetite rim of the zoned spinel may also enclose adjacent pentlandite (Plate 38). Sulphide and silicate minerals may occur at the sharp interface between chromite and magnetite (Plates 20 and 37). The continuous ferritchromit-magnetite compositional zoning characteristic of Area III has not been observed in Area I. Some homogeneous spinels are without rims.

2 Simply Zoned Spinels

Simply zoned spinels contain a core of homogeneous chromite surrounded by a rim of magnetite. Simple zoning is rare and generally observed in a spinel totally or partially enclosed by sulphide (Plate 37). Electron microprobe analyses of the core of a simply zoned spinel (#1031) are shown in Table V.4 and X-ray raster scans in Plate 44.

3 Multiply Zoned Spinels

The chromite cores to multiply zoned spinels in Area I are surrounded by zones of magnetite and a member of the pyroaurite-group of minerals (Plates 34 and 39). The appearance of multiply zoned spinels, with frittered and scalloped contacts suggests that they are derived from simply zoned spinels by the subsequent development of pyroaurite within them. The composition of the spinel phases is similar to those of the simply zoned spinels.

Table V.4 Electron microprobe analyses of simply and multiply zoned spinels from Area I.

	1	2	3	4	5	6	7	8
Al_2O_3	11.74	10.11	.05	.05	24.28	.00	11.44	.62
Cr_2O_3	38.07	39.20	.78	.09	30.88	.31	38.09	.32
TiO_2	.58	.54	.07	.09	.50	.06	.79	.02
MgO	7.90	6.94	2.56	.11	11.30	.90	5.93	.33
NiO	.16	.16	.02	.27	.59	.04	.32	.35
FeO	21.51	22.70	27.09	30.61	18.07	29.61	24.33	30.30
Fe_2O_3	20.04	20.35	69.42	68.78	14.39	69.07	19.09	68.06
	100.00	100.00	100.00	100.00	100.00	100.00	100.00	100.00
Cr/Cr+Al	.74	.77	.86	1.00	.52	1.00	.74	.33
$Fe^3/Fe^3+Cr+Al$	.28	.28	.99	1.00	.18	1.00	.27	.98
$Mg/Mg+Fe^2$	.34	.30	.12	.00	.46	.04	.25	.01

Specimen 1031 - simply zoned spinel
Plate 37:- 1. centre of chromite core; 2. margin of chromite core; 3. inner portion of magnetite rim; 4. outer portion of magnetite rim.

Specimen W13 - multiply zoned spinel
Plate 34, Fig.V.1:- 5. chromite core (average of 8 analyses); 6. magnetite rim (average of 5 analyses).

Specimen 2246 - multiply zoned spinel
Plate 39:- 7. chromite core (average of 5 analyses); 8. magnetite rim (average of 3 analyses).

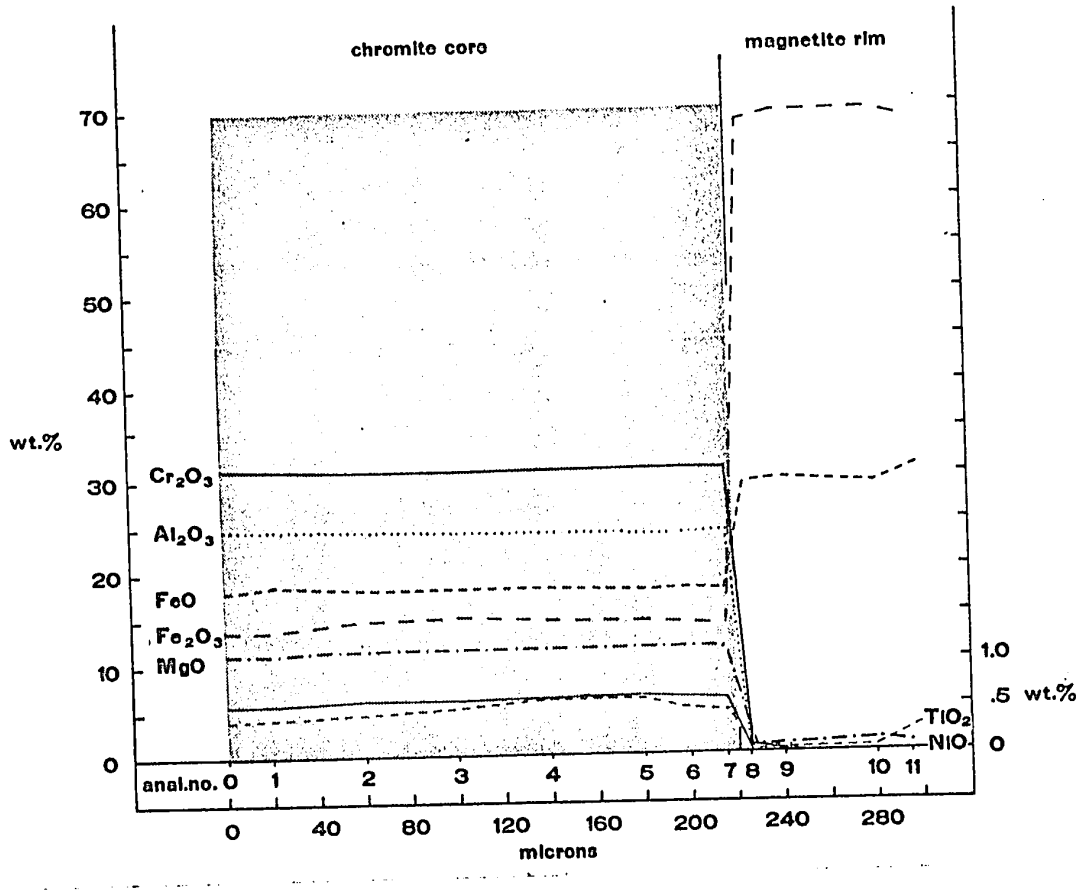

Fig.V.1. Compositional variation across a simply zoned spinel, W13 (Plate 34), with a chromite core and a magnetite rim. The analyses numbers refer to analyses listed in Appendix V, Table X. The microprobe traverse is from the centre of the grain outwards to one rim.

4 Homogeneous Spinels

Homogeneous chrome spinels are rarely observed in Area I; they have irregular outline and show evidence of fragmentation around the margins where they appear to be replaced by phlogopite. There is no surrounding rim of magnetite. Their composition is that of ferritchromit, although small fractures which extend through the grains may be filled with magngtite or hematite (Plate 36). The uniform composition is illustrated in Table V.5 and in the electron beam image photographs in Plate 45. Spinels with incomplete magnetite rims (Plate 35) have chromite cores of composition similar to that of homogeneous chromite (Table V.5); they too are closely associated with phlogopite.

5 Exsolution Textures

The chromite cores of some otherwise simply zoned spinels show textures indicating exsolution of dark and light phases. These exsolved cores are surrounded by rims of homogeneous magnetite. The appearance of the exsolution textures varies from grain to grain, but a crude zoning is apparent (Plates 19, 30 and 31). These zones are from the outside inward:- (a) a zone of magnetite surrounding the grain; (b) a narrow dark zone of chromite; (c) a narrow zone of light ferritchromit enclosing patches of dark chromite continuous with a reticulate network of similar texture and (d) an extremely fine acicular intergrowth of light and dark phases. This intergrowth is too fine to permit electron probe analysis of individual phases but average compositions are obtained using a wide beam.

Table V.5 Electron microprobe analyses of homogeneous spinels and spinels with incomplete magnetite rims.

	1	2	3	4	5	6	7	8	9	10
Al_2O_3	.60	5.20	4.94	1.73	.43	1.90	1.67	.00	1.24	1.19
Cr_2O_3	49.73	44.10	44.88	42.69	45.73	48.62	49.31	1.15	24.35	22.85
TiO_2	.32	.46	.51	.53	.24	.22	.15	.03	.66	.80
MgO	5.06	8.25	7.67	7.82	.67	1.08	1.01	.13	3.36	3.48
NiO	.12	.07	.10	.17	.13	.08	.00	.00	.61	.73
FeO	24.03	19.94	20.77	19.83	30.67	30.41	30.57	30.85	25.90	25.57
Fe_2O_3	20.15	21.99	21.13	27.23	22.12	17.70	17.34	67.84	43.88	45.39
	100.01	100.01	100.00	100.00	99.99	100.01	100.00	100.00	100.00	100.00
Cr/Cr+Al	.99	.88	.89	.95	.99	.96	.96	1.00	.94	.94
$Fe^3/Fe^3+Cr+Al$	.28	.30	.29	.37	.32	.25	.25	.98	.63	.65
$Mg/Mg+Fe^2$	.22	.36	.34	.35	.03	.05	.04	.01	.15	.16

Specimen 980 - homogeneous spinel. 1 average scan on core.
Specimen 2372 - homogeneous spinel. 2,3 and 4, left side, centre and right side of spinel.
Specimen 2375 - simply zoned spinel with incomplete magnetite rim (Plate 35). 5 centre of core, 6 & 7 opposite margins of core, 8 centre of magnetite rim.
Specimen 1027 - homogeneous spinel. 9 and 10, average analyses of two spinels from same polished section.

In the simplest stage of exsolution (Plate 19) euhedral chromite (zone d) is composed of very fine intersecting acicular lamellae of dark and light phases. Traced outwards the direction of one of the sets of lamellae becomes dominant and the exsolved phases coarser and somewhat vermicular in shape (zone c). The outermost portion of the chromite remains as a homogeneous rim (zone b), separated from the homogeneous magnetite (zone a) by a sharp contact. Analyses of chromite and magnetite are presented in Table V.6.

In more highly exsolved spinels, the pattern appears more complicated but the zonal structure is still recognizable (Plates 30 and 31). The chromite rim (zone b) presents a sharp outer margin to the magnetite rim (zone a) and a slightly irregular one to the inner zone c. Electron microprobe analyses (Table V.8) show that the dark phase in zone c is chromite with an irregular composition and the light phase in zone c is ferritchromit. The fine two-phase intergrowth in zone d yields an intermediate composition when analyzed with a wide beam. This may represent the bulk composition of the spinel prior to exsolution.

The continuous chromite shell may be broken by the magnetite rim (zone a) cutting through the grain (Plates 31 and 41) or it may be removed entirely (Plate 20), both of which result from recementing a fractured chromite grain by magnetite.

The large chromite core in the spinel in Plate 38 exhibits poor exsolution texture; the small one is homogeneous. The composition of both is similar when analyzed by electron microprobe using a wide beam (Table V.7).

Table V.6 Analyses of phases in some exsolved spinels from Specimen W747.

	1	2	3	4	5
Al_2O_3	31.87	31.77	.00	11.45	.02
Cr_2O_3	30.19	29.28	.11	29.79	.41
TiO_2	-	-	.09	.61	.41
MgO	14.36	15.35	.77	7.06	1.13
NiO	.11	.10	.02	.21	.00
FeO	15.19	13.66	29.84	22.58	29.31
Fe_2O_3	8.27	9.84	69.16	28.31	69.09
Cr/Cr+Al	.45	.44	1.00	.69	1.00
Fe^3/Fe^3+Cr+Al	.11	.13	1.00	.39	.99
$Mg/Mg+Fe^2$	.57	.61	.03	.30	.05

Spinel 1 (not illustrated): 1 and 2 chromite rim; 3 magnetite rim.
Spinel 2 (Plate 19) : 4 chromite rim to exsolved core; 5 magnetite rim.

Table V.7 Electron microprobe analyses of fine two phase intergrowth (zone d) in exsolved spinels using a wide beam.

	747.6	747.8	747.8	747.9	747.9	747.9	747.9	747.11
Al_2O_3	4.83	4.83	3.54	4.74	3.13	4.75	4.18	4.31
Cr_2O_3	20.08	22.04	23.18	29.70	25.10	29.01	23.23	21.07
TiO_2	.89	1.08	-	.87	1.06	1.00	-	-
MgO	5.69	4.14	5.12	3.27	2.56	3.44	3.04	3.79
NiO	.87	.46	.58	.33	.55	.56	.58	.88
FeO	22.67	25.49	23.60	27.04	27.59	26.56	26.94	25.49
Fe_2O_3	44.77	41.97	43.98	34.03	40.04	34.68	42.01	44.47
Cr/Cr+Al	.78	.80	.81	.81	.84	.80	.79	.81
$Fe^3/Fe^3+Cr+Al$	.63	.60	.60	.47	.56	.48	.58	.63
$Mg/Mg+Fe^2$	.26	.18	.28	.18	.14	.19	.17	.17

Table V.8 Electron microprobe analyses of phases in a zoned spinel with exsolved chromite core.

	1	2	3	4	5	6	7	8	9	10	11	12	13
Al_2O_3	24.75	21.59	28.64	24.37	30.74	30.85	2.17	1.66	1.81	.00	4.52	6.10	4.02
Cr_2O_3	29.66	30.93	28.20	30.51	30.28	31.60	17.18	15.86	15.64	.39	21.52	23.55	22.01
TiO_2	.31	.29	.15	.22	-	-	1.29	1.10	.90	-	1.22	-	-
MgO	11.61	10.24	15.33	14.71	12.93	13.16	2.47	2.75	2.18	1.09	4.86	3.97	3.83
MnO	.31	.07	.11	.14	.11	.11	1.12	1.33	1.25	.03	1.00	1.10	1.28
FeO	17.91	19.70	13.07	13.24	17.20	16.88	26.86	26.10	27.07	29.36	23.80	25.36	24.99
Fe_2O_3	15.60	17.18	14.49	16.80	8.72	7.39	48.92	51.21	51.15	68.89	43.08	39.89	43.87
	100.15	100.00	99.99	99.99	99.98	99.99	100.01	100.01	100.00	99.76	100.00	99.97	100.00
Cr/Cr+Al	.51	.55	.46	.52	.46	.47	.87	.89	.88	1.00	.81	.77	.83
$Fe^3/Fe + Al+Cr$	.25	.23	.19	.22	.11	.10	.71	.74	.74	1.00	.61	.54	.62
Mg/Mg+Fe^2	.48	.42	.62	.60	.51	.52	.11	.13	.10	.05	.22	.18	.17

1 and 2 - chromite rim - zone b
3 to 6 - dark patches inside rim } zone c
7 to 9 - light patches inside rim }
10 outer (magnetite) rim - zone a
11 to 13- fine two phase intergrowth - zone d (bulk analyses using wide beam)
See Plate 31

Table V.9 Electron microprobe analyses of magnetite from Area I.

	1	2	3	4	5	6	7
Al_2O_3	.00	.00	.02	.01	.09	-	.67- 1.30
Cr_2O_3	.02	.02	.02	.36	.45	-	.50- 5.00
TiO_2	-	.00	.03	.07	.11	-	.20- 4.20
MgO	.94	.40	.35	.84	.88	-	2.85-15.10
NiO	.01	.00	.00	.03	.09	-	.09- 8.14
FeO	29.60	30.42	30.50	29.73	29.62	31.03	-
Fe_2O_3	69.20	69.16	69.09	68.98	68.80	68.97	-

1- Magnetite grain W747
2 and 3- Magnetite grains W729
4 and 5- median and arithmetic mean of 8 analyses of magnetite rimming chromite from Area I (Tables V.3, Anal.3,4,6,and 8; V.4, Anal.8; V.8, Anal.10; V.5, Anal.3 and 5.
6- Theoretical composition of magnetite
7- Range of trace element content of magnetite from ultramafic rocks given by Frietsch (1970, Table 17).

6 Magnetite

Magnetite occurs as individual grains or aggregates within mesh centres as well as rims to chrome spinels. It is normally euhedral when occurring as individual grains. Analyses of magnetite are given in Table V.9.

E SULPHIDES

1 Introduction

Sulphides are irregularly distributed through the ultramafic rocks of Area I, the content varying from 0 to about 5%. Pentlandite is the predominant nickel sulphide associated with millerite and heazlewoodite and rare violarite and polydymite. Chalcopyrite occurs in small amounts as an exsolution phase in pentlandite. Pyrite and pyrrhotite are rare.

Sulphide concentrations of variable magnitude (Fig.V.6) occur in layers 25 to 40 feet thick in serpentinized dunite and peridotite. Between these layers the total nickel content of the ultramafic rocks may drop to background, about .3% Ni, and sulphides may be completely absent. There is no evidence of gravity settling contributing to the sulphide concentrations.

The sulphides occur in two grain sizes:- (a) coarse sulphides, pentlandite and millerite up to about 1.0 mm in size, occur interstitially to serpentinized silicates, normally olivine. The shape of the grains varies, some have euhedral outlines and occur as discrete crystals, others are anhedral and interstitial to serpentinized olivine (Plates 28, 29 and 40); (b) fine sulphide grains, down to about 2 microns in diameter, pentlandite,

millerite, heazlewoodite, and rarely violarite and polydymite are scattered through the ultramafic. They occur with the coarse sulphides but also in sections devoid of coarse sulphide. The shape of the fine grains is quite irregular, anhedral, scalloped and vermicular shapes being predominant. The fine sulphides occur in the following associations:- (i) within patches of carbonate, talc or other secondary minerals associated with post-serpentinization events; (ii) within the serpentine minerals of serpentinized and partially serpentinized olivine; (iii) as trains of grains, with magnetite, along the median parting in mesh rims; (iv) as fine grains at the contact between chromite or ferritchromit cores and magnetite rims to zoned spinels, and (v) along cleavage planes in anthophyllite and phlogopite at the contact between serpentinite and granite.

2 Nickel Sulphides

a Pentlandite

Pentlandite $(Fe,Ni)_9S_8$ is the most common sulphide in Area I, occurring as both fine and coarse grains. The coarser grains are normally interstitial to serpentinized olivine, resulting in a characteristic cuspate shape (Plate 28): euhedral grains also occur interstitially. All the grains are somewhat fragmented, but this may have been enhanced as a result of polishing. Rarely pentlandite occurs as part of a complex intergrowth, or in narrow late veins, with pyrrhotite. Some pentlandite grains completely enclose euhedral pseudomorphs which now consist of spongy or vermicular pentlandite, pentlandite and magnetite or pentlandite and serpentine (Plates 40 and 42). The shape of the pseudomorphs

closely resembles that of euhedral chromite or magnetite. Electron microprobe analyses show that the pentlandite in the pseudomorph is richer in Co relative to that in the surrounding pentlandite.

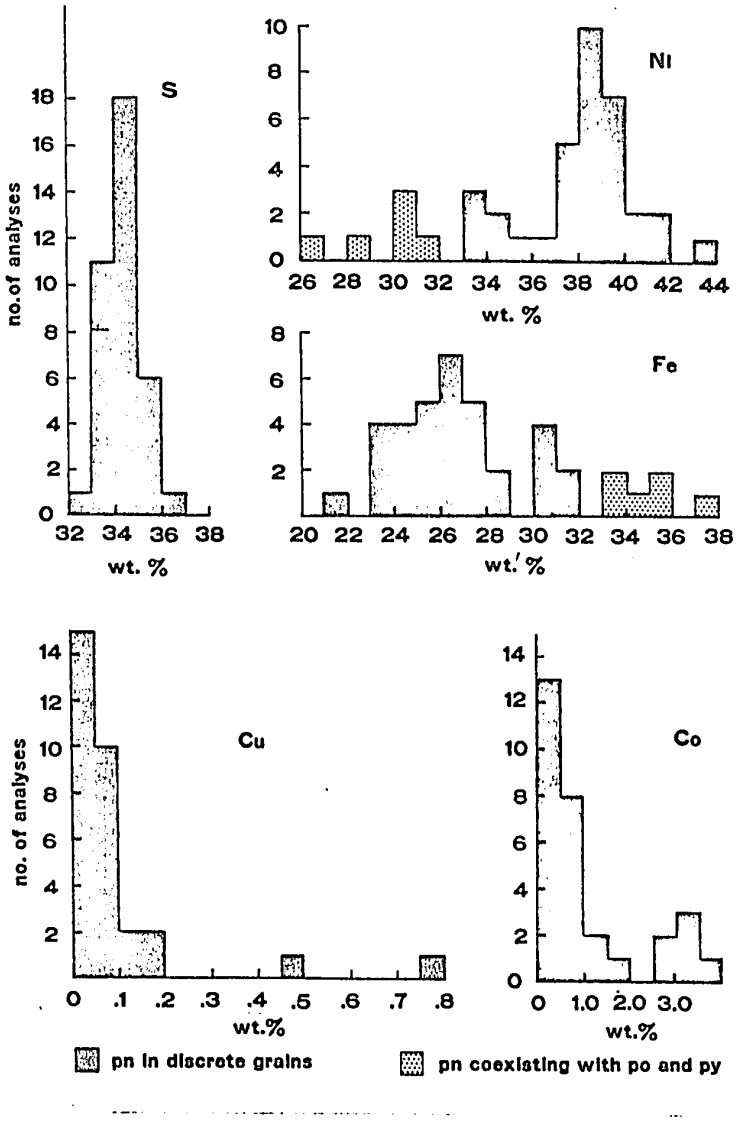

Fig.V.2. Range of pentlandite composition, Area I.

The composition of the pentlandite in both the coarse and fine grains is summarized in the histograms for Ni, Fe, Co, Cu and S (Fig.V.2). The pentlandite is Ni rich, with an Fe:Ni ratio between .57 and .94, averaging .69.

Pentlandite also occurs as part of a complicated sulphide intergrowth with pyrrhotite and pyrite. Occasional narrow veins of pentlandite and pyrrhotite cross-cut all other minerals. In these associations pentlandite is Ni-poor having a Fe:Ni ratio of about 1.15 (Fig.V.2).

The composition of pentlandite is clearly related to the sulphide minerals with which it is associated; it is Ni-rich in association with nickel sulphides, and Ni-poor in association with iron sulphides.

b Millerite

Millerite (NiS) occurs as both coarse and fine grains. Under crossed nicols the coarse grains appear polycrystalline. A few analyses only are available (Fig.V.3); these indicate no marked compositional difference between millerite in Areas I and III (compare Fig.IV.15).

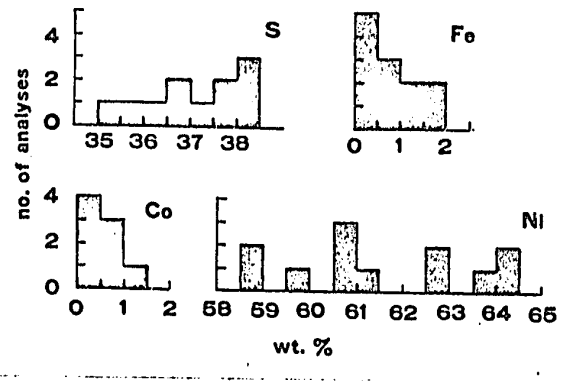

Fig.V.3. Range in millerite composition, Area I.

c Violarite

Violarite (Table V.10) is rare, occuring either as small grains or as an alteration of pentlandite and millerite surrounded by phlogopite.

Table V.10. Electron microprobe analyses of violarite from Area I

	1	2
Ni	41.58	42.02
Fe	13.84	13.18
S	43.69	43.77
Cu	.03	.05
Co	.87	.98
	100.00	100.00

1. Grain from W740-$Ni_{2.08}Fe_{0.73}Co_{0.04}S_{4.00}$

2. Grain from W740-$Ni_{2.10}Fe_{0.69}Co_{0.05}S_{4.00}$

d Heazlewoodite

Heazlewoodite (Ni_3S_2) Occurs as small grains scattered throughout the sulphide-rich sections. The composition is illustrated in figure V.4.

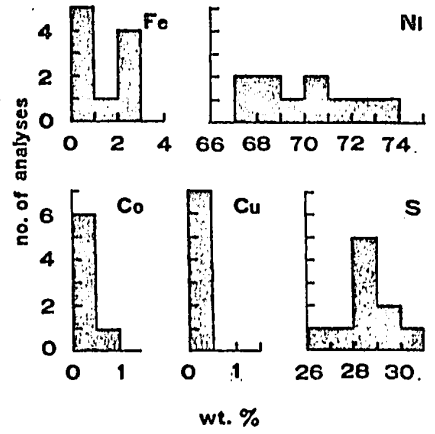

Fig.V.4. Composition of heazlewoodite in Area I

Table V.11 Electron probe analyses of coexisting nickel and iron sulphides.

	pyrite			pyrrhotite			pentlandite		
Ni	.05	.26	.21	4.33	.52	.15	31.96	30.16	26.60
Fe	47.36	44.03	44.12	58.75	60.08	61.03	33.44	33.42	35.99
Cu	.14	.00	.00	.00	.41	.00	.00	.75	1.60
Co	.30	.70	.65	.10	.06	.00	.18	.16	.45
S	52.14	55.01	55.02	36.82	38.93	38.82	39.42	35.51	35.35
	100.00	100.00	100.00	100.00	100.00	100.00	100.00	100.00	100.00

3 Iron Sulphides

Pyrite and pyrrhotite occur only rarely in Area I serpentinites,but both are found at the base of one mineralised section where they are intergrown with pentlandite.Analyses of these phases are shown in Table V.11.The iron sulphide is with one exception low in nickel,whereas the coexisting pentlandite is iron-rich (Fig.V.2).

Late veins of pyrrhotite alone are also known,bearing a distinct cross-cutting relationship to all other constituents. Analyses are given in Table V.12.

Table V.12. Electron microprobe analyses of pyrrhotite in late veins.

Ni	.33	2.34
Fe	62.91	60.58
Cu	0.00	0.00
Co	0.19	0.00
S	36.58	37.08
	100.00	100.00

F DISTRIBUTION OF NICKEL AND SULPHUR

The total nickel content of the serpentinites in Area I lies between 0.1% and 2.0%,with a few scattered erratic higher values;the mode is in the 0.3% to 0.4% class interval (Fig.V.5). The distribution is markedly left skewed and in general the nickel values are higher than average for dunite and serpentinite (Table IV.5).

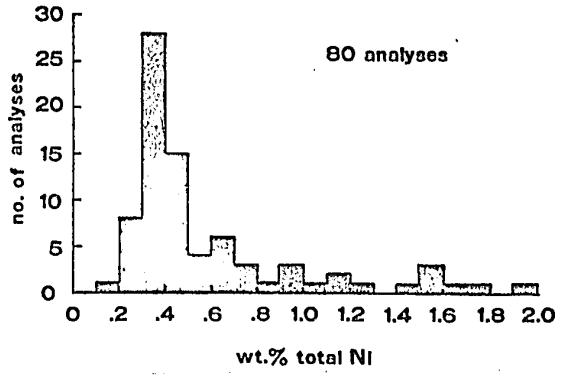

Fig.V.5. Distribution of total nickel in Area I serpentinites. Data from three drill holes.

The simple relation between sulphide and silicate nickel demonstrated for Area III (Fig.IV.12) is not apparent in Area I. Sulphide nickel values vary between zero and about 2.0%, whereas silicate nickel values vary between .05% and about .5% (Fig.V.6). For total nickel values below about 0.4% there is a tendency for sulphide and silicate nickel to have an inverse relationship. Above 0.4% there is no clear relation and the silicate nickel tends to stay at a constant value relative to the sulphide nickel.

The distribution of sulphur in the ultramafic rocks of Area I is shown in Figure V.7. The modal value is in the class interval .1% to .2%, and the arithmetic mean is .41%. These values indicate that the sulphur content of the ultramafics of Area I is somewhat higher than normal (see p.85).

G CONTACT METAMORPHISM AND METASOMATISM

Many of the contacts between the serpentinite and granite are faults, so that original relations are destroyed. A significant number of contacts are, however, marked by monomineralic selvedges of biotite, anthophyllite and talc between the granite and

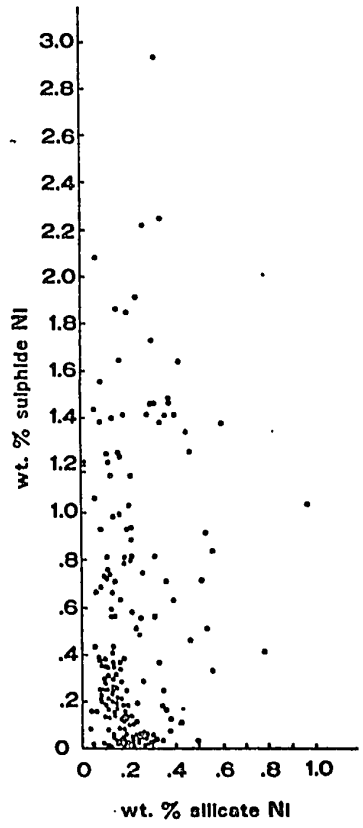

Fig.V.6. Relation between silicate and sulphide nickel in Area I serpentinites. Data from four drill holes.

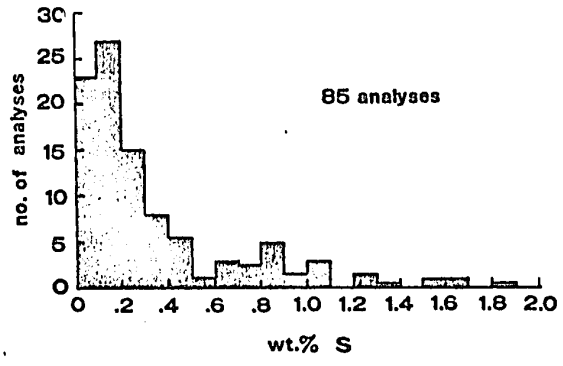

Fig.V.7. Distribution of total sulphur in Area I serpentinites. Data from three drill holes.

serpentine. These selvedges are all narrow, never more than about $1\frac{1}{2}$ inches in width, and frequently $\frac{1}{4}$ inch or less; the contacts are all sharp.

Monomineralic zones of this type occur at contacts of ultramafic rocks either as a result of amphibolite facies regional metamorphism (Phillips and Hess, 1936; Read, 1934) or by the intrusion of granite dykes into an ultramafic body (Larsen, 1928; Greenwood, 1963). The production of zones from the intrusion of granite pegmatite has been observed at the Manibridge Mine (location 4, Fig.II.2); (Coats and Brummer, 1971) and elsewhere in the Manitoba Nickel Belt (Coats, 1966; Wilson et al., 1969).

Greenwood (1963, Figs. 1 and 3) has shown that anthophyllite is stable in the presence of water between about 680°C and 780°C at a total pressure of 4 kbars. Extrapolation of data to higher pressures indicates an increase in these temperatures, and to lower pressures a decrease. These temperatures are above the stability range of serpentine, and anthophyllite only forms within the stability range of serpentine at pressures around 1 kbar at high molar concentrations of CO_2 (Johannes, 1969).

At constant temperature and pressure which will exist during regional metamorphism the formation of the monomineralic zones necessitates a steep gradient in the activity of H_2O (Greenwood, 1963). Regional metamorphism will result in the initial conversion of the serpentinite to an assemblage of chlorite and amphibole (O'Hara, 1967, Fig.4). Alternatively, the metamorphism may have occurred prior to serpentinization. The activity gradient in H_2O is reduced if a thermal gradient is present, a situation that would exist along the margin of a dyke. In this case anthophyllite

would develop adjacent to the dyke down to the appropriate temperature at which stage the reaction anthophyllite + vapour = talc + forsterite will occur. Thus anthophyllite can be produced locally i.e., along a dyke margin, without dehydration and conversion of the whole serpentine body. These stability relations imply a zone of forsterite and talc between the serpentinite and anthophyllite which may be reserpentinized on cooling.

It may be concluded that if anthophyllite forms as a result of regional metamorphism producing pervasive high temperature, then the whole serpentine body must convert to a higher temperature assemblage. Anthophyllite may also form locally under the influence of a thermal gradient away from a dyke; the serpentine beyond the range of the contact metasomatism is not affected.

An ultramafic rock containing anthophyllite which formed as a result of either regional or thermal metamorphism may subsequently be serpentinized. Amphiboles serpentinize readily (Wicks, 1969; Francis, 1965) and those in Area I are entirely serpentinized (Plate 12). Thus, it can be concluded that the anthophyllite selvedges developed subsequent to the serpentinization.

Cleavage in the serpentinite is occasionally truncated by the monomineralic selvedges. In one serpentinite fragment, cleavage is truncated by the intrusive contact and intruded by fine veins of the granite.

It is concluded that in Area I, these selvedges have been formed due to the post-serpentinization intrusion of granitic dykes.

In the Manibridge mine, (Fig.I.2), intrusive pegmatite dykes up to 50 feet in width intersect the ultramafic body to produce

similar contact zones (Coats and Brummer, 1971, p.159) suggesting that the whole body has been shattered and invaded by the granite pegmatite (Wicks, personal communication, 1972).

Phlogopite is ubiquitous in Area I serpentinites. It occurs as colourless to light green euhedral crystals throughout the serpentinites but is concentrated slightly towards the margins of the bodies. It is frequently closely associated with spinel which lacks a magnetite rim (Plate 36). In other examples the rim is incomplete and appears to have been disrupted (Plate 35). The margin of the chromite adjoining the phlogopite frequently shows signs of intergrowth, (Plates 36 and 45). The margin of the chromite illustrated in Plate 45 is fragmented, resulting in a chequer-board texture with fragments enclosed by phlogopite. Homogeneous chromite rimmed by magnetite (Table V.3) but not associated with phlogopite contains more Al_2O_3 than chromite associated with phlogopite.

It is shown in Chapter VII that the magnetite rim results from serpentinization; hence, if the magnetite rim is disrupted by phlogopite, it must be post-serpentinization.

It is difficult to determine the phlogopite distribution in diamond drill core but it appears to be developed in contact zones. It is certainly not present in uniform amounts and its presence is reflected by the bulk composition of the serpentinites (Table V.1).

It is concluded that phlogopite develops at a late post-serpentinization stage probably associated with the intrusion of the granitic dykes.

H SUMMARY

The serpentinites of Area I, originally dunite and peridotite, are lensoid in shape and have been intricately faulted and sliced along with the granite country rocks west of the metavolcanic and metasedimentary units (Fig.II.1).

The ultramafic rocks are in an advanced stage of serpentinization, but patches of fresh olivine are common. Mesh-textured serpentine pseudomorphs the olivine and bastite the pyroxene. Some serpentinized amphibole is also present. Only lizardite has been identified in the serpentine textures; clinochrysotile and antigorite have not been observed. Brucite has not been recognized. Chrome spinel is either homogeneous or exsolved into two phases. It has a variable composition and is usually surrounded by a magnetite rim that formed during serpentinization. Continuously zoned ferritchromit rims have not been observed. The primary silicates appear to have had an interlocking texture and relict cumulus texture is far less common than in Area III. Phlogopite and chlorite are common post-serpentinization minerals.

Pentlandite, millerite and minor heazlewoodite, violarite and polydymite are irregularly distributed throughout the serpentinite. The sulphide mineralogy is secondary, but coarse pentlandite and millerite occur interstitially to serpentinized olivine with a texture suggestive of replacement of primary sulphide. Fine-grained pentlandite, millerite and heazlewoodite probably formed during serpentinization. There is no evidence that gravity concentration has operated in the formation of the coarse sulphides.

VI COMPARISON OF SERPENTINITES IN AREAS I AND III

Data on the serpentinites in Areas I and III have been presented in Chapters IV and V. This data is now summarized (Table VI.1) and conclusions drawn about the geological history of the respective serpentinites.

The ultramafic rocks in Area III are serpentinized dunite with lizardite and clinochrysotile mesh textures (after cumulus olivine) partly replaced by antigorite. Accessory chromite is rimmed by ferritchromit which varies continuously in composition towards magnetite. Sulphides are scarce; secondary millerite formed during serpentinization predominates. Antigorite is interpreted as resulting from medium to low-grade metamorphism subsequent to serpentinization.

The wall-rocks are garnetiferous quartz-mica schist, plagioclase amphibolite and tremolite-chlorite schist in the epidote-amphibolite facies of metamorphism.

Mineral assemblages on either side of the contact are consistent with equilibration between the serpentinite and wall-rock as a result of low- to medium-grade metamorphism.

It can be concluded that the ultramafic was regionally metamorphosed after serpentinization to the epidote-amphibolite facies.

Post-serpentinization and post-metamorphism CO_2 metasomatism has obscured much of the contact relationship.

No contact metamorphic aureole has been observed in the wall-rocks. This, taken in conjunction with the disrupted nature of the serpentinite, suggest tectonic emplacement rather than magmatic

emplacement. However, the serpentinite is not sheared except at the contacts and there are no structures indicative of pre-serpentinization deformation. This is interpreted to mean that if tectonic emplacement occured then the margins of the ultramafic were able to absorb all the stress so as to preclude all internal deformation. It may be that the talc evident in the talc-carbonate schist provided the horizon along which all movement occured.

The ultramafic rocks in Area I are serpentinized dunite and harzburgite with lizardite mesh textures after olivine and lizardite bastite after pyroxene. Antigorite and chrysotile have not been observed. Relict chromite has a variable composition indicating a complex history, prior to serpentinization. Chromite has a magnetite rim but ferritchromit has not been observed. Sulphides, principally millerite and pentlandite are common, with textures suggesting that they replaced primary (magmatic) sulphides.

The serpentinites are in places heavily sheared and intermingled with country rock. The contacts are marked by selvedges of biotite-anthophyllite and talc, which are interpreted to result from the late intrusion of granitic dykes. Phlogopite, abundant towards the contacts, is also a result of late metamorphism.

Serpentinites with characteristics of those in Area I are not found in Reservation 34 outside of Area I. The remaining serpentinites all have the characteristics of those in Area III.

The Area III serpentinites which are enclosed in supracrustal rocks are poor in Ni and have been metamorphosed to the epidote-amphibolite facies subsequent to serpentinization. The Area I serpentinites contain a greater amount of Ni, are emplaced

in granitic rocks and have undergone local metasomatism but not regional metamorphism subsequent to serpentinization.

The serpentine textures in Area I (Plates 26 and 27) are very similar to the sub-rectangular mesh textures and the close spaced sub-parallel veinlets of fibrous serpentine illustrated and described by Coats, (1968) as two of the common serpentine textures of the Manitoba Nickel Belt. The mesh texture illustrated in Plate 26 is regarded by Wicks (personal communication, 1972) as typical of Manitoba Nickel Belt serpentinites.

Area III serpentinites, containing lizardite-chrysotile mesh textures replaced by antigorite, do not fit into the sequence of serpentine mineralogy established by Wicks (1969)(Fig.I.3), which serves to emphasize their distinct nature from the Manitoba Nickel Belt-type serpentinites. If Area III serpentinites are to be fitted into the Manitoba Nickel Belt sequence of serpentinites on the basis of mineralogy and texture, then they would be expected to outcrop to the NE of location 1, Figure I.3, as they contain antigorite in addition to lizardite-chrysotile mesh textures. The fault mechanism that would have to be postulated to accomplish this is unreasonable. It is more likely that they have a different origin entirely; their wall-rocks are consistent with their being part of an Archaean greenstone belt and it is possible that a portion of the Cross Lake sub-Province extends beneath Reservation 34 (Fig.III.1).

It is clear that Area I serpentinites closely resemble those from the Manitoba Nickel Belt and that they differ in mineralogy, texture and evolution from those in Area III. Thus within a short distance of each other are representatives of two different groups

Table VI.1. Salient differences between Area I and III ultramafic rocks.

	AREA I	AREA III
Protolith	Dunite and herzburgite	Dunite
Serpentine mineralogy	Mesh-textured serpentine with lizardite rims and centres.	Mesh-textured serpentine with lizardite centres and lizardite-clinochrysotile rims. Antigorite (and minor chlorite and tremolite) replaces the mesh-textured serpentine.
Spinel mineralogy	Chromite with a variable but homogeneous composition or a two-phase exsolution texture surrounded by magnetite rims. Magnetite also occurs as discrete grains.	Chromite with ferritchromit alteration rims. Magnetite may occur at the outer margin of some rims and as discrete grains in the serpentinite.
Sulphides	Coarse interstitial grains of pentlandite, heazlewoodite and millerite apparently replacing a primary sulphide. Fine disseminated grains of millerite, heazlewoodite and pentlandite. Violarite, pyrite, pyrrhotite and chalcopyrite also occur.	Minor millerite and pyrite as fine disseminated grains.
Contact metamorphism	Anthophyllite $\pm$ talc and biotite as selvedges separating serpentinite from late granite dykes.	Obscured by later contact metasomatism.
Contact metasomatism	nil	Talc-carbonate alteration.
Country-rocks	Granite, gneissic granite with minor amphibolite. Amphibolite facies of metamorphism.	Argillite, quartz-magnetite schist, plagioclase-amphibolite and tremolite-chlorite schist. Epidote-amphibolite facies of metamorphism.
Ni-content	Very variable from 0.2% to 2.0% total Ni.	About .22% total Ni, which corresponds to the average Ni content of dunite.

of ultramafic rocks.

In Chapter VIII the zoning in the chrome spinels in both areas is examined in the light of these conclusions.

VII COMPOSITIONAL VARIATION IN CHROMITE

A INTRODUCTION

Spinels from Reservation 34 exhibit zoning and inhomogeneities involving chromite, ferritchromit and magnetite. In chapter VIII these features are used to interpret the geological history of the serpentinites and it is therefore necessary to discuss the spinel group of minerals from the point of view of their occurrence in ultramafic and mafic rocks. Compositional trends due to magmatic, late magmatic and post-magmatic crystallization are reviewed in order to interpret the observed zoning in chromite from Reservation 34.

The chapter is a summary, a discussion and an interpretation of data reviewed from the literature and presented in more detail in Appendix I.

B THE SPINEL GROUP OF MINERALS

The spinel group of minerals, of general formula $R^{2+}R_2^{3+}O_4$ is divided into the spinel series, the magnetite series and the chromite series, depending on whether the trivalent cation is Al, Fe or Cr respectively. The type structure is that of the mineral spinel, $MgAl_2O_4$, which is cubic close packed and has eight formula units per unit cell. Extensive solid solution between end members, variations in cation coordination and cation deficient structures occur in all spinel group minerals.

A convenient means of representing the spinel group minerals is by a triangular prism (Stevens, 1944). The triangular faces represent the divalent oxides MgO and FeO, and the three prism

axes the trivalent oxides Fe_2O_3, Cr_2O_3 and Al_2O_3 (Fig.VIII.4). Thus the six important end members are represented by the corners of the prism; these are, with their mnemonic abbreviations:

$FeCr_2O_4$ ferrochromite (chromite) FC	$MgCr_2O_4$ magnesiochromite MC
$FeAl_2O_4$ hercynite FA	$MgAl_2O_4$ spinel MA
Fe_3O_4 magnetite FF	$MgFe_2O_4$ magnesioferrite MF

Spinel compositions may be represented by three types of planar projection from the prism devised by Stevens (1944), (Fig.VIII.4).

Experimental work indicates extensive solid solution between end members of the spinel group at about 1300°C (Ulmer, 1969; 1970), a temperature at which spinel might crystallize from an ultramafic crystal-liquid mush. Limits of solid solution at lower temperatures are less well known. There is a miscibility gap between magnesioferrite and spinel (S.S.) at 1250°C, (Kwestroo, 1959), and between magnetite and hercynite below 860°C (Turnock and Eugster, 1962). Stability of spinel group minerals varies with fo_2 (Ulmer, 1969).

Cation deficient structures, resulting from a replacement of three divalent cations by two trivalent cations, are more numerous in synthetic than in naturally occurring spinels (Ulmer, 1970, p.264). The negligible departure of natural chromite from the ideal formula has been demonstrated by Irvine (1965, p.650).

Ferritchromit is a term first used by Spangenberg (1943) to describe highly reflecting borders to chromite in some serpentinized ultramafic rocks. These borders are depleted in MgO and Al_2O_3 compared to the chromite core, and thus ferritchromit describes an Al- and Mg-poor chromite. It does not represent a mineral of specific composition.

C LITHOLOGICAL ASSOCIATIONS OF CHROMITE, MAGNETITE AND FERRITCHROMIT

Chromite is an early crystallizing mineral in ultramafic rocks, characteristically associated with olivine in peridotites. It is also found in pyroxenites though there is a tendency for chromite and pyroxene to be mutually exclusive. Chromite occurs in chromitite segregations, or as an accessory mineral.

Magnetite is normally associated with the later products of differentiation: gabbro, anorthosite and basalt. It also occurs as a secondary mineral resulting from various oxidation processes, including serpentinization. The separation in both space and time of magnetite and chromite has been verified experimentally by Hill (1969), and theoretically explained by Irvine (1967, Fig.3).

Ferritchromit has been described only as a zone around chromite and not as discrete crystals. Five of the chromite analyses listed by Stevens, (1944, Fig.4) are ferritchromit but no further information is given.

D ACCESSORY CHROMITE AS A PETROGENETIC INDICATOR

The use of chromite as a petrogenetic indicator is based on a correlation of geologic environment with compositional changes in chromite. Thayer (1970) and Irvine (1967) have distinguished the compositional fields of chromite from layered and Alpine-type ultramafic intrusions (Fig.VII.1, VIII.2); Irvine (1967), from ultramafic nodules in basalt (Fig.VIII.2); and Aumento and Loubat (1971), from Mid-Atlantic Ridge serpentinites (Fig.VIII.2). More information is available on the composition of layered or podiform ore chromite than on accessory chromite from the enclosing ultramafic rock. Chromite segregations have not been observed in the

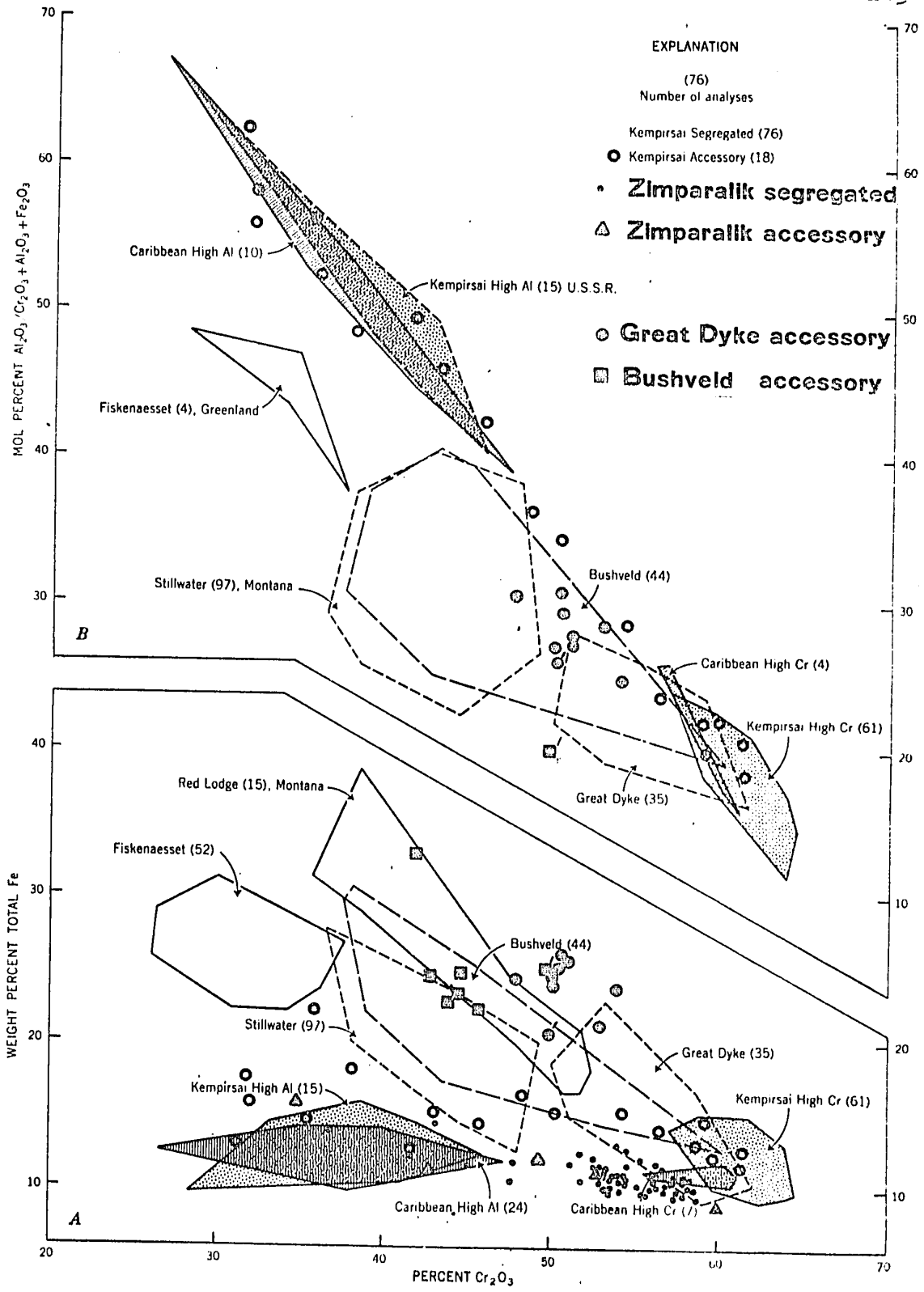

Fig.VII.1. Variation diagram illustrating the trend of chromite composition from layered and podiform chromitites (Thayer, 1970). Data points for the Great Dyke, the Bushveld and Zimparalik chromite have been added by the author, and their significance is discussed in the text.

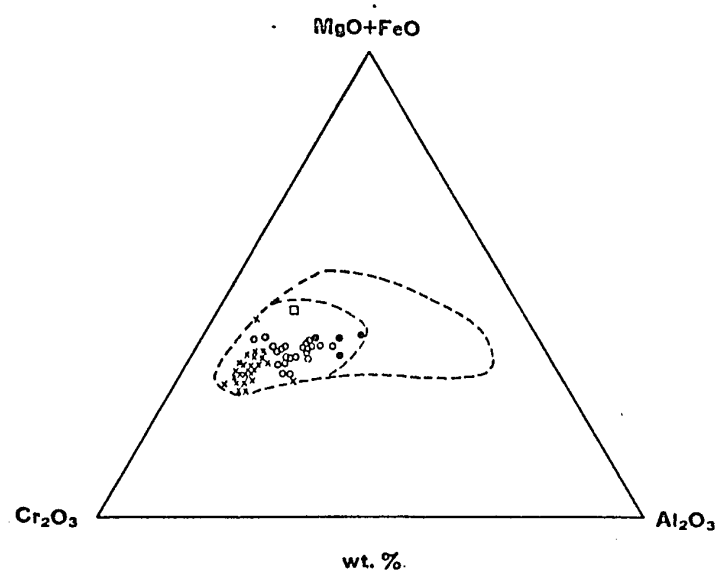

Fig.VII.2. Compositional variation in chromite from ultramafic rocks. All iron plotted as FeO.

- ∘ Chromite associated with settled plagioclase from the Fiskenaesset and Sittampundi Complexes.
- ∘ Chromite associated with settled orthopyroxene from the Bushveld Complex.
- × Chromite associated with settled olivine from the Bushveld Complex, the Great Dyke, the Stillwater Complex and from eastern Sierra Leone.
- □ Chromite associated with anorthositic gabbro from the Bushveld Complex.

Source of data:-
Bushveld Complex-van der Walt, 1941; Cameron and Emerson, 1959; Cameron and Desborough, 1969.
Fiskenaesset Complex-Ghisler and Windley, 1967.
Great Dyke-Worst, 1960.
Sierra Leone-Dunham et al., 1968.
Sittampundi-Subramaniam, 1956.
Stillwater-Beeson and Jackson, 1969.

The additional data to show the extended field of chromite composition from orogenic type ultramafic rocks, and ultramafic nodules in olivine basalt* have been derived from Stevens, 1944; Ross, Foster and Myers, 1954; Green, 1964; Frisch, 1971).

*(indicated by a dashed line).

serpentinites of Reservation 34. If the existing data on chromite is to be used to interpret the geological history of Reservation 34 serpentinites, it is necessary to establish that accessory chromite displays the same compositional trends as segregated chromite in the same ultramafic body.

Thayer (1970) has plotted analyses of ore and accessory chromite from the Kempirsai Pluton (Pavlov and Chuprynina, 1967) and in this case the compositional trend of the two is similar. The writer has plotted analyses of both ore and accessory chromite from Alpine-type intrusions in SW Turkey (Engin and Hirst, 1970) and these are found to follow a similar trend (Fig.VII.1). Accessory chromite from the Western Bushveld (van der Walt, 1941) the Eastern Bushveld (Cameron and Emerson, 1959) and the Great Dyke (Bichan, 1969; Appendix V, Table XI) have also been added to the variation diagram; the trend apparent from the ore chromite is continued or exemplified by the accessory chromite (Fig.VII.1). Thus, in an ultramafic body with no chromite segregations, compositional trends of accessory chromite are comparable to those from ore chromite, allowing the use of accessory chromite as a petrogenetic indicator.

E COMPOSITIONAL VARIATION IN MAGMATIC CHROMITE

Variation diagrams to distinguish fields of chromite from various types of ultramafic intrusion have been devised by Thayer, (1970), Engin and Hirst, (1970) and Irvine, (1967; 1965). These diagrams show that chromite from different types of ultramafic rocks have distinct, although sometimes overlapping, fields of composition. Thayer's diagrams also illustrate different

compositional trends for chromite from stratiform and podiform chromitites.

In chromite from stratiform complexes total Fe and Al_2O_3 increase with decreasing Cr_2O_3; in chromite from podiform and other intrusions, total Fe remains constant, and Al_2O_3 increases rapidly with decreasing Cr_2O_3. The compositional trend for chromite from stratiform complexes (Fig.VII.1) also reflects a differentiation trend: chromite from the Great Dyke is associated with settled olivine, from the Bushveld Complex with settled olivine and pyroxene and from the Fiskenaesset Complex with settled plagioclase. The same trend is apparent on a ternary plot of Al_2O_3-Cr_2O_3-(total FeO + MgO) to which the compositional field of chromite from non-stratiform intrusions has been added (Fig.VII.2).

These trends are recognized in individual intrusions. Van der Walt (1941) showed the Cr_2O_3 content of chromite in the Western Bushveld to decrease with elevation in the layered series; this decrease is compensated by an increase in Al_2O_3 in the lower seams and Fe_2O_3 in the upper (Irvine, 1967, p.87). Chromite from the Hartley Complex of the Great Dyke of Rhodesia (Worst, 1960, Table 30) shows systematic inverse relations between Cr_2O_3 and total iron, while Al_2O_3 tends to remain constant. The trends in chromite composition in non-stratiform intrusions are not always easily related to coexisting mineralogy. Other factors such as pressure (Green, 1964) affect Al-content of the spinel. However, in New Caledonia, the main peridotite mass is cut by dunite which is transitional in the upper section to noritic gabbro and

anorthosite. There is a rise in Al_2O_3 content of the chrome spinel in passing from dunite through the pyroxene- and plagioclase-bearing rocks of the transition zone to gabbro and anorthosite (Guillon and Lawrence, 1971, p.425).

Lapham (1964) notes that spinel in dunites of the Mayaguez serpentinite is Cr-Fe rich whereas spinel in augite harzburgite is Mg-Al rich.

Early chromite from the Makaopuhi Lava flow, Hawaii (presumably a xenocryst from an ultramafic body shows increasing Al_2O_3 with decreasing Cr_2O_3, a trend interpreted as of primary magmatic origin (Evans and Moore, 1968). Thayer (1970) showed that the increase in total Fe with decreasing Cr_2O_3 which was such a noticeable feature of chromite from layered intrusions is only slight in the case of podiform deposits from orogenic ultramafic bodies (Fig.VII.1). Chromite from partially serpentinized peridotite, harzburgite and lherzolite from SW Turkey (Engin and Hirst, 1970), conform to this (Fig.VII.1). However, van der Kaaden's (1959) variation diagrams of ultramafic rocks in the same general area suggest a very slight decrease in total Fe, an increase in Al_2O_3 and an irregular but slight decrease in MgO with decreasing Cr_2O_3. It is reasonable to conclude that there is an increase in Fe and Al with decreasing Cr, but not necessarily both together. This is apparent on the variation diagram in Figure VII.2 as a trend away from the Cr_2O_3 corner towards the (MgO + FeO) - Al_2O_3 boundary. The fact that either Fe or Al increases may be due to the fact that in the hercynite-magnetite series Fe or Al enrichment is dependent on fO_2 (see Appendix I).

Trends involving TiO_2 are not consistent and to some degree depend on whether Ti occupies a divalent or trivalent site in the crystal lattice (Appendix I). A tendency for TiO_2 to increase with continued magmatic crystallization is expected by analogy with lunar spinels (see below) and terrestrial chrome spinels included as xenocrysts in basalt. Hill (1969, Fig.16) has observed experimentally an increase in TiO_2 with decreasing Cr_2O_3 although the trend is very slight in the chromite compositional field as compared to the magnetite field. No clear relation between TiO_2 and Cr_2O_3 could be found in the Great Dyke (Worst, 1960; Bichan, 1969) or in the Rhum intrusion (Henderson and Suddaby, 1971), although locally it is possible to demonstrate an increase in TiO_2 with decreasing Cr_2O_3. In the Makaopuhi Lava lake, Hawaii, the trend of markedly increasing TiO_2 with decreasing Cr_2O_3 is only apparent at a comparatively late magmatic stage when early crystallized chromite is re-equilibrating to an ulvospinel-magnetite solid solution while enclosed in a basaltic magma.

Henderson and Suddaby (1971) have presented evidence from the Rhum ultramafic intrusion for a magmatic alteration whereby olivine and plagioclase react with interstitial liquid to produce spinel ($MgAl_2O_4$) and liquid. The spinel enters into solid solution with previously formed chromite to produce picotite. The composition of these spinels has been plotted in Figure VII.3. Spinels 13 and 15* are enclosed by olivine crystals and insulated from further magmatic reaction; they may be taken as being representative of

*The numbers refer to the analysis numbers given by Henderson and Suddaby.

Figure VII.3-Explanation

The field of chromite from layered and Alpine-type intrusions is based on Thayer (1970,fig.2) but generalised to include the writer's data presented in figure VII.1.

◇——◇ Primary and altered chromite from the Makaopuhi lava flow (Evans and Moore,1968).

▫ ▫ Primary and altered chromite from Apollo 12 basalts (Haggerty and Meyer,1970).

△------△ Primary and altered chromite from Apollo 12 basalts and gabbros (Reid,1971).

• Chromite from the Rhum layered intrusion (Henderson and Suddaby,1971).The numbers refer to the authors' analyses from which the data points were plotted.

o Chrome spinel from transition basalts,British Tertiary Volcanic Province (Ridley,1972).

The chromite is surrounded by,or altered to,a Ti-rich phase (except that from the Rhum intrusion No.s 3 to 15).Ti is not a variable in the diagram nor does it have a spinel structure and so the variation diagram does not entirely represent the compositional change.The zoning is the result of the substitution $Ti + (Mg, Fe^{2+})$ for $2(Cr + Al)$;at an advanced stage of substitution the mol.% $Al_2O_3 / Al_2O_3 + Cr_2O_3 + Fe_2O_3$ fluctuates and becomes meaning less because of the small quantities involved.For this reason the most Ti-rich phases have not been plotted on the diagram utilising this ratio as a variable.

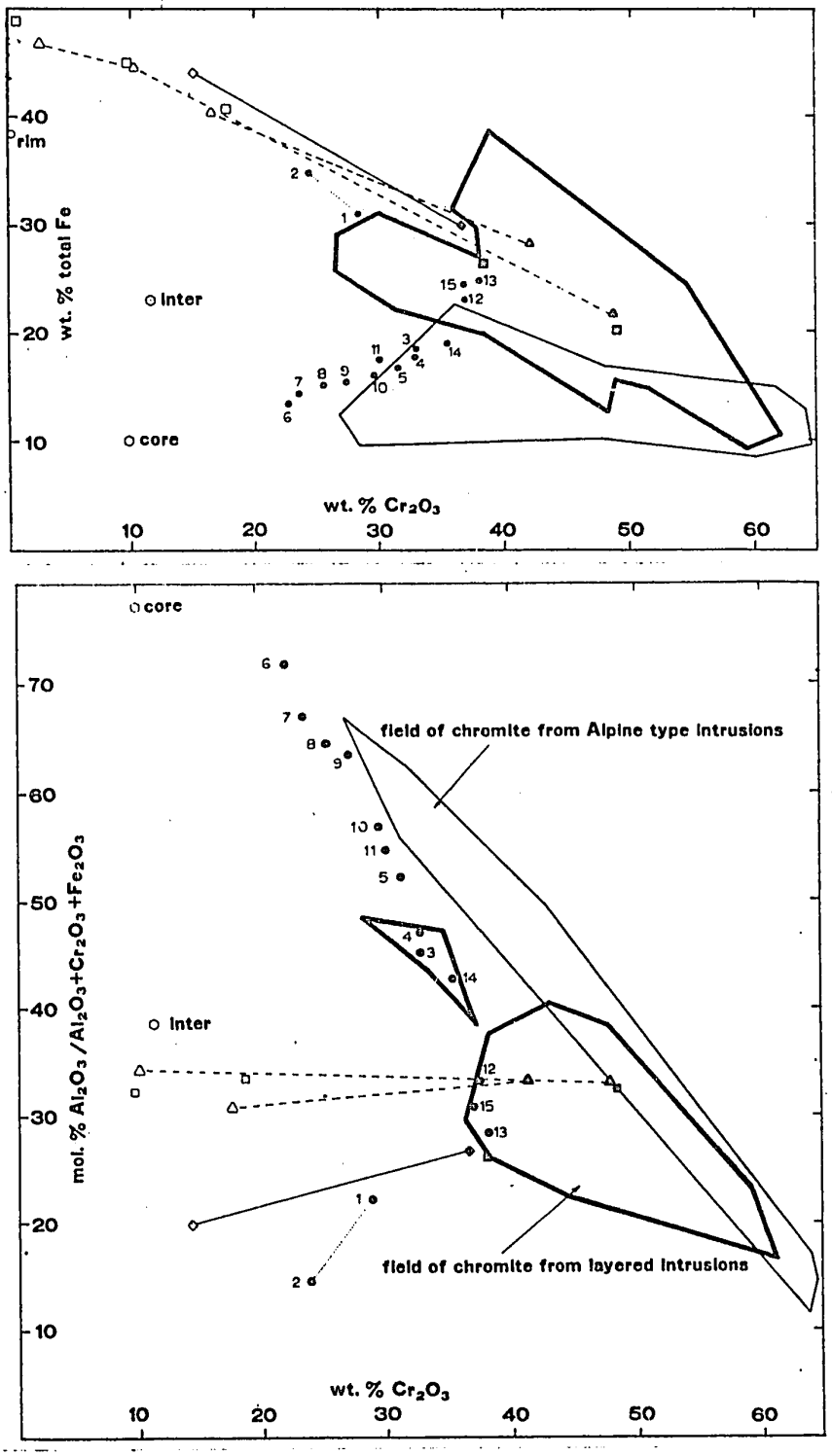

Fig.VII.3.. Compositional trends in chrome spinel resulting from magmatic and late magmatic reactions. (The explanation is on the facing page).

the original chromite composition. Chromites 12 and 14 are partly enclosed by olivine and have undergone some later reaction. The remaining chrome spinels have undergone the reaction outlined above that involves an increase in Mg and Al and a decrease in Cr and Fe. The trend of these chromites is parallel to and extends that of the Alpine-type intrusions on both diagrams of Figure VII.3. The overall trend is towards spinel, $MgAl_2O_4$.

Ridley (1972) has described chrome spinels from basalts in the British Tertiary igneous province where the eruptive rocks are generally regarded as related to the intrusive rocks, of which the Rhum layered intrusion is one example (e.g., Hatch, Wells and Wells, 1961). Note that the core of a chrome spinel from one of these basalts falls along the extension of the compositional trend of the chromite from the Rhum layered intrusion (Fig.VII.3).

Chromite may undergo magmatic corrosion resulting in the removal of MgO and Al_2O_3 with the concomitant production of silicates, notably pyroxene, anorthite and olivine (Thayer, 1956, p.42; 1946, p.206). Zoning has not been recorded in corroded spinels. A similar reaction has been postulated by Ridley (1972) whereby at a late magmatic stage and at 'low' temperature aluminous chromite reacts with liquid to produce Al-poor chromite and plagioclase. Ridley's results are available only in abstract form; it is not clear whether this reaction produces zoning of the spinel. The compositional trends would be in the reverse direction to those depicted in Figures VII.1 and VII.2.

Zoning has not been recorded in primary magmatic chromite in unserpentinized ultramafic rocks (Henderson and Suddaby, 1971;

Beeson and Jackson, 1969; Thayer, 1969; Golding and Bayliss, 1968; Jackson, 1963). A microprobe scan by the author across an accessory chromite in the Great Dyke, Rhodesia, similar to the one shown in Plate 32 , showed that the composition was constant (Table XI, Appendix V).

The following conclusions are drawn from the above data concerning the compositional variation in chromite resulting from magmatic crystallization:- (1) primary chrome spinels are homogeneous in composition; (2) early-formed chrome spinels are enriched in Cr_2O_3 whereas late-formed spinels are depleted in Cr_2O_3 and enriched in Al_2O_3 and Fe_2O_3; there may also be a slight increase in TiO_2; (3) the compositional fields of chromite from layered intrusions, Alpine-type intrusions, ultramafic nodules and Mid-Atlantic ridge serpentinites are distinct though overlapping; (4) chromite in layered and Alpine-type intrusions have divergent compositional trends.

F ZONED CHROMITE RESULTING FROM LATE MAGMATIC REACTIONS

1 Ultramafic Nodules in Basalt

Zoning is recorded in chromite in ultramafic nodules enclosed as xenoliths in alkali basalt (Frisch, 1971; Muir and Tilley, 1964; White, 1966). The opaque highly reflecting margins are depleted in Cr and Al and enriched in total Fe relative to the dark chromite core (Table VII.1). The microprobe traverse of a chromite grain in an ultramafic nodule from Lanzarote in the Canary Islands (Frisch, 1971) shows that the altered margin has the composition of ferritchromit. The compositional variation between core and rim is shown in Table VII.2 and in figures VII.4 and VII.5.

Table VII.1 Summary of the relative changes of major oxides between the chromite core and ferritchromit rim of zoned spinels.

	CHROMITE FROM ULTRAMAFIC INCLUSIONS IN BASALT.(3)		CHROMITE IN OLIVINE PHENOCRYSTS IN BASALT.(6)		CHROMITE FROM SERPENTINITES.(17)			
	core richer	rim richer	core richer	rim richer	core richer	rim richer	no change	
Al_2O_3	9,25		8,12,14		1,3,4,6,7,8,13, 17,19,20,21,24			Al_2O_3
FeO				8	4,10	1,3,17		FeO
Fe_2O_3			8			1,3,10,17,20		Fe_2O_3
Total Fe		9,18,25		2,8,11,12,26		7,14,19,21,22, 24		Total Fe
MgO	9		2,8,12,26		1,3,4,6,7,10,13, 14,17,19,20,21. 24			MgO
Cr_2O_3	9,18		2,8,11,12,26		3,6,17,20,24	3,4,7,15,19,24	7,14,17,21	Cr_2O_3
TiO_2		9		2,8,11,12,26		17	3	TiO_2
MnO		9				17	10	MnO
NiO		9				5,9,10,15,17,20 23	14	NiO
SiO_2	9					10,14		SiO_2
S						14	14	S
V_2O_3		9						V_2O_3
ZnO	9		8					ZnO

1 Amin,1948
2 Babkine,1965
3 Beeson and Jackson,1969
4 Den Tex,1955
5 De Waal and Hiemstra,1966
6 De Wijkerslooth,1943
7 Engin and Aucott,1971
8 Evans and Moore,1968
9 Frisch,1971
10 Golding and Bayliss,1968
11 Gunn,et al.,1970
12 Haggerty and Meyer,1970
13 Horninger,1941
14 Lepham,1964
15 Mihalik and Hiemstra,1966
16 Mihalik and Seager,1968
17 Miller,1953
18 Muir and Tilley,1964
19 Panagos and Otteman,1966
20 Simpson and Chamberlain,1967
21 Spangenberg,1943
22 Stephenson,1940
23 van der Kaaden,1970
24 Weiser,1966,1967
25 White,1966
26 Wright,1967

Table VII.2 Analyses of chromite and associated ferritchromit from zoned spinels.

	1	2	3	4	5	6	7	8
	Chromite							
Al_2O_3	18.60	19.30	10.97	31.80	24.17	13.00	30.60	10.70
Cr_2O_3	47.10	46.50	54.49	34.10	36.41	56.62	32.00	36.60
TiO_2	.71	.72	.26	.10	.00	-	.30	4.30
Fe_2O_3	2.10	1.42	3.62	6.30	12.84	-	7.40	14.90
FeO	19.70	21.10	19.68	7.70	2.55	18.22*	17.10	26.30
MgO	10.00	9.20	9.52	16.50	18.90	12.16	12.70	7.00
NiO	-	-	.05	0.00	-	-	.18	-
V_2O_3	-	-	-	.10	-	-	-	-
MnO	-	-	.29	.20	-	-	.20	.27
CaO	-	-	.31	.10	-	-	.01	-
SiO_2	-	-	-	.70	-	-	.09	-
ZnO	-	-	-	-	-	-	.25	.20
	98.20	98.24	100.01	97.60	94.87	100.00	101.00	100.27
	Ferritchromit							
Al_2O_3	3.10	6.60	2.41	20.20	11.84	2.50	19.60	3.60
Cr_2O_3	42.00	53.70	54.84	44.80	39.01	62.53	32.00	15.50
TiO_2	1.04	.72	.30	.10	.00	-	.40	18.40
Fe_2O_3	22.40	8.40	13.62	15.40	31.21	-	19.00	14.10
FeO	30.16	32.10	21.74	6.60	3.46	26.53*	17.20	43.90
MgO	2.10	1.68	5.87	11.50	10.86	8.42	11.30	2.80
NiO	-	-	.09	-	-	-	.24	-
V_2O_3	-	-	-	.10	-	-	.18	-
MnO	-	-	.44	.20	-	-	.21	.27
CaO	-	-	.35	.10	-	-	.02	-
SiO_2	-	-	-	.20	-	-	.10	-
ZnO	-	-	-	-	-	-	.04	.17
	100.80	103.20	99.66	99.20	96.38	100.01	100.30	98.74

Columns 1 to 6 contain analyses of chromite and ferritchromit from serpentinites;column 7 from an ultramafic nodule in basalt;and column 8 from a xenocryst in basalt.* indicates total iron. Col.1 and 2,Stillwater Complex (Beeson and Jackson,1969);col.3, Webster-Addie Complex (Miller,1953);col.4,Coolac serpentinite (Golding and Bayliss,1968);col.5,Barramia serpentinite (Amin,1948); col.6,Andizlik-Zimparalik area(Engin and Aucott,1971);col.7,Lanzarote (Frisch,1971);col.8,Makaopuhi lava flow (Evans and Moore,1968).

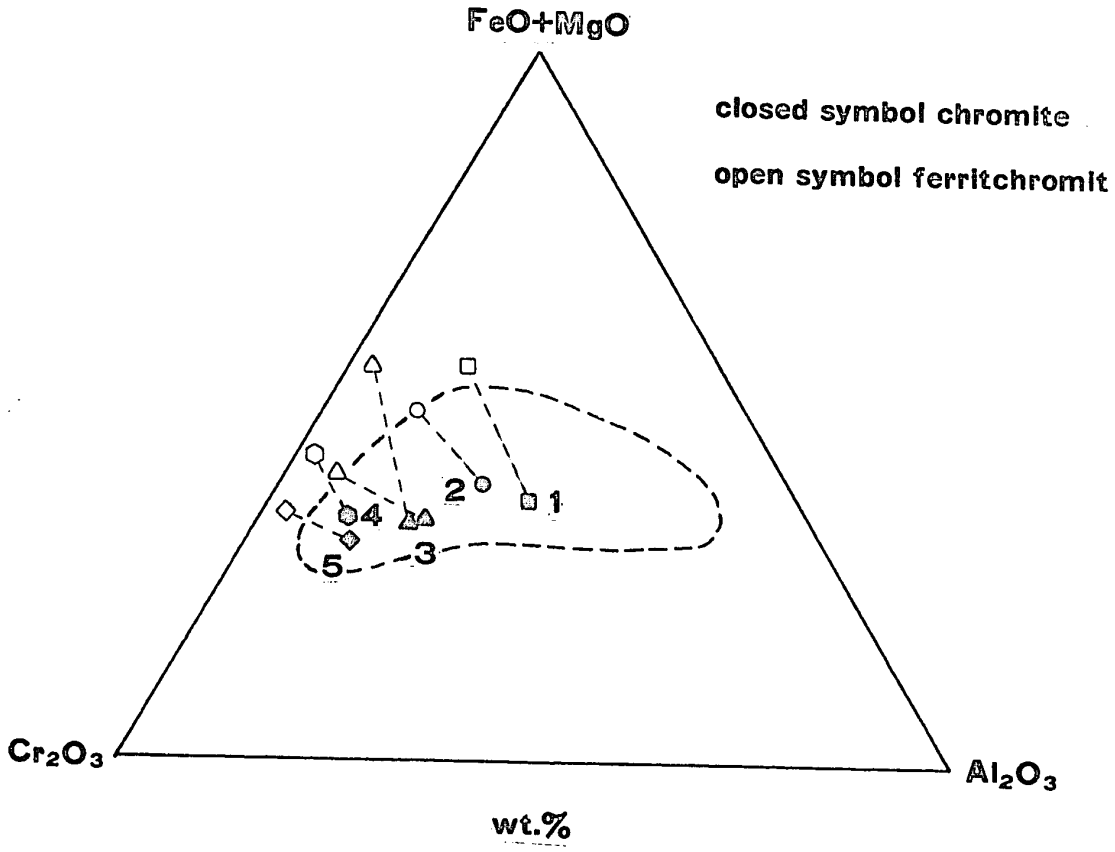

1 Lanzarote, Canary Islands (Frisch, 1971)
2 Barramia, Egypt (Amin, 1948)
3 Stillwater, Montana (Beeson and Jackson, 1969)
4 Webster-Addie Complex, N. Carolina (Miller, 1953)
5 Andizlik-Zimparalik, Turkey (Engin and Aucott, 1971)

1 Chromite from dunite nodule
2-5 Chromite from serpentinite

Fig.VII.4. Ternary variation diagram to illustrate the compositional trend of ferritchromit alteration (Plotted in weight percent). The field of chromite from ultramafic intrusions is taken from Fig.VII.2.

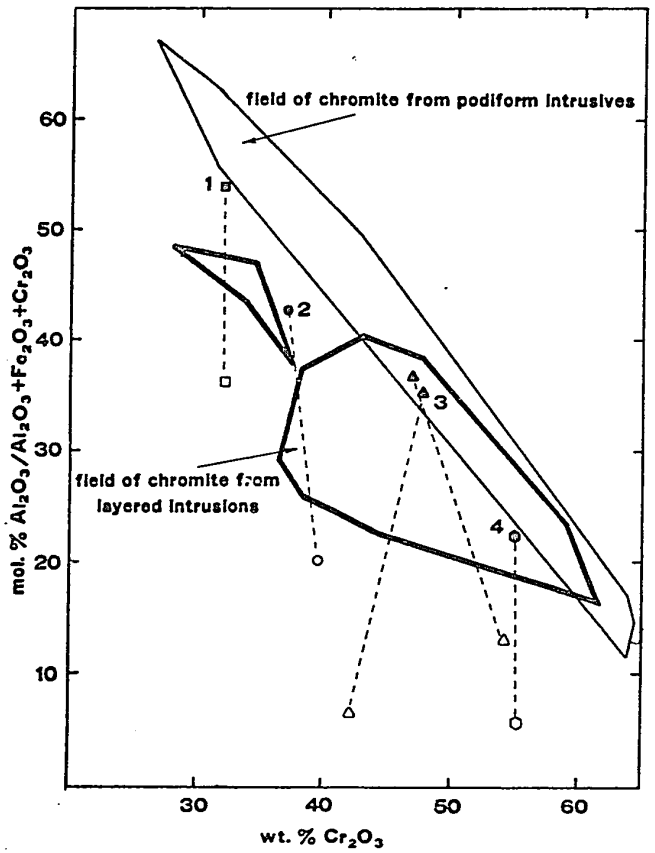

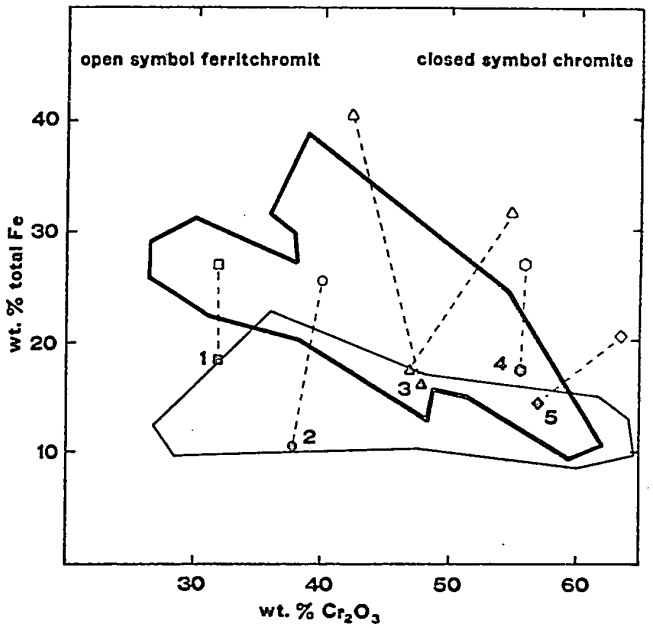

chromite from serpentinite, 2,3,4 and 5

chromite from a dunite nodule in alkali basalt, 1.

Fig.VII.5. Compositional plot of the trend of ferritchromit alteration. The compositional fields of chromite from layered and podiform chromitites are generalized from the data in Figure VII.1.

1. Lanzarote, Canary Islands (Frisch, 1971) 2. Barramia, Egypt (Amin, 1948) 3. Stillwater, Montana (Beeson and Jackson, 1969) 4. Webster-Addie Complex, N.Carolina (Miller, 1953) 5. Andizlik-Zimparalik, Turkey (Engin and Aucott, 1971).

Zoning in chromite from these nodules is not ubiquitous; the writer has made a microprobe traverse across a chrome spinel from a dunite nodule in basanite lava from the Grand Canyon (Best, 1970) and found it to be homogeneous.

2 Alkali Basalt

Chromite is found enclosed in olivine and orthopyroxene phenocrysts in alkali basalt. It may be unzoned (Wright, 1967), but more frequently it is zoned in a manner similar to that described for chromite from ultramafic nodules (Tables VII.1 and VII.2) (Ridley, 1972; Evans and Moore, 1968; Babkine, 1965). Chromite occuring in the groundmass of these rocks is frequently rimmed by ulvospinel or titanomagnetite which also occurs as discrete crystals in the groundmass (Gunn et al., 1970; Wright, 1967).

3 Lunar Basalts and Gabbros

Chrome spinel in lunar basalts is often surrounded by chrome ulvospinel of variable composition which in turn is surrounded by homogeneous ilmenite (Haggerty and Meyer, 1970) or by an ulvospinel only (Reid, 1971). Chrome spinel in lunar gabbros varies smoothly in composition from chromite cores to ulvospinel rims (Reid, 1971).

4 Discussion

Where chromite grains have been in contact with basalt magma they normally become zoned towards a titaniferous magnetite or an ulvospinel. Only rarely does ferritchromit occur between the core and the Ti-rich phase. This zoning is a result of the substitution of $Ti \pm (Mg,Fe)$ for $2(Cr \pm Al)$. The Al_2O_3 content decreases with

decreasing Cr_2O_3 content so that in the variation diagram involving Al_2O_3 (Fig.VII.3) the trend is a variance with the magmatic trend because Cr and Al are not replaced by Fe^{3+}. This trend is clearly illustrated for spinels from the Makaopuhi lava flow (Evans and Moore, 1968) from British Tertiary basalt (Ridley, 1972) chromite from some lunar rocks (Reid, 1971; Haggerty and Meyer, 1970). Two chromites from an olivine cumulate in the Rhum layered intrusion (Henderson and Suddaby, 1971, analyses 1 and 2) that have reacted with trapped pore fluid follow the same trend.

In the variation diagram in which total Fe is a variable (Fig.VII.3) the change to the Ti-rich spinel phase shows an increase in Fe^{2+} so that the compositional trend of chromite from layered intrusions is continued.

Chromite grains within ultramafic nodules, olivine or orthopyroxene phenocrysts in basalt tend to be surrounded by a zone with progressively decreasing amounts of Al_2O_3 and Cr_2O_3 and increasing Fe_2O_3 towards the rim, thus approaching the composition of ferritchromit. This implies migration of elements through the surrounding silicates. In some cases chromite enclosed in olivine is surrounded by a Ti-rich phase in addition to ferritchromit (Gunn et al., 1970).

It is concluded that chromite immersed in basaltic magma is surrounded by a rim of a Ti-rich spinel which is the stable crystallizing phase from that magma. Chromite insulated within silicate minerals from direct contact with the magma undergoes alteration whereby Al, Mg and Cr diffuse outwards and Fe, and sometimes Ti diffuse inwards to alter the chromite to ferritchromit.

This type of alteration is also evident in some spinels in direct contact with magma.

F ZONED CHROMITE IN SERPENTINITES

The simplest type of compositional zoning in chromite results from the formation of a rim of magnetite around a core of chromite. This has been observed in Casper Mountain, Wyoming (Stephenson, 1940); in the Red Lodge district, Montana (James, 1946); New Caledonia (Maxwell, 1949); the Abitibi area,(MacRae, 1969); the Great Dyke, Rhodesia (Plate 32) and in serpentinites dredged from the Mid-Atlantic Ridge (Aumento and Loubat, 1971, p.649) and the Palmer Ridge (Cann, 1971, p.613). There is no aluminous silicate associated with the alteration which has been correlated with the "Buckskin weathering" type of serpentinite, commonly enclosed by low-grade, unfoliated, metamorphic rocks (Thayer, 1956, p.653).

The chromite is homogeneous and surrounded by narrow selvedges of magnetite, with which it may or may not be in direct contact. Magnetite may line fractures through the chromite and also occurs as discrete grains throughout the serpentinite. The boundary between the chromite and magnetite is compositionally sharp and optically visible due to the higher reflectivity of the magnetite. This type of zoning is an additive process involving the deposition of magnetite, released on serpentinization of silicates, around the margins of chromite grains. Extremely sharp margins and corners of chromite beneath the magnetite rim (Plate 32) indicates that there has been no replacement of chromite.

Alternatively chromite in serpentinites may be surrounded by ferritchromit (Poitevin, 1931; Horninger,1941; Spangenberg, 1943;

de Wijkerslooth, 1943; Amin, 1948; Miller, 1953; Lapham, 1964; den Tex, 1955; Weiser, 1966, 1967; Panagos and Otterman, 1966; Mihalik and Hiemstra, 1966; de Waal and Hiemstra, 1966; Simpson and Chamberlain, 1967; Golding and Bayliss, 1968; Beeson and Jackson, 1969; Engin and Aucott, 1971). An aluminous silicate is invariably associated with ferritchromit. The alteration is correlated with the 'verde antique' type of serpentinization characteristic of foliated rocks in the greenschist and amphibolite facies of metamorphism (Thayer, 1956, p.693).

Chromite associated with the 'verde antique' type of serpentinization is rounded and optically zoned with the margins having a higher reflectivity than the core. The dark chromite core is homogeneous and passes with a sudden compositional change to light ferritchromit which then grades to magnetite at the rim (Plate 22). MgO and Al_2O_3 are invariably depleted and FeO and Fe_2O_3 enriched in the rim; Cr_2O_3 fluctuates erratically and may be enriched, depleted or remain constant; TiO_2 increases or remains constant (Table VII.1). The alteration occurs in two stages in which the first is an immediate loss of MgO and Al_2O_3 to yield ferritchromit and the second a more gradual decrease in MgO and Cr_2O_3 to change the composition of the ferritchromit towards magnetite. The presence of magnetite in the outer portion of the zoned spinel is rarely recorded (Table VII.2). The trend of this alteration of Thayer's (1970) variation diagrams (Fig.VII.5) and on a (MgO + FeO)-Cr_2O_3-Al_2O_3 ternary plot (Fig.VII.4) is markedly different from compositional variations due to magmatic stages of chromite crystallization.

The evidence suggests that the alteration of chromite to ferritchromit is a replacement process in which FeO and Fe_2O_3 replace Al_2O_3, MgO and to a lesser degree, Cr_2O_3. Photographs of zoned chromites (Miller, 1953; Golding and Bayliss, 1968; Beeson and Jackson, 1969; Simpson and Chamberlain, 1967; this thesis, Plates 22, 23, etc.) with well rounded cores and rims support this view. If the process was additive, that is, ferritchromit was crystallizing around chromite, then angular outlines similar to those illustrated in Plate 32 would be expected. Furthermore, if ferritchromit were a stable crystallizing phase discrete, interstitial crystals of ferritchromit in the serpentinite would be expected; they have never been recorded.

The compositional trend of ferritchromit alteration is away from the fields of primary magmatic chromite from ultramafic rocks and is in contrast to the trend characteristic of the magmatic phase of chromite development (Figs. VII.4 and VII.5, data points 2,3,4 and 5). The trend of ferritchromit alteration, that is, increasing total iron, decreasing Al_2O_3 with little variation of Cr_2O_3, is the same for chromite of widely different composition.

G ARTIFICIALLY HEATED CHROMITE

Compositional zoning has been described from a used refractory brick consisting of 40% magnesite and 60% raw chrome ore (Berry, Allan and Snow, 1950). Adjacent to the cold face of the brick the chromite develops a reticulate network of a highly reflecting constituent, probably Fe_2O_3. Inwards from the cold face a crystallographically orientated intergrowth of a highly reflecting material develops inside the chromite, while the margin is

surrounded by a lacey fringe of a highly reflecting material. As the fringe becomes better developed, the intergrowth disappears and the chromite develops a grey centre with a lacey fringe. Immediately adjacent to the hot face the chromite becomes a more uniform and complex solid solution with a dark rim. Chemical analyses show that in passing from the cold to the hot face the chromite becomes depleted in MgO, Al_2O_3 and Cr_2O_3 and enriched in Fe_2O_3. The authors conclude that $MgAl_2O_4$ in the chromite is more soluble than $MgCr_2O_4$ in the silicate matrix.

Silicate and direct bonded chrome-periclase refractory bricks show euhedral or angular secondary Fe-rich spinel as rims on chromite or as discrete crystals in the groundmass (Padfield et al. 1967). The secondary spinel may be separated from the chromite core by a line of irregular pore spaces. The formation of the secondary spinel causes expansion in bricks.

Brownell (1942) heated chromite from the Bird River sill, Manitoba, to 700°C and observed an exsolution phase which he assumed was hematite. Gait (1964) investigated this phenomenon further, heating specimens in air from 12 to 144 hours at 1000°C. Hematite exsolved in a Widmanstatten pattern, initially at the rims, but subsequently extending to the centre of the chromite. The Bird River chromite is altered; a highly reflecting Fe-rich phase surrounds, and penetrates through a chromite core. A homogeneous chromite from the Great Dyke of Rhodesia, similar to that illustrated in Plate 32 was heated for 6 weeks in air at 900°C. It exsolved into two phases (Plate 33) with a zonal arrangement that resembles that for the naturally occurring spinels (p.118).

Electron probe analyses showed that the dark phase was enriched in Al_2O_3 and MgO compared to the light phase.

H ZONED DETRITAL CHROMITE

Detrital chromite grains with more highly reflecting borders than cores occur in the Basal Reef of the Wiwatersrand System (Mihalik and Saager, 1968). The borders contain more Fe, and sometimes more Cr, but less Al and Mg than do the cores, and are intensified by adjacent radioactive uraninite. The authors conclude that at least some of the chromite heterogeneity resulted from alteration in the sedimentary environment.

Radioactive haloes have been described from chromite grains in the Elsberg Reef in the Orange Free State (Ramdohr and Schidlowski, 1965), but no chemical data are supplied.

Chromite grains in a Triassic conglomerate near Grenoble, France, have altered margins whereas those in a Carboniferous conglomerate do not. Grains in both conglomerates are supposed to have been derived from the Belledonne ultramafic body which contains chromite with altered borders. This led den Tex (1955) to suggest that the alteration of the chromite occurred after consolidation of the sediment and hence of the Belledonne ultramafic body.

I SUMMARY AND DISCUSSION

Chromite is associated with peridotite, and magnetite with the later products of differentiation, gabbro and anorthosite. The two are rarely found together as primary magmatic minerals. Ferritchromit occurs as a zone around chromite in both serpentinized and non-serpentinized ultramafic rocks and in some other rocks.

Chromites from rocks of differing origin occupy distinct fields in compositional variation diagrams and can be used as a petrogenetic indicator.

Various compositional trends of chromite may be recognized and are due to (1) primary magmatic crystallization of chromite; (2) late magmatic reactions and (3) post-magmatic reactions.

The magmatic trend involves an increase in Al_2O_3 and sometimes Fe_2O_3 with decreasing Cr_2O_3. In stratiform intrusions the increase of both Al_2O_3 and Fe_2O_3 with decreasing Cr_2O_3 is marked (Fig.VII.3). In Alpine-type intrusions the increase of Al_2O_3 with decreasing Cr_2O_3 is more marked than with stratiform intrusions, but total Fe tends to remain constant or even decrease slightly (Fig.VII.3). The decrease in total Fe is more pronounced in chromite from the Rhum ultramafic where a late magmatic reaction has resulted in an increase in Al_2O_3 and MgO with a decrease in Cr_2O_3 and total Fe (Fig.VII.3). Magmatic chromite is homogeneous and both segregated and accessory chromite follow the same compositional trends.

The late magmatic trend involves the crystallization of a titanium oxide, titaniferous magnetite, ilmenite or ulvospinel around a chromite core immersed in a basaltic magma. The titanium-rich oxide is the stable oxide phase crystallizing from this liquid, rimming the chromite and forming discrete crystals in the groundmass. Some sequential zoning results from the substitution of $Ti + (Mg,Fe)$ for $2(Cr + Al)$ but because Ti is involved the compositional variation is not properly represented on the normal spinel variation diagrams. The decrease of Al_2O_3 with decreasing Cr_2O_3 leads to a distinct trend on the variation diagram (Fig. VII.3).

The most simple post-magmatic compositional trend involves the deposition of a magnetite rim around chromite in serpentinites that are unmetamorphosed, or of low grade only (Buckskin-weathering type of serpentinites). The magnetite forms from Fe released on serpentinization of the silicates and rims chromite grains (Plate 32).

Ferritchromit rims of varying composition are found around chromite in certain serpentinites, refractory bricks, detrital chromite and in ultramafic nodules. The ferritchromit compositional trend shows a decrease of Al_2O_3 and an increase of Fe_2O_3 at constant Cr_2O_3 composition followed by increasing FeO and Fe_2O_3 with decreasing MgO and Cr_2O_3.

Chromite, surrounded by rims of ferritchromit which vary continuously in composition towards magnetite, is associated with an aluminous silicate in serpentinites frequently enclosed by rocks metamorphosed to the greenschist or amphibolite facies (verde antique-type of serpentinite).

The compositional trend resulting from ferritchromit alteration involves a loss of Al_2O_3, initially with little or no loss of Cr_2O_3, and a gain in Fe_2O_3. The compositional trends are in marked contrast to those established as magmatic.

Many authors ascribe the formation of zoned chromites of the verde antique association to the process of serpentinization (Spangenberg, 1943; Amin, 1948; Miller, 1953; Lapham, 1964; de Waal and Hiemstra, 1966; Golding and Bayliss, 1968; Beeson and Jackson, 1969). Others suggest that the alteration occurs subsequent to serpentinization (de Wijkerslooth, 1943; Den Tex, 1955; Engin and Aucott, 1971). Occasionally the suggestion is made that it

may be a late magmatic reaction (Simpson and Chamberlain, 1967). It would appear that serpentinization alone is not sufficient to cause zoning in the spinels because the buckskin-weathering-type of serpentinization produces a rim of magnetite around chromite but no intermediate zone of ferritchromit (James, 1946; Maxwell, 1949; Golding and Bayliss, 1968; MacRae, 1969; Aumont and Loubat, 1971 and this thesis (Plate 32). Furthermore, the type of zoning found in chromite associated with the verde antique-type of serpentinization is very similar to that found in chromite in xenoliths and xenocrysts in basalt, in refractory bricks and possibly in sedimentary environments.

The production of ferritchromit in any of these environments involves the loss of MgO and Al_2O_3, a common factor in all cases being an elevation of temperature. Homogeneous, magmatic chromite will form at an fO_2 between 10^{-5} and 10^{-7} atm.(Ulmer, 1969), temperatures from about 500°C to 1300°C and probably high pressure. If an ultramafic rock containing such chromite is emplaced at a higher level in the crust, in an environment of lower temperature and pressure but higher fO_2, it may be metastable. The reaction to produce the spinel stable under the new conditions is initiated by an elevation of temperature.

J CONCLUSIONS

Trends of ferritchromit alteration in serpentinites are quite distinct from compositional trends due to magmatic and late magmatic reactions. It is concluded that the formation of ferritchromit around chromite is unlikely to be due to a magmatic reaction.

Ferritchromit alteration is not confined to chromite in serpentinites but is found in non-serpentinized rocks that have been subjected to elevated temperature subsequent to the formation of the chromite. Furthermore, serpentinites in which ferritchromit alteration is found are associated with low-grade metamorphic wall-rocks. Many serpentinites do not contain chromite with ferritchromit alteration rims; instead the chromite is surrounded by a rim of magnetite. Such serpentinites are associated with unmetamorphosed wall-rocks. It is concluded that serpentinization is itself not sufficient to produce ferritchromit. An elevation of temperature in a rock containing pre-existing chromite appears to be necessary for the formation of ferritchromit.

VIII DISCUSSION OF THE SPINELS IN AREAS I AND III

A INTRODUCTION

The details of the spinel mineralogy in Areas III and I have been presented in Chapters IV and V respectively. The chrome spinels in Area III are always zoned and consist of a homogeneous chromite core surrounded by ferritchromit varying in composition towards magnetite. The chrome spinels in Area I are also zoned, but the chromite core, which may be homogeneous or exsolved into two phases, is surrounded by magnetite. Homogeneous chrome spinel also occurs. The origins of these features are now discussed in the light of the data presented in Chapter VII.

B CHROMITE CORES IN AREA III

The composition of chromite cores from spinels in Area III lies entirely within the field of chromite from layered intrusions, or overlapping the fields of layered and Alpine-type intrusions depending upon the diagram used (Figs.VIII.1 and VIII.2). The composition (Fig.VIII.1) also falls beyond the field of chromite associated with dunite (from the Great Dyke) but within the field of chromite associated with peridotite (from the Stillwater Complex) and pyroxenite (from the Bushveld Complex). This is at first sight anomalous because the ultramafic rocks of Area III are almost entirely serpentinized dunite. It has already been shown that accessory chromite lies slightly further along the variation trend than does segregated chromite from the same body (Fig.VII.1). Thus the accessory chromite from Area III is of a composition consistent with its association with dunite.

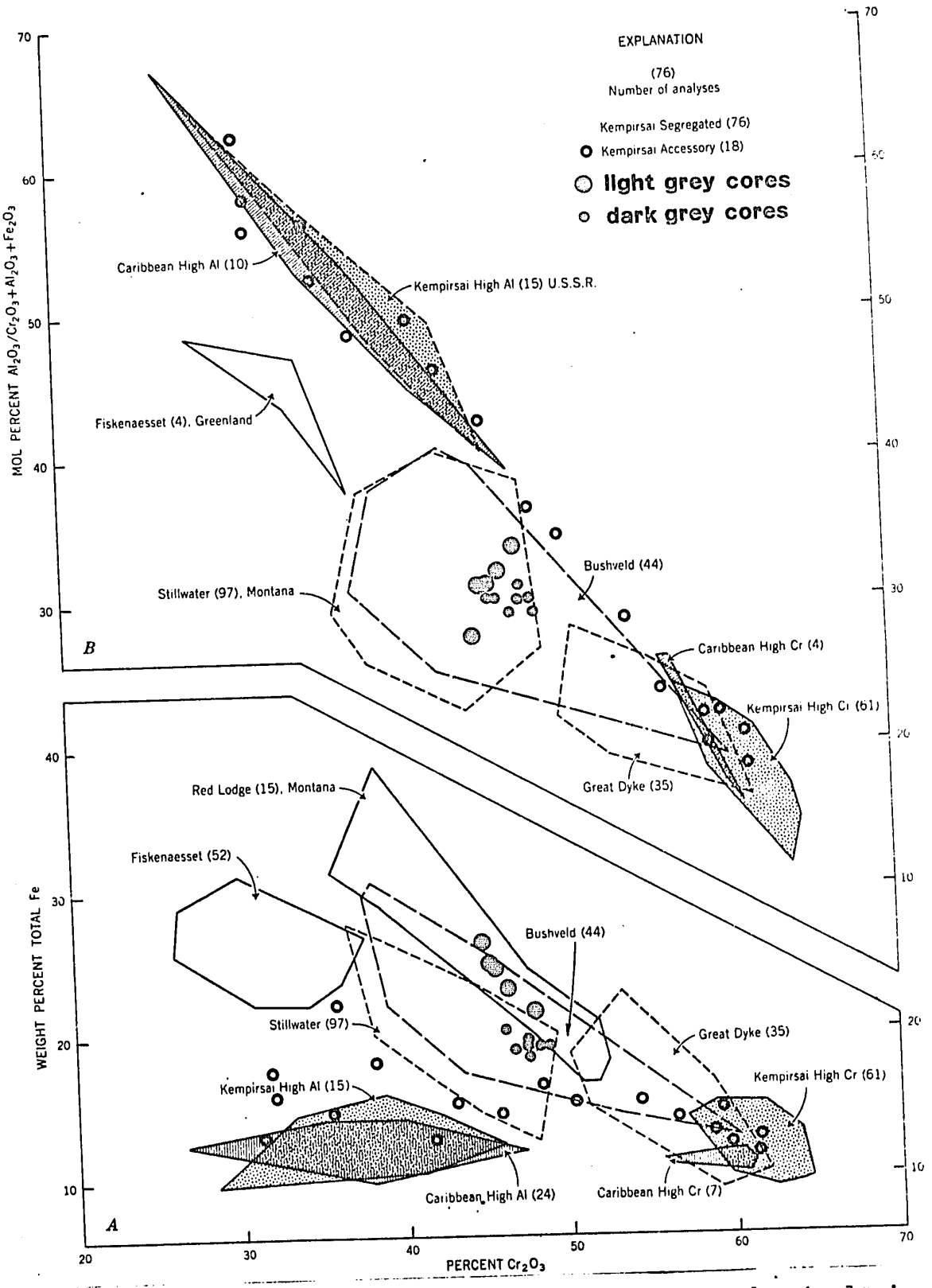

Fig.VIII.1. Compositions of chromite cores from zoned spinels in Area III (Table IV.3) compared to compositional fields of chromite from podiform and layered intrusions. The data is plotted on a variation diagram devised by Thayer (1970).

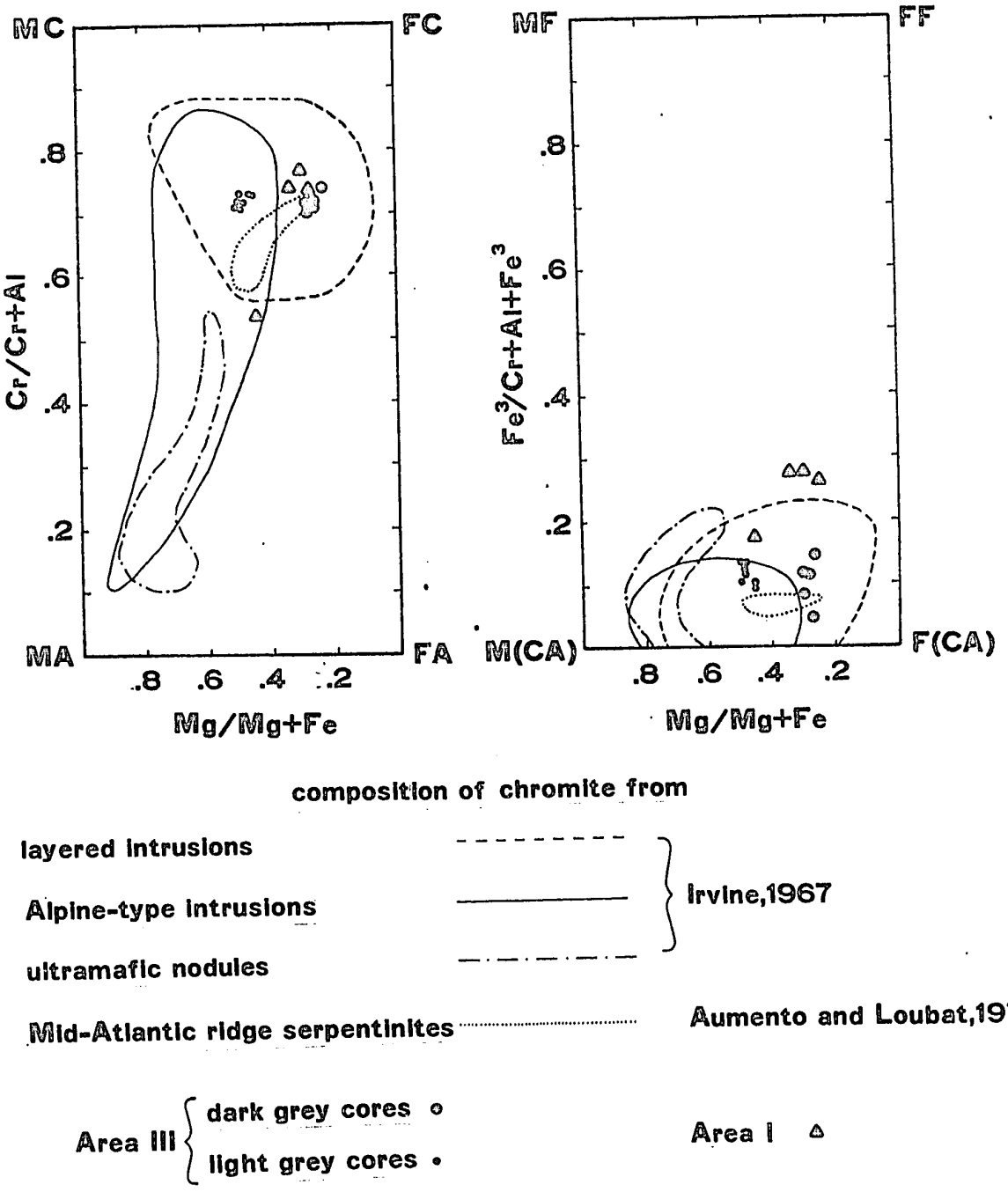

Fig.VIII.2. Compositional variation diagram of chromite cores from zoned spinels in Area I (Table V.4, cols. 1, 2, 5 and 7) and Area III (Table IV.3). The derivation of the plots is shown in figure VIII.4.

For the following reasons the dark grey chromite cores to the zoned spinels are interpreted as relics of the original magmatic chromite:- (1) the cores are homogeneous in composition, a feature that appears to be characteristic of primary magmatic chromite (p.156).(Slight compositional variations that do occur are between, not within, grains); (2) the composition falls within the field of chromite from layered intrusions where it overlaps the field from Alpine-type intrusions (Figs.VIII.1 and VIII.2).

Where slight compositional differences occur between the homogeneous grains total Fe and Al_2O_3 increase slightly with decreasing Cr_2O_3 a trend characteristic of the magmatic phase of chromite development (p.151). The variation in Cr_2O_3 content is small (Table IV.3) hence it would be unwise to place too much reliance on this relation.

The light grey chromite cores may also be original chromite; they are homogeneous and fall within the compositional field of chromite from layered intrusions (Fig.VIII.1). Light and dark grey cores differ mainly in MgO and FeO content. Studies of silicate-oxide systems have shown that the trend of FeO or MgO enrichment in spinel is determined by fo_2 (p.252). The slight compositional differences between these chromites may be attributed to fluctuating fo_2 at the time of crystallization. On the other hand the compositional variation for the light grey chromite core shows a reversal compared to the dark chromite cores. TiO_2, MgO, FeO and Al_2O_3 decrease with decreasing Cr_2O_3. The range in Cr_2O_3 content is again small (Table IV.3) and any interpretation

must be cautious. However, the trends between the light grey cores are similar to the trends in the ferritchromit rims suggesting a post-magmatic process may have operated.

Irvine (1965, Fig.11) has devised theoretical fo_2 isobars for spinel series solid solutions in equilibrium with olivine and orthopyroxene (Fig.VIII.3 a & b). Orthopyroxene was rare in the Area III ultramafic rocks; nevertheless, the data may be used to gain an indication of the fo_2 at which the chromite crystallized. The dark grey chromite contains about 15% Al_2O_3 and lies near the MF-FF-FC-MC face of the spinel prism; it must therefore lie between the contour for Cr-free and Al-free spinel at any one fo_2 but slightly nearer the contour for Al-free spinel (Fig.VIII. 3b). This places the chromite approximately on the -1 isobaric surface. Now the figures on the isobars, when added to $\log_{10}K_m$, estimated to be about -7 at 1250°C (Irvine, 1965, p.669), give $\log_{10}fo_2$, indicating that the chromite crystallized at an fo_2 of the order of 10^{-8} atm.. This value is in accordance with that to be expected for melts at these temperatures (MacLean, 1969, Fig. 13). In the system MgO-FeO-Fe_2O_3-SiO_2, the assemblage olivine, pyroxene spinel and liquid does not occur below $fo_2 = 10^{-7}$ atm., though the assemblage olivine and spinel does (Ulmer, 1969, p.120).

The light grey chromite cores have a slightly different composition being depleted in MgO, indicating (Fig.VIII.3b) that they crystallized at a slightly lower fo_2. It is known from experimental evidence that spinel that crystallizes with decreasing fo_2 becomes depleted in $MgFe_2O_4$ and enriched in Fe_3O_4 (Appendix I) (Spiedel & Osborn, 1967). This is a further indication that the

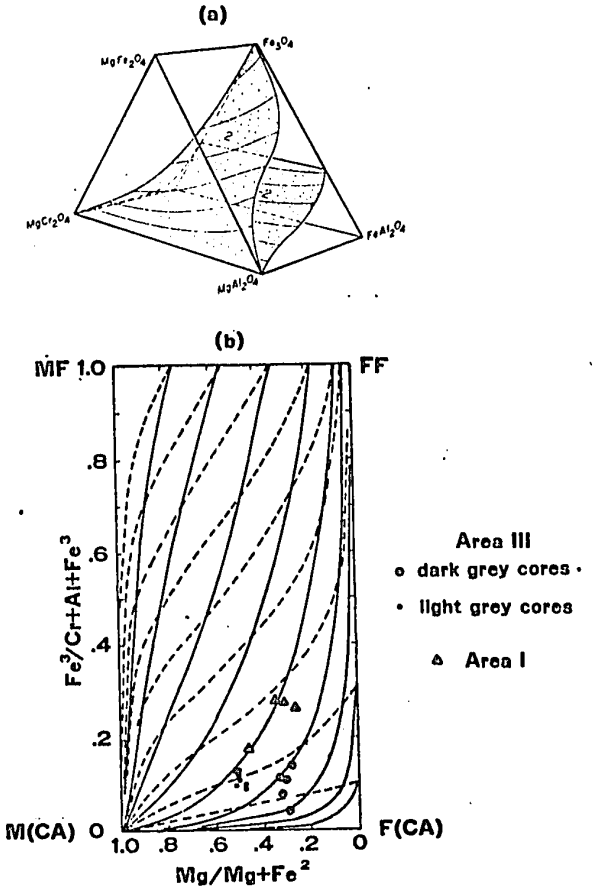

Fig.VIII.3 (a) Theoretical configuration of two fo_2 isobaric surfaces in the spinel compositional prism where spinel solid solutions coexisted in equilibrium with olivine and orthopyroxene at constant temperature and pressure (Irvine, 1965).
(b) Type B projection from spinel prism of theoretical fo_2 isobaric surfaces for spinels crystallizing under conditions in (a). The solid lines are isobars in the MF-FF-FC-MC face representing Al-free spinel; the dashed lines are isobars in the MF-FF-FA-MA face representing Cr-free spinel. The isobaric surfaces are continuous between the two faces. The diagram has been redrawn from Irvine, (1965, Fig.4) with compositions of chrome spinels in Areas I (Table V.4) and III (Table IV.3) added.

light grey chromite cores are also originally magmatic in origin.

Thus it is concluded that the dark grey chromite cores represent, and the light grey possibly represent, original magmatic chromite. The chromite is thus the only remnant of the primary mineralogy of the ultramafic rock which could be part of a disrupted layered intrusion.

These conclusions support the evidence presented in Chapter IV that the Area III serpentinites were derived from cumulates.

C FERRITCHROMIT RIMS TO CHROME SPINELS IN AREA III

1 Discussion

Ferritchromit rims surround chromite in Area III only. These rims are separated from chromite by a sharp compositional boundary, beyond which the ferritchromit varies continuously in composition towards magnetite. The composition of magnetite may not be reached.

The ferritchromit-magnetite rims are interpreted as an alteration of an original (magmatic) chromite rather than the addition of a new spinel phase around the original chromite for the following reasons:- (1) the rounded shape of the grey cores indicates an alteration process affecting a pre-existing grain from all directions. Chromite grains in ultramafic rocks tend to be euhedral, or at least to show some evidence of crystal faces; the addition of a new phase would leave the euhedral outline intact, as in Area I (Plate 19), but no such outlines have been observed in Area III spinels. The boundary between ferritchromit and magnetite is gradational, and concentric to the core. In occurrences where magnetite or hematite has been added to the rim of a chromite grain, angular outlines and corners of grain

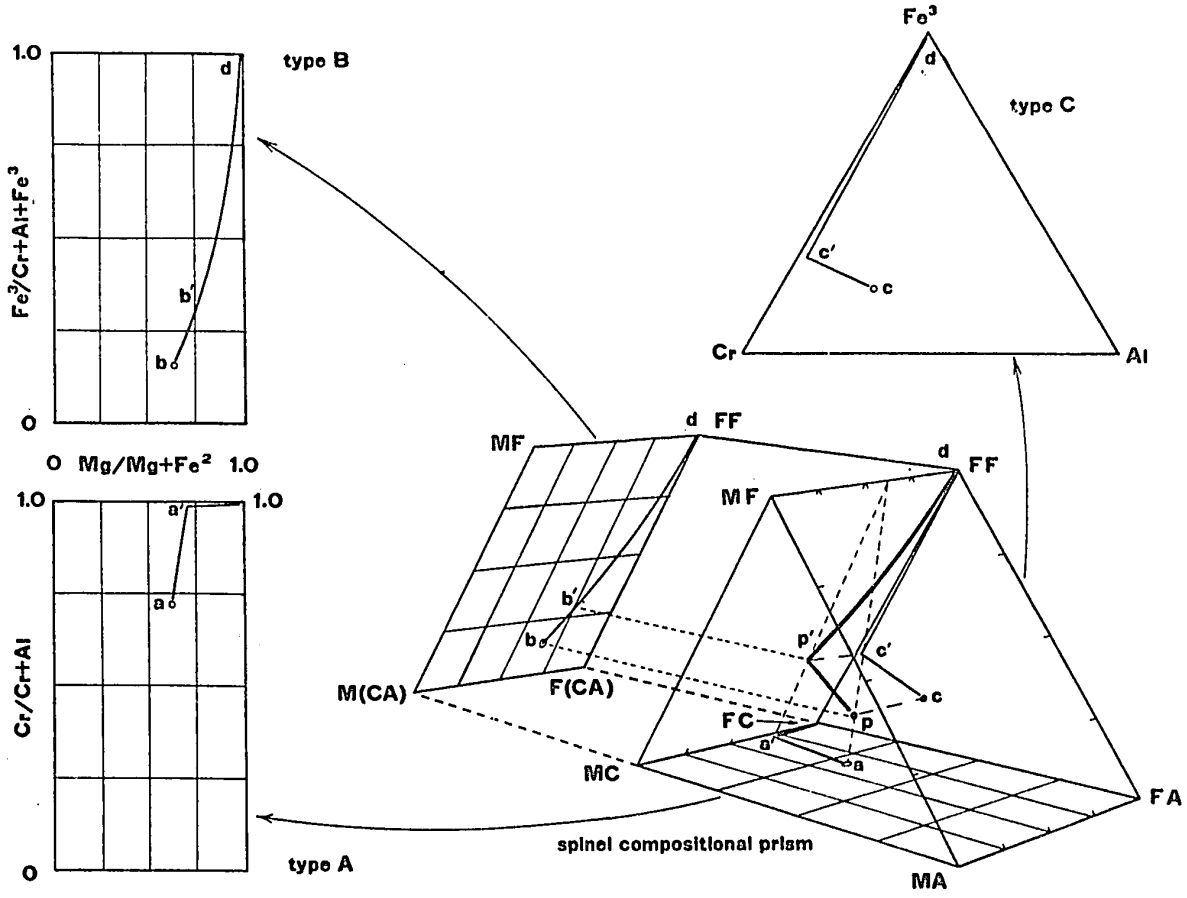

Fig.VIII.4. The spinel prism and the derivation of three projections from the prism.

Chromite of composition p is surrounded by ferritchromit of composition varying between p' and d. The trace of these compositional changes is shown in the three planar projections (for further discussion see pp.180 - 181). (Based on Irvine, 1965, Fig.2).

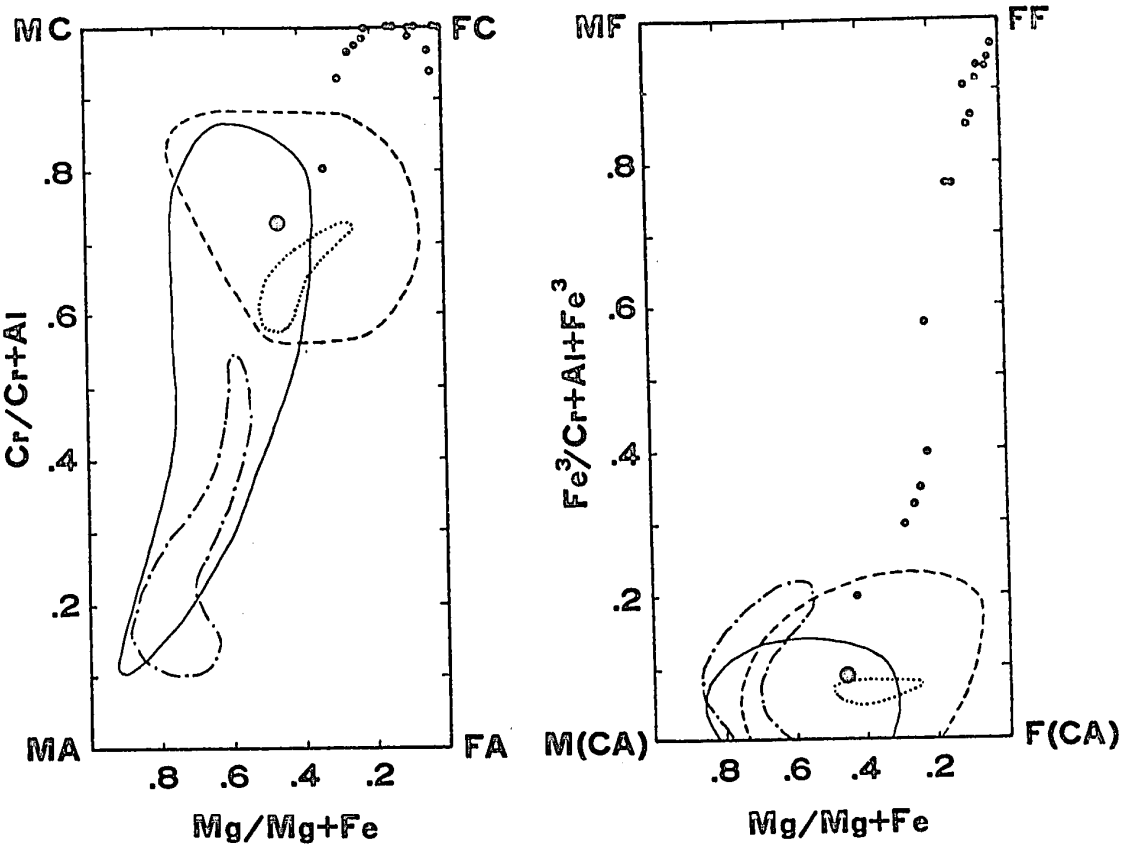

Fig.VIII.5. Variation diagrams to show ferritchromit alteration in a simply zoned spinel (W269). The large data point is the parent chromite. The fields of chromite compositions are explained in the caption to Figure VIII.2.

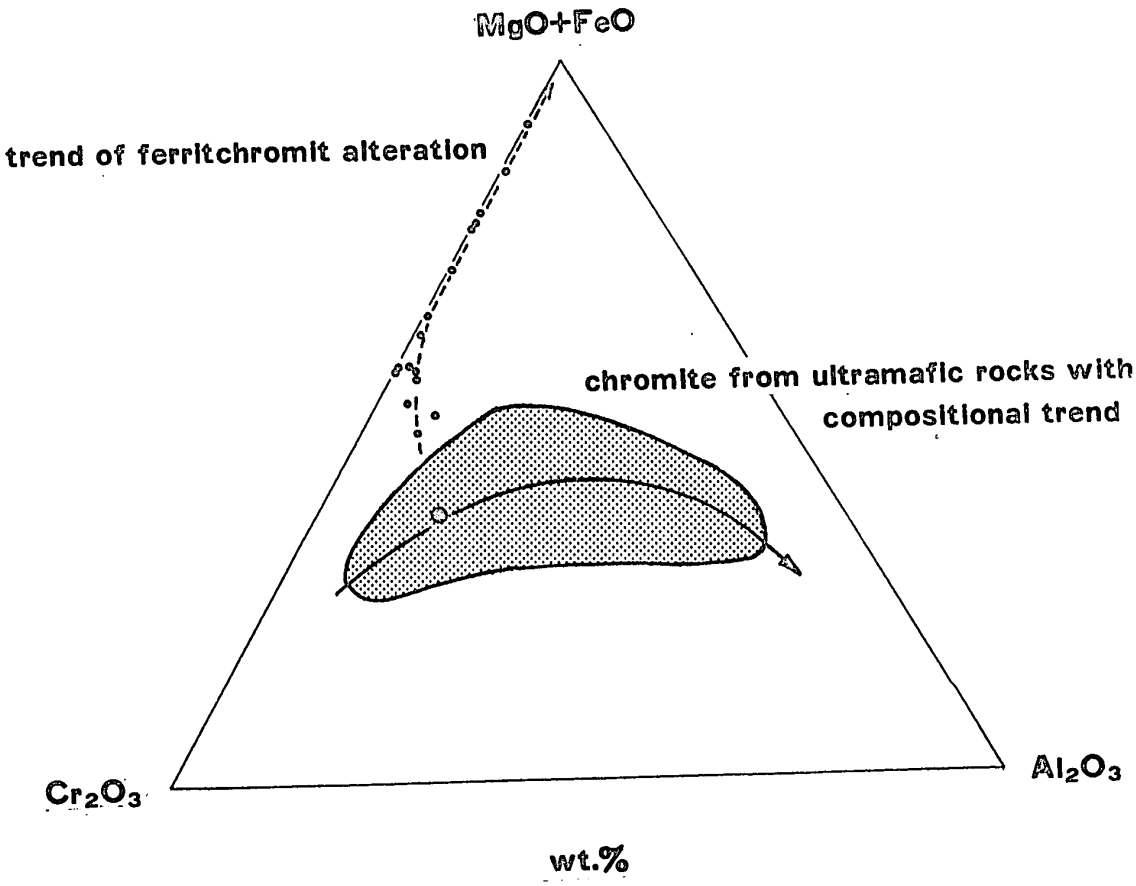

Fig.VIII.6. Ternary variation diagram illustrating the trend of ferritchromit alteration in W91 (Table IV.4). The large data point is an average analysis of the chromite core (Table IV.3, col.9). The trend of magmatic chromite composition is derived from figure VII.2.

fragments are preserved beneath the added portion (Plate 32). (2) The lack of silicate and sulphide minerals at the boundary of ferritchromit and chromite suggests that as presently situated the contact does not represent an original mineral interface. Some zoned chromites do however contain a concentric zone of silicate inclusions within the ferritchromit rim (Plate 23), the significance of which is discussed on p.192. (3) The chemical gradients whereby Al_2O_3, MgO and Cr_2O_3 in the ferritchromit decrease towards the margin of the grain and FeO, Fe_2O_3, TiO_2 and NiO increase towards the margin suggest movement of these oxides along compositional gradients (Fig.IV.8). That is iron, NiO and TiO_2 diffused inwards and replaced Al_2O_3, MgO and Cr_2O_3 which diffused outwards. The Al_2O_3 is fixed in antigorite which in Area III contains over 3% Al_2O_3 (Table IV.3).

If the ferritchromit is then an alteration of chromite, at what stage in the history of the ultramafic rocks did the alteration occur? Compositional alteration could possibly occur (a) during the magmatic stage, (b) during serpentinization and (c) during regional metamorphism either before or after serpentinization. All three have been suggested in the literature as responsible for ferritchromit alteration (see discussion, p.166).

Ferritchromit alteration is illustrated in the spinel prism (Fig.VIII.4). Chromite of composition **p** is surrounded by ferritchromit that is non-aluminous chromite, of composition **p'**; the ferritchromit then changes composition toward magnetite along the path **p'd**. The compositional change **p-p'-d** may be represented on projections from the prism by the paths **a-a'-d** for the type A

projection, **b-b'-d** for the type B and **c-c'-d** for the type C.

Compositional variation across a zoned chromite (W269) plotted on types A & B projections is shown in Fig.VIII.5. Type C projection has not been used; instead a wt.% ternary plot of Cr_2O_3-Al_2O_3-(MgO + FeO) which gives a similar variation curve has been employed (Fig.VIII.6), because trends in chromite composition have been established using this plot (Figs.VII.2 and VII.4). These diagrams emphasize two points; firstly, that ferritchromit falls outside the compositional field of magmatic chromite and has a compositional trend opposite to the magmatic trend of chromite; secondly, the very rapid compositional change from chromite to ferritchromit. This suggests the instability of Al-chromite under the conditions at which ferritchromit formed.

Compositional variation is also plotted on Thayer's (1970) variation diagrams (Fig.VIII.7 and VIII.8). These emphasize not only the divergent compositional trends of ferritchromit and chromite but the divergent trends of ferritchromite and late magmatic alteration of chromite.

Thus the compositional evidence suggests that the ferritchromit is not a consequence of magmatic reaction. This conclusion gains support from the fact that homogeneous grains of ferritchromit have not been observed in Area III serpentinites. Grains without chromite cores are cryptically zoned, indicating derivation from chromite. Homogeneous chromite occurs as core to the spinels and homogeneous magnetite grains occur throughout the serpentinite. This suggests that chromite and magnetite but not ferritchromit were, at different times, stable crystallizing phases.

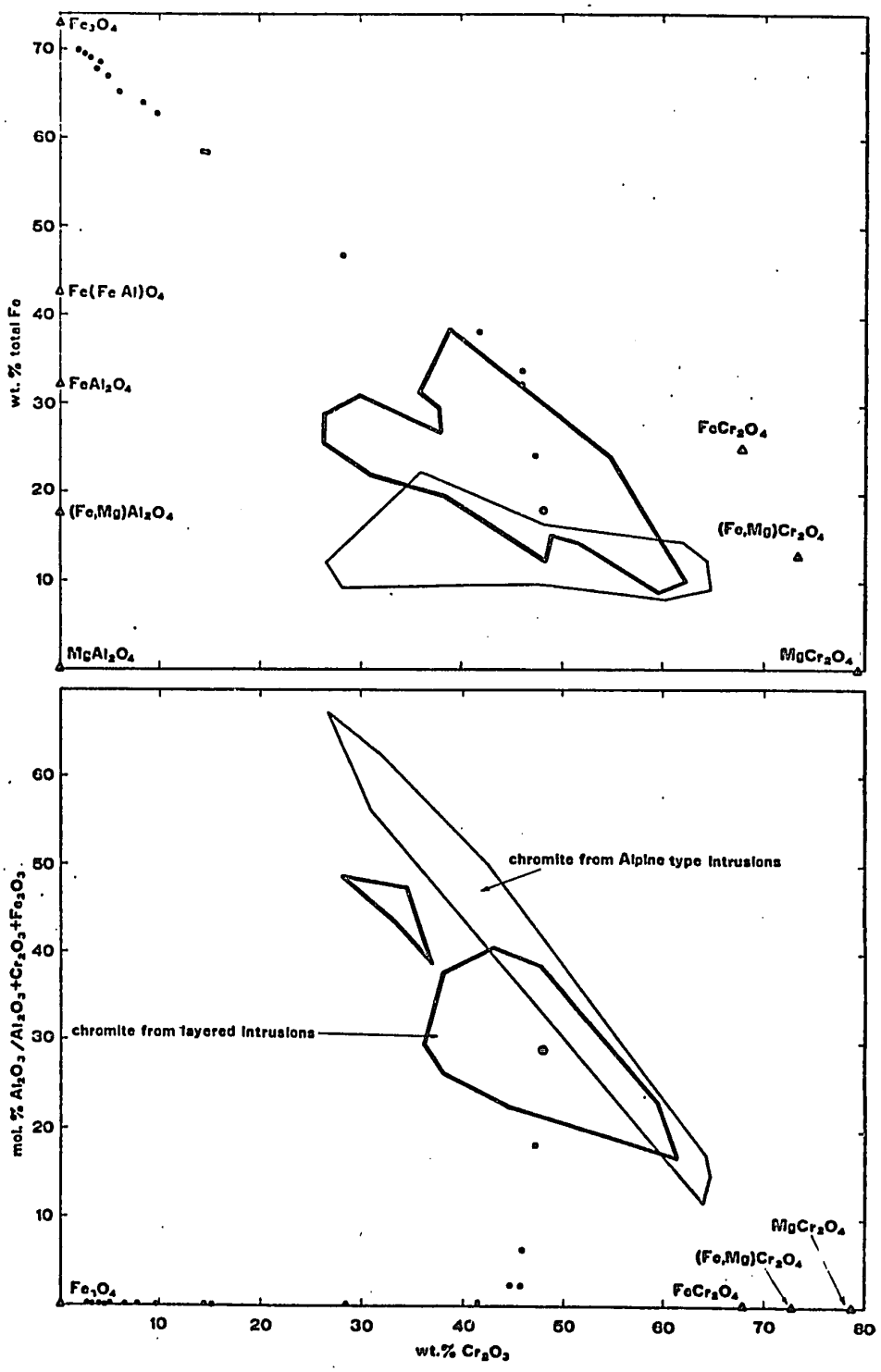

Fig.VIII.7. Plot of compositional trend of ferritchromit alteration (W269, Area III, Fig.IV.9) variation diagram after Thayer (1970).

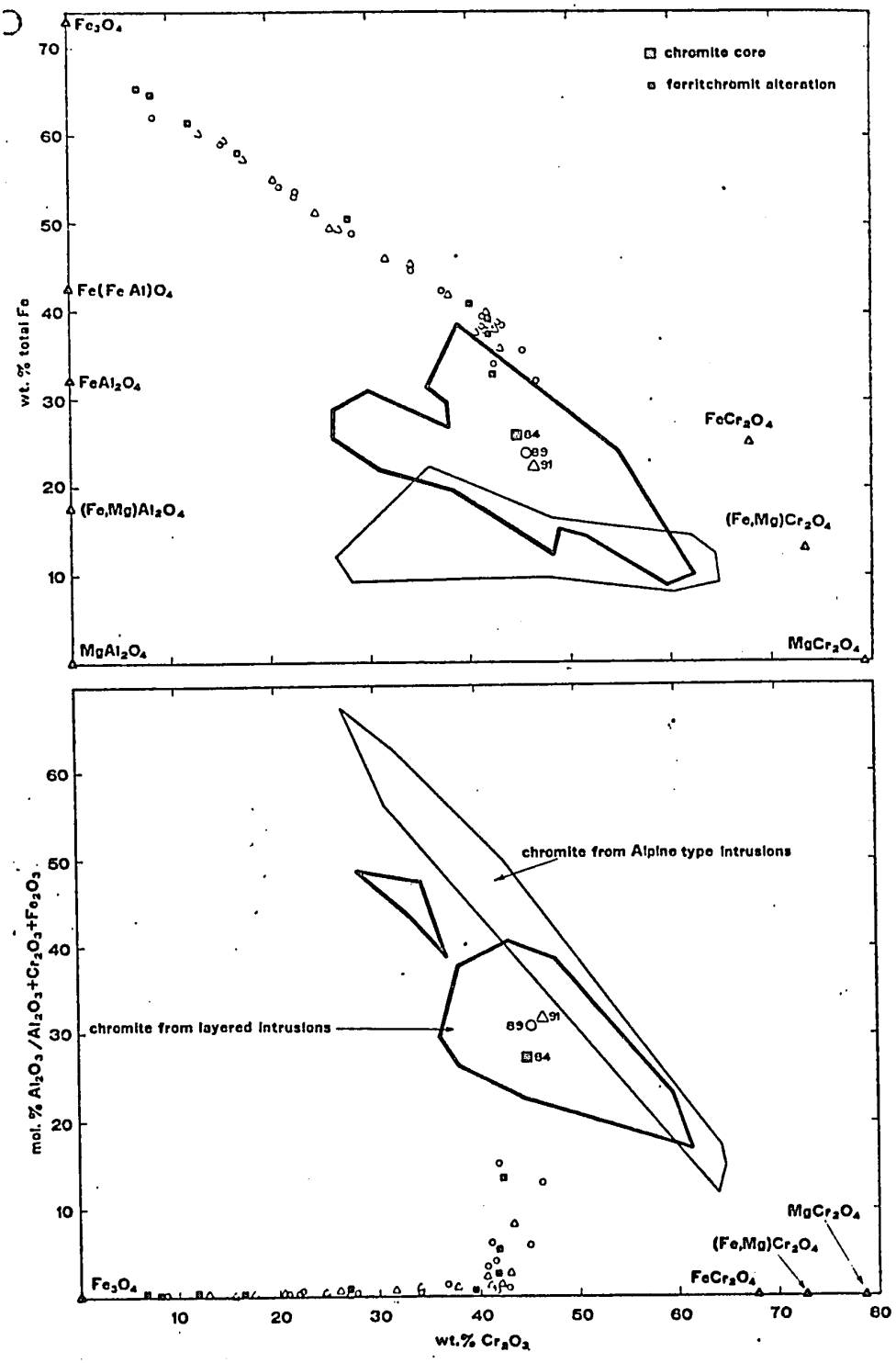

Fig.VIII.8. Plot of compositional trend of ferritchromit alteration (W84, 89 and 91, Area III, Figs.IV.4-IV.6).

If the alteration of the chromite is the result of serpentinization only, it remains to be explained why so many serpentinites do not contain chromite with ferritchromit rims and furthermore why ferritchromit occurs around chromite in environments other than serpentinites. The evidence from the literature survey (Chapter VII, and Appendix I) clearly indicates that serpentinization itself is not sufficient for the formation of ferritchromit. The formation of secondary magnetite during serpentinization does however result in magnetite forming both rims to chromite and discrete grains throughout the serpentinite.

This leaves only the third possibility that the ferritchromit may result from regional metamorphism of chrome spinels.

Irvine (1965) constructed theoretical equipotential surfaces within the spinel prism on which chemical potential, or free energy, of the oxide pairs MgO-FeO and any pair of the trivalent oxides, Al_2O_3, Cr_2O_3 or Fe_2O_3 differ by a constant amount. The individual chemical potentials become fixed if the spinel is in equilibrium with olivine and orthopyroxene, a refinement that cannot be made here because pyroxene is absent from the Area III ultramafic rocks. Irvine derives these equipotential surfaces from a theoretical reaction

$$AM_2O_4 + BN_2O_4 = AN_2O_4 + BM_2O_4 \text{.....1}$$

where the equilibrium constant K will vary according to the identity of the divalent cations A and B and the trivalent cations N and M. The production of ferritchromit from chromite involves the elimination of $MgAl_2O_4$; if $FeCr_2O_4$ is taken to represent ferritchromit then the alteration can be represented by the

equation

$$MgCr_2O_4 + FeAl_2O_4 = MgAl_2O_4 + FeCr_2O_4 \ldots\ldots\ldots 2$$

Ln K for this reaction is estimated at 3 (Irvine, 1965), and hence the general equipotential curves corresponding to Ln K = 3 (Irvine, 1965, Fig.7) may be labelled for Mg-Fe^{2+} and Cr-Al equipotential surfaces. This corresponds to a type A plot of Cr/Cr + Al against Mg/Mg + Fe^{2+}. The spinel compositional variations have been plotted on this diagram (Fig.VIII.9) and they follow closely the Mg-Fe^{2+} equipotential surfaces until Al_2O_3 is eliminated. After this, variation in the Mg/Mg + Fe^{2+} ratio moves the spinel composition towards magnetite. This variation is on, or closely parallel to, the MC-FC join. (Compare path **a-a'**-FC in Figure VIII.4). This stage may be represented by the equation

$$FeCr_2O_4 + MgFe_2O_4 = MgCr_2O_4 + Fe_3O_4 \ldots\ldots\ldots 3$$

In terms of the general case, equation 1, the equipotential surfaces for Cr-Fe^{3+} and Mg-Fe^{2+} may be derived. The projection that represents these variations is a type A plot (Fig.VIII.10). In this case the spinel also tends to follow the Mg-Fe^{2+} equipotential surface.

Thus the varying ferritchromit compositions all lie along a surface on which the difference in chemical potential between Mg and Fe^{2+} is constant. They do not lie along surfaces in which the differences in Cr-Al or Cr-Fe^{3+} chemical potential is constant. This suggests that Mg and Fe^{2+} were buffered during the formation of the ferritchromit. The serpentine minerals comprising the silicate phase of the rock would, along with an aqueous fluid

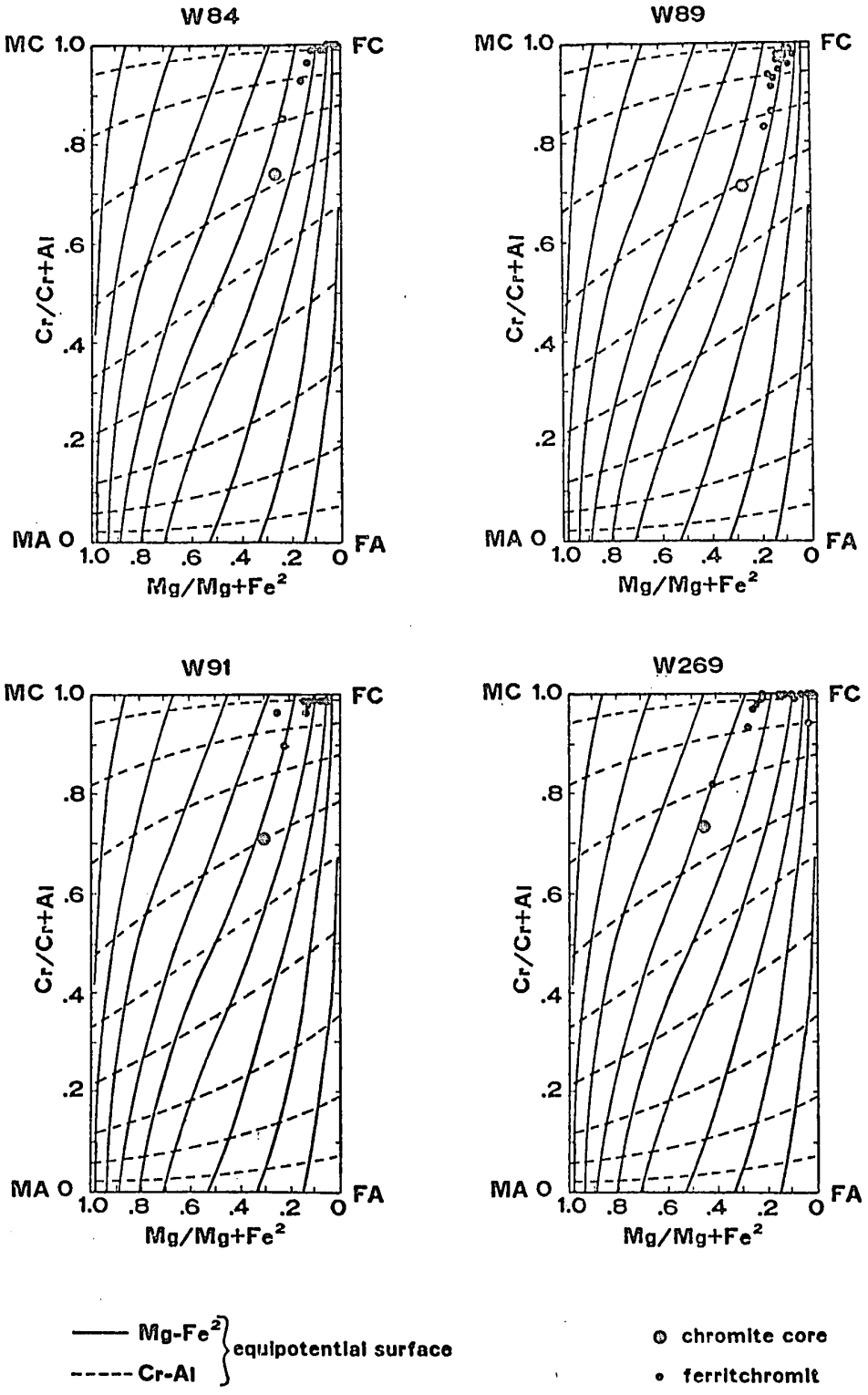

Fig.VIII.9. Composition of ferritchromit alteration to spinels in Area III with reference to Cr-Al and Mg-Fe^{2} equipotential surfaces.

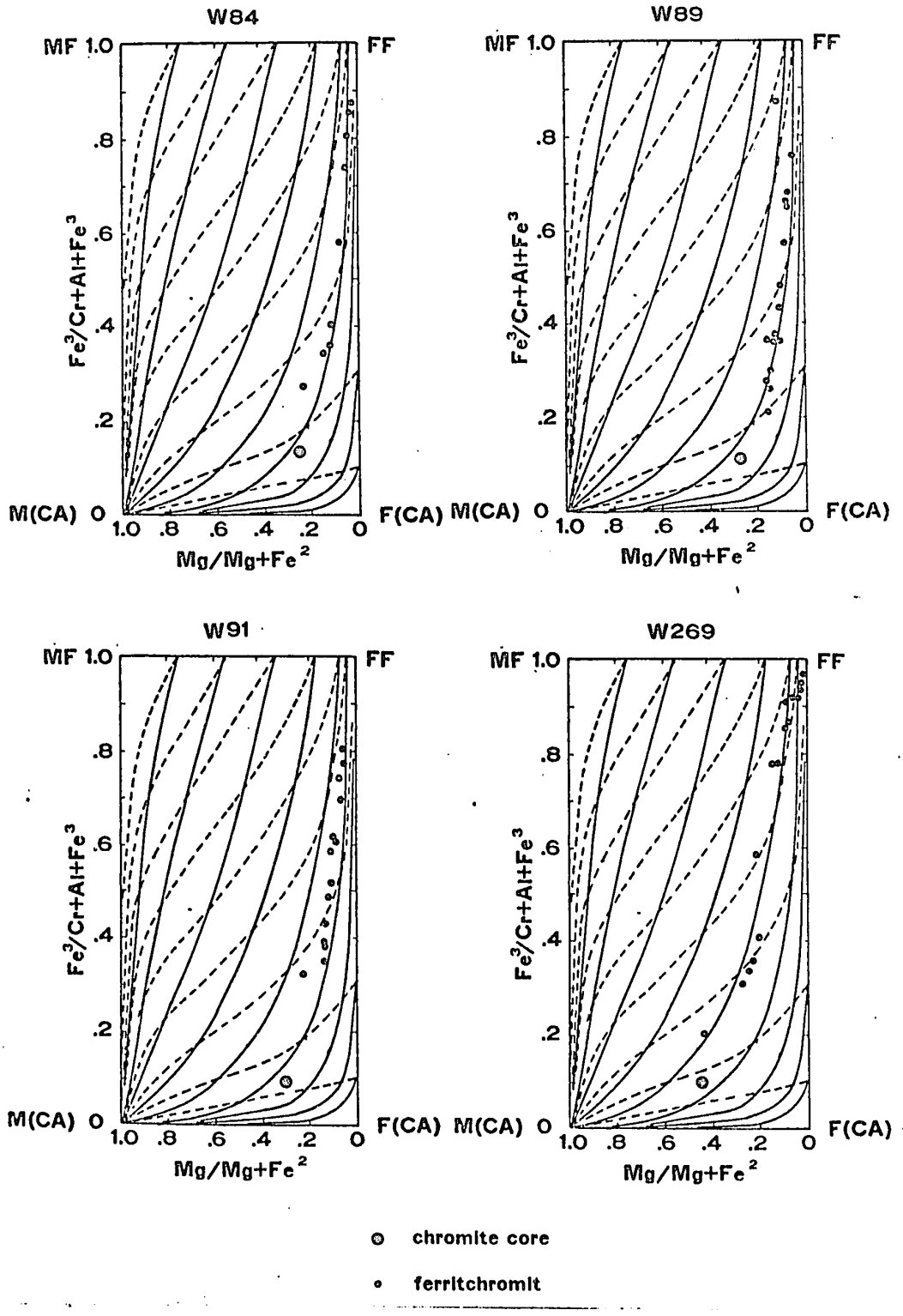

Fig.VIII.10. Compositions of ferritchromit alteration to spinels in Area III with reference to $Cr\text{-}Fe^3$ and $Mg\text{-}Fe^2$ equipotential surfaces.

phase, buffer Mg and Fe^{2+} during alteration. Cr and Al are not present in the silicates, except for extremely small amounts, and cannot buffer the Cr and Al in the spinels so as to maintain constant differences in chemical potential. Fe^{3+} in the spinel would also be buffered by silicate minerals and the fluid phase, but since Cr and Al are not, the composition cannot follow equipotential surfaces for these elements. Cr, Fe^{3+} and Al could only buffer chromite formation during the magmatic stage.

Spinel compositions near the parent chromite and the secondary magnetite (Fig.VIII.10) tend to lie off the equipotential surface on which the intervening ferritchromit is located. This indicates that ferritchromit formed when neither chromite nor magnetite was the stable spinel phase, and thus as a reaction between magnetite and chromite producing a spinel stable under the existing conditions.

Specimen W269 illustrates the alteration in an early stage (Fig.VIII.10, VIII.9 and VIII.7). The composition of the spinel phases tends to be near magnetite or chromite with few analyses of intervening ferritchromit. The points are only poorly aligned along the trace of an equipotential surface. The data points in the other specimens, W84, 89 and 91 (Fig.VIII10, VIII.9 and VIII.8) are more evenly distributed throughout the whole range of ferritchromit composition and are closely coincident with an equipotential surface. Specimen W91 contains no magnetite, has the largest compositional gap between the chromite and the ferritchromit, and the least range in ferritchromit composition. Thus it appears possible that ultimately the ferritchromit could

become homogeneous.

Irvine (1965) has also constructed theoretical isobaric surfaces for fo_2 within the spinel prism (Fig.VIII.11) on which the ferritchromit compositional trend for Area III spinels is nearly coincidental with such a surface for an Al-free spinel. Examination of Figure VIII.3 shows that an aluminous spinel must project above the isobar for the continuous solid solution at the same pressure and temperature. The parent chromite falls below the isobar on which the ferritchromit alteration plots. This indicates that the chromite core and the ferritchromit rim did not form on the same isobaric surface and suggests that it formed at a lower fo_2 than the ferritchromit alteration. The fo_2 of the chromite formation has been estimated at 10^{-7} atm. (p.175), but the fo_2 of the ferritchromit cannot be estimated due to the lack of thermodynamic data (Irvine, 1965). The magnetite also plots off the ferritchromit isobaric surface, because it too formed under different conditions to the ferritchromit. It will be shown in the next section that the magnetite rims in Area I chromite formed as a result of the iron released during serpentinization.

Thus all the evidence indicates that chromite and magnetite formed under different conditions but at different times and ferritchromit formed subsequently to either under different conditions again. In Chapter VII evidence was presented to show that ferritchromit forms from chromite under the influence of rising temperature. The complex serpentine mineralogy in Area III has already been interpreted as resulting from regional

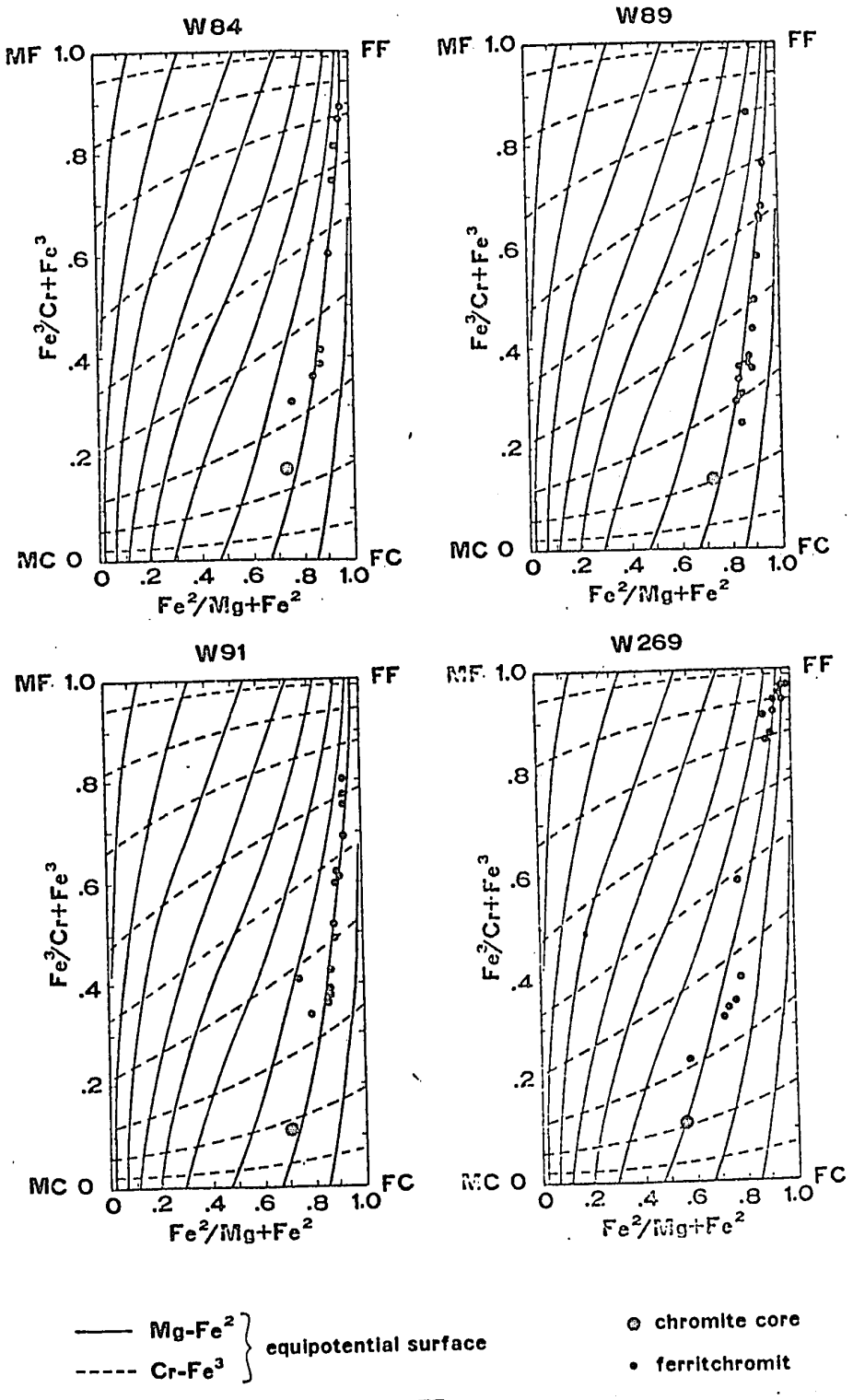

Fig.VIII.11. Compositions of ferritchromit in Area III with reference to isobaric surfaces within the spinel prism.

metamorphism of a serpentinite.

It is therefore concluded that the ferritchromit formed also as a result of the regional metamorphism which promoted a reaction between a chromite core and a magnetite rim in a serpentinized ultramafic.

In other words magmatic chromite, whose range of composition has been clearly outlined (Figs.VII.1 and VIII.2) is metastable when removed from the pressure, temperature and fo_2 conditions prevailing at the time of its formation. Elevation of temperature promotes the formation of ferritchromit which has a composition stable under the new conditions of temperature, pressure and fo_2. In regional metamorphism of a serpentinite a reaction between chromite and magnetite leads to the formation of ferritchromit. Ferritchromit also forms around chromite in environments where no magnetite rim was present, for example fresh dunite nodules in basalt (pages 157 and 160). In this case inward diffusion of Fe must have been derived from a source other than magnetite.

It is also concluded that the concentric zone of silicate inclusions found in some spinels (Plate 23 and p. 181), marks the original boundary between chromite and magnetite. The reaction between magnetite and chromite to produce ferritchromit obscures the original compositional boundary, leaving the 'marker horizon' intact. It is also reasonable to suggest that the pyroaurite-group mineral found as a zone in multiply zoned spinels is somehow derived from silicate inclusions originally at a chromite magnetite interface.

2 Summary and Conclusions

The arguments for the metamorphic origin of ferritchromit in Area III presented above may be summarized as follows:-

(1) Chromite cores to zoned spinels have a composition consistent with a magmatic origin.

(2) Ferritchromit is an alteration of, and not an addition to, a magmatic chromite grain.

(3) Compositional trends of ferritchromit alteration are very different to compositional trends resulting from magmatic and late magmatic alteration.

(4) Magnetite rims form around chromite during serpentinization.

(5) Serpentinization itself is not sufficient to form ferritchromit; not all serpentinites contain ferritchromit and those that do may frequently be shown to have been metamorphosed. Ferritchromit rims to chromite also occurs in refractory bricks, ultramafic nodules in basalt and other environments where an elevation of temperature has occured subsequent to the initial chromite formation.

(6) The silicate mineralogy of the serpentinites and wall-rocks in Area III shows them to have been regionally metamorphosed to the epidote-amphibolite facies.

(7) It is concluded that ferritchromit formed during regional metamorphism of a serpentinite as the result of a reaction between primary chromite grains and magnetite rims produced during serpentinization.

D MAGNETITE RIMS ON CHROME SPINELS IN AREA I

The chrome spinels in Area I are all surrounded by rims of

magnetite which for the following reasons are interpreted as having been added to a homogeneous or exsolved chromite grain:-

(1) Euhedral outlines of primary chromite are preserved beneath the magnetite (Plates 37 & 19).

(2) The interface between chromite and magnetite is sharp and often marked by small inclusions of silicate (Plate 34) or sulphide (Plate 20), indicating a time gap, separating the formation of magnetite and chromite.

(3) The magnetite rim is always homogeneous; the chromite core is also homogeneous except in the case of the exsolved spinels. There is no compositional gradient between the two.

(4) Small euhedral magnetite grains are present throughout the serpentinite.

(5) The magnetite forming the rims on the two-phase spinels, cuts cleanly across the exsolution textures (Plate 31) and may enclose disrupted fragments with exsolution textures (Plate 41). The primary chromite had crystallized, exsolved and subsequently fractured before the formation of the magnetite.

(6) Magnetite is not a primary mineral in ultramafic rocks (see p.145). Serpentinization of primary iron-bearing silicates releases Fe, in excess of the small amount that can be accommodated in serpentine, which is usually oxidized to magnetite.

The serpentine mineralogy indicates that the serpentinization history has been simple. There has been no subsequent 'event' to modify the pervasive lizardite mesh texture. The presence of homogeneous magnetite rims supports this interpretation.

E CHROMITE CORES IN AREA I

The homogeneous chromite in Area I occurs either as cores to simply and multiply zoned spinels or as homogeneous spinels with no, or only fragmentary, magnetite rims. They exhibit a diverse composition which displays a linear trend (Fig.VIII.12).

The chromite cores to simply and multiply zoned spinels are closest to the compositional field of magmatic chromite, while the chromite without magnetite rims is furthest away and has the composition of ferritchromit. This trend is explained if chromite whose composition is that of W13 loses Al_2O_3 and MgO, resulting in a relative or absolute gain in Cr_2O_3 and Fe_2O_3. There is evidence that this could be a late magmatic reaction; such reactions involving loss of Al_2O_3 and MgO from chromite and production of plagioclase have been described on p.156. This reaction will reverse the compositional trend of the earlier magmatic stages of chromite crystallization. The homogeneous nature of the resulting chromite and the variation of Cr_2O_3 content also suggest that the reaction is magmatic. However this late magmatic trend is not well established by chemical analyses and until further documentation is available the possibility that it is post-magmatic must be considered. Since some chromite in Area I has the composition of ferritchromit, the possibility arises that it originated by homogenization of a zoned spinel consisting of a magnetite or ferritchromit rim and a chromite core. This implies the possibility of an early serpentinization in Area I, prior to the serpentinization responsible for the magnetite rims around homogeneous and two-phase chrome spinel.

The homogenization of artificially zoned spinels at high temperatures has been observed in refractory bricks (p.164), and the possibility that ferritchromit rims in Area III are tending to homogenize has been noted (p.189).

The least altered spinels in Area I crystallized at an fo_2 of 10^{-7} atm. (p.175). In the system $MgO-FeO-Fe_2O_3-SiO_2$ the assemblage olivine, pyroxene, spinel and liquid becomes stable above an $fo_2 = 10^{-7}$ atm.; the Area I serpentinites all contain relict pyroxene, in contrast to the serpentinized dunite of Area III that have crystallized at a slightly higher fo_2.

The exsolved chromite cores, which have been observed from one short section of drill core, are not easy to interpret. The composition of various phases is shown in Fig.VIII.5. The exsolution involves separation into a dark Al-rich phase and a light, Al-poor, ferritchromit phase (Fig.VIII.13). This separation must have been achieved prior to the deposition of the magnetite rim produced during serpentinization (Plate 31).

Bulk analyses of the fine two phase intergrowths of the type shown in Plate 31, determined using a wide beam on the electron microprobe, have the composition of ferritchromit (Fig.VIII.13).

The highly exsolved spinel illustrated in Plate 31 is composed of a dark Al-rich phase and a light Al-poor phase surrounded by a dark Al-rich chromite rim. Much of the two phase intergrowth is so fine that it can only be resolved under very high magnification (Plate 30). A planimeter was used to estimate*

* The intergrowth pattern is so complicated that even with a planimeter it is only possible to make an estimate of the relative proportions of the phases.

the areas occupied by the dark rim, the dark and light phases in the centre and the finely intergrown phases. As analyses are available for all these phases it is possible to weigh these according to area and thus to estimate a bulk analysis of the chromite grain (Table VIII.1). The calculated bulk analysis corresponds closely to those for less complicated fine two-phase intergrowths (Plates 19 and 38 and Fig.VIII.13), all of which lie on a trend of ferritchromit alteration.

The two-phase cores in Area I correspond to exsolution products of an original chromite grain represented by the bulk composition determined by weighted mean (Table VIII.1) or wide-beam electron microprobe analyses (Fig.VIII.13). These phases are ferritchromit and a chrome spinel enriched in Al_2O_3 and MgO. The two exsolved phases and the bulk composition all lie on the ferritchromit trend (Fig.VIII.13). In the formation of sequentially zoned ferritchromit, Al_2O_3 leaves the spinel and becomes fixed in an Al-silicate which in Area III is antigorite. The formation of the Al-rich exsolution phase means that in this case not all excess Al_2O_3 has migrated out of the spinel.

The bulk analysis of the chromite cores falls well outside the field of chromite from layered and Alpine-type ultramafic rocks (Fig.VIII.13), and is in fact ferritchromit. Furthermore, the homogeneous chromite (Fig.VIII.13), has the composition of ferritchromit although it has not developed exsolution textures. These ferritchromit cores may have formed as in Area III where chromite cores and magnetite rims reacted to form ferritchromit which under suitable conditions homogenized. The reason for the subsequent exsolution is not clear; exsolution can be artificially

Table VIII.1 Estimation of the bulk composition of the exsolved chromite grain in Plate 31 and Table V.8.

	DARK RIM		LIGHT PHASE		TWO PHASE		DARK PHASE		
	Av.	x.156	Av.	x.033	Av.	x.777	Av.	x.034	Weighted
Al_2O_3	23.17	3.61	1.88	0.06	4.88	3.79	28.65	0.97	8.43
Cr_2O_3	30.30	4.73	16.23	0.54	22.36	17.37	30.15	1.03	23.67
TiO_2	0.30	0.05	1.10	0.04	1.22	0.95	0.19	0.01	1.05
MgO	10.93	1.71	2.47	0.08	4.22	3.28	14.03	0.48	5.55
NiO	0.19	0.03	1.23	0.04	1.13	0.88	0.12	0.00	0.95
FeO	18.81	2.93	26.68	0.88	24.72	19.21	15.10	0.51	23.53
Fe_2O_3	16.39	2.56	50.43	1.66	42.28	32.85	11.85	0.40	37.47

The first column in each pair is an average analysis of each phase listed in Table V.8.The second column is this analysis multiplied by the proportion it occupies of the total area of the exsolved portion of the grain.(The area of the exsolved portion of the grain is taken as 1).The third column is the weighted mean,which approximates the bulk composition of the grain.

Fig.VIII.12. Compositional variation of the cores of some simply zoned and homogenous spinels in Area I. The solid circles represent the homogenous chromite cores to the zoned spinels in Table V.4; the open circles the homogenous spinels in Table V.5.

Fig.VIII.13. Compositional variation of the phases in the exsolved chromites of the type shown in Plates 30 and 31. The solid squares represent the dark (chromite) phases (Tables V.6 and V.8),the open squares the light (ferritchromit) phases (Table V.8),the solid circles the average analyses of the two-phase intergrowths using a wide beam (Table V.7) and the bisected square the weighted average composition of the exsolved grain in Plate 31 (Table VIII.1).

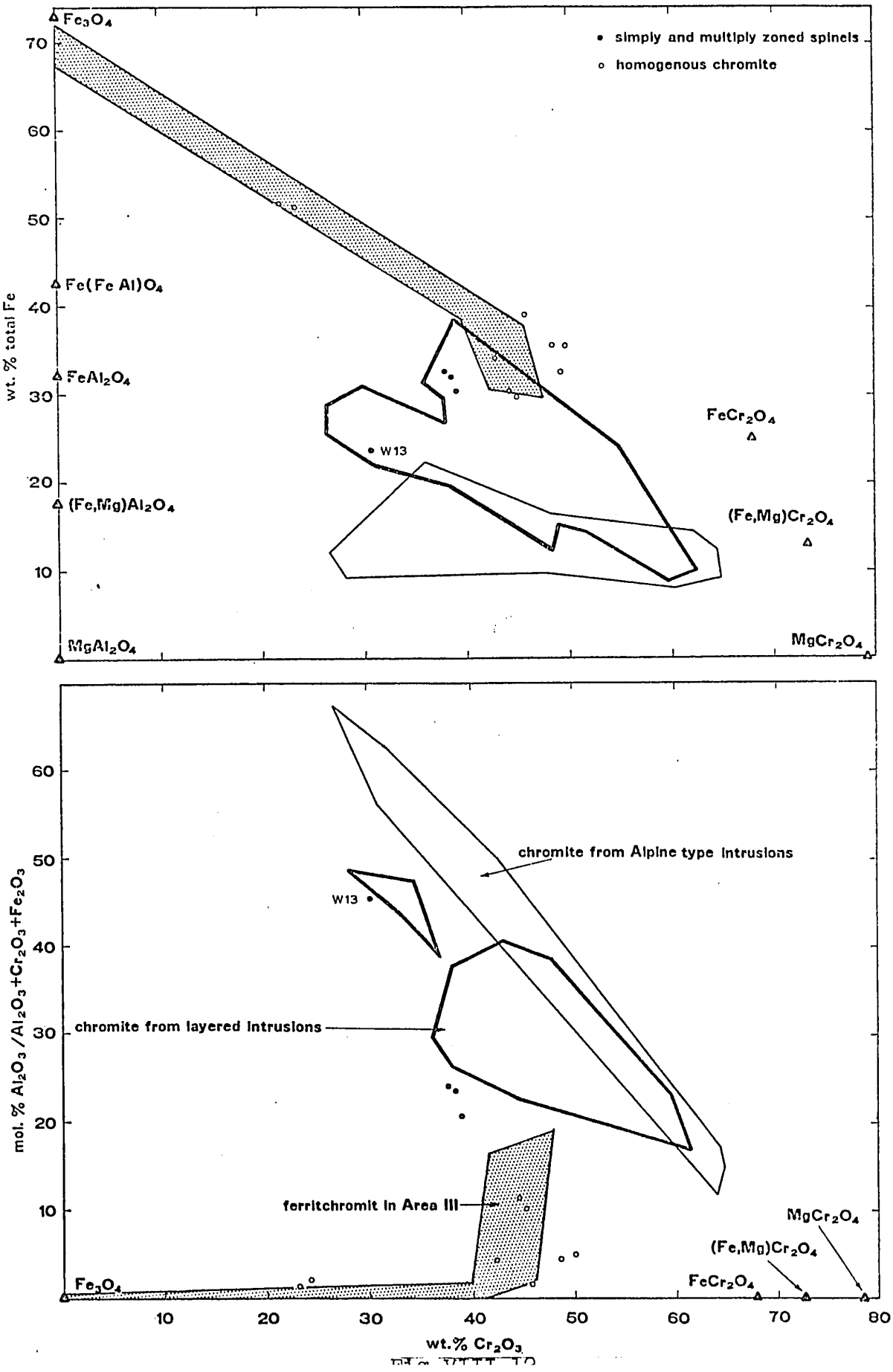
• simply and multiply zoned spinels
o homogenous chromite
wt. % total Fe
Fe_3O_4
$Fe(Fe\ Al)O_4$
$FeAl_2O_4$
$(Fe,Mg)Al_2O_4$
$MgAl_2O_4$
$FeCr_2O_4$
$(Fe,Mg)Cr_2O_4$
$MgCr_2O_4$
W13
mol. % $Al_2O_3/Al_2O_3+Cr_2O_3+Fe_2O_3$
chromite from Alpine type intrusions
chromite from layered intrusions
ferritchromit in Area III
wt.% Cr_2O_3

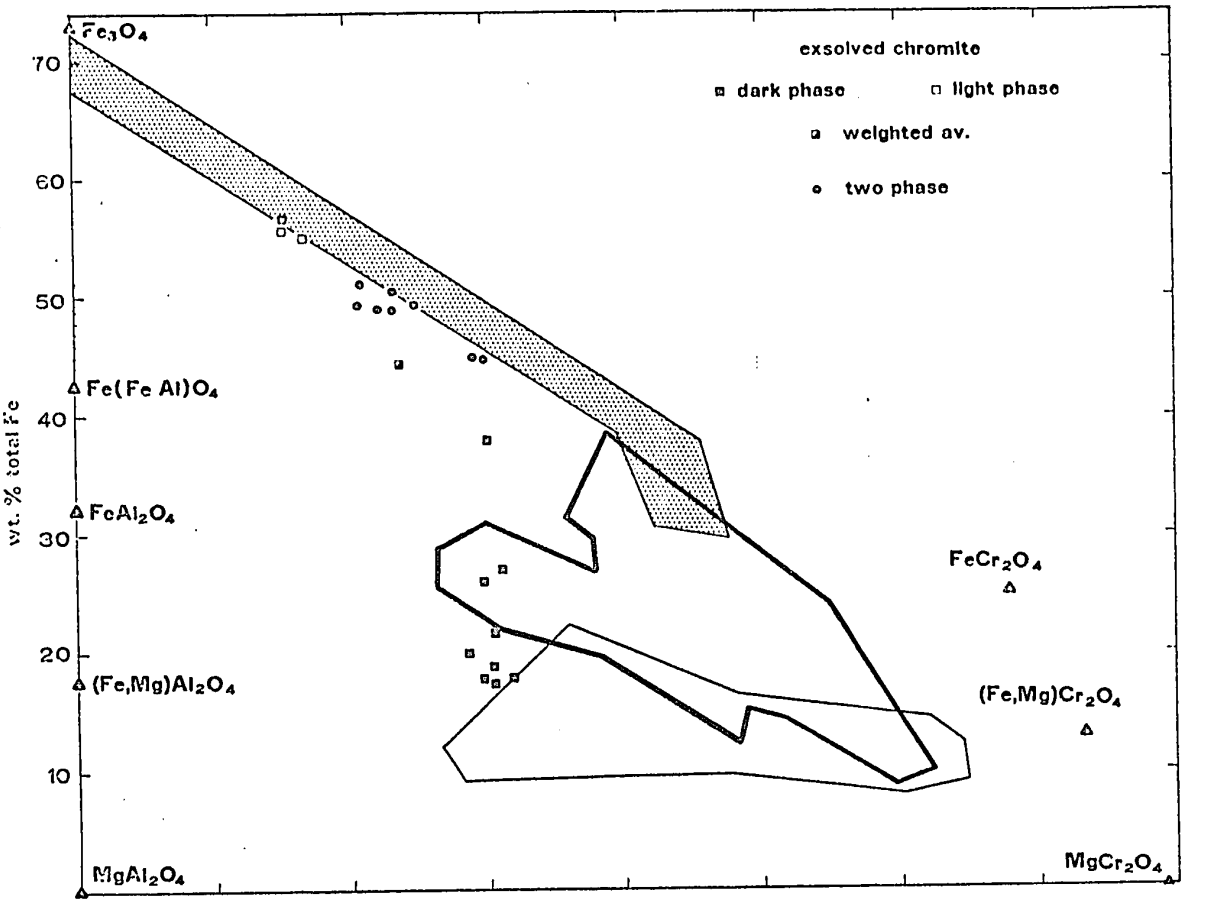
exsolved chromite
dark phase
light phase
weighted av.
two phase
Fe_3O_4
$Fe(Fe\ Al)O_4$
$FeAl_2O_4$
$(Fe,Mg)Al_2O_4$
$MgAl_2O_4$
$FeCr_2O_4$
$(Fe,Mg)Cr_2O_4$
$MgCr_2O_4$
wt. % total Fe
70
60
50
40
30
20
10

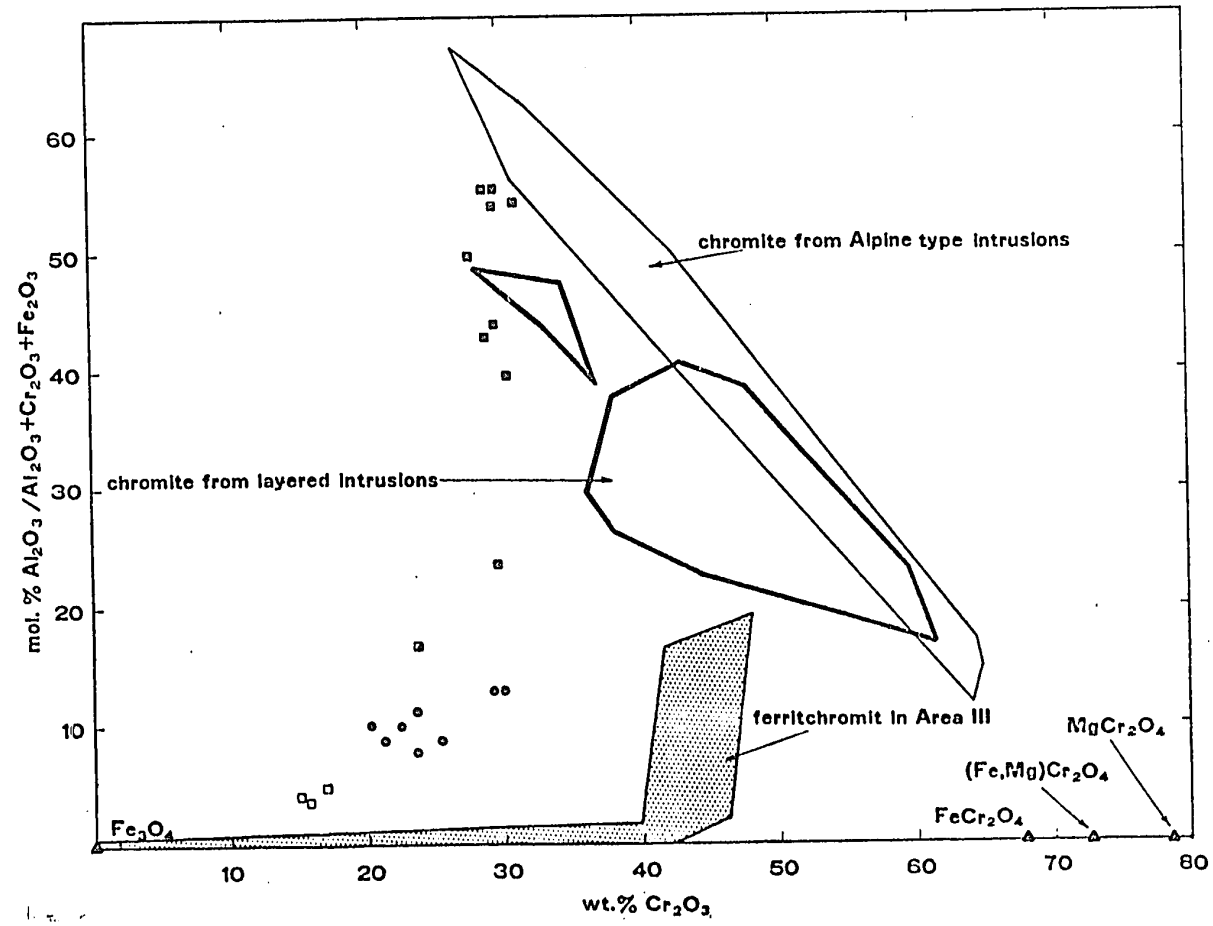
chromite from Alpine type intrusions
chromite from layered intrusions
ferritchromit in Area III
Fe_3O_4
$FeCr_2O_4$
$(Fe,Mg)Cr_2O_4$
$MgCr_2O_4$
mol. % Al_2O_3 / Al_2O_3+Cr_2O_3+Fe_2O_3
wt.% Cr_2O_3
60
50
40
30
20
10
10
20
30
40
50
60
70
80

induced in chrome spinels by heating under high oxygen fugacities. It is possible that in Area I exsolution results from rise in temperature of the serpentinite adjacent to a late granitic dyke.

The serpentine and chromite mineralogy in Area III serpentinites has been interpreted as indicating regional metamorphism of serpentinites; in spite of this complicated history, relicts of the original chromite are common. The serpentine mineralogy in Area I where lizardite only is present is interpreted as indicating a less complicated geological history subsequent to serpentinization. It would be expected that remnants of the original chromite would be well in evidence in Area I; in fact they are not, and this together with the 'non-magmatic' composition indicates that chromite has undergone a complicated history prior to serpentinization, and subsequent to crystallization.

It is concluded that the composition and textures of the chromite in Area I indicate that some geological event occured prior to present serpentinization, an event which altered the composition of the chromite. The nature of this event can only be speculated upon at present.

The serpentinites in Area I contain a pervasive serpentine mesh texture (Plate 26) in which relict interstitial material has been reduced to a minimum (Plate 29), and a relict interlocking texture of original silicates is apparent. Such interlocking textures are characteristic of recrystallization of primary silicates either during deformation or under high grade metamorphism. Serpentinized amphibole, which is clearly later than the original olivine (Plate 12) is common throughout the

ultramafics, and has a texture consistent with it being a late, metamorphic mineral, transacting all other constituents.

It is suggested that the ultramafics underwent high grade regional metamorphism prior to the present serpentinization, which recrystallized the silicates to an interlocking mosaic and altered the chromite to homogeneous ferritchromit. It is not certain whether the homogeneous ferritchromit formed on metamorphism from chromite in a fresh ultramafic rock or from composite chromite-magnetite grains in a serpentinite.

F CONCLUSIONS

The following conclusions may be drawn concerning the origin of chrome spinel in Reservation 34:-

(1) The homogeneous chromite cores in the zoned spinels in Area III are original magmatic chromite.

(2) Ferritchromit rims of variable composition surround the magmatic chromite cores in Area III and result by reaction of chromite and magnetite rims formed during serpentinization. The reaction was promoted by post-serpentinization regional metamorphism.

(3) The chromites in Area I have undergone a complicated post-crystallization but pre-serpentinization history, probably as a result of high grade regional metamorphism.

(4) Homogeneous magnetite rims formed around the chromite in Area I during serpentinization.

The following conclusions may be drawn about chrome spinel generally:-

The compositional field of magmatic chromite is well-defined and is controlled by the physical conditions pertaining at the time of crystallisation.Chromite is however nct stable under conditions of pressure,temperature and fo_2 different from those under which it originally crystallised.An elevation of temperature will promote a reaction to produce a chrome spinel, ferritchromit,stable under the new conditions.

The evidence of the reaction is provided by the occurence of ferritchromit rims,of variable composition,around chromite in metamorphosed ultramafic rocks,and in other environments in which an elevation of temperature occurs.The correlation between the occurence of ferritchromit,together with antigorite,or other Al-silicate,shows that chrome spinel may be used as a metamorphic petrogenetic indicator up to the epidote-amphibolite facies.The occurence of homogeneous ferritchromit,whose composition lies outside the field of magmatic chromite,indicates that at higher grades of metamorphism,the alteration product may homogenise.The use of chromite as a metamorphic indicator extends therefore to higher grades but the nature of the alteration is less certain.

G SUGGESTIONS FOR FUTURE WORK

The experimental work on chromite has been directed towards an understanding of the various spinel solid solutions involving the chromite molecule.The writer knows of no published work concerning the stability of chromite when subjected to physical conditions different to those under which it formed. It would be informative to heat chromite,and chromite-bearing rocks, under controlled conditions of temperature,pressure and fo_2,and

to examine the alteration products.This would more clearly establish the nature and mechanism of the alteration.

An examination of further examples of metamorphosed ultramafic bodies,both serpentinised and fresh,would yield more data on the relation of chromite composition to metamorphism.Ideally this study should be conducted on ultramafic rocks that can be traced from unmetamorphosed to metamorphosed.

An examination of sulphides coexisting with altered chromite would establish whether sulphide mineralogy reflects the metamorphic changes as well as the spinels.Further work on the sulphides in Areas I and III is now being undertaken.

IX GEOLOGICAL HISTORY OF SERPENTINITES IN RESERVATION 34

The salient differences between the serpentinites in Areas I and III (Table VI.1) have been presented in Chapter VI. The conclusions drawn from these differences are supported by the additional evidence of the chrome spinels. It is now possible to propose a sequence of events for Area I (Manitoba Nickel Belt-Type) and Area III serpentinites (Table IX.1).

A AREA III SERPENTINITES

(1) A dunite containing an average amount of nickel was emplaced as a magma, or crystal-liquid mush such that it could crystallize to a cumulate. The lack of features associated with protoclastic deformation suggest that if it was emplaced tectonically; it was thoroughly lubricated at the contact to preclude internal deformation. Small amounts of Fe-rich, Fe-Ni sulphides were formed.

(2) The dunite was serpentinized, without accompanying deformation resulting in lizardite and clinochrysotile mesh-textured pseudomorphs after olivine. Magnetite released upon serpentinization of the silicates formed rims on the primary chromite and many small grains throughout the serpentinite; minor amounts of Ni-rich sulphides formed from the release of Ni from the serpentinized silicates and S released by oxidation of original magmatic pyrrhotite.

(3) The serpentinite and wall-rocks were regionally metamorphosed to the epidote-amphibolite facies. Antigorite, and possibly clinochrysotile, and a small amount of tremolite formed from the mesh-textured serpentine. Chromite grains reacted with

their magnetite rims to produce ferritchromit of varying composition around the relict chromite cores.

(4) The margins of the serpentinites were subjected to CO_2 metasomatism, which affected both the wall rocks and the serpentinites to form talc-carbonate schist.

(5) Phlogopite is of very minor occurrence in Area III type ultramafics near granite contacts, and indicates late stage hydrothermal activity possibly associated with granite intrusion.

B AREA I SERPENTINITES

(1) Ni-rich dunite and peridotite consisting of olivine, pyroxene, accessory chromite and a sulphide phase belonging to the mono-sulphide solid solution series was formed. It is unlikely that they were intruded in their present position.

(2) The ultramafic rocks may then have been serpentinized, resulting in the formation (inter alia) of magnetite rims to chromite grains.

(3) The ultramafic rocks underwent regional metamorphism to a high grade. This caused recrystallization, or regeneration, of olivine and pyroxene giving rise to an interlocking texture, and a recrystallization of chrome spinels. Some amphibole was developed.

(4) The metamorphosed ultramafic rock was re-serpentinized, resulting in the formation of lizardite mesh-textures and the addition of a magnetite rim to the altered chromite. Primary Fe-rich sulphides were replaced by Ni-rich ones.

(5) Minor metamorphic or hydrothermal activity resulted in the production of phlogopite throughout the serpentinite and in

anthophyllite-biotite contact zones between granitic dykes and serpentinites.

C CONCLUSIONS

Within a very short distance serpentinites of differing geologic history sub-outcrop. This is to be expected since the geology beneath Reservation 34 is not a simple extension of the Manitoba Nickel Belt (p.33).

When the evolution of the two types is compared (Table IX.1) there is only one event common to both, namely event (5), the production of phlogopite and some contact equilibration effects at a late stage. Even this is only poorly developed in Area III, being most common in those serpentinites nearer to the granite. Phlogopite is better developed in Area II(Fig.II.1) where the serpentinites are similar to those in Area III.

It is possible that the regional metamorphic event (3) that affected the two bodies is coeval and that a higher grade was achieved in Area I than Area III. If so then Area III type serpentinites were serpentinized before Area I-type and it is possible that the CO_2 metasomatism that affected Area III is related to the period of serpentinization in Area I.

The juxtaposition of serpentinites with very different evolutions suggests that a major tectonic break exists between Area I and the remainder of the Reservation. This break may occur between the Superior Province and Churchill Province with the Area I serpentinites belonging to the Manitoba Nickel Belt type and Area III type serpentinites being part of an Archaean greenstone belt; an extension of the Cross Lake sub-Province.

Table IX.1 Illustration of the contrasting evolution of serpentinites in Reservation 34.

AREA I		AREA III	
	PHLOGOPITE-SERPENTINITE Minor development of phlogopite. Biotite and enthophyllite selvedges develop at the contact between serpentinite and granitic dykes.		PHLOGOPITE-SERPENTINITE Minor and sporadic development of phlogopite.
(5) Hydrothermal activity & intrusion of granitic dykes.	SERPENTINITE Mesh-textured lizardite pseudomorphs olivine; magnetite rims chrome spinel of variable composition. Replacement of primary Fe-sulphides by Ni-sulphides.	(5) Hydrothermal activity	TALC-CARBONATE SCHIST Talc and carbonate develop in both wall-rocks and serpentinite on either side of the contact.
(4) Serpentinisation.	METAMORPHOSED ULTRAMAFIC Recrystallisation of either (a) original dunite and harzburgite to produce interlocking olivine and pyroxene, and ferritchromit from chromite or (b) serpentinite to regenerate olivine and pyroxene, and composite magnetite-chromite grains to react to form homogeneous ferritchromit	(4) CO_2 metasomatism	ANTIGORITE-SERPENTINITE Antigorite, together with minor tremolite and chlorite, develops; composite magnetite-chromite grains react to form ferritchromit of varying composition.
(3) Regional metamorphism to the amphibolite facies or greater.	SERPENTINITE Production of serpentinite minerals and magnetite rims to chromite grains.	(3) Regional metamorphism to epidote-amphibolite facies	SERPENTINITE Lizardite and clinochrysotile mesh-textured serpentinite pseudomorphs olivine; magnetite rims chromite grains; millerite forms.
(2) Serpentinisation ?	ULTRAMAFIC INTRUSION Formation of dunite and harzburgite consisting of olivine, pyroxene, accessory chromite and sulphides.	(2) Serpentinisation	ULTRAMAFIC INTRUSION Formation of dunite consisting of olivine, accessory chromite and rare Fe-sulphide.
(1) Intrusion or emplacement of ultramafic crystal mush		(1) Intrusion or emplacement of ultramafic melt.	
EVENT	RESULTING ROCK	EVENT	RESULTING ROCK

D SUGGESTIONS FOR FUTURE WORK

The implications regarding the conclusions that there are two different types of ultramafic body sub-outcropping beneath Reservation 34 are important from the point of view of regional geology and the continuation of the Manitoba Nickel Belt beneath the Palaeozoic rocks. The conclusion can only be properly evaluated as more becomes known about the geology in the vicinity of the Nickel Belt.

Wicks (seep.9) has established characteristics of the serpentine mineralogy in the Nickel Belt between Manibridge and Thompson and it would be interesting to examine the chromite mineralogy to see what correlation exists. Clinochrysotile occurs towards Thompson and it is possible that this indicates metamorphism to the greenschist facies.If this is so then some alteration might be expected in the chromite analogous to that demonstrated in Area III.as a result of metamorphism.

The Area I serpentinites are similar to those in the exposed portion of the Manitoba Nickel Belt and conform to the sequence of serpentine minerals established by Wicks.The assignment of Area I serpentinites to the Manitoba Nickel Belt would be confirmed if the chromite mineralogy was found to be consistent.

It was concluded that the Area III serpentinites were not part of the Manitoba Nickel Belt sequence and that they were likely to be part of an Archaean greenstone belt.Detailed descriptions of ultramafic rocks in the Cross Lake sub-Province would facilitate the comparison.

CLAIMS AS TO ORIGINAL WORK

Original work in this thesis pertains to the regional geology at the SW end of the Manitoba Nickel Belt and to chrome spinel mineralogy.

Manitoba Nickel Belt

(1) Knowledge of the geology of the Manitoba Nickel Belt has been extended SW beneath the Palaeozoic cover.

(2) It has been shown that the ultramafic rocks of different type sub-outcrop beneath Reservation 34. One type (Area I) has wall-rocks, mineralization and serpentine mineralogy consistent with them belonging to the Manitoba Nickel Belt. The other sequence of ultramafic rocks has had a more complex serpentinization history, and its environment and mineralogy are not typical of the Manitoba Nickel Belt sequence. It is possible that these serpentinites are part of an Archaean schist belt extending west beneath the Palaeozoic from the Superior Province.

Spinel Mineralogy

(1) Ferritchromit rims of chrome spinel have been shown to have resulted from regional metamorphism and not as previously thought from serpentinization.

(2) This leads to the possibility of using chrome spinel as a metamorphic petrogenetic indicator. Further work is needed in both the field and the laboratory to establish this conclusion. Spinel mineralogy could be a powerful tool in elucidating the metamorphic history of ultramafic rocks that have undergone serpentinization at a late stage in their history.

ACKNOWLEDGEMENTS

The invitation to work on the ultramafic rocks came from Dr.J.A.Hansuld of Amax Exploration Inc.,Toronto.Amax Exploration supplied financial support during the first portion of the investigation,technical assistance,free access to diamond drill core and geological data and, transport and living accomodation in the field.This support is gratefully acknowledged,as is that supplied by Dr.J.E. Gill,through N.R.C. grant No.NRC A-1511,**and by Dr.J.S. Stevenson through microprobe operating grant NRC A-4258.**

I would like to acknowledge the help and encouragement of my thesis supervisor,Dr.W.H.Maclean,who also provided instruction in the use of the electron microprobe and financial assistance to defray computer and other costs through N.R.C. grant No.NRC A-7719.

I would also like to thank:-

Dr.F.J.Wicks of the Royal Ontario Museum who made the X-ray microbeam determinations of serpentine and other minerals and who provided much stimulating discussion on serpentinites and their mineralogy.

Dr.R.E.T.Hill of Amax Exploration Inc.,who acted as guide in the initial stages of the project and provided data and discussion.

Dr.R.Martin of McGill University for critically reading the manuscript.

J.B.Brown of McGill University who cooperated in making X-ray diffraction determinations.

M.Firth of McGill University for electron microprobe

instruction.

Drs.H.Helmstaedt and J.S.Stevenson of McGill University, Dr.A.J.Naldrett of Toronto University, Drs.C.K.Bell and T.N. Irvine of the Geological Survey of Canada, D.C.Cranstone of the Manitoba Mines Branch, Dr.T.Thayer of the United States Geological Survey, Dr.S.A.de Waal of the National Institute for Metallurgy, Johannesburg, and many others for discussion on many aspects of the thesis topics.

PLATES

The photomicrographs, Plates 1-42, were taken by a Leitz Photomicroscope 35mm camera, (with automatic exposure) using Kodak Panatomic X film and normal commercial developing and printing. The bar scale on each photograph represents 0.1mm.

The electron beam images, Plates 43-45, were taken through the optical microscope of an Acton-cameca electron microprobe.

The X-ray microbeam images, Plate 46, were taken by Dr. F.J. Wicks of the Royal Ontario Museum, using a Norelco microbeam X-ray camera.

Plate 1 Olivine replaced by mesh textured serpentine (Area III). Irregular white lizardite mesh rims enclose dark mesh centres of clinochrysotile and lizardite. Antigorite (white) is in turn replacing the mesh-textured serpentine. Dusty magnetite is aggregated into some mesh centres. The texture is relict cumulus. (W 87, transmitted light).

Plate 2 Relict cumulus texture in serpentinized dunite (Area III). Euhedral to sub-hedral olivine replaced by mesh textured serpentine (dark) in turn replaced by antigorite (light), largely around the margins. Secondary magnetite forms trains outlining the original olivine and fills the interstitial spaces. Large rounded spinels are relicts of primary chromite. (W 162, transmitted light photograph of a polished thick section).

Plate 3 Olivine replaced by mesh-textured serpentine (Area III). The euhedral outline of the original olivine is clearly visible. Bipartite veins of α-serpentine, lizardite, enclose mesh centres of isotropic lizardite and clinochrysotile. Antigorite (colourless) is replacing the margin of the pseudomorph. These 3 interstitial spinel grains are present. (The fine grid is the microprobe beam scar) W 89, transmitted light.

Plate 4 Mesh-textured serpentine typical of Area III. Olivine pseudomorphed by lizardite and clinochrysotile mesh-textured serpentine, with the individual pseudomorphs clearly outlined by interstitial material. (W 63, crossed nicols).

Plate 5 Mesh-textured serpentine partially replaced by fine antigorite (Area III). Similar orientation of mesh rims in widely separated remnants indicates a lack of deformation accompanying the formation of antigorite. (W 201, crossed nicols).

Plate 6 'Curtain' antigorite (Area III); mesh-textured serpentine replaced by fine antigorite and coarse 'curtain' antigorite developing from a fracture through the pseudomorph. A portion of the pseudomorph margin has a fringe of coarse antigorite as well. (W 201, crossed nicols).

Plate 7 Lizardite ribbon mesh rim continuous across a grain boundary between two olivine pseudomorphs (Area III). (W 219, crossed nicols).

Plate 8 Bipartite mesh rim (Area III). The vein is separated into two zones of lizardite by a median of nearly isotropic serpentine. (W 87, crossed nicols).

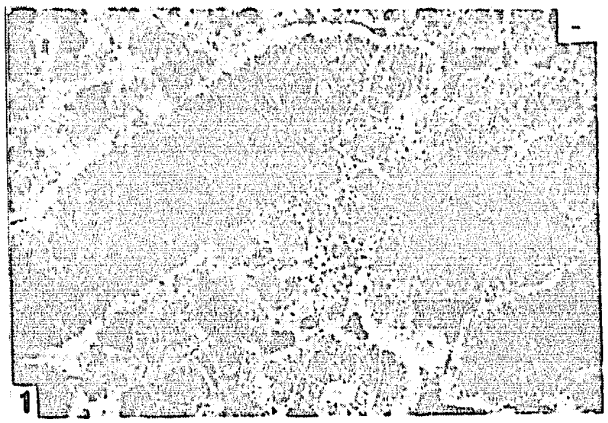
1

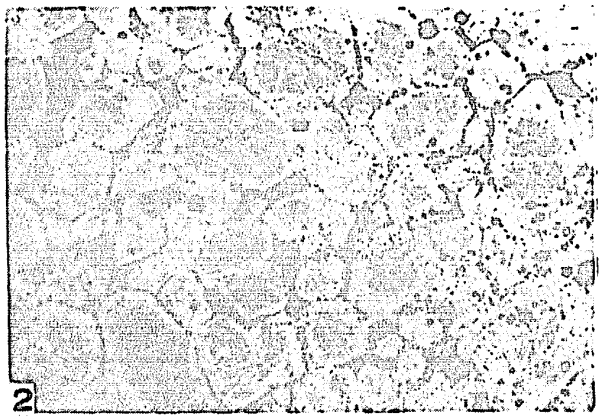
2

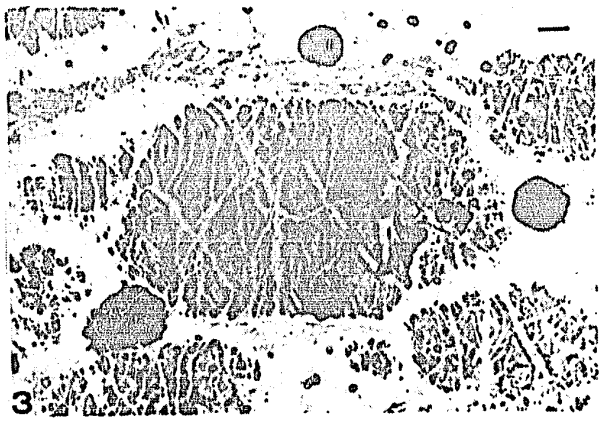
3

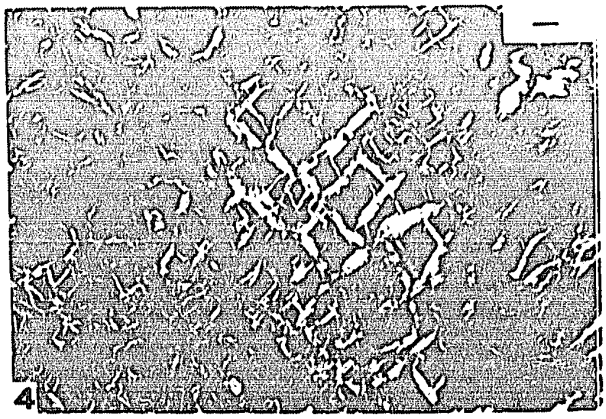
4

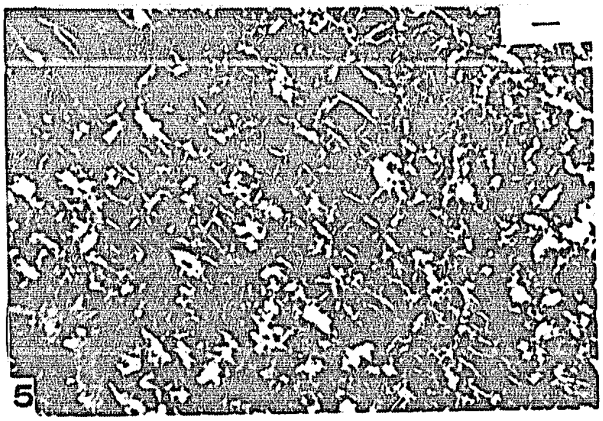
5

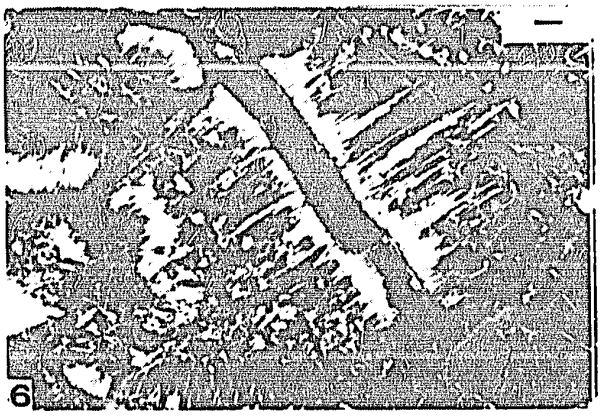
6

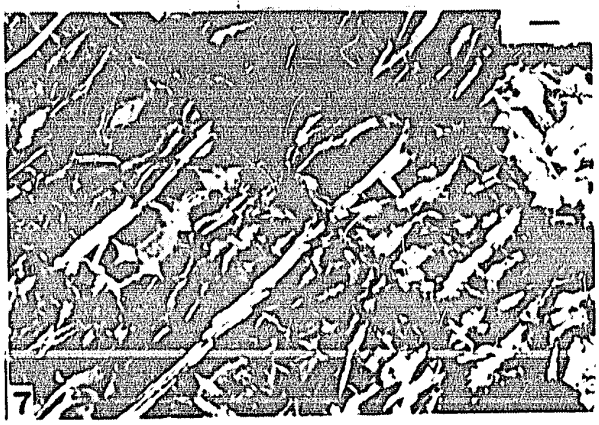
7

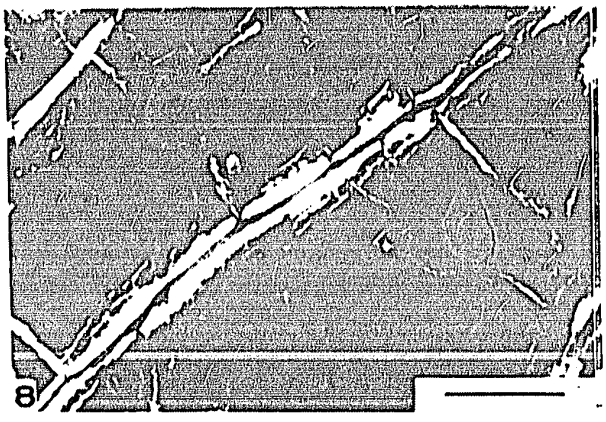
8

Plate 9 Mesh-textured serpentine (Area III) in which the mesh centres consist of fibro-lamellar patches of orientated clino-chrysotile. (W 201, crossed nicols).

Plate 10 Exterior mesh rim to serpentinized olivine (Area III). Isotropic mesh centres are separated by mesh rims of lizardite. The exterior mesh rim is present around the margin of the olivine pseudomorph, an uncommon feature. (W 63, crossed nicols).

Plate 11 Partially serpentinized olivine remaining in a mesh centre (Area I). (2228, crossed nicols).

Plate 12 Serpentinized amphibole laths (Area I) in serpentinized dunite. The smaller of the two pseudomorphs cuts through a serpentinized olivine. (W 749, crossed nicols).

Plate 13 Bastite pseudomorph after pyroxene (Area III). The prominent orthogonal parting may be a relic of the (110) pyroxene cleavage. (2241, crossed nicols).

Plate 14 Serpentinized amphibole (Area III). The amphibole pseudomorphs cut through the serpentinized olivine (W 335, crossed nicols).

Plate 15 Bastite pseudomorph (Area I) after a longitudinal section of pyroxene enclosed in mesh textured serpentine after olivine. (W 467, transmitted light).

Plate 16 Bastite pseudomorphs (Area III) after pyroxene. Interstitial space between serpentinized olivine (white) is occupied by magnetite (black) and bastite (grey). The bastite on the left side shows an outline and cleavage suggestive of a pyroxene cross-section. (W 55, plain light).

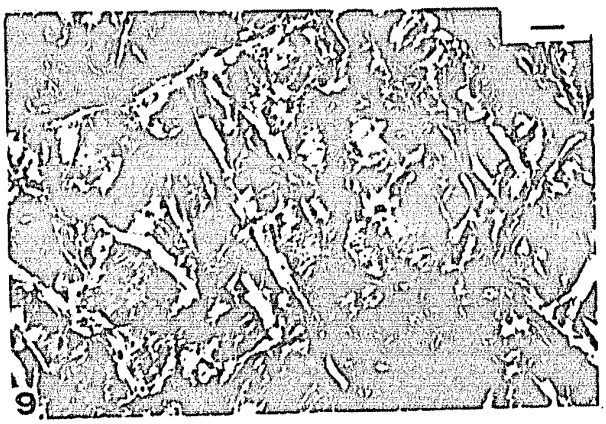
9

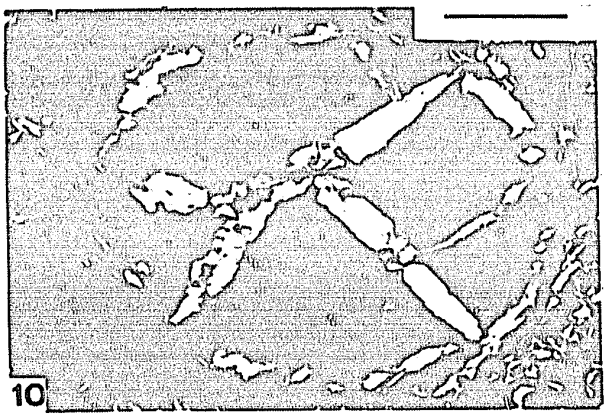
10

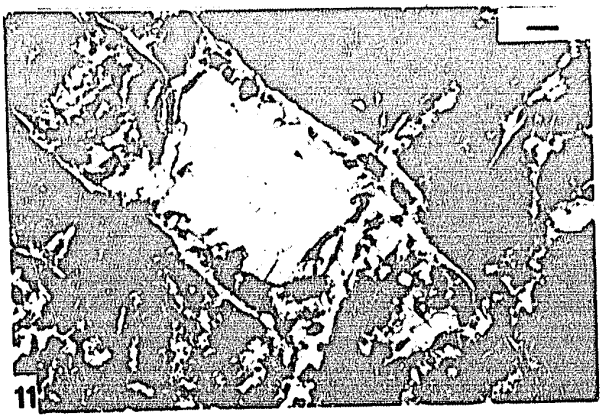
11

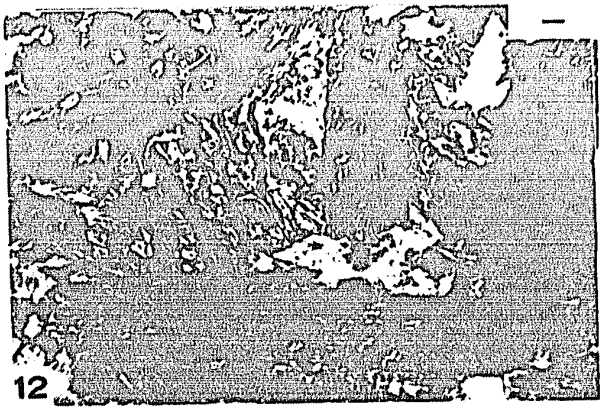
12

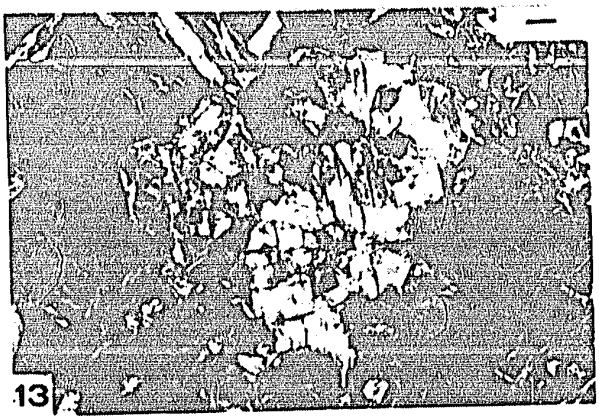
13

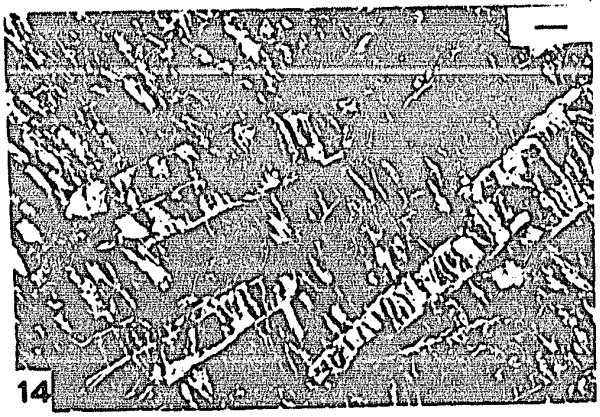
14

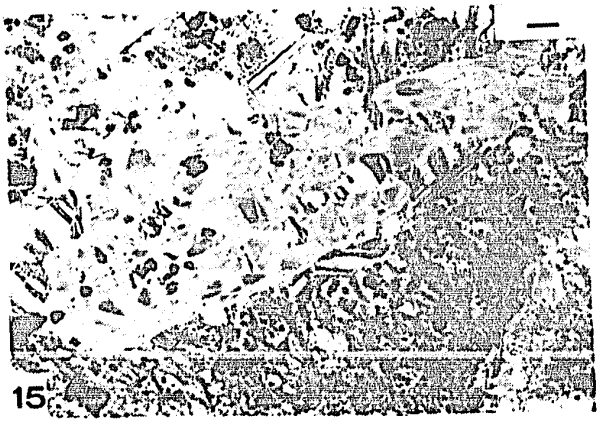
15


16

Plate 17 Deformed dunite from Mount Albert, P.Q. Granulation of the dunite results in porphyroblastic olivine in a fine matrix: a bimodal texture (Specimen SDM 57/593 made available by Dr. F.J. Wicks; transmitted light, crossed nicols).

Plate 18 Serpentinized deformed peridotite from Glen Urquhart, Scotland (Francis, 1965). The bastite pseudomorphs are bent; the mesh textured serpentine consists of both large and small olivine pseudomorphs, resulting from the serpentinization of a granulated olivine similar to that in Plate 17. (Specimen Glen Urquhart 18508 made available by Dr. F.J. Wicks; transmitted light, crossed nicols).

Plate 19 Exsolution textures in the core of a zoned spinel (Area I). The centre of the chromite core contains fine exsolution lamellae of a light and dark phase. The chromite rim is homogeneous as is the more highly reflecting magnetite rim. The very highly reflecting material at the margin of the photograph is pentlandite. The numbers refer to analyses in Table V.6; the letters to zones described on p.119 (W 747, reflected light, oil immersion).

Plate 20 Rounded and exsolved chrome spinel (Area I) enclosed in a grain of euhedral magnetite. Small grains of pentlandite are enclosed by the magnetite. (W 747, oil immersion, reflected light).

Plate 21 Multiply zoned spinel (Area I) in which the magnetite rim is incomplete apparently having been removed from part of the grain. The grain has been badly fractured and a light, highly reflecting, sponge-textured magnetite (Table IV.5) partly fills the fractures and extends as a plume to one side of the grain. (W 264, oil immersion, reflected light).

Plate 22 Simply and optically zoned spinel (Area III) with a dark grey chromite core. The highly reflecting material around the edge of the spinel is hematite. (W 269, reflected light, oil immersion).

Plate 23 Simply and optically zoned spinel (Area III) with a train of silicate inclusions, near the outer margin of the grain, interpreted to represent the magnetite-chromite interface prior to the reaction which produced ferritchromit. (W 84, partially crossed nicols, reflected light, oil immersion).

Plate 24 Multiply zoned spinel (Area III). A dark grey core of homogeneous chromite is surrounded by ferritchromit with increasing reflectivity towards the magnetite at the rim. The ferritchromit is partially replaced by a pyroaurite-group mineral, giving rise to an 'atoll' structure. Fractures in the spinel are filled by serpentine and have a narrow zone of magnetite along their margin. The white spots in the centre are electron beam scars (see also Plate 43) (W 264, oil immersion, reflected light).

Plate 25 Simply and cryptically zoned spinel (Area III). The spinel consists entirely of ferritchromit of varying composition but with negligible reflectivity differences; hence the cryptic zoning. (W 84, reflected light, oil immersion).


17

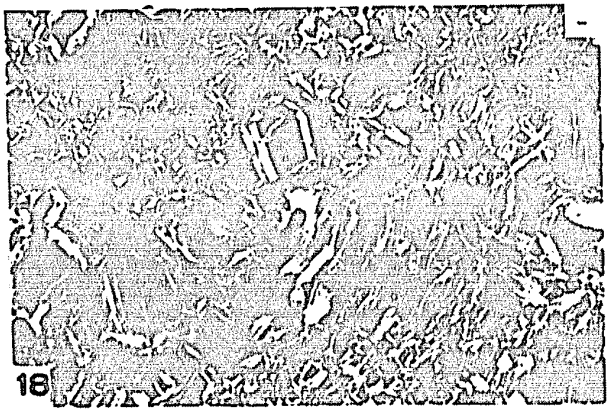
18

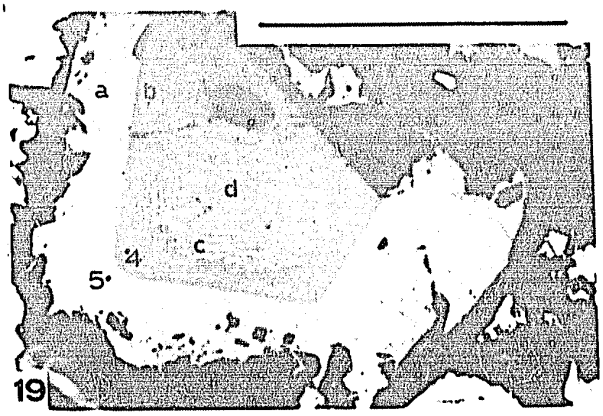

19

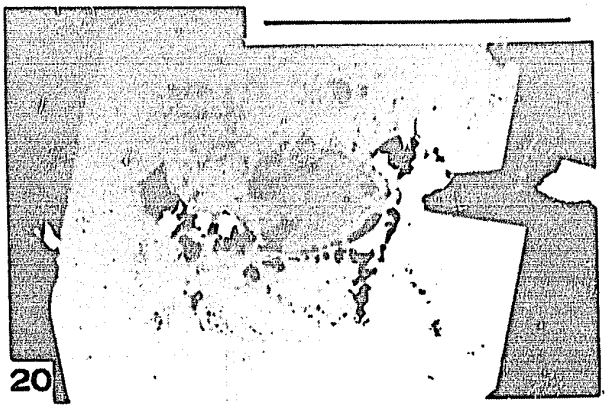
20

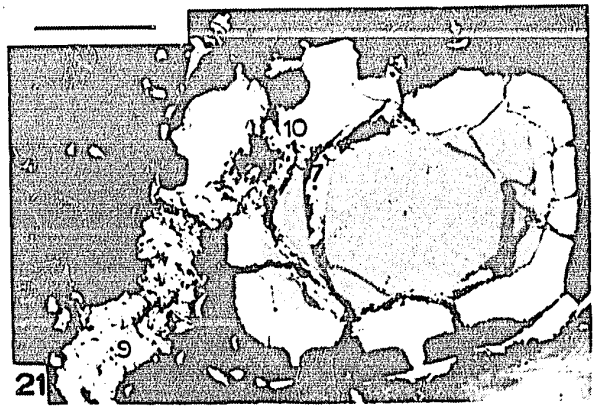

21


22

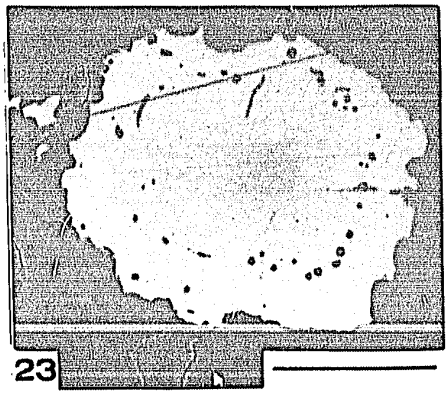
23

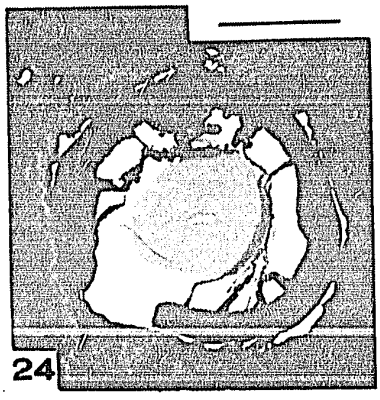
24

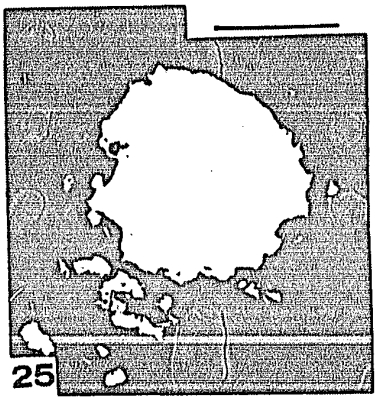
25

Plate 26 Mesh textured serpentine typical of Area I. Birefringent mesh rims of α-serpentine enclose mesh centres of isotropic lizardite. Some light, irregularly shaped bastite pseudomorphs are also present. Individual olivine pseudomorph outlines are not readily apparent. The texture compares closely with that from near Wabowden (Coats, 1968, Fig.2). (2240, crossed nicols).

Plate 27 Black serpentine with ribbon mesh texture (Area I). Alpha serpentine mesh rims, with irregular fringes of γ-serpentine mesh rims, with irregular parting of magnetite and isotropic serpentine separates the γ-serpentine from the isotropic serpentine of the next mesh. (W 473, plain light). This is similar to the texture of an ultramafic from near Setting Lake (Coats, 1968, Fig.3).

Plate 28 Pentlandite surrounding serpentinized olivine (Area I). Outlines of rounded olivine pseudomorphs are visible, with pentlandite occupying intergranular spaces and grain boundaries. (2384, reflected light).

Plate 29 Serpentinized olivine (Area I) with interstitial and intergranular pentlandite. Apart from the sulphide the intercumulus material is entirely eliminated, resulting in a sulphide net texture. (2386, reflected light).

Plate 30 Detail of exsolution textures in the core of a zoned spinel (Area I). The upper portion of the spinel shown in Plate 31. The letters refer to the zones described on p. 117. (Oil immersion, reflected light).

Plate 31 Exsolution textures in the core of a zoned spinel. A dark rim of chromite encloses a reticulate network of veins consisting of a light and dark phase. These veins divide the core of the spinel into areas consisting of very fine exsolution lamellae. Magnetite rims the chromite and penetrates the spinel. The numbers refer to analyses in Table V.5, the letters to zones described on p.117. (W 747.7, oil immersion, reflected light).

Plate 32 Accessory chromite from the Great Dyke, Rhodesia. The light grey chromite has been fractured and veined by serpentine. White magnetite has been deposited around the margin of some of the chromite fragments and extends into the serpentine. The chromite outlines beneath the magnetite are angular suggesting that the magnetite has been added to the chromite and not replaced it. Reflected light.

Plate 33 Artificially induced exsolution in chromite. An homogeneous chromite from the Great Dyke, similar to the one above, heated for 6 weeks at 900°C.

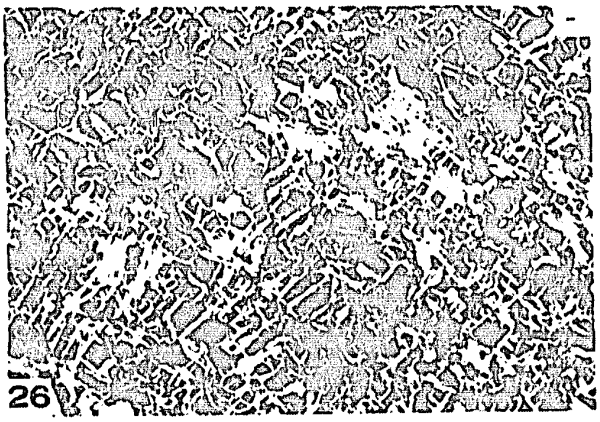
26


27


28


29

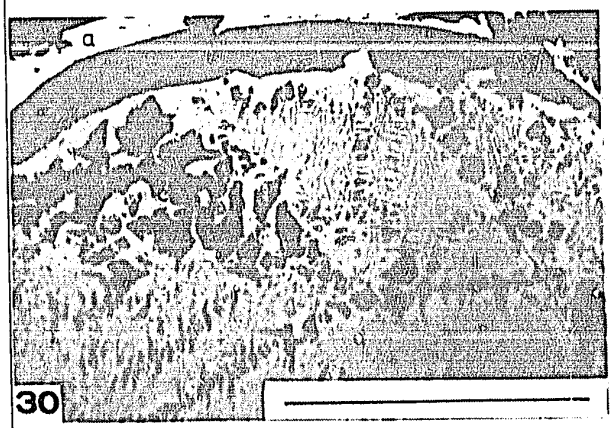

30

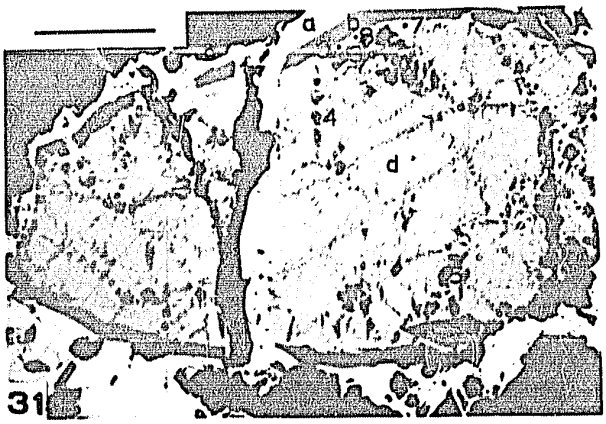

31

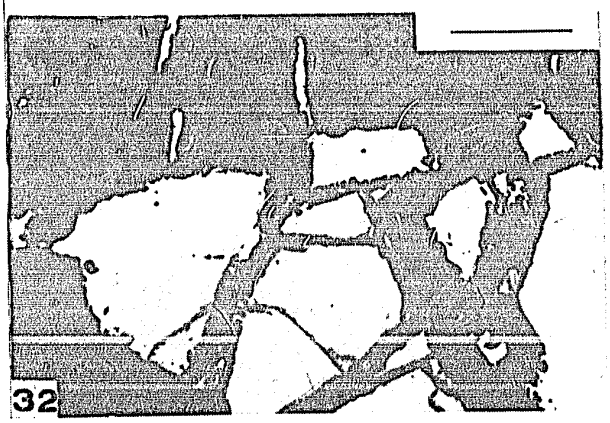
32

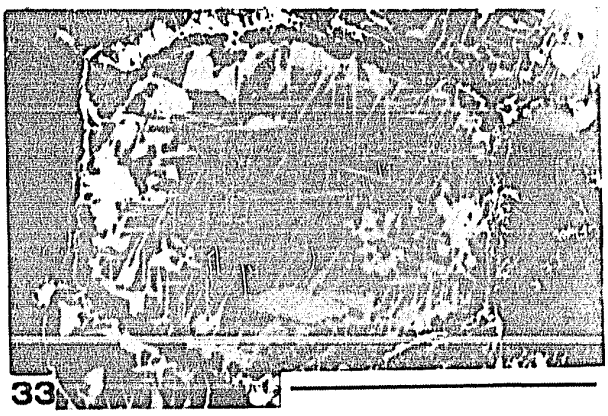
33

Plate 34 Multiply zoned spinel with a chromite core and a magnetite rim separated from each other by an incomplete zone of a pyroaurite-group mineral. The numbers refer to the analyses in Fig.V.1. (W 13, reflected light).

Plate 35 Simply zoned spinel consisting of a ferritchromit core with remnants of a magnetite rim. Phlogopite surrounds the spinel. The numbers refer to analyses in Table V.4. (2375, reflected light).

Plate 36 Homogeneous chromite with a scalloped margin adjacent phlogopite. (1027, reflected light).

Plate 37 Simply zoned spinel with chromite core and magnetite rim enclosed by pentlandite. The numbers refer to the analyses in Table V.4. (1031, reflected light).

Plate 38 Exsolved chrome spinel surrounded by a magnetite rim which also encloses an adjacent pentlandite grain. The exsolution texture is only poorly developed. (W 747, reflected light).

Plate 39 Multiply zoned spinel in which the chromite core and magnetite rim are also entirely replaced by stichtite. Pentlandite adjoins the spinel on the right side. (2246, reflected light).

Plate 40 Pentlandite in serpentinite. The large pentlandite grain surrounds a pseudomorph whose shape suggests it was spinel (compare Plates 19 and 37). Rounded, serpentinized olivine grains are outlined by interstitial pentlandite. (2247, reflected light).

Plate 41 Magnetite rim around a zoned and exsolved spinel. Fragments of the exsolved core have clearly been broken off and rotated during formation of the later magnetite rim (reflected light, oil immersion).

Plate 42 Pentlandite surrounding a pseudomorph of magnetite and pentlandite, probably after chromite. Compare the shape of the pseudomorph with the chromite core in Plate 37. (W 971, reflected light).

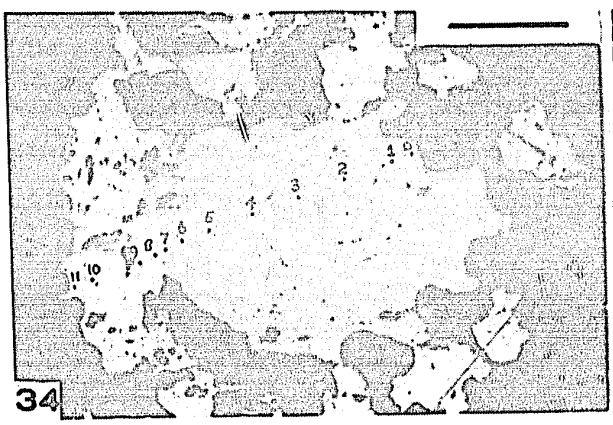
34

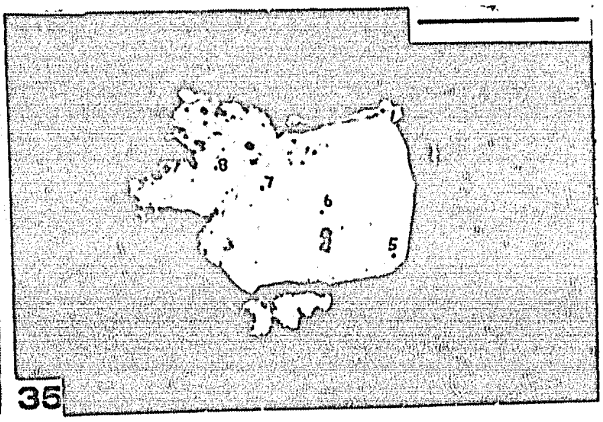
35

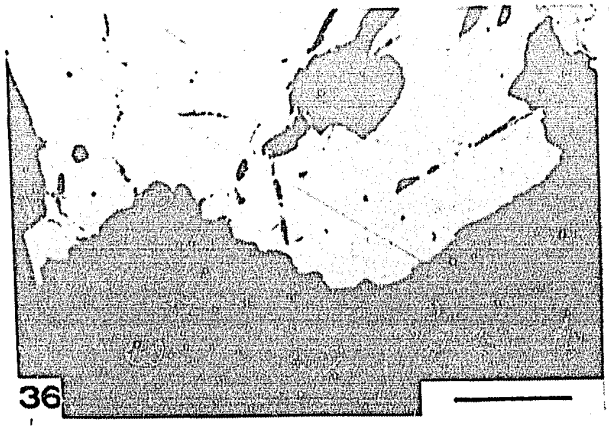
36

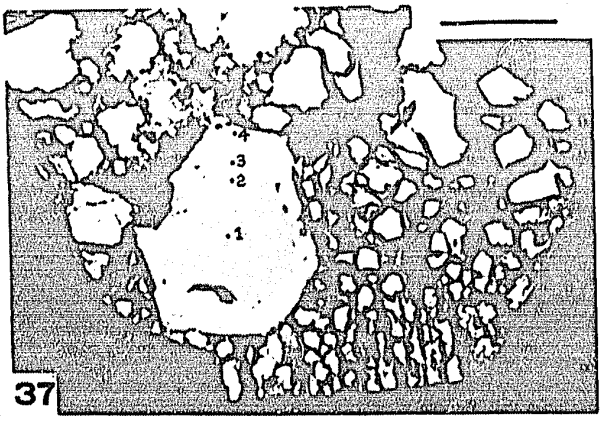
37

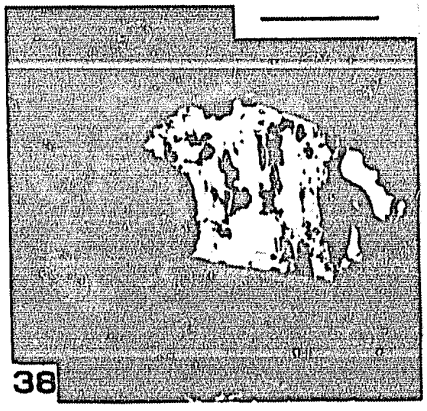
38

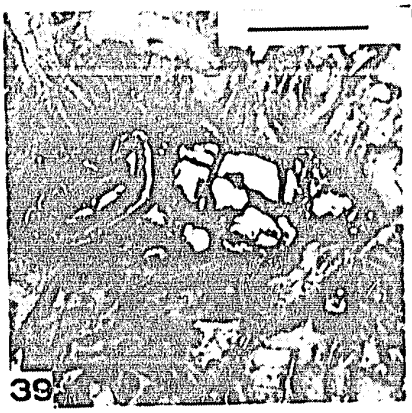
39

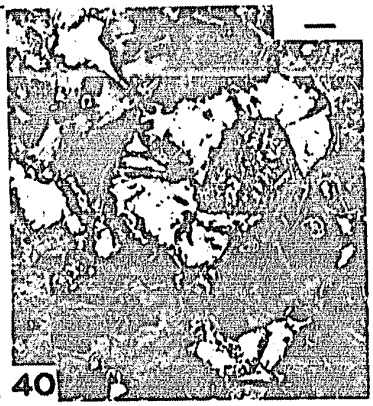
40

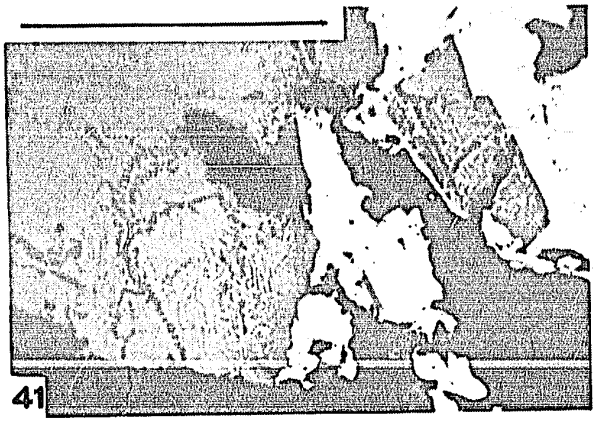
41

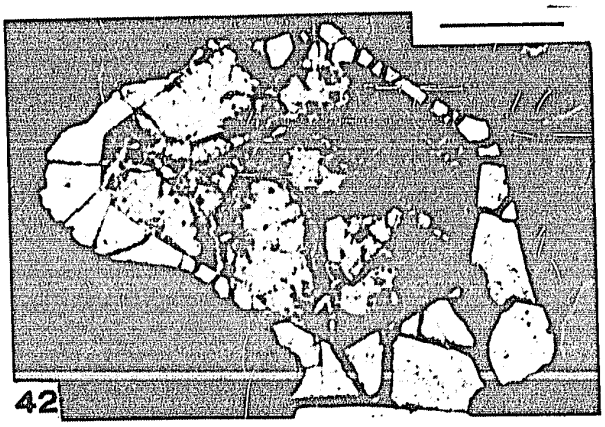
42

Electron beam images for Mg, Fe, Al, Ni and Cr in the multiply zoned spinel in Plate 24. The sharp compositional change between chromite core and ferritchromit rim for all elements other than Cr is apparent. The compositional change within the ferritchromit rim is not readily apparent except for Cr. The pyroaurite-group mineral which occurs between the magnetite rim and ferritchromit contains Mg, Cr and Fe suggesting it is a mixture of pyroaurite and stichtite (p.78). The serpentine-filled fractures are also apparent. The numbers on the key diagram refer to analysis numbers in Figure IV.9. The scale for the key diagram is slightly larger than the bar scale for the remainder.

PLATE 43

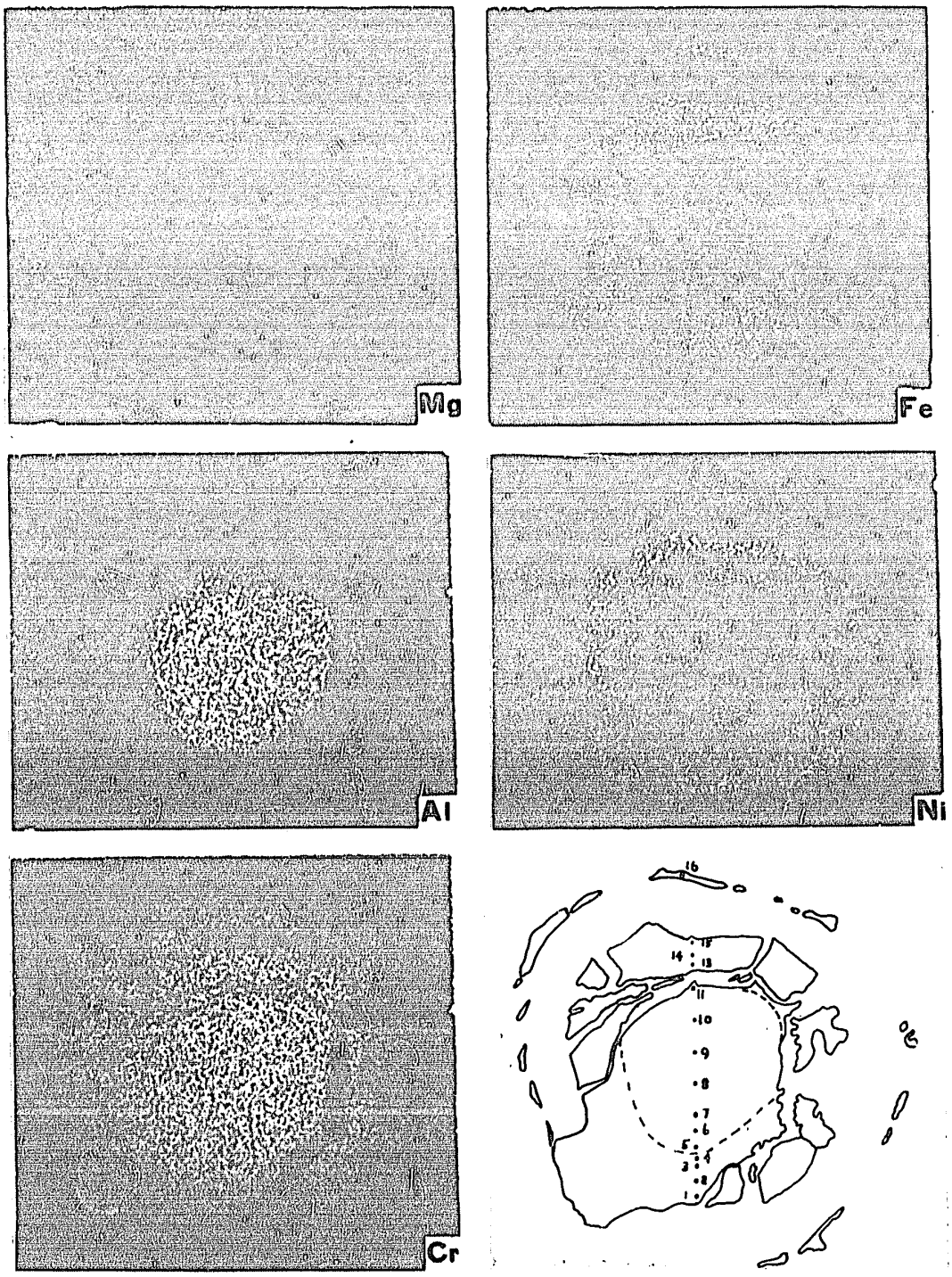
Mg
Fe
Al
Ni
Cr
16
15
14
13
12
11
10
9
8
7
6
5
4
3
2
1
.1 mm

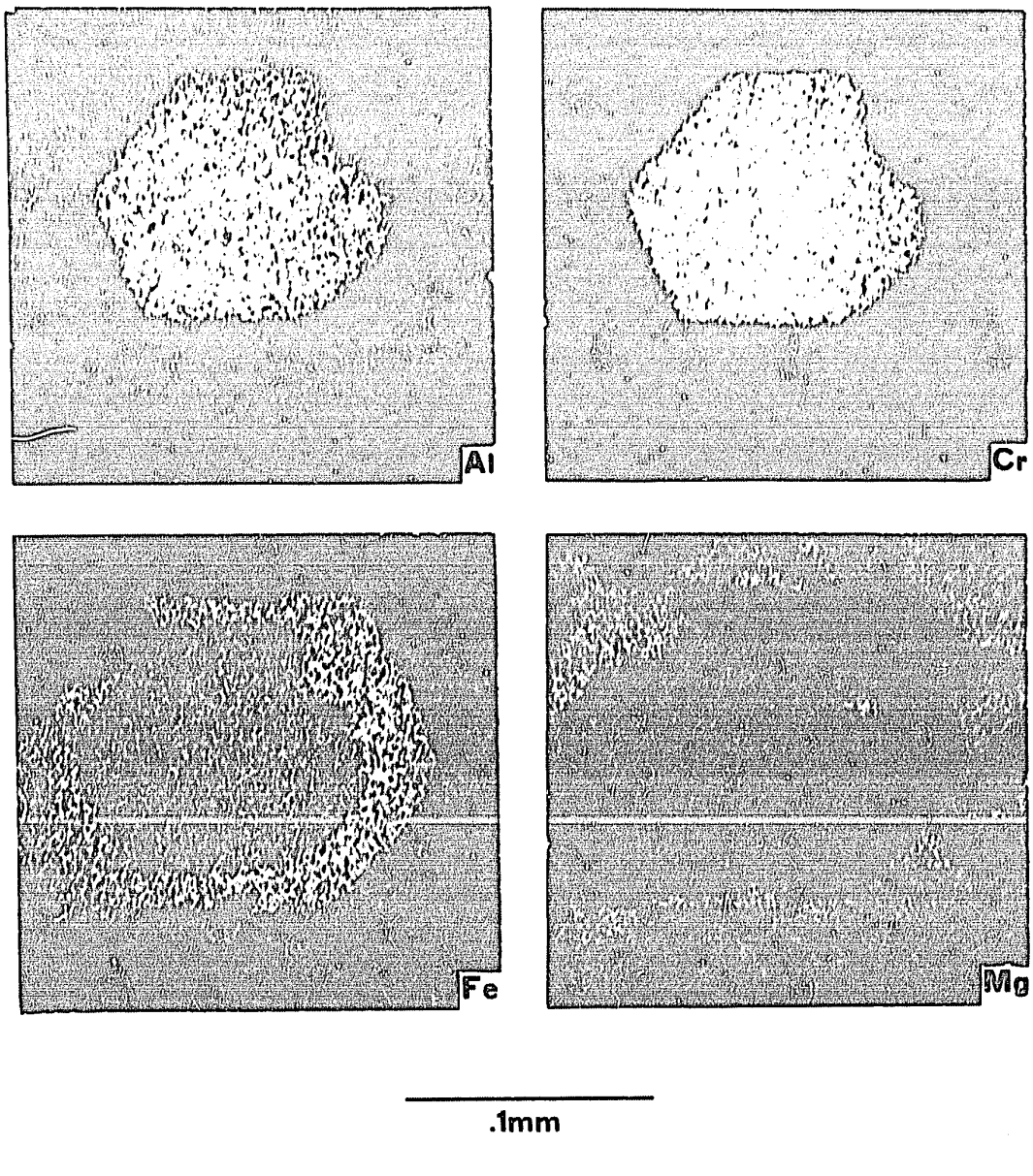

Electron beam images for Al, Cr, Fe and Mg in a simply zoned spinel, 1031. The chromite core is clearly marked by the Cr and Al, which is absent from the magnetite rim, the surrounding pentlandite and serpentine. The concentration of Fe and the depletion of Mg in the magnetite rim shows clearly in contrast to the concentrations of these elements in the core and the surrounding silicate and sulphide. An optical image of this spinel is shown in Plate 37 and analyses in Table V.4.

PLATE 44

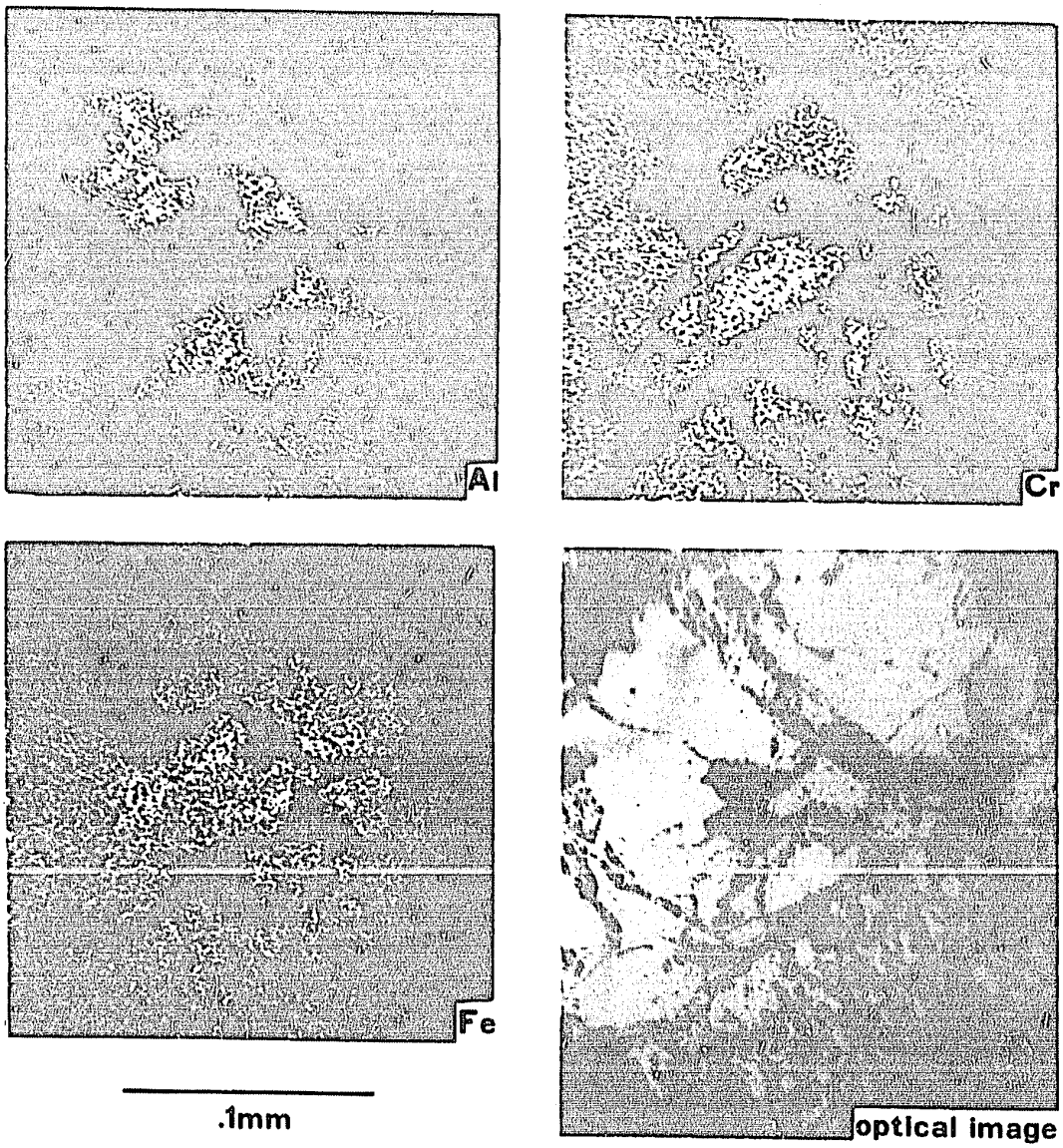

Electron beam images for Al,Cr and Fe and an optical image for a portion of a homogeneous spinel W980.Fe and Cr are distributed uniformly while Al is virtually absent.The silicate surrounding the spinel is phlogopite.The scale of the optical image is slightly larger than the bar scale for the electron beam images.

PLATE 45

6585	6688	6691
clinochrysotile and ?lizardite	clinochrysotile	clinochrysotile

6624	6587a	6631
clinochrysotile lizardite	lizardite (type I)	lizardite (type I)

6687	6714	6745
antigorite	lizardite (type I)	lizardite (type I)

6734	6730	6638
lizardite (type II)	lizardite (type I)	lizardite (type I)

6678	6789
pyro-aurite group	pyro-aurite group

Key to X-ray microbeam photographs in Plate 46

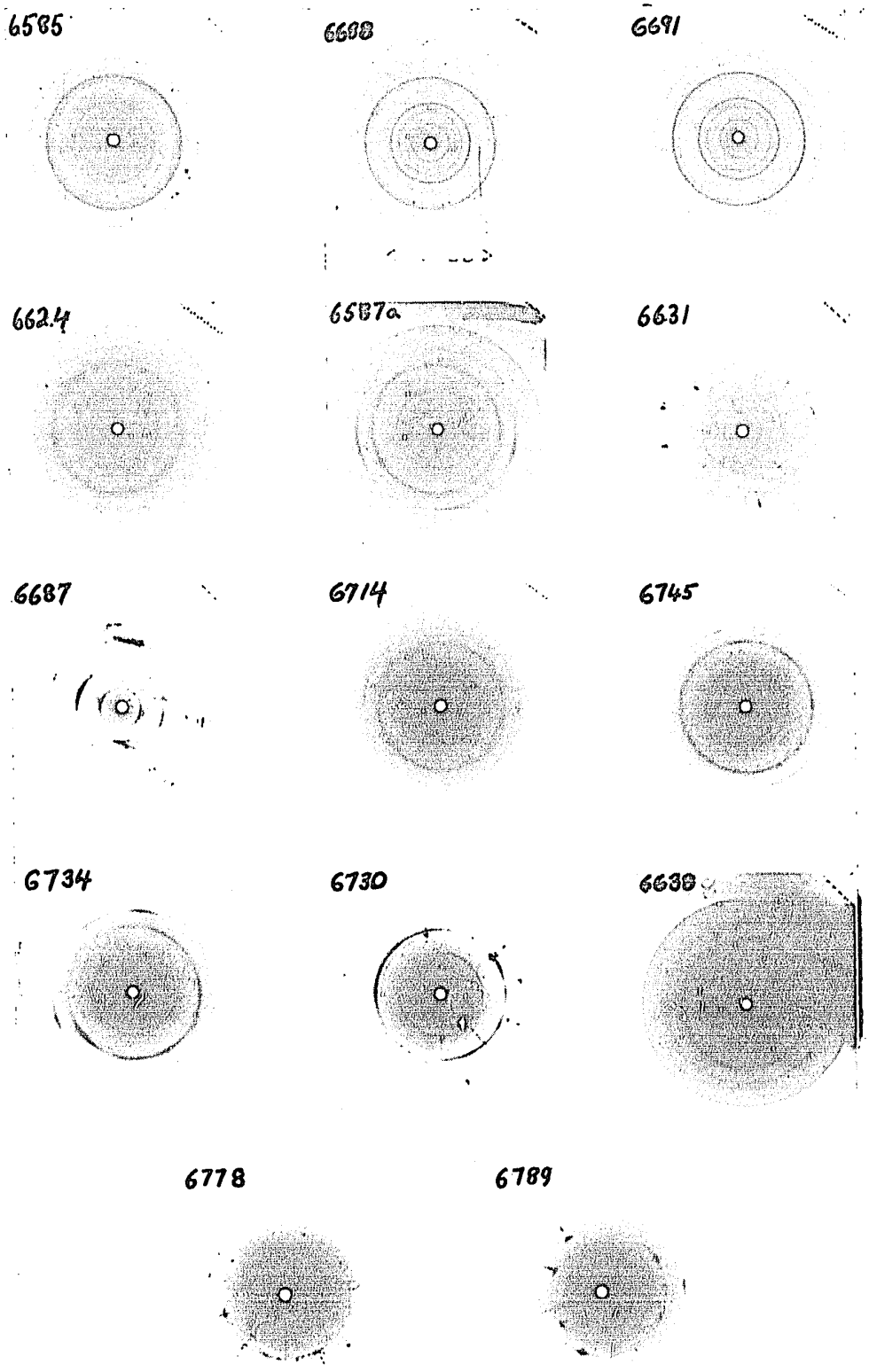

X-ray microbeam photographs of serpentine and the pyroaurite group mineral.(See Appendix II).

PLATE 46

LIST OF REFERENCES

Abdullaev, Z.B., Shcherbina, V.V. and Efendiev, G.Kh., 1967. The geochemistry of nickel and cobalt in ultrabasic rocks of the ophiolite formation of the Lesser Caucasus (Azerbaidzhan). Geokhimiya, 4, 425-432.

Allard, G.O., 1970. The Dore Lake Complex - a metamorphosed Bushveld-type layered intrusion. In: Geol.Soc.S.Afr., Spec.Pub. #1, 477-491.

Amin, M.S., 1948. Origin and alteration of chromites from Egypt. Econ.Geol., 43, 133-153.

Atlas, L.M. and Sumida, W.K., 1958. Solidus, sub-solidus and sub-dissociation phase equilibria in the system Fe-Al-O. J.Amer. Ceram.Soc., 41, 150-160.

Aumento, F., and Loubat, H., 1971. The Mid-Atlantic Ridge near 45° N. XVI. Serpentinized ultramafic intrusions. Can.Jour.Earth Sci., 8, 6, 631-663.

Babkine, J., 1965. Contribution a l'etude petrographique et magnetique des basaltes de la region de Monistrol-d'Allier (Haute-Loire). Bull.Soc.Franc.Min.Crist., 88, 306-318.

Barry, G.S., 1959. Geology of the Oxford House-Knee Lake area, Oxford Lake and Gods Lake Mining Districts. Man.Mines Branch, Pub. 58-3.

Beeson, M.H. and Jackson, E.D., 1969. Chemical composition of altered chromites from Stillwater Complex, Montana. Am.Min., 54, 1084-1100.

Bell, C.K., 1971. Boundary geology, Upper Nelson River area, Manitoba and northwestern Ontario. Geol.Soc.Can., Spec.Pub.#9, 11-39.

---------- 1966. Churchill-Superior Province boundary in northeastern Manitoba. In Jenness, S.E., (Ed), Geol.Surv.Can., Paper 66-1, 133-136.

Berry, T.F., Allen, W.C., and Snow, R.B., 1950. Chemical changes in basic brick during service. J.Amer.Ceram.Soc., 33, 121.

Best, M.G., 1970. Kaersutite-peridotite inclusions and kindred megacrysts in basanitic lavas, Grand Canyon, Arizona. Contr. Min. and Pet., 27, 25-44.

Bichan, R., 1969. Origin of chromite seams in the Hartley Complex of the Great Dyke. In Wilson, H.D.B. (Ed): Magmatic ore deposits, Soc.Econ.Geol., Mono.#4, 95-113.

Bliss, N.W. and Stidolph, P.A., 1971. The Rhodesian Basement Complex: A review. In: Geol.Soc.S.Afr., Spec.Pub.#2, 305-334.

Brindley, G.W. and Zussman, J., 1957. A structural study of the thermal transformation of serpentine minerals to forsterite. Am.Min., 42, 461-474.

Brown, E.H., 1967. The greenschist facies in part of Eastern Otago, New Zealand. Cont.Min. and Pet., 14, 259-292.

Brownell, G.M., 1942. Chromite in Manitoba.Precambrian, 15, 12, 3-5.

Burns, R.G., 1970. Mineralogical applications of crystal field theory. Cambridge Univ.Press.

Cameron, E.N. and Desborough, G.A., 1969. Occurrence and characteristics of chromite deposits-Eastern Bushveld Complex. In: Wilson, H.D.B. (Ed), Magmatic ore deposits, Soc.Econ.Geol., Mono.#4, 23-40.

---------- and Emerson, M.E., 1959. The origin of certain chromite deposits of the Eastern part of the Bushveld Complex. Econ.Geol., 54, 7, 1151-1213.

Cann, J.R., 1971. Petrology of basement rocks from Palmer Ridge, NE Atlantic. Phil.Trans.Roy.Soc., Lond., A, 268, 605-617.

Cerny, P., 1968. Comments on serpentinization and related metasomatism. Am.Min., 53, 1377-1385.

Challis, G.A., 1965. The origin of New Zealand ultramafic intrusions. J.Pet., 6, 322-364.

Cheney, E.S. and Lange, I.M., 1967. Evidence for sulfuritization and the origin of some Sudbury type ores. Min.Dep., 2, 80-94.

Chidester, A.H., 1962. Petrology and geochemistry of selected talc-bearing ultramafic rocks and adjacent country rocks in north-central Vermont. U.S.G.S., Prof.Pap., 345.

Coats, C.J.A., 1968. Serpentine minerals from Manitoba. Can.Min., 9, 322-347.

---------- 1966. Serpentinized ultramafic rocks of the Manitoba Nickel Belt. Ph.D thesis, Univ. of Manitoba, Unpub..

---------- and Brummer, J.J., 1971. Geology of the Manibridge nickel deposit, Wabowden, Manitoba. Geol.Soc.Can., Spec.Pub. #9, 155-166.

Coleman, R.G., 1966. New Zealand serpentinites and associated metasomatic rocks. N.Zealand Geol.Surv.Bull., n.s. 76, 102pp.

---------- 1963. Serpentinites, rodingites and tectonic inclusions in Alpine-type mountain chains. Geol.Soc.Amer., Spec.Pap. 73, 130 (abst).

Collett, L.S. and Bell, C.K., 1971. The use of AFMAG in geological interpretation. C.I.M. Bull, 64, 706, 39-47.

Cotterill, P., 1969. The chromite deposits of Selukwe, Rhodesia. In: Wilson, H.D.B., (Ed), Magmatic ore deposits, Soc.Econ. Geol., Mono.#4, 154-186.

Cranstone, D.A. and Toogood, T.J., 1969. Pakwa Lake. Preliminary Map 1969 D-1, 63J-15. Manitoba Mines Branch.

---------- 1969a. Pistol Lake. Preliminary Map 1969 D-2. Manitoba Mines Branch.

Dana, E.S., 1932. A textbook of mineralogy, 4th Ed., J. Wiley and Sons.

Davies, J.F., Bannatyne, B.B., Barry, G.S. and McCabe, H.R., 1962. Geology and Mineral Resources of Manitoba. Manitoba Mines Branch Publication.

Deer, W.A., Howie, R.A. and Zussman, J., 1962. Rock forming minerals, vols. 1-5. Longmans Green.

Den Tex., E., 1955. Secondary alterations of chromite. Amer.Min., 40, 353-355.

de Waal, S.A., 1969. On the origin of hydrogrossularite and other calcium silicates in serpentinites. Trans.Geol.Soc.S.Afr., LXXII, 23-27.

---------- and Hiemstra, S.A., 1966. The investigation of six samples of serpentinite from the Barberton Area. Nat.Inst., for Met., Pretoria, Rpt.#86.

de Wijkerslooth, P., 1943. Mikroskipische beobachtungen an anatholischen chromerzen. Maden.Tetkik.Arama.(Ankara) 2/30, 259-264.

Dunham, K.C., Phillips, R., Chalmers, R.A., and Jones, D.A., 1958. The chromiferous ultrabasic rocks of eastern Sierra Leone. Overseas Geol. and Min.Res., Supp.Ser., Bull.Sup.#3.

Engin, T. and Aucott, J.W., 1971. A microprobe study of chromites from the Andizlik-Zimparalik area, southwest Turkey. Min. Mag., 38, 76-82.

--------- and Hirst, D.M., 1970. The alpine chrome ores of the Andizlik-Zimparalik area, Fethiye, southwest Turkey. Inst. Min. & Met., London, Trans., 79, 759, B16-29.

Evans, B.W. and Moore, J.G., 1968. Mineralogy as a function of depth in the prehistoric Makaopuhi tholeiitic lava lake. Contr.Min. & Pet., 17, 85-115.

Evans, R.C. 1964. An introduction to crystal chemistry. Cambridge Univ.Press.

Faust, G.T. and Fahey, J.J., 1962. The serpentine group minerals. U.S.G.S., Prof.Paper, 384-A.

---------- Murata, K.J. and Fahey, J.J., 1956. Relation of minor element content of serpentines to their geological origin. Geochem.et Cosmochem.Acta., 10, 316-320.

Fawley, A.P., 1959. Mwahanza Hill Nickel Deposit, Central Province. Rec.Geol.Surv.Tanganyka, v.7 (for 1957), 49-54.

Francis, G.H., 1956. The serpentinite mass in Glen Urquhart, Inverness hire, Scotland. Amer.J.Sci., 254, 201-226.

Friedman, G.M., 1959. Identification of carbonate minerals by staining methods. J.Sed.Pet., 29, 87-97.

Frietsch, R., 1970. Trace elements in magnetite and hematite mainly from northern Sweden. Sveriges Geologiska Undersokning, Ser.C, NR 646, Arsbok 64 NR 3.

Frisch, T., 1971. Alteration of chrome spinel in a dunite nodule from Lanzarote, Canary Islands.

Frondel, C., 1941. Constitution and polymorphism of the pyroaurite and sjogrenite groups. Am.Min., 26, 5, 295-315.

Gait, R.I., 1964. The mineralogy of the chrome spinels of the Bird River Sill, Manitoba. M.Sc. thesis, Univ. of Manitoba.

Ghisler, M. and Windley, B.F., 1967. The chromite deposits of the Fiskenaesset Region, West Greenland, Rep.Geol.Surv. Greenland, 12.

Gibb, R.A., 1968. A geological interpretation of the Bouguer anomalies adjacent to the Churchill-Superior boundary in Northern Manitoba. Can.Jour.Earth Sci., 5, 439-453.

Godard, J.D., 1968. Geology of the Halfway Lake area (West half). Manitoba, Dept.Mines and Nat.Res., Mines Branch Pub. 64-5.

---------- 1966. Geology of the Hambone lake area, Manitoba. Manitoba, Dept.Mines and Nat.Res., Mines Branch Pub. 63-1.

Golding, H.G. and Bayliss, P., 1968. Altered chrome ores from the Coolac serpentine belt, New South Wales, Australia. Am.Min., 53, 162-183.

Goles, G.G., 1967. Trace elements in ultramafic rocks. In: Wyllie, P.J. (Ed), Ultramafic and related rocks. J. Wiley and Sons, 352-362.

Green, D.H., 1964. The petrogenesis of the high temperature peridotite intrusion in the Lizard area, Cornwall. Jour.Pet., 5, 134-188.

---------- 1961. Ultramafic breccias from the Musa Valley, Eastern Papua. Geol.Mag., XCVIII, 1-26.

Greenwood, H.J., 1963. The synthesis and stability of anthophyllite. Jour. of Pet., 4, 317-351.

Grudnin, M.I. and Letnikov, F.A., 1969. Geochemistry of nickel in ultrabasic rocks in the magmatic and post-magmatic stage. Endogennos orudenie Pribaikal'ya, Nauka, Moscow.

Guillon, J.H. and Lawrence, L.J., 1971. Ni-Fe-Cu sulphides in New Caledonia ultramafic bodies with special reference to the Great South-eastern Massive. Pacific Sci.Assoc., 12th Congress, Canberra, Aust., Rec. of proc., v.1, abst., 425-426.

Gunn, B.M., et al., 1970. Geochemistry of an oceanite-ankaramite basalt suite from East Island, Crozet Archipeligo. Contr. Min. & Pet., 28, 319-339.

Haggerty, E., and Meyer, H.O.A., 1970. Apollo 12: Opaque oxides. Earth and Plan.Sci.Let., 9, 5, 379-387.

Hatch, F.H., Wells, A.K. and Wells, M.K., 1961. Petrology of the igneous rocks. 12th Ed., Murby, London.

Haughton, S.H., 1969. Geological History of Southern Africa. Geol.Soc.S.Afr., Johannesburg, Tvl..

Hawkes, H.E. and Webb, J.S., 1962. Geochemistry in Mineral Exploration. Harpers Geoscience Series.

Hawley, J.E., 1962. The Sudbury Ores: their mineralogy and origin. Min.Assoc.Can..

Henderson, P. and Suddaby, P., 1971. The nature and origin of the chrome-spinel of Rhum Layered ultrabasic intrusion. Contr. Min. and Pet., 33, 21-31.

Hess, H.H., Smith, R.J. and Dengo, G., 1952. Antigorite from the vicinity of Caracas, Venezuela. Am.Min., 37, 68-75.

Hey, M.H., 1954. A new review of the chlorites. Min.Mag., 30, 277.

Hill, R.E.T., 1969. The crystallization of basaltic melts as a function of oxygen fugacity. Ph.D thesis, Queens Univ., Kingston, Ont..

Horninger, G., 1941. Beobachtungen am erzinhalt von gesteinen und an chromerz aus tampadel in schlesien. Mineral.Petrogr.Mitt., 52, 316-346.

Hughes, C.J., 1970. Major rhythmic layering in ultramafic rocks of the Great Dyke, Rhodesia, with particular reference to the Hartley Area. In: Geol.Soc.S.Afr., Spec.Pub. #1, 594-609.

Irvine, T.N., 1967. Chromian spinel as a petrogenetic indicator. Part II petrologic applications. Can.Jour.Earth Sci., 4, 71-103.

---------- 1965. Chromian spinel as a petrogenetic indicator. Part I-theory. Can.Jour.Earth Sci., 2, 648-672.

---------- and Findley, C.C., 1972. Alpine-type peridotite, with particular reference to the Bay of Islands igneous complex. In: Irving, E. (Ed). Pub.Earth Physics Branch, Dept.Energy Mines and Resources, 42, 3, 97-128.

---------- and Smith, C.H., 1969. Primary oxide minerals in the Muskox intrusion. In: Wilson, H.D.B., (Ed), Magmatic ore deposits, Soc.Econ.Geol., Mono,#4, 76-94.

Jackson, E.D., 1963. Stratigraphic and lateral variation of chromite composition in the Stillwater Complex. In: Fisher et al., eds., Symposium on layered intrusions, Min.Soc.Amer., Spec.Pap. #1, 46-54.

---------- and Thayer, T.P., 1972. Some criteria for distinguishing between stratiform, concentric and Alpine peridotite-gabbro complexes. 24th I.G.C., Section 2 (Petrology), 289-296.

Jahns, R.H., 1967. Serpentines of the Roxbury District, Vermont. In: Wyllie, P.J., (Ed), Ultramafic and related rocks, John Wyllie and Sons., 137-160.

James, H.L., 1946. Chromite deposits near Red Lodge, Carbon County, Montana. U.S.G.S., Bull. 945-F, 151-189.

Johannes, W., 1969. An experimental investigation of the system $MgO-SiO_2-H_2O-CO_2$. Amer.Jour.Sci., 267, 1083-1104.

Katsura, T. and Muan, A., 1964. Experimental study of equilibriae in the system $FeO-MgO-Cr_2O_3$ at 1300°C. Trans.Met.Soc.AIME, 230, 77-84.

Kilburn, L.C. et al., 1969. Nickel sulphide ore related to ultra-basic intrusions in Canada. In: Wilson, H.D.B., Ed., Magmatic ore deposits, Soc.Econ.Geol., Mono. #4, 276-293.

Kornik, L.J., 1969. An aeromagnetic study of the Moak Lake-Setting Lake Structure in northern Manitoba. Can.Jour.Earth Sci., 6, 373-381.

Krauskopf, K.B., 1967. Introduction to geochemistry. McGraw Hill Book Co..

Kullerud, G. and Yoder, H.S., 1964. Sulphide-silicate reactions. Geophysical Lab., Washington, Ann.Rpt., 1963-1964, 218-222.

---------- 1963. Sulphide-silicate reactions. Geophysical Lab., Washington, Ann.Rpt., 1962-1963, 215-218.

Kwestroo, W., 1959. Spinel phase in the system $MgO-Fe_2O_3-Al_2O_3$. Jour.Inorg.Nucl.Chem., 9, 65-70.

Lapham, D.M., 1964. Spinel-orthopyroxene compositions and their bearing on the origin of the serpentinite near Mayaguez, Puerto Rico. In: Hess, H.H., and Otalora,G.,Eds., A study of serpentinite, NAS-NRC Pub.1188, 134-144.

Larsen, E.S., 1928. A hydrothermal origin of corundum and albitite bodies. Econ.Geol., 23, 398-433.

Lauder, W.R., 1970. Origin of the Merensky Reef. Nature, 227, 5256, 365-366.

Leech, G.B., 1953. Geology and mineral deposits of the Shulaps Range, south-western British Columbia. B.C.Dept.Mines., Bull.32.

Lipman, P.W., 1964. Structure and origin of an ultramafic pluton in the Klamath Mountains, California, Amer.Jour.Sci., 262, 199-222.

Lyons, J.B., 1955. Geology of the Hanover Quadrangle, New Hampshire, Vermont. Bull.Geol.Soc.Amer., 66, 105-146.

MacLean, W.H., 1969. Liquidus phase relations in the FeS-FeO-Fe_3O_4-SiO_2 system and their application in geology. Econ. Geol., 64, 8, 865-884.

MacRae, N.D., 1969. Ultramafic intrusions in the Abitibi Area, Ontario. Can.Jour.Earth Sci., 6, 281-303.

McDonald, J.A., 1960. A petrological study of the Cuthbert Lake ultrabasic and basic dyke swarm; a comparison of the Cuthbert Lake ultrabasic rocks to the Moak Lake type serpentine. M.Sc. thesis, Univ.Manitoba, Unpub..

Maxwell, J.C., 1949. Some occurences of chromite in New Caledonia. Econ.Geol., 44, 525-550.

Mihalik, P. and Hiemstra, S.A., 1966. Quantitative electron-probe investigations of the distribution of nickel in serpentinites and associated minerals and rocks from the Barberton Area. Nat.Inst.for Met., Pretoria.Rpt.#88.

---------- and Saager, R., 1968. Chromite grains showing altered borders from the basal reef, Witwatersrand System. Amer.Min., 53, 1543-1550.

Miller, R., 1953. The Webster-Addie ultramafic ring, Jackson County, North Carolina, and the secondary alteration of its chromite. Amer.Min., 38, 1134-1147.

Miyashiro, A., 1953. Calcium-poor garnet in relation to metamorphism. Geochim. et Cosmochim.Acta., 4, 179-208.

Muan, A. and Osborn, E.F., 1956. Phase equilibrium relationships at liquidus temperatures in the system FeO-Fe_2O_3-Al_2O_3-SiO_2. J.Amer.Ceram.Soc., 39, 121-140.

Muir, I.D. and Tilley, C.E., 1964. Basalts from the northern part of the rift zone of the Mid-Atlantic Ridge. Jour.Pet., 5, 409-434.

---------- and Scoon, J.H., 1957. Contribution to the petrology of Hawaiian basalts.1.The picrite basalts of Kilauea. Amer.Jour.Sci., 255, 241-253.

Nagy, B., and Faust, G.J., 1956. Serpentines: natural mixtures of chrysotile and antigorite. Amer.Min., 41, 817-838.

Naldrett, A.J., 1966. Talc-carbonate alteration of some serpentinized ultramafic rocks S. of Timmins, Ont.. Jour.Pet., 7, 489-499.

---------- Bray, J.G., Gasparrini, E.L., Podolsky, T., and Rucklidge, J.C., 1970. Phase layering and cryptic variation in the Sudbury Nickel irruptive. In: Geol.Soc.S.Afr., Spec.Pub.#1, 532-546.

---------- 1970a. Cryptic variation and the petrology of the Sudbury Nickel irruptive. Econ.Geol., 65, 122-155.

---------- and Gasparrini, E.L., 1971. Archaean nickel sulphide deposits in Canada: Their classification, geological setting and genesis with some suggestions as to exploration. In: Glover, J.E. (Ed), Symposium on Archaean rocks, Geol.Soc.Aust.Inc.,Spec.Pub.#3, 201-226.

Nelson, B.W., and Roy, R., 1958. Synthesis of the chlorites and their structural and chemical constitution. Am.Min., 43, 707-725.

O'Hara, M.J., 1967. Mineral facies in ultrabasic rocks. In: Wyllie, P.J. Ed., Ultramafic and related rocks, 7-18. J. Wiley and Sons.

Osborn, E.F., 1962. Reaction series for sub-alkaline igneous rocks based on different oxygen pressure conditions. Am.Min., 47, 211-226.

Padfield, R.C., Beechan, C.R., and Thwaite, R.D., 1967. Linear changes in basic brick under cycled temperatures. Amer. Ceram. Bull., 46, 5, 527-533.

Panagos, A., and Otteman, J., 1966. Chemical differentiation of chromite grains in the nodular-chromite from Rodiani (Greece). Mineral.Dep., 1, 72-75.

Patterson, J.M., 1963. Geology of the Thompson-Moak Lake area. Manitoba Mines Branch, Pub. 60-4.

Pavlov, N.V., and Chuprynina, I.I., 1967. The composition of the chrome spinellids and genetic types of chrome mineralisation in the Kempirsay plutonic body. Geochemistry, 1967, Pt.1, 214-227.

Phillips, A.H. and Hess, H.H., 1936. Metamorphic differentiation at contacts between serpentinite and siliceous country rocks. Amer.Min., 6, 333-362.

Poitevin, E., 1931. Chemical and mineralogical studies of some Quebec chromites. Canadian Dept.Mines., Geol.Survs., Summ. Rpt., 1930, Pt.D, 15-21.

Presnall, D.C., 1966. The join forsterite-diopside-iron oxide and its bearing on the crystallization of basaltic and ultramafic magmas. Amer.Jour.Sci., 264, 753-809.

Prinz, M., 1967. Geochemistry of basalts: trace elements. In: Hess, H.H., and Poldervaart, A., (Eds), Basalts. The Poldervaart treatise on rocks of basaltic composition. V.1., 271-323.

Quirke, T., Cranstone, D.A., Bell, C.K., and Coats, C.J.A., 1970. Geology of the Moak-Setting Lakes Area, Manitoba. Field Trip No.1, Guide Book, GAC-MAC, Winnipeg Meeting, 1970.

Ragan, D.M., 1963. Emplacement of the Twin Sisters Dunite, Washington. Amer.Jour.Sci., 261, 549-565.

Raleigh, C.B., 1967. Experimental deformation of ultramafic rocks and minerals. In: Wyllie, P.J. (Ed), Ultramafic and related rocks, J.Wiley and Sons Ltd., 191-199.

---------- and Patterson, M.S., 1965. Experimental deformation of serpentine and its tectonic implications. Jour.Geophys. Res., 70, 16, 3965-3985.

Ramdohr, P. and Schidlowski, M., 1965. Ein radioaktiver hof in chromit. Neues Jahrb. Mineral.Monatsch., 8, 225-227.

Rance, H., 1966. Superior-Churchill structural boundary, Wabowden, Manitoba. Ph.D thesis, Univ.Western Ontario, London, Ont., Unpub..

Read, H.H., 1934. On zoned association of antigorite, talc, actinolite, chlorite and biotite in Unst, Shetland Islands. Min.Mag., 145, 23, 519-540.

Reid, J.B., 1971. Apollo 12 spinels as petrogenetic indicators. Earth and Plan.Sci.Let., 10, 3, 351-356.

Richards, R.G. and White, J., 1954. Phase relationships of the iron oxide containing spinels. Pt.I. Relationships in the system Fe-Al-O. Pt.II. Relationships in the systems Fe-Cr-O, Fe-Mg-O, Fe-Al-Cr-O and Fe-Al-Cr-Mg-O. Trans. British Ceram.Soc., 53, 233-270 and 422-459.

Ridley, W.I., 1972. Zoned spinels in some British Tertiary Basalts. Trans.A.G.U., 53, 4, 548 (abstr).

Rittman, A., 1962. Volcanoes and their activity. (Eng.Ed), Interscience Publishers.

Roeder, P.L., and Osborn, E.F., 1966. Experimental data for the system MgO-FeO-Fe_2O_3-$CaAl_2Si_2O_8$ and their petrologic implications. Amer.Jour.Sci., 264, 428-480.

Ross, C.S., Foster, M.D. and Myers, A.T., 1954. Origin of dunites and of olivine-rich inclusions in basaltic rocks. Amer.Min., 39, 693-737.

Rousell, D.H., 1965. Geology of the Cross Lake area, Manitoba. Manitoba Dept. Mines Nat.Res., Mines Branch Pub. 62-4.

Rucklidge, J., and Gasparrini, F.L., 1968. Specifications for a computer programme for processing electron microprobe analytical data. Univ.of Toronto.

Sampson, E., 1931. Varieties of chromite deposits. Econ.Geol., 26, 833.

Schwellnus, J.S.I., 1970. Andalusite-staurolite relationships in the northeastern metamorphic aureole of the Bushveld Complex. In: Geol.Soc.S.Afr., Spec.Pub.#1, 326-335.

Scoates, R.F.J., 1971. A description and classification of Manitoba ultramafic rocks. In: Geol.Assoc.Can., Spec. Pub.#9, 89-96.

---------- 1969. Ultramafic rocks of Manitoba. Prelim.Map 1969 A, Manitoba Mines Branch.

Shaw, D.M., 1954. Trace elements in pelitic rocks. Bull.Geol. Soc.Amer., 65, 1151-1182.

Simpson, P.R., and Chamberlain, J.A., 1967. Nickel distribution in serpentinites from Puddy Lake, Ontario. Proc.Geol.Assoc. Can., 18, 67-91.

Spangenberg, K., 1943. Die chromitlaagerstatte von tampadel in Zobten. Z.Pract.Geol., 51, 13-35.

Speidel, D.H., 1967. Phase equilibria in the system MgO-FeO-Fe_2O_3: the 1300° isothermal section and extrapolations to other temperatures. Jour.Amer.Ceram.Soc., 50, 5, 243-248.

---------- and Osborn, E.F., 1967. Element distribution among coexisting phases in the system MgO-FeO-Fe_2O_3-SiO_2 as a function of temperature and oxygen fugacity. Am.Min., 52, 1139-1152.

Spry, A., 1969. Metamorphic textures. Pergammon Press.

Stephenson, H.K., 1940. Contributions to the mineralogy of chromite based on the chromite deposits of Casper Mountain, Wyo.. Ph.D thesis, Princeton Univ.Unpub..

Stevens, R.E., 1944. Composition of some chromites of the western hemisphere. Am.Min., 29, 1-34.

Stout, J.H., 1972. Phase petrology and mineral chemistry of coexisting amphiboles from Telemark, Norway, J.Pet., 13, 1, 99-145.

Stueber, A.M., and Goles, G.G., 1967. Abundances of Na, Mn, Sc, and Co in ultramafic rocks. Geoch. et Cosmoch.Acta., 31, 75-93.

Subramaniam, A.P., 1956. Mineralogy and petrology of the Sittampundi Complex Salem,District, Madras State, India. Bull.Geol.Soc.Amer., 67, 317-390.

Thayer, T.P., 1970. Chromite segregations as petrogenetic indicators. In: Geol.Soc.S.Afr., Spec.Pub.#1, 380-390.

---------- 1969. Gravity differentiation and magmatic re-emplacement of podiform chromite deposits. In: Wilson, H.D.B., (Ed), Magmatic ore deposits, Soc.Econ.Geol., Mono. #4, 132-146.

---------- 1960. Some critical differences between Alpine-type and stratiform peridotite-gabbro complexes. XXI st Int. Geol.Cong., Pt.13, 247-259.

---------- 1956. Mineralogy and geology of Chromium. In: Udy, M.J. (Ed), Chromium, Vol.1, chemistry of chromium and its compounds. Am.Chem.Soc., Mono.#132, 14-52.

---------- 1946. Preliminary chemical correlation of chromite with the containing rocks. Econ.Geol., 41, 202-217.

---------- 1942. Chrome resources of Cuba. U.S.G.S., Bull., 935-A, 1-74.

Thompson, J.B., and Norton, S.A., 1968. Paleozoic regional metamorphism in New England and adjacent areas. In: An Zen, E., et al., (Eds), Studies of Appalachian geology northern and maritime. Interscience Pub., 319-327.

Turekian, K.K. and Wedepohl, K.H., 1961. Distribution of the elements in some major units of the earth's crust. Bull. Geol.Soc.Amer., 72, 175.

Turner, F.J., 1968. Metamorphic petrology, McGraw Hill Book Co.

---------- 1948. Mineralogical and structural evolution of the metamorphic rocks. Geol.Soc.Amer., Mem.30.

Turnock, A.C., and Eugster, H.P., 1962. Fe-Al oxides: phase relations below 1000°C. Jour.Pet., 3, 3, 533-565.

Ulmer, G.C., 1970. Chromite spinels. In: Alper, A.M. (Ed)., High temperature oxides, Pt.1, Magnesia, lime and chrome refractories, 251-314. Refractory Materials v.5.

---------- 1969. Experimental investigations of chromite spinels. In: Wilson, H.D.B. (ed) Magmatic ore deposits, Soc.Econ. Geol.,Mono.#4,114-131

---------- and Smothers, W.J., 1968. The system MgO-Cr_2O_3-Fe_2O_3 at 1300°C in air. Jour.Amer.Ceram.Soc., 51, 6, 315-319.

van der Kaaden, G., 1959. On relationship between the composition of chromites and their tectonic magmatic position in peridotite bodies in the SW of Turkey. Bull.Min.Res. and Expl.Inst. of Turkey, 52, 1-14.

van der Walt, C.F.J., 1941. Chrome ores of the western Bushveld Complex.Geol.Soc.S.Afr., XLIV, 79-112.

van Zyl, J.P., 1970. The petrology of the Merensky Reef and the associated rocks on Swartklip 988, Rustenberg District. In: Geol.Soc.S.Afr., Spec.Pub.#1, 80-107.

Viljoen, R.P., Saager, R., and Viljoen, M.J., 1969. Metallogenesis and ore control in the Steyndorp goldfield, Barberton Mountain Land, South Africa. Econ.Geol., 64, 7.

Vinogradov, A.P., 1962. Average contents of chemical elements in the principal types of igneous rocks of the earth's crust. Geochemistry, 641-664.

Vogt, J.H.L., 1923. Nickel in igneous rocks. Econ.Geol., 28, 305-353.

Wager, L.R. and Brown, G.M., 1968. Layered igneous rocks. Oliver and Boyd, Edinburgh.

---------- and Mitchell, R.L., 1953. Trace elements in a suite of Hawaiian Lavas. Geochim. cosmochim Acta., 3, 217-223.

Warshaw, I, and Keith, M.L., 1954. Solid solution and chromium oxide loss in part of the system $MgO-Al_2O_3-Cr_2O_3-SiO_2$.Jour. Amer.Ceram.Soc., 37, 161.

Wanless, R.K., Stevens, R.D., Lachance, G.R. and Edmonds, C.M., 1967. Age determinations and geologic studies. K-Ar isotopic ages, Rpt.#7. Geol.Surv.Can., Paper 66-17.

---------- and Rimsaite, J.Y.H., 1966. Age determinations and geologic studies. K-Ar isotopic ages. Rpt.#6. Geol.Surv.Can., Paper 65-17.

1965. Age determinations and geologic studies. Part 1 - isotopic ages, Rpt.5. Geol.Surv.Can., Paper 64-17 Part 1.

Weiser, T., 1967. Untersuchungen mit der electronenmikrosonde uber die zizammensetzung von chromiten. Neuse.Jahrb.Mineral. Ablandl.107 (2) 113-143.

---------- 1966. Geochemische untersuchungen and chromiten mit det electronenmikrosonde. Ph.D thesis, Ludwig-Maxmilians Unerversitat, Munchen.

Whittaker, E.J.W., and Wicks, F.J., 1970. Chemical differences among the serpentine "polymorphs": a discussion. Amer.Min., 55, 1025-1047.

White, R.W., 1966. Ultramafic inclusions in basaltic rocks from Hawaii. Cont.Min.Pet., 12, 245-314.

Wicks, F.J., 1969. X-ray and optical studies on serpentine minerals. Ph.D thesis, Oxford Univ., Unpub..

Wilde, W.T. and Rees, W.J., 1943. The ternary system $MgO-Al_2O_3-Cr_2O_3$. Trans.British Ceram.Soc., 42, 7, 123-155 (also in Ceram.Abst., 23, 1, 27, 1944).

Wilkinson, J.F.G., 1953. Some aspects of the Alpine-type serpentinites of Queensland. Geol.Mag., XC, 5, 305-321.

Wiles, J.W., 1957. The geology of the eastern portion of the Hartley gold belt. Geol.Surv.S.Rhodesia, Bull.44, pt.1.

Willemse, J., 1969. The geology of the Bushveld igneous complex, the largest depository of magmatic ore deposits in the world. In: Wilson, H.D.B. (Ed), Magmatic ore deposits, Soc.Econ. Geol., Mono.#4, 1-22.

---------- 1959. The "floor" of the Bushveld igneous complex and its relationships, with special reference to the Eastern Transvaal.Geol.Soc.S.Afr., Trans. 62, XXI-IXXX.

Williams, G.J., 1965. Minerals associated with ultramafic rocks. In: Economic geology of New Zealand, v.4, of Proc. of 8th Com.Min. and Met.Conf., Australia and N.Z., 1965, 143-166.

Wilson, H.D.B., 1953. Geology and geochemistry of base metal deposits. Econ.Geol., 48, 370-407.

---------- and Anderson, D.T., 1959. The composition of Canadian sulphide ore deposits. Trans., Can.Inst.Min. and Met., 62, 325, 337.

---------- Andrews, P., Moxham, R.L., and Ramlal, K., 1965. Archaean volcanism in the Canadian Shield. Can.Jour.Earth Sci., 2, 161-175.

---------- and Brisbin, W.C., 1962. Tectonics of the Canadian Shield in northern Manitoba. In: Stevenson, J.S., (Ed)., Tectonics of the Canadian Shield, Roy.Soc.Can., Spec.Pub.#1, 60-75.

---------- 1961. Regional structure of the Thompson-Moak Lake nickel belt. Can.Inst.Min., Bull. 64, 815-822.

---------- Kilburn, L.C., Graham, A.R., and Ramlal, K., 1969. Geochemistry of some Canadian ultrabasic intrusions. In: Wilson, H.D.B. (Ed), Magmatic ore deposits. Soc.Econ.Geol., Mono.#4, 294-309.

Winchell, A.N. and Winchell, H., 1951. Elements of optical mineralogy, 4th Ed.. J. Wiley and Sons.

Wolfe, W.J., 1967. Petrology, mineralogy and geochemistry of the Blue River ultramafic intrusion, Cassiar District, British Columbia. Ph.D thesis, Yale Univ., Unpub. (also on University microfilms, Inc., Ann Arbour, Michigan).

Worst, B.G., 1960. The Great Dyke of Southern Rhodesia, Geol. Surv.S.Rhodesia. Bull,#47.

Wright, J.B., 1967. The iron-titanium oxides of some Dunedin (New Zealand) lavas, in relation to their palaeomagnetic and therm-magnetic character (with an appendix on associated chromiferous spinel. Min.Mag., 36, 1, 425-435.

Wyckoff, R.W.G., 1965. Crystal structures. 2nd ed. v.3 Inorganic compounds $R_x(MX_4)_y$, $R_x(M_nX_p)_y$, hydrates and ammoniates. Interscience publishers.

Wyllie, P.J., 1970. Ultramafic rocks and the upper mantle. Min. Soc.Amer., Spec.Pap.#3, 3-32.

---------- 1967. Review (of petrogenesis of ultramafic and ultrabasic rocks). In: Wyllie, P.J. (Ed)., Ultramafic and related rocks. J.Wiley and Sons, 403-406.

Yoder, H.S. and Tilley, C.E., 1962. Origin of basalt magmas: an experimental study of natural and synthetic rock systems. Jour.Pet., 3, 342-532.

Zurbrigg, H.F., 1963. Thompson mine geology. Can.Inst.Min. and Met., Bull.66, 451-460.

Zachos, K., 1969. The chromite mineralisation of the Vourinos ophiolite complex, Northern Greece. In: Wilson, H.D.B. (Ed)., Magmatic ore deposits, Soc.Econ.Geol., Mono.#4, 147-153.

APPENDIX I

THE SPINEL GROUP OF MINERALS IN ULTRAMAFIC ROCKS

THE SPINEL GROUP OF MINERALS IN ULTRAMAFIC ROCKS

A INTRODUCTION

The spinel group of minerals has the general formula, $R^{2+}R^{3+}_2O_4$ and is divided into the spinel, magnetite and chromite series depending on whether the trivalent cation is Al, Fe^{+3} or Cr. The type structure is taken as that of the mineral spinel, $MgAl_2O_4$, which is cubic close packed and contains eight formula units per unit cell, namely 32 oxygen atoms and 24 cations. It is convenient to express the formula in terms of the unit cell, $R^{2+}_8R^{3+}_{16}O_{32}$.

Extensive solid solution between end members, variation in cation coordination and cation deficient structures occur in the spinel group of minerals. The cations occupy two structural positions, the tetrahedral (A) and octahedral (B) sites. The distribution of cations between the A and B sites determines the type of spinel structure, inverse or normal:-

	A site	B site	formula
normal spinel	8 R^{2+}	16 R^{3+}	$R^{2+}_8\ R^{3+}_{16}\ O_{32}$
inverse spinel	8 R^{3+}	8 R^{3+} & 8 R^{2+}	$R^{3+}_8\ (R^{3+}_8\ R^{2+}_8)\ O_{32}$

The actual distribution may in fact lie between the two extremes of normal and inverse structures (Wyckoff, 1965, p.77); when the A site is occupied by, say, 7 trivalent and one divalent cation then the structure is said to be 7/8 inverse (Burns, 1970, p.111). Experimental determination of cation distribution in the common spinels leads to the following types of structure (from Burns, 1970, Table 6.1):-

	Al^{3+}	Cr^{3+}	Fe^{3+}
Mg^{2+}	7/8 I	N	I
Fe^{2+}	N	N	I
Ni^{2+}	3/4 I	N	I

I inverse spinel
N normal spinel

The factors determining the type of spinel structure were for some time obscure and although it was to be expected that the tetrahedrally coordinated sites would be filled by the smaller cations this was not found to be the case.

Empirical predictions of structure may be made from a knowledge of the constituent cations which are arranged in a series so that of any two cations in a spinel, the one standing higher in the table will preferably occupy the tetrahedral site (Evans, 1964, p.173). This series is as follows:-

increase in preference for tetrahedral coordination	↑	Zn^{2+} Cd^{2+}	increase in preference for octahedral coordination
		Fe^{3+} In^{3+} Ga^{3+}	
		other divalent cations	
		other trivalent cations	
		quadrivalent cations	↓

Recently crystal field theory has been partially successful in predicting spinel structures. The octahedral site preference energy (Burns, 1970, p.111) is a measure of the affinity of a cation for an octahedral coordination site, over that for a tetrahedral site, in an oxide mineral. Hence the higher the energy, the more likely is the cation to occupy an octahedral site. When the trivalent cations have high octahedral site preference energy relative to the divalent cations normal spinels result, when the reverse is true inverse spinels result.

Cation deficient solid solution occurs when two trivalent cations replace three divalent cations. This is apparent on phase diagrams by an extension of the solid solution field towards sesquioxide enrichment. Cation deficient structures are more frequent in synthetic than in naturally occuring spinels (Ulmer, 1970, p.264) and the negligible departure of chrome spinel from the ideal formula has been demonstrated by Irvine (1965, p.650). However Al may substitute for Mg in the A site leading to a spinel with a γ-Al_2O_3 structure.

A convenient means of representing spinel group mineral compositions is by a triangular prism (Stevens, 1944, fig.3) on which the faces of the prism represent the divalent oxides, MgO and FeO and the three prism axes or corners the trivalent oxides Al_2O_3, Cr_2O_3 and Fe_2O_3 (Figure 1). Thus the six important compositional end members are represented:-

$FeCr_2O_4$ ferrochromite (chromite) FC	$MgCr_2O_4$ magnesiochromite (MC)
$FeAl_2O_4$ hercynite (FA)	$MgAl_2O_4$ spinel (MA)
Fe_3O_4 magnetite (FF)	$MgFe_2O_4$ magnesioferrite (MF)

Spinel compositions are represented by various planar projections from the prism (Stevens, 1944; Thayer, 1946, 1956; Jackson, 1963; Irvine, 1965, 1967).

Type A projections result from the projection of a point within the spinel prism from one corner of the prism on to the opposite rectangular face; there are thus three possible type A projections. A chromite, of composition **p** projects onto the MC-FC-FA-MA face at **a** (in Figure 1). This point is determined by plotting mol.% Cr/Cr + Al against Mg/Mg + Fe^{2+}. The projection of a point on the MF-FF-FC-MC face is found by plotting Fe^{3+}/Fe^{3+} + Cr

against $Mg/Mg + Fe^{2+}$, and on the MF-FF-MA-FA face by plotting $Fe^{3+}/Fe^{3+} + Al$ against $Mg/Mg + Fe^{2+}$(Fig.1)

Type B projections result from the projection of a point within the prism along a line parallel to one rectangular face of the prism on to one or other of the two remaining faces. The point **p** projects to **b** (Figure 1) in a plane parallel to the MC-FC-FF-MF face. This projection is achieved by plotting $Fe^{3+}/Fe^{3+} + Cr + Al$ against $Mg/Mg + Fe^{2+}$. Type B projections also result from plotting Al^{3+}/R^{3+} and Cr/R^{3+}, against $Mg/Mg + Fe^{2+}$.

If one component of the R^{3+} group is reduced to zero, then a type B plot changes to a type A. For example the factor $Fe^{3+}/Fe^{3+} + Cr + Al$ used in a type A plot becomes $Fe^{3+}/Fe^{3+} + Cr$, used in a type B, when Al is zero.

Type C projections are obtained by projection of a point within the prism on to one or other of the triangular faces in a direction normal to that face. This plot is achieved by making a ternary plot of Al, Cr and Fe^{3+}.

The term ferritchromit was first used by Spangenberg (1943) to describe highly reflecting margins to chromite in some serpentinized ultramafic rocks. Ferritchromit is an Al- and Mg-poor chromite, of variable composition. In terms of the spinel prism (Fig.1) the composition lies in the MC-MF-FF-FC face between **p'** and **d**, which is the composition of magnetite FF.

B EXPERIMENTAL WORK ON SPINEL GROUP MINERALS

1 Oxide Systems

Complete solid solution exists between magnetite and chromite at 1300°C in the system Cr_2O_3 -FeO-Fe_2O_3 at an f_{O_2} between 10^{-11}

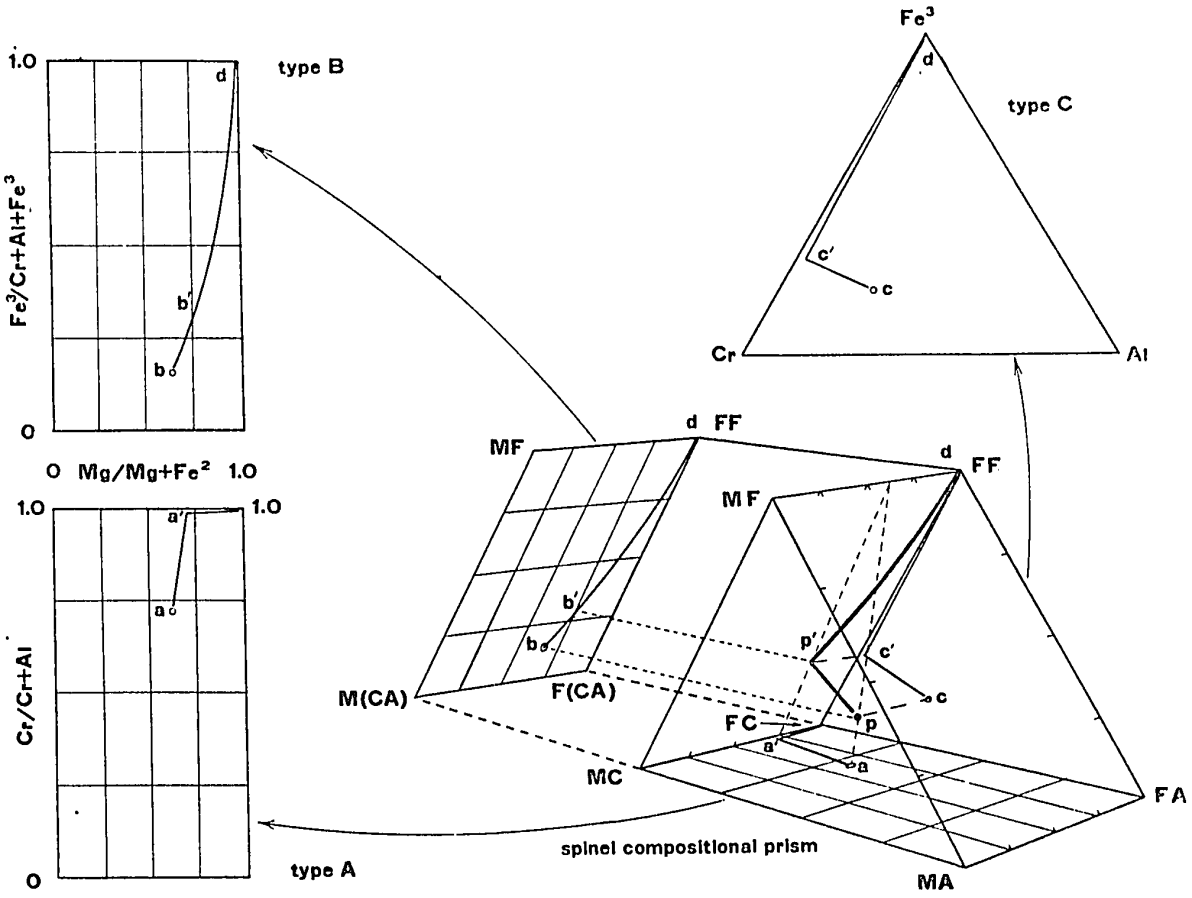

Fig.1. The spinel prism and the derivation of the type A,B and C projections from the prism.Further description of these projections is given in Appendix I,p.248.

and 10^{-2} atm. (Katsura and Muan, 1964).

The chromite-magnesiochromite stoichiometric join lies in a plane in the system Cr_2O_3-Fe_2O_3-FeO-MgO. At 1300°C, 1 atm. total pressure and controlled oxygen partial pressure this solid solution series is cation deficient and so does not lie along the stoichiometric join (Ulmer, 1969, Fig.9; 1970, Fig.14).

The magnetite-magnesioferrite join lies in the system MgO-FeO-Fe_2O_3 where at 1300°C and various fo_2 there is complete solid solution with cation deficient structures becoming more extensive towards the Fe-rich side (Speidel, 1967).

The magnetite-hercynite join lies within the system Al_2O_3-FeO-Fe_2O_3 (Ulmer, 1969, Fig.6). Atlas and Sumido (1958) and Richards and White (1954) found complete solid solution between 1000°C and 1300°C. Turneck and Eugster (1962) demonstrated a miscibility gap in the binary system magnetite-hercynite below about 860°C; exsolution is almost complete at 500°C.

The magnesiochromite-magnesioferrite join is in the system MgO-Fe_2O_3-Cr_2O_3 where complete solid solution exists in air at 1300°C (Ulmer and Smothers, 1968).

The magnesioferrite-spinel join is in the system MgO-Fe_2O_3-Al_2O_3. Kwestroo (1959) found a miscibility gap between the two end members along the stoichiometric join at 1250°C although a complete series of cation deficient spinels is found, Ulmer (1969, p.116) has suggested that the miscibility gap becomes more extensive at low temperatures.

The spinel-magnesiochromite join is in the system MgO-Al_2O_3-Cr_2O_3 where complete solid solution exists between the two end members down to 510°C (Warshaw and Keith, 1954; Wilde and Rees, 1943)

The spinel-hercynite stoichiometric join is in the system Al_2O_3-Fe_2O_3-FeO-MgO (Ulmer, 1969, Fig.9; 1970, Fig.15). At 1300°C 1 atm. total pressure and controlled oxygen partial pressures the spinel series is cation deficient containing excess Fe^{3+}.

There is no experimental work involving the pair chromite-hercynite that is known to the author.

The following conclusions, based on consideration of the data at 1300°C, may be drawn:-(1) Spinel stability varies with fo_2 (Ulmer, 1969, p.119); (2) the extent of solid solution between the end members of the spinel group of minerals is limited only by fo_2 except in the case of the spinel-magnesioferrite series, and at low temperatures the magnetite-hercynite series; (3) an fo_2 of 10^{-5} to 10^{-7} atm. is required for the formation of chromite (Ulmer, 1969, p.119; Stevens, 1944); (4) both chromite and magnetite may form at the same fo_2 about 10^{-7} atm; (5) there is complete solid solution between $MgAl_2O_4$ and $FeCr_2O_4$ and minerals of intermediate composition are common.

2 Silicate-Oxide Systems

The Mg/Fe ratio of phases crystallizing in the system MgO-FeO-Fe_2O_3-SiO_2 is a function of temperature and fo_2 (Spiedel and Osborn, 1967). Crystallization of the assemblage olivine-pyroxene-magnesioferrite-liquid under decreasing fo_2 results in the spinel phase (Magnesioferrite-magnetite) becoming enriched in Fe_3O_4. Crystallization under constant or increasing fo_2 results in the spinel becoming enriched in $MgFe_2O_4$.

Ulmer (1969, Fig.15) has compiled the work of Osborn (1962) and Presnall (1966) on the system CaO-MgO-SiO_2-iron oxide and

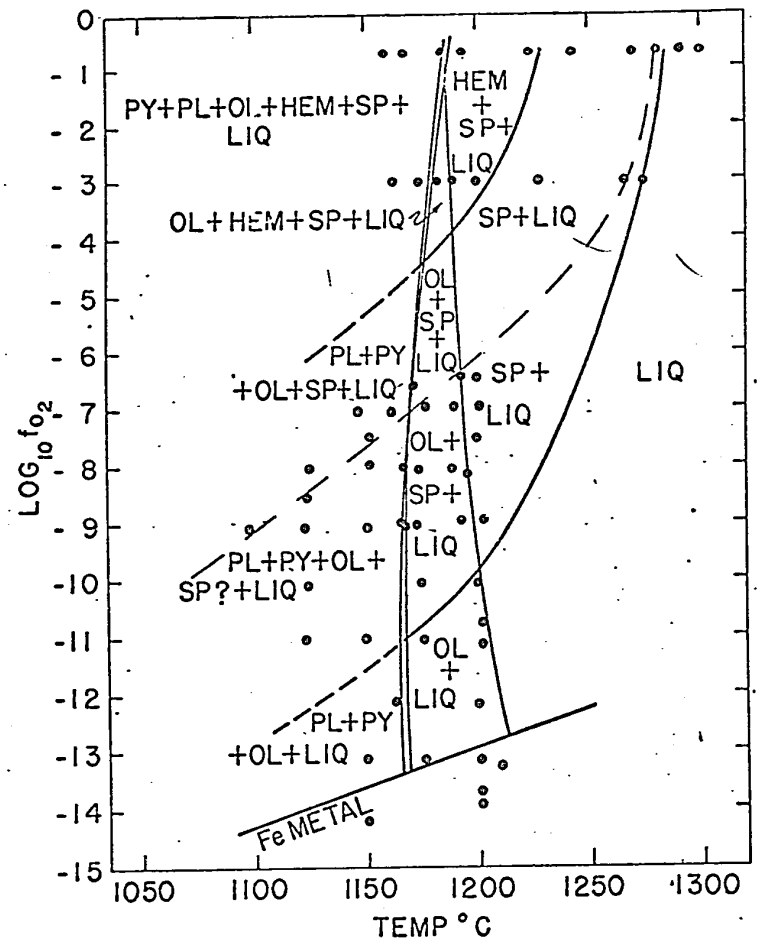

An oxygen fugacity ($-\log_{10} f_{O_2}$) versus temperature (°C) projection illustrating the effect of the variation of oxygen fugacity (10^{-14} atm. to $10^{-0.68}$ atm.) and temperature on the stability of the various phases in G1 1921, a basaltic glass prepared from the 1921 Kilauea olivine tholeiite. Heavy solid curves delineate the limit of stability of the particular phase assemblage stable to the left of the curves, and each curve depicts the effect of oxygen fugacity on the temperature of first appearance of a separate phase. The light weight dashed curve separates that spinel which was optically identified as magnetite (to the left) from that identified as chrome spinel. The phase assemblages within the stability field of metallic iron have not been determined in detail and have been omitted. Each solid circle represents the conditions of one experimental run.

Abbr. SP = Spinel
OL = Olivine
PY = Pyroxene
PL = Plagioclase
HEM = Hematite-ilmenite
Fe = Metallic iron
LIQ = Liquid

(Hill, 1969, Fig.6)

Figure 2

concluded that coprecipitation of pyroxene and magnesioferrite can occur down to,but not below,an fo_2 of 10^{-6} atm.. Similar relations were shown for the system $MgO-FeO-Fe_2O_3-CaAl_2Si_2O_8-SiO_2$ (Roeder and Osborn, 1966), where spinel (magnesio ferrite-magnetite) and pyroxene precipitate together down to an fo_2 of 10^{-9} atm. but below this pyroxene precipitates with other silicates rather than spinel.

Crystallization at constant total composition under increasing fo_2 in the system $FeO-Fe_2O_3-Al_2O_3-SiO_2$ causes a decrease in the Al_2O_3 content of the spinel formed (Muan and Osborn, 1956).

The silicate-oxide systems described above are more pertinent to mafic than to ultramafic rocks, however, the following conclusions may be drawn:-(1) the nature of silicate-oxide assemblages is a function of temperature and fo_2; (2) the trend of either Fe or Mg enrichment in the magnetite-magnesioferrite series depends upon fo_2. The reaction $Mg^{2+} + FeFe_2O_4 = MgFe_2O_4 + Fe^{2+}$ goes to the right with increasing fo_2; (3) the trend of Fe or Al enrichment in the series hercynite-magnetite depends upon fo_2. The reaction $Fe^{3+} + FeAl_2O_4 = FeFe_2O_4 + Al^{3+}$ goes to the right with increasing fo_2.

3 Silicate Melts

Hill (1969) examined the silicate and oxide mineral assemblages that resulted from cooling melts of Hawaiian basalt under varying conditions of temperature and fo_2. Optical and chemical data confirm the existence of a complete solid solution field between chromite and magnetite-ulvospinel. At constant fo_2 chromite is the higher temperature stable phase; at constant temperature magnetite is stable at the higher fo_2. Increase in the Cr content of the melt extended the stability field of chrome spinel to lower

fo_2 and higher temperatures. The Cr/Fe and Cr/Ti ratios increased continuously with lowering fo_2 and rising temperature. Below an fo_2 of 10^{-7} atm. and at temperatures below the olivine-pyroxene phase boundary (Fig.2), the amount of chromite crystallizing decreases as the temperature decreases (this is the stability field labelled Pl+PY+OL+SP?+LIQ). At an fo_2 of 10^{-9} atm. chrome spinel disappears at 1160° to be replaced by magnetite below 1100°C. This is an experimental verification of the observed separation of chromite and magnetite in igneous rocks. At an fo_2 above 10^{-7} atm. the crystallization of spinel is continuous between high and low temperatures with magnetite crystallizing along with pyroxene below 1175°C.

Yoder and Tilley (1962) recognized chrome-rich spinels at high temperatures and magnetites at low temperatures in their experimental runs with Kilauea olivine tholeiite, the same basalt as used by Hill (1969).

C LITHOLOGICAL ASSOCIATIONS

The compositional field of chromite from the Western hemisphere was first established by Stevens (1944, Fig.4), who showed that naturally occuring chromite was an Al-bearing magnesiochromite confined to a compositional field subsequently shown by Irvine (1967, Figs.5 and 9) to be characteristic of ultramafic rocks. Microprobe analyses of chromite by Weiser (1967, 1966) have shown that pure ferrochromite and magnesiochromite did not occur naturally although pure magnetite did.

Chromite is an early crystallizing mineral in ultramafic rocks, characteristically associated with olivine in dunites and

peridotites, and with a tendency to be antipathetic to pyroxene. It occurs either disseminated or segregated into layered or podiform masses. As a result of early crystallization it tends to be euhedral; on the other hand Ramdohr (1955) contends that chromite normally occurs as rounded grains. Sampson (1931) suggested that chromite could form hydrothermally at a post-magmatic stage contemporaneous with serpentinization but Thayer (1956) has advanced reasons why this is unlikely. References in the literature to secondary chromite normally refer to ferritchromit (Spangenberg, 1943), an altered chromite depleted in MgO and Al_2O_3 but enriched in total iron.

Magnetite is a comparatively late mineral normally associated with the later products of differentiation and fractional crystallization: anorthosite, gabbro, basalt and mafic pegmatite. Magnetite may occur as a secondary mineral as the result of the oxidation of olivine and the serpentinization of olivine and pyroxene. Experimental sulphuritization of iron bearing silicates also leads to the production of magnetite.

The crystallization of magnetite and chromite is separated in both space and time and they rarely occur together as primary minerals. "A gap in the spinel series appears to exist between the cessation of chromite and the advent of Fe-Ti oxide crystallization...." (Wager and Brown, 1968, p.551). An experimental verification of this (Hill, 1969) is described above.

In the Muskox intrusion, N.W.T., both segregated and accessory chromite occur in the olivine-rich rocks but are absent from rocks containing cumulus pyroxene. Magnetite occurs in gabbro and to a lesser extent in the upper, pyroxenite, part of the intrusion

(Irvine and Smith, 1969).

Layered ultramafic intrusions in the Abitibi District of Ontario contain cumulus chromite in dunite and peridotite, post-cumulus magnetite in clinopyroxenite and feldspathic clino-pyroxenite, and cumulus magnetite in gabbro (MacRae, 1969, p.284).

Worst (1960, p.65) suggested that chromite had ceased to crystallize in the Great Dyke of Rhodesia by the time pyroxenite was forming. He cites only three occurences of accessory chromite in pyroxenite although orthopyroxene enclosing chromite and olivine is recorded from olivine pyroxenite (Worst, 1960, p.57). Hughes (1970, p.606) found cumulus chromite and orthopyroxene together in the Hartley Complex and suggests that original olivine reacted with magma to form orthopyroxene. Primary magnetite occurs in gabbroic rocks in the upper layers of the Dyke (Worst, 1960; Wiles, 1957, p.66).

Layered chromitite occurs in the Critical Zone of the Bushveld Complex, Transvaal, R.S.A., where it is associated with norite, pyroxenite and anorthosite (Willemse, 1969, Fig.5). Some chromitite seams are developed in pyroxenite and harzburgite in the underlying Basal Zone. The Bushveld Complex is one of the few ultramafic intrusions which contain a consistent association of chromite and orthopyroxene (Irvine, 1967, p.76). Magnetite occurs in gabbro, anorthosite and troctolite in the Upper Zone (Willemse, 1969, p.9 and Fig.5). Magnetite and chromite occur together in the Merensky reef (van Zyl, 1970, p.101).

The Skaegaard and Sudbury complexes are layered intrusions of predominantly mafic character. In the Skaergaard, accessory chromite occurs with olivine gabbro at the base of the exposed

Layered Series and in the Border Group (Wager and Brown, 1968, p.48). Magnetite and Fe-Ti oxides are associated with both the ores and the host rocks in the Sudbury eruptive (Hawley, 1962; Naldrett et al., 1970a, 1970).

The Vourinos ophiolite complex in Greece consists of a basal zone of dunite and harzburgite, a middle zone of pyroxenite and minor dunite and an upper zone of gabbro (Zachos, 1969). Chromite is found in dunite and harzburgite as both segregations and accessory grains; it is rare in pyroxenite and gabbro. Magnetite is not mentioned.

The Alpine-type ultramafic sequence in the vicinity of Mugla, SW Turkey*, consists largely of chromite-bearing peridotites. Gabbros belonging to the same magmatic cycle were intruded into the ultramafic sequence and carry magnetite as an accessory mineral (van der Kaaden, 1959).

Chromite ores of Cuba occur only in dunite and troctolite although accessory chromite is scattered throughout all the rocks including pyroxenite and anorthosite. Both accessory chromite and magnetite are found in the anorthosite (Thayer, 1942, p.12 and p.24).

These examples of spinel associations from ultramafic bodies illustrate the general relationship of early chromite and late magnetite.

Magnetite occurs as a secondary mineral in both mafic and

---

* This area includes the smaller area of Andizlik-Zimparalik from which certain features of chromites are illustrated in this thesis (Engin and Hirst, 1970).

ultramafic rocks. Olivine may be oxidized to form magnetite and orthopyroxene (Muir, Tilley and Scoon, 1957, p.252). During serpentinization Fe is released from the primary silicates and in the presence of sufficient oxygen is converted to magnetite. If insufficient oxygen is present native iron may result in addition to magnetite. Magnetite may also result from the sulphuritization of Fe-bearing silicates in the laboratory (Kullerud and Yoder, 1963; 1964). The addition of S in this way is in fact an oxidation process:

$$4MgFeSiO_4 + S = FeS + Fe_3O_4 + 4MgSiO_3$$

$$4MgFeSiO_4 + 2S = FeS_2 + Fe_3O_4 + 4MgSiO_3$$

Cheyney and Lange (1967, p.88) have summarized the geological evidence for these reactions.

The occurence of ferritchromit is clearly recorded in zones around chromite and a detailed account is given below. As far as the author knows, there is no confirmed instance of ferritchromit as a discrete crystal or grain. Only four of the chromites plotted by Stevens (1944, Fig.4) have the composition of ferritchromit. They could, however, be heavily zoned chromite. The range of chromite content in magnetite from ultramafic rocks (Frietsch, 1970, p.67) between .5 and 5.0% suggests that ferritchromit does not occur as discrete grains.

A number of conclusions may be reached concerning the lithological associations of magnetite, chromite and ferritchromit:-

(1) Primary magmatic magnetite and chromite are separated in layered ultramafic and mafic intrusions; chromite is associated with the earlier crystallizing olivine-rich rocks and magnetite

with the later gabbroic or plagioclase-rich rocks. Ferritchromit occurs as rims to chromite.

(2) In the orogenic, or non-stratiform, type of ultramafic body the same relation appears to hold, although the later gabbroic phases are not as well developed as they are in stratiform intrusions.

(3) Chromite and pyroxene tend to be antipathetic, the Bushveld Complex providing the major exception to this generalization. The appearance of pyroxene is normally accompanied by magnetite.

(4) Secondary chromite is not found although ferritchromit, in effect a non-aluminous chromite, is found as a secondary mineral.

(5) Secondary magnetite forms in ultramafic and mafic rocks as a result (a) of direct oxidation of olivine to enstatite and magnetite; (b) of the serpentinization of olivine and possibly also of pyroxene, and (c) possibly of the sulphuritization of olivine to produce an iron sulphide, enstatite and magnetite.

D COMPOSITIONAL VARIATION IN CHROMITE

1 Trends of Chromite Composition in Ultramafic Rocks

Thayer (1970) has presented two variation diagrams illustrating the distinctive compositional trends of chromite from podiform and stratiform deposits. The variation diagrams show that in stratiform chromitites, total iron content increases rapidly with decreasing Cr_2O_3, whereas in podiform chromitites, and accessory chromite, total iron tends to remain constant or increase only slightly with decreasing Cr_2O_3. The Al_2O_3 content of

chromitites increases with decreasing Cr_2O_3 more rapidly for podiform chromitites than for stratiform chromitites.

Irvine (1965) has presented variation diagrams which are projections from the spinel prism (Fig.1) to illustrate spinel compositions from various types of ultramafic body to which Aumento and Loubat (1971) have added the field for spinels from the Mid-Atlantic Ridge.

Engin and Hirst (1970) have shown that chromite from a wide variety of ultramafic rocks occupies overlapping fields in an Al_2O_3-Cr_2O_3-(total FeO + MgO) ternary plot.

From these diagrams it can be firmly concluded that chromite from chromitite segregations have compositional fields characteristic of their mode of origin, although these fields may overlap.

Zoning in chromite from unserpentinized ultramafic rocks is not recorded in the literature, although Wager and Brown (1968, p.550) suggest that it might occur.

In describing nodular and orbicular chromite from podiform deposits, Thayer (1969, p.140) noted the absence of zoning and concluded that this coupled with the large grain size, necessitated slow cooling. Internal homogeneity is characteristic of Stillwater chromite (Jackson, 1963, p.51), and post-cumulus overgrowths on chromite above the H zone have essentially the same composition as the settled chromite (Beeson and Jackson, 1969, p.1086). Qualitative microprobe scans of Coolac chromite (Golding and Bayliss, 1968) show an overall consistency of composition in unaltered chromite. Chromite may show remarkable compositional variations between adjacent homogeneous grains (Henderson and Suddaby, 1971).

2 Zoned Chromite in Magmatic Environments

a Ultramafic Nodules in Alkali Basalts

Zoning is apparent in some chrome spinels found in ultramafic nodules in alkali basalts.

Muir and Tilley (1964) describe octahedral chromite with coffee brown cores and opaque margins enclosed in, or adjacent to, fresh olivine in xenocrysts from Mid-Atlantic Ridge basalt. The high Cr content in the cores decreases rapidly to the margin, whereas Fe content is doubled between core and rim, suggesting that the rim has the composition of ferritchromit.

Spinel grains at, or near, boundaries of lherzolite inclusions in Hawaiian basalt have either been converted to a fine grained opaque aggregate with feldspar or have developed solid, opaque, margins (White, 1966). The opaque portion is strongly enriched in total Fe and depleted in Al relative to the primary spinel.

Alteration in chrome spinels in a dunite nodule from Lanzarite in the Canary Isles (Frisch, 1971), occurs around borders of and along fractures in grains, enclosed by and adjacent to, olivine. Chemical analyses show that the alteration product corresponds closely to ferritchromit; the unaltered cores are homogeneous. The alteration is interpreted as having occured at high temperature at a late magmatic stage subsequent to the crystallization of the olivine (Fig.3c).

b Alkali Basalts

Zoning is apparent in chrome spinels within olivine and orthopyroxene phenocrysts in alkali basalts.

Zoned spinels from basanites in the Upper Loire Valley, France, which occur within olivine phenocrysts are chromiferous

magnesian picotites with titanomagnetite rims (Babkine, 1965). Chrome spinel in basanite from the Dunedin Volcano, New Zealand, is found within olivine and titanaugite phenocrysts where it is unzoned, and outside the phenocrysts where it is rimmed by titanomagnetite. Titanomagnetite also occurs as discrete crystals (Wright, 1967). Chromian spinels from an oceanite-ankaramite suite in the Crozet archipelago, which occur as inclusions in olivine and in the groundmass of the volcanics, are frequently rimmed by ulvospinel (Gunn et al., 1970). The chrome spinel in the Makaopuhi Lava Lake, Hawaii shows a wide range in composition (Evans and Moore, 1968). The Al content of the low-chrome chromites decreases with decreasing Cr content and the authors' suggest that it is the result of a process which post-dates the eruption of the lava. These low-chrome chromites are typically located near the margins of olivines adjacent to fractures. This is in contrast to the high-chrome chromites, which are poikilitically enclosed within olivine, where the Al content decreases with increasing Cr, a trend which is characteristic of the magmatic stage of spinel development. Concentric zoning is rare in the altered, or low-chrome chromites; chemical variability occuring between rather than within grains, but in one sample where zoning does occur, the centre of the grain is richer in Cr, Mg, Al and Zn than the margin, but poorer in Ti and Fe. Spinel occurs enclosed in olivine in British Tertiary Basalts (Ridley, 1972), and where they have been in contact with the basaltic liquid they are continuously zoned as follows:-

molecular species	core %	inter. %	rim %
spinel	75	32	7
chromite	9	15	1
magnetite	15	39	33
ulvospinel	1	14	59

c Lunar Basalts and Gabbros

Zoning, similar to that in terrestrial basalts, has been recorded in lunar chrome spinels and interpreted as of magmatic origin (Haggerty and Meyer, 1970). Cores of chrome spinel are surrounded by chrome-ulvospinel which are in turn surrounded by ilmenite. The chrome spinel and ilmenite phases are homogeneous; the chrome-ulvospinel varies continuously and regularly in composition. Reid (1971) notes that the coarse lunar gabbros contain spinels which vary continuously and smoothly in composition from chromite cores to ulvospinel rims. The fine basalts contain spinels with chromite cores separated from ulvospinel rims by a sharp compositional boundary.

3 Zoned Chromites from Refractory Bricks

Compositional zoning has been described from a used refractory brick consisting of 40% magnesite and 60% raw chrome ore (Berry, Allan and Snow, 1950). Adjacent to the cold face of the brick the chromite develops a raticulate network of a highly reflecting constituent, probably Fe_2O_3. Inwards from the cold face a crystallographically orientated intergrowth of a highly reflecting material develops inside the chromite, while the margin is surrounded by a lacey fringe of a highly reflecting material. As the fringe becomes better developed, the intergrowth disappears and the chromite develops a grey centre with a lacey

fringe. Immediately adjacent to the hot face the chromite becomes a complex solid solution with a dark rim.Analyses show that in passing from the cold to the hot face the chromite becomes depleted in MgO,Al_2O_3 and Cr_2O_3 and enriched in Fe_2O_3.The authors' conclude that $MgAl_2O_4$ in the chromite is more soluble in the silicate matrix than $MgCr_2O_4$.

Silicate and direct bonded chrome-periclase refractory bricks show euhedral and angular secondary Fe-rich spinel as rims on chromite or discrete grains in the groundmass (Padfield et al., 1967).The secondary spinel may be separated from the chromite core by a line of irregular pore spaces.

5 Zoned Detrital Chromite

Detrital chromite grains with differing reflectivity and single grains with more highly reflecting borders than cores have been observed in the Basal Reef of the Witwatersrand System (Mihalik and Saager,1968).The chromite with higher reflectivity contains more Fe and sometimes more Cr but less Al and Mg.The alteration is intensified by the radioactivity of adjacent uraninite.The authors' conclude that at least some of the chromite alteration occured in the sedimentary environment.

Radioactive haloes have been described from chromite grains in the Elsberg Reef in the O.F.S. (Ramdohr and Schidlowski,1965) but no chemical data is supplied.

Chromite grains in a Triassic conglomerate,Grenoble,France, have altered margins,whereas those in Carboniferous conglomerate do not.Grains in both conglomerates are thought to have been derived from the adjacent Belledonne ultramafic intrusion

(see p.268), which contains chromite with altered borders. This led Den Tex (1955) to suggest that the alteration of the chromite occured after consolidation of the ultramafic and was unconnected with deuteric activity.

Alteration of detrital chromite is effected by radioactivity. There is insufficient information to know whether other processes such as diagenesis or regional metamorphism can bring about the formation of ferritchromit in situ from detrital grains.

5 Zoned Chromite in Serpentinites

a Examples

The simplest type of zoning results from the formation of a rim of magnetite around a core of chromite. This has been observed in the Red Lodge ultramafic, Montana (James, 1946), New Caledonia (Maxwell, 1949, p.538), Casper Mountain, Wyoming (Stephenson, 1940), the Abitibi area, Ontario (MacRae, 1969), and in serpentinites dredged from the Mid-Atlantic Ridge (Aumento and Loubat, 1971, p.649) and from the Palmer Ridge (Cann, 1971, p.613).

Zoning in chromite may be more complicated and involve the migration of material between the chromite and enclosing silicates, resulting in the formation of spinel phases intermediate in composition between magnetite and chromite and in the formation of an Al-bearing silicate around the zoned chromite.

Poitevin (1931) noted the oxidation of brown-red translucent cores to an opaque,black, oxide around the periphery,and along fractures,in some Quebec chromites. Chromiferous penninite is associated with the oxidized chromite.

Horninger (1941) termed the more highly reflecting material on the margin of chromite as "grey magnetite". He suggested that this was an alteration resulting from the transfer of material between the host rock and the chromite; a removal of Al and Mg from, or an addition of Fe to, the chromite.

Spangenberg (1943) was the first to use the term ferritchromit to describe highly reflecting margins of chromite found in some serpentinized ultramafic rocks. He suggests that as a consequence of serpentinization the $MgAl_2O_4$ component of the spinel migrates to the country rock, the Fe_3O_4 migrates into the spinel from the country rock and the Cr_2O_3 content remains constant.

De Wijkerslooth (1943) described post-serpentinization hydrothermal alteration of chromite from Turkey. He concluded that hematite initially develops from the chromite, either as crystallographically orientated lamellae or along the margin of fractures. This is followed by the progressive development of silicates containing MgO, Al_2O_3 and Cr_2O_3 derived from the chromite and CaO, Na_2O and SiO_2 introduced by the hydrothermal solutions until ultimately the chromite is entirely replaced. The Al_2O_3 and MgO in the chromites is more readily removed than is the Cr_2O_3 and iron oxide.

The alteration of primary chromite in a serpentinized peridotite near Barramia in the Eastern Desert of Egypt has been described by Amin (1948). Secondary, or ferriferous chromite, occurs at the margin of primary chromite lens, adjacent to cracks within the lens and in bodies of talc-carbonate schist. Disseminated chromite has been marginally altered to ferriferous chromite.

Compared to the primary chromite the ferriferous chromite is poorer in Al_2O_3 and MgO but richer in FeO and Fe_2O_3 (Table VII.2). The removal of Al_2O_3 from the primary chromite leads to the formation of chlorite adjacent to the ferriferous chromite.

Chromite in the Webster-Addie ultramafic ring complex (Miller, 1953) has been replaced during serpentinization by a black opaque ferriferous chromite (Table VII.2). When compared to the primary chromite the ferriferous chromite is poorer in Al_2O_3 and MgO, richer in FeO and Fe_2O_3, slightly richer in TiO_2, MnO and NiO and identical in Cr_2O_3. The chromiferous chlorite, kammererite forms initially round the margin of the chromite and subsequently may replace it.

Scattered chromite grains in a serpentinized ultramafic in the Belledonne Massif, Grenoble, France,are coated with a highly ferromagnetic, black opaque material which appears to be magnetite and which also penetrates along fractures in the chromite (Den Tex, 1955). The altered chromite is relatively enriched in Cr_2O_3 by removal of Al_2O_3, MgO and FeO; a colourless chlorite surrounds the altered chromite presumably utilizing the released Al_2O_3. Some detrital chromite in adjacent conglomerates is not altered so it is suggested that the alteration post-dates the consolidation of the ultramafic and is not the result of late magmatic, deuteric activity.

The composition of spinels associated with dunite and augite-harzburgite from the Mayaguez serpentinite, Puerto Rico was investigated by Lapham (1964). The dunite contains small grains of chromite which are of uniform composition from core to rim and consist almost entirely of Al_2O_3, Cr_2O_3, MgO and iron oxides

Table I. Compositional variation in zoned spinels from the Mayaguez Serpentinite, Puerto Rico (Lapham, 1964).

	Chromite	Spinel	Magnetite	Spinel	Magnetite & Fe-sulphs.	
	Dunite	Augite-harzburgite		Augite-harzburgite		
		Core	Rim	Core	Inner rim	Outer rim
Al_2O_3	11.0	48.5	7.6	48.5	5.8	5.8
Cr_2O_3	54.5	15.5	15.3	12.1	13.0	12.0
MgO	8.6	22.2	9.3	21.8	11.0	10.0
NiO	1.0	1.0	1.0	1.0	1.0	1.0
FeO	25.2	13.5	59.4	11.8	43.0	35.0
SiO_2	1.0	1.0	8.0	1.0	5.0	12.0
S	1.0	1.0	1.0	1.0	18.0	6.0
Total	99.3	98.7	99.5	94.2	96.8	80.8

(Table 1, col.1). The augite-harzburgite contained zoned spinels which have a core of spinel (s.s.) and a margin, in one case of chromiferous magnetite and in the other of a chrome-iron sulphide and magnetite. Lapham suggests that at a high temperature Mg-Al spinel associated with forsterite crystallized at a depth between 675° and 1650°C and was followed by low temperature crystallization of iron sulphide and magnetite associated with serpentinization.

Weiser (1966; 1967) examined chromites from 35 deposits in serpentine and observed two types of alteration:- (1) an increase in Fe and Cr with a decrease in Mg and Al between the core and rim, leading to the formation of ferritchromit and (2) an increase in Fe and a decrease in Mg, Al and Cr between core and rim leading to the formation of magnetite. The type of alteration may vary from deposit to deposit, even in the same chromite province, but normally only one type of alteration is observed in a single deposit.

Chromite from strongly serpentinized ultramafics in Northern Greece exhibits a narrow marginal alteration phase that is richer in Fe and Cr but poorer in Al and Mg than the cores (Panagos and Otterman, 1966). Their microprobe scanning photographs suggest that the boundary between the two phases is sharp rather than gradational.

The distribution of Ni in serpentinites from the Barberton Area, Transvaal, R.S.A., has been investigated by Mihalik and Hiemstra (1966). They observed composite spinel grains with chromite cores and magnetite rims. The Ni content was higher in the magnetite rims than in the chromite cores. Further investigations by de Waal and Hiemstra (1966) confirmed this observation

and suggested a correlation between the amount of Ni in the chromite and the magnetite. There was no impoverishment in Ni in the silicates adjacent to the spinel and they suggested that the zoning was the result of the redistribution of Ni in the chromite as it was replaced by magnetite at a late stage of serpentinization. Chlorite is not recorded from the mineral assemblages.

Zoned chromian spinels have been described and illustrated by Simpson and Chamberlain (1967) from an Archaean serpentinite at Puddy Lake, Ontario. The cores of the spinels are rich in Cr, Al and Mg and are surrounded by a lighter and softer rim of chromian magnetite which contains less Cr and Al but more ferric iron. Nickel in general increases from core to rim where it is higher in sulphur-deficient than in sulphur-rich rock. The authors are undecided as to whether the zoning is a result of serpentinization or late magmatic crystallization.

The altered chromite from the Coolac Belt, N.S.W., Australia, is found in two mineralogical associations (Golding and Bayliss, 1968):-(1) Chloritic assemblages in which chromite is altered by oxidation to ferritchromit; (2) Serpentine assemblages containing unaltered chromite rimmed by secondary magnetite. The ferritchromit characteristically occurs as (a) parallel, or rosette shaped, crystallographically orientated replacement lamellae; (b) marginal replacement of individual chromite grains; (c) isolated areas of pitted appearance within primary chromite; and (d) zonal sequences with primary chromite and a non-polishing Fe, Mg and Cr rich material. The ferritchromit showed an increase in Cr and Fe and

decrease in Mg and Al compared to the primary chromite (Table VII.2 and Fig.3.b). There may be minor variations between the different modes of occurence.Magnetite occurs as rims to chromite from which it may be separated by a narrow selvedge of material having a reflectivity resembling that of ferritchromit.There is about 1.0% Ni in the magnetite but none in the chromite.Primary magnetite has not been recognised.It is suggested that some of the chlorite with which the ferritchromit is associated developed as a result of the release of Al_2O_3 from the primary chromite upon oxidation during serpentinisation.The non-chloritic assemblages developed under conditions of low oxygen activity in which the chromite will apparently not alter.

Beeson and Jackson (1968) examined 100 polished sections from chromite zones in the Stillwater Complex and found that of these 10 contained ferritchromit along crystal borders and fractures within the chromite.The alteration was complete to magnetite in some sections.Two specimens were collected from cumulus chromite layers for more detailed examination and found to exhibit slightly different alteration patterns (Table VII.2). Microprobe traverses across part of the first grain showed an increase in total iron,a decrease in Cr_2O_3,Al_2O_3 and MgO and virtually no change in TiO_2 content in passing from the chromite core to the ferritchromi rim.The change was abrupt and there was no variation in composition within each phase.Magnetite is presented around the margin of the grain adjacent to the ferritchromit from which it is clearly demarcated.The second specimen examined showed a similar sequence of relative changes between

the chromite core and the ferritchromit margin except for Cr_2O_3 content, which increased towards the margin. The amounts of Cr_2O_3, Fe_2O_3 and Al_2O_3 in the chromite were constant while that of FeO rose and MgO fell towards the boundary with ferritchromit. The composition of the ferritchromit varies continuously (Fig.3.a). Chlorite replaces the serpentine as the silicate mineral surrounding the altered spinels and its formation is attributed to the release of Al_2O_3 from the chromites on alteration to ferritchromit and ultimately to magnetite. The alteration is considered a direct consequence of serpentinization.

Ore chromites from partially serpentinized harzburgite in the Andizlik-Zimparalik area of Turkey show sporadic alteration along fractures and around grain margins (Engin and Aucott, 1971). Electron microprobe analyses show that the ferritchromit is poorer in MgO and Al_2O_3 and richer in total Fe than the original chromite (Table VII.2). The Cr_2O_3 content of the ferritchromit is either similar to or greater than that of the original chromite. Analyses of three accessory chromites show a decrease in Cr_2O_3/FeO ratio and an increase in Al_2O_3/MgO ratio from core to rim. However the matrix of one specimen is not serpentinized so these variations might be due to a magmatic process. The authors' suggest that the development of ferritchromit is the result of hydrothermal activity during which the Al_2O_3 and MgO were preferentially removed from chromite leaving zones enriched in Cr_2O_3 and Fe_2O_3. It is possible that some pyroxene and tremolite was formed at the same time as the ferritchromit.

b Summary

Two types of chromite alteration may be recognized in the

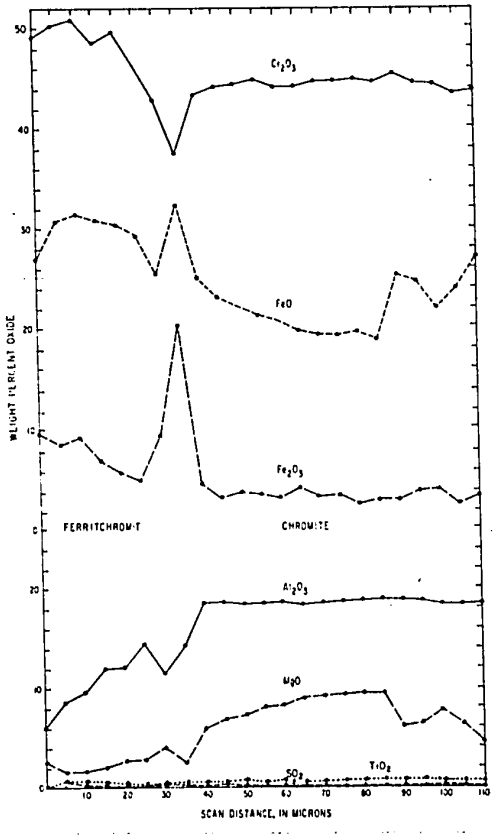

(a)

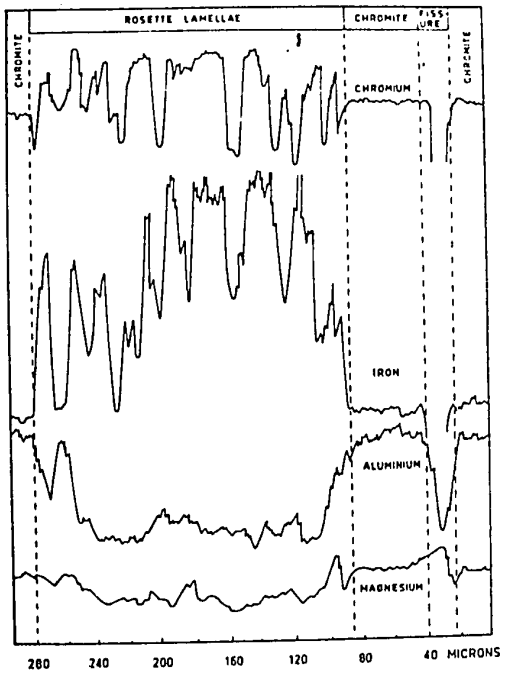

(b)

Fig.3. Electron microprobe scans across altered chromite from serpentinite and an ultramafic nodule.

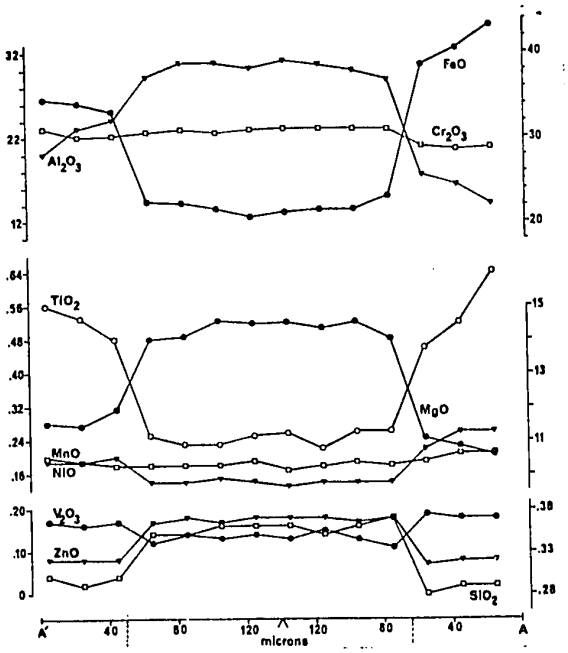

(c)

(a) Stillwater Complex, Montana (Beeson and Jackson, 1969).

(b) Coolac serpentine belt, Australia (Golding and Bayliss, 1968).

(c) Ultramafic nodule in alkali basalt, Lanzarote, Canary Islands (Frisch, 1971).

examples listed above. In the first, chromite is altered around the margin to ferritchromit, and occasionally to magnetite, and an aluminous silicate (chlorite) is normally found adjacent to the altered chromite. This type of alteration has been correlated with the "verde antique" type of serpentine by Thayer (1956). In the second type of alteration, chromite grains are surrounded by magnetite rims but are otherwise unaltered and are not accompanied by an aluminous silicate. This type of alteration is correlated with the "buckskin weathering" type of serpentinization (Thayer, 1956). It is not always clear from descriptions which type of alteration is being described and it is only the advent of the electron microprobe that makes it possible to clearly determine which is present in any particular case.

The characteristics of the verde antique type of serpentinite have been sumarized by Thayer (1956, p.693):-"In the verde antique variety, well described by Chidester (1962) lamellar or platy serpentine and antigorite form a felted fabric which makes the rock tough. Concentration of magnetite in grains of appreciable size commonly leaves the native green colour of the serpentine unobscured when the rock is cut for ornamental use. In this rock chromite characteristically is attacked hydrothermally, and may be extensively replaced by chromian chlorite (Miller, 1953; Thayer, 1956).....In general, I believe that verde antique is associated with talc in foliated greenschist or amphibolite-facies country rocks and near younger dioritic or more silicic plutonic intrusions".

The associated chromite grains are rounded and optically zoned with the margins having a higher reflectivity than the core. The dark chromite core passes with a sudden compositional change to lighter ferritchromit which then grades in composition towards magnetite at the rim.

The characteristics of the buckskin weathering type of serpentinite have been summarized by Thayer (1956, p.693):-"The buckskin weathering facies is named from its characteristic yellow-brown or brownish-red colour on weathered surfaces and is very brittle. In this rock the serpentine forms a very characteristic mesh of minute cross-fibre veins along grain boundaries and fractures in olivine; much of the magnetite is extremely fine and dusty, imparts a sooty gray or black colour on fresh surfaces, and weathers readily to brown limonite. The magnetite in this kind of serpentinite commonly accretes on chromite to form simple sharply bounded rims.....The buckskin weathering facies is preeminent in low-grade unfoliated country rock environments such as Cuba, Oregon, California and Cyprus."

Chromite associated with buckskin weathering type of serpentinite may be surrounded by narrow selvedges of magnetite, which may or may not be in direct contact with the chromite. Magnetite may also penetrate along the margins of fractures in the chromite. The boundary between the chromite and magnetite is compositionally sharp and optically visible due to the higher reflectivity of the magnetite.

APPENDIX II

X-RAY MICROBEAM DETERMINATIONS OF SERPENTINE

X-RAY MICROBEAM DETERMINATIONS OF SERPENTINE

AREA III

Mesh Centres W89 Three photographs 6585, 6688 and 6691 show the isotropic mesh centres to be composed of randomly orientated clinochrysotile. One centre (6585) may also contain a small amount of lizardite. These centres would be called serpophite unless proper identification were carried out.

Mesh Centres W201 The centre consisted of a central featureless zone surrounded by fibrous material; both were included in the X-ray beam and gave a diffraction pattern of a mixture of clinochrysotile and lizardite (6624).

Mesh Rims W89 The mesh rims are lizardite in Type 1 orientation (α-serpentine) (6587a).

Mesh Rims W201 An α-serpentine rim adjacent to a spinel was X-rayed (6631) and found to be lizardite in Type 1 orientation.

Antigorite W89 Fibro-lamellar γ-serpentine was confirmed by X-ray microbeam to be antigorite (6687).

AREA I

Mesh Textures After Olivine W972 The mesh centres contain lizardite in Type 1 orientation (6714). Very fine mesh-textured serpentine, in which both rims and centres were included in the X-ray beam (6745), is composed of lizardite in Type 1 orientation.

Bastite Serpentine W972 This consists of γ-serpentine, which X-ray diffraction shows to be lizardite in Type II orientation (6734).

Serpentine After Amphibole W972 This consists of α-serpentine which X-ray diffraction shows to be lizardite in Type 1 orientation (6730).

Serpentine After Amphibole 1027 This consists of α-serpentine which X-ray diffraction shows to be lizardite in Type 1 orientation (6638) with weak reflections from a 14Å- chlorite-like substance. 14Å structures have previously been described as an intermediate stage between olivine and lizardite (Wicks, 1969, p.280), and between serpentine minerals generally and olivine (Brindley and Zussman, 1957).

X-RAY MICROBEAM DETERMINATIONS OF MULTIPLY ZONED SPINELS

The non spinel phase (Plate 24) in a multiply zoned spinel W264 was determined to have a pyroaurite-type structure. Both photographs were severely darkened by secondary fluorescence from iron in the spinel (6778, 6789).

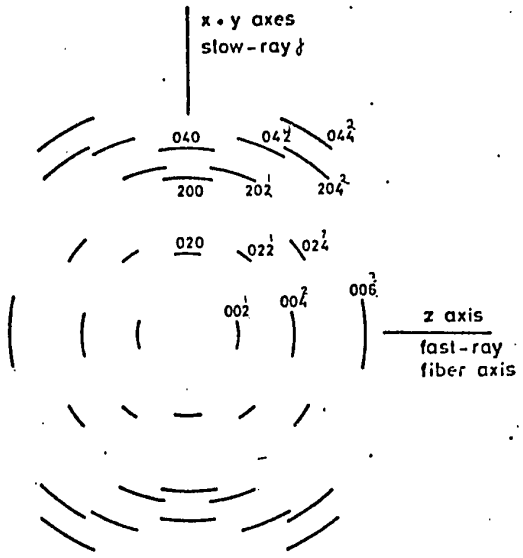

(a)Lizardite-type I orientation

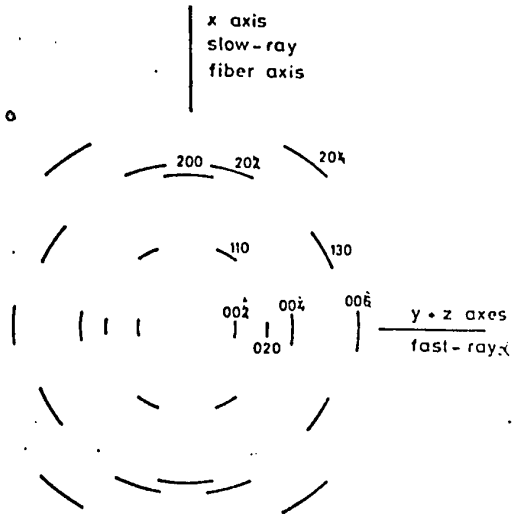

(b)Lizardite-type II orientation

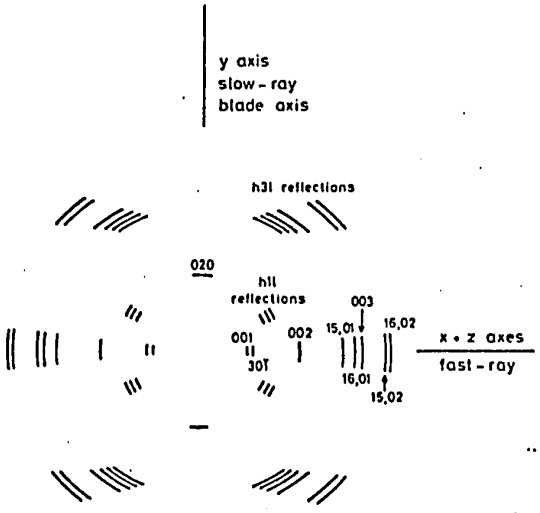

(c)Antigorite

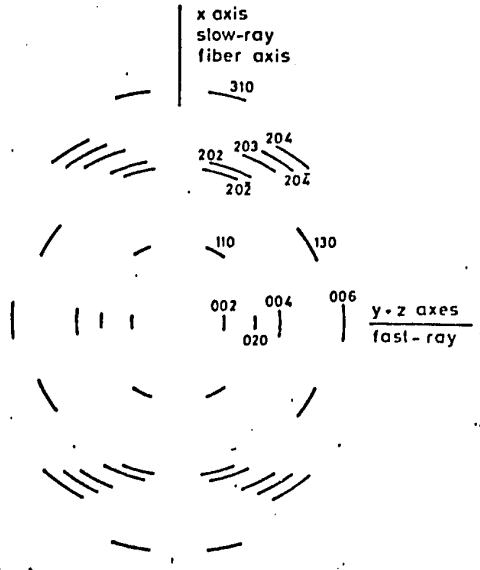

(d)Clinochrysotile

Fig.1. Microbeam diffraction patterns for serpentine minerals (from Wicks,1969,figs.5.3,5.10,5.24 and 5.37).

The symmetrically arranged intensity maxima are those that occur when the long axis of the mineral is normal to the incident X-ray beam.When this is not so the maxima will still occur in groups of four but will be asymmetrically arranged and will form arcs or even continuous rings rather than sharp spots.

APPENDIX III

ELECTRON MICROPROBE ANALYSES

ELECTRON MICROPROBE ANALYSES

Oxide, sulphide and silicate minerals were analyzed with an Acton-Cameca MS 64, electron microprobe. Quantitative analyses were made at 15 KV accelerating potential, 0.04μA sample current and a 10 second integration time.

The following standards were used:-

(1) Chromium metal

(2) Titanium metal

(3) Hematite #80

(4) Garnet #14 Mg, 6.95; Al, 11.72; Si, 18.22; Ca, 3.00; Ti, .05; Mn, .10; Fe, 17.12.

(5) Pyrrhotite (artificial) #531 Fe, 61.25; Ni, .50; S, 38.25.

(6) Millerite #505 Ni, 61.80; S, 38.20.

(7) Chalcopyrite #537 Fe, 32.00; S, 32.50; Cu, 34.50; Co, 1.00.

(8) Olivine #67 Mg, 27.50; Si, 18.71; Fe, 11.00.

(9) Tremolite #53 Na, .12; Mg, 6.35; Al, .10; Si, 24.44; Ca, 8.05; Ti, .03; Mn, .19; Fe, 17.54; K, .06.

(10) Plagioclase #153 Na, 6.14; Al, 13.02; Si, 28.55; Ca, 4.32.

(11) Enstatite #12 Na, .060; Mg, 20.10; Al, 2.31; Si, 25.39; Ca, .60; Ti, .10; Mn, .12, Fe, 4.49; Cr, .23.

(12) Feldspar #60 Na, .24; Mg, .06; Al, 9.16; Si, 30.43; K, 13.37; Ca, .21; Fe, .02.

(13) Feldspar #61 Na, 8.68; Al, 10.32, Si, 32.11; K, .08.

(14) Plagioclase #39 Na, 4.47; Al, 14.37; Si, 26.63, K, .49; Ca, 6.56.

(15) Quartz #77 Si, 46.70.

The standards used in spinel analyses were as follows:

(1) Cr

(2) Ti

(3) Fe

(4) Mg, Al

(5) Ni

The raw microprobe data was reduced using the McGill revision of the Empadr V program (Rucklidge and Gasparrini, 1968).

APPENDIX IV

RECALCULATION OF SPINEL ANALYSES

(PROBELEMATIC COMPUTER PROGRAMME)

PROBE-LEMATIC

I OBJECT

The output of silicate and oxide analytical data from the computer programme (Rucklidge and Gasparrini, 1968), used at McGill University to correct the raw electron micro-probe data, is tabled in three ways:-

(1) Element weight percentages.

(2) Molecular proportions based on 24 cations.

(3) Oxide weight percentages.

Spinels from the Manitoba Nickel Belt have been analyzed for Ni, Fe, Al, Cr, Ti and Mg and the oxides of these elements account for about 98% of the spinel composition. In practice the total of the oxides calculated from the analyses does not normally exceed more than about 91% because all iron is calculated as FeO and all chrome as CrO and hence the oxygen weight equivalent of the trivalent oxides has to be added. Analytical error and the presence of small amounts of other elements such as Mn and Zn may also contribute to a deficiency.

The Probe-lematic programme was written to recalculate the microprobe analyses to 100%, to report chrome as Cr_2O_3, to allocate the total iron content as FeO and Fe_2O_3 and to calculate a number of significant oxide and element ratios.

The programme, written for the IBM 360 series computers, was devised by the author and translated into Fortran IV by Dr. M. Schneider.

BASIS OF RECALCULATION

The spinel group minerals have the general formula

$$R^{2+}R_2^{3+}O_4$$

which may be written

$$\underbrace{R_8^{2+}R_{16}^{3+}}_{24}O_{32}$$

Thus there are a total of 24 cations in the expanded formula unit, the basis to which the molecular proportions are calculated in the micro-probe output data. This provides a convenient starting point for the recalculation.

Microprobe analyses are incomplete in that they do not distinguish between the oxidation state of constituent oxides and in order to recalculate the analyses it is necessary to make some assumptions. Firstly, the oxidation state of the elements determined is assumed to be:-

R^{3+}group	Al_2O_3	R^{2+}group	FeO
	Cr_2O_3		MgO
	Ti_2O_3		NiO
	Fe_2O_3		

The programme is written for these seven oxides, although it would be relatively easy to add others and easier still to substitute any other oxide for an existing one.

Secondly, it is assumed that there are no vacant sites, or cation deficiencies in the spinel structure; there are a total of 24 cations which are divided into 8 R^{2+} and 16 R^{3+}. Fe^{3+} and Fe^{2+} are allocated from total Fe to complete the two groups after allocating the other elements. To do this it is necessary to recalculate the molecular proportions to 24.

III METHOD OF RECALCULATION

A manual example of the recalculation that is performed by the computer programme is shown in Table I. The molecular proportions from the data output are listed in column 1 and this is the input data for the Probe-lematic programme.

The molecular proportions are normalized to 100% and allocated to their correct groups after which the total iron can be split and allocated to complete the R^{2+} group to 8 and the R^{3+} group to 16 (Column 2).

Column 3 shows the assumed molecular form of the elements.

The figures in column 2 are divided by the atomic proportions of the elements present in the oxides in column 3, 2 for the R^{3+} group and 1 for the R^{2+} group to produce the correct molecular proportions in column 4.

These molecular proportions are multiplied by the molecular weight in column 5 to give the weight proportion in column 6. The normalized weight proportions are the oxide weight percentages in column 7.

Column 8 shows the weight percentages recalculated to 100% from the oxide weight percentages in the Empadr output. Differences are apparent because in the probe-lematic programme chrome is calculated as Cr_2O_3 and not CrO as in the Empadr; Ti is calculated as Ti_2O_3 and not TiO as in the Empadr, and the total iron is allocated to FeO and Fe_2O_3. This column is included here for comparison only, it is not part of the computer programme.

The second half of the programme headed "data for graph", calculates ten oxide and element ratios. The minor constituents Ni and Ti are eliminated from the element weight percentage column

Table I. A spinel analysis recalculated mechanically using an electronic calculator.

	1	2	3	4	5	6	7	8
	Mol. proport. from anal.	Mol. proportion recalculated to 100%	Mol.	Mol. proport.	Mol. weight	Weight proport.	Wt.%	Wt% recalcul from anal.
Al	.076	.077	Al_2O_3	.039	99.96	3.898	.22	.23
Cr	5.353	5.423	Cr_2O_3	2.712	152.02	412.28	22.88	21.97
Ti	.270	.274	Ti_2O_3	.137	143.80	19.70	1.09	1.30
Fe^3	-	10.288	Fe_2O_3	5.114	159.70	816.71	45.33	-
								73.59
Fe^2	16.969	6.962 (17.190)	Fe O	6.962	71.85	500.22	27.77	
Mg	.826	.837	MgO	.837	40.32	33.75	1.87	2.01
Ni	.198	.201	NiO	.201	74.71	15.02	.83	.89
Totals	23.692	24.002				1801.56	100.00	99.99

The oxide weight percentages are recalculated from the molecular proportions which appear in the output from the corrected microprobe data.

which is then normalized. The ratios

$$\frac{Fe^{3+} + Fe^{2+} + Mg}{Al^{3}}$$

$$Cr^{3}$$

can be plotted on ternary diagrams after the manner of Engin and Hirst (1970). The ratios

$$Cr/Cr + Al$$

$$Fe^{3+}/Fe^{3+} + Cr + Al$$

$$Mg/Mg + Fe^{2+}$$

$$Fe/Mg + Fe^{2+}$$

can be plotted on compositional variation diagrams based on Stevens prism (Irvine, 1965).

In cases where Al^{3+} is nil a line of stars appears in place of a number opposite Cr^{2+}/Al^{3+}.

A printout of the programme will be found at the end of this appendix.

IV INPUT FORMAT

Each analysis occupies one data card, an example of which is shown in Figure 1. The sample identification occupies the first 16 spaces and may be entered in alpha-numeric, e.g., Deer, p.427, Col.#1. It is not necessary to fill all 16 spaces and the word sample which appears on the output is not included in the entry.

The data is entered in 6 f10.3 in the following order:-

Al.....initial numeral in column 20
Cr..... 30
Ti..... 40
Mg..... 50
Ni..... 60
Fe..... 70

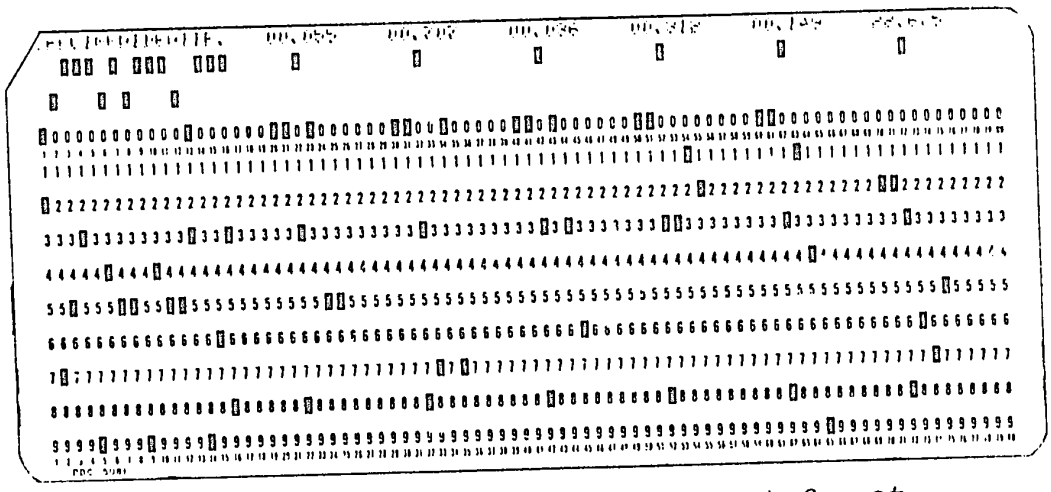

Fig.1. Example of data card showing input format.

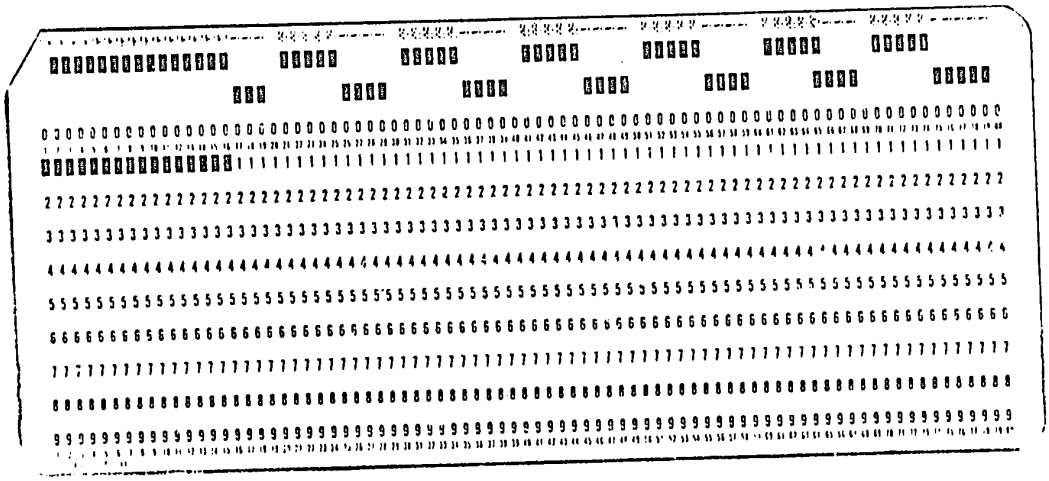

Fig.2. Drum card.

V OUTPUT

An example of the output is displayed in Table III and is self-explanatory.

VI DRUM CARD

The drum card used with the programme is shown in Figure 2. This card allows the choice of alpha-numeric in sample identification, automatic skip between all entries provided the numerals are punched as six figure groups and automatic numeric punching for the data columns.

VII OBJECT DECK

The programme is shown in Table IV. . An object deck may be obtained and data treated at the same time by submitting the following deck:-

```
                        job card
//S1 EXEC FORTGCLG
//  PARM.FORT="NOLIST,EBCDIC,SOURCE,DECK,MAP,LOAD,ID"
//FORT.SYSIN DD *
                        source deck


/*
//GO.SYSIN DD  *
                        data cards
END
/*
```

Alterations and additions to the programme may be checked on Watfor using the source deck and the following control cards:-

```
$WATFOR 123456-GEOLOGICAL SCIENCES-BLISS,RUN=FREE,KP=29
                        source deck
$data
                        data cards
END
$
```

VIII VALIDITY OF THE PROGRAMME

The programme is valid within the assumptions made at the start of this appendix.

It is necessary to analyze for sufficient elements to account for about 95% of the total composition, so that serious errors are not introduced in recalculation. In chrome spinel the oxides MgO, FeO, Cr_2O_3, Al_2O_3 and Fe_2O_3 account for 98% of the constituent (Irvine, 1965, p.649).

The molecular proportions calculated from two spinel analyses by Deer, Howie and Zussman (1966), were recalculated back to the oxide analyses using the Probe-lematic programme. The results are given in Table II, where they are compared to the original analyses.

Table II A comparison of analyses given by Deer, Howie and Zussman, (1966) with those recalculated by the problematic programme.

	1.	2.	3	4.	
Al	15.344	15.344	3.142	3.142	
Cr	-	-	12.178	12.178	
Ti	.020	.020	.028	.028	
Mg	6.592	6.592	4.852	4.852	Molecular proportions
Ni	-	-	-	-	
Fe	1.983	1.983	3.702	3.702	
Zn	.025	*	-	-	
Mn	.017	*	.031	*	
Ca	-	-	.039	*	
	23.98	23.939	23.972	23.902	
SiO_2	-	-	.12	-	
Al_2O_3	65.40	64.92	10.28	10.12	
Cr_2O_3	-	-	59.40	59.68	
Ti_2O_3	.13	.12	.14	.14	Oxide weight percent.
MgO	22.23	22.50	12.62	12.61	
NiO	-	-	-	-	
FeO	8.03	8.44	14.09	14.43	
Fe_2O_3	4.32	4.02	3.30	3.02	
ZnO	.24	*	-	-	
MnO	.10	*	.14	*	
CaO	-	-	.14	*	
	100.45	100.00	100.23	100.00	

1. Hercynite, Deer, Howie and Zussman, 1966, p.427, col.1.
2. Recalculation of the relevant portions of the molecular proportions of 1. by Probe-lematic programme to give oxide weight percentages.
3. Chromite, Deer, Howie and Zussman, 1966, p.427, col.7.
4. Recalculation as for col.2.

\- not determined

* deleted from calculation because oxide not catered for in Probe-lematic programme.

Table III. Example of the output.

PROBE-LEMATIC SAMPLE DEER,P427,CCL#7.

ION	OXIDE	INPUT	NORM	WT. PROP	OXIDE WT. PCT.	ELEMENT WT. PCT.
AL3+	AL2O3	3.142C	3.1549	157.681C	10.1248%	5.3560%
CR3+	CR2O3	13.179C	13.2279	323.4446	59.6802%	40.8213%
TI3+	TI2O3	C.C28C	C.0281	2.0215	C.1298%	C.0973%
MG2+	MGC	4.852C	4.8719	196.4347	12.6132%	7.6058%
NI2+	NIC	C.CCCC	C.CCCC	C.CCCC	C.CCCC%	C.CCCC%
FE2+	FEC	3.702C	3.1281	224.7546	14.4316%	11.2134%
FE3+	FE2O3	***	C.5691	47.0371	3.0203%	2.1112%
**	SUMS	** 23.902C	24.0CCC	1557.372C	99.9999%	67.2049%

INPUT NORMALIZATION FACTOR= 1.C041
OXIDE NORMALIZATION FACTOR= C.C642

DATA FOR GRAPH

ION	ELEMENT WT. PCT. NOT NORM	NORM
AL3+	5.356C	7.9812
CR3+	40.8213	6C.829C
MG2+	7.6C5E	11.3337
FE2+	11.2134	16.7095
FE3+	2.1112	3.146C
SUMS	67.1C76	1CO.00CC

NORMALIZATION FACTOR= 1.49C1

(FE3+ + FE2+)	19.8555
(FE3+ + FE2+ + MG2+)	31.1892
CR3+/(FE3+ + FE2+)	3.C636
NI2+/CR3+	C.CCCC
MG2+/(MG2+ + FE2+)	C.4C42
CR3+/(CR3+ + AL3+)	C.884C
FE3+/(CR3+ + AL3+ + FE3+)	C.C437
FE2C3/FEC	C.2C93
FE2+/(MG2+ + FE2+)	C.5556
CR2+/AL2+	7.6216
MG2+/FE2+	C.6783

Table IV. Probelematic programme.

```
      $WATFOR 701090-GEOLOGICALSCIENCES=BLISS,RUN=FREE,KP=29
      C      PROGRAM TO WORK UP PROBE DATA
 1           DIMENSION ATS(8),PM(7),AN(7),T(11),ATN(8),AT(8),WTPN(8),OXIDE(8),N
     $A(3,8),ATW(8),ID(4)
 2           DATA NA(1,1),NA(2,1),NA(3,1),PM(1),T(1),AN(1)/'AL3+',' AL2',103  '
     $,99,96,2,0,0,529/
 3           DATA NA(1,2),NA(2,2),NA(3,2),PM(2),T(2),AN(2)/'CR3+',' CR2',103  '
     $,152,02,2,0,0,684/
 4           DATA NA(1,3),NA(2,3),NA(3,3),PM(3),T(3),AN(3)/'TI3+',' TI2',103  '
     $,143,80,2,0,0,750/
 5           DATA NA(1,4),NA(2,4),NA(3,4),PM(4),T(4),AN(4)/'MG2+',' MGO','    '
     $,40,32,1,0,0,603/
 6           DATA NA(1,5),NA(2,5),NA(3,5),PM(5),T(5),AN(5)/'NI2+',' NIO','    '
     $,74,71,1,0,0,786/
 7           DATA NA(1,6),NA(2,6),NA(3,6),PM(6),T(6),AN(6)/'FE2+',' FEO','    '
     $,71,85,1,0,0,777/
 8           DATA NA(1,7),NA(2,7),NA(3,7),PM(7),T(7),AN(7)/'FE3+',' FE2',103  '
     $,159,70,2,0,0,699/
 9           DATA NA(1,8),NA(2,8),NA(3,8)/'**  ','SUMS',' **'/
10           DATA IEND /'END '/
11           NTIW=5
12           NTOUT=6
13           ATS(7)=100,00
      C      FIX UP MOLE PROP
14           DO 10 I=1,7
15      10   PM(I)=PM(I)/T(I)
      C$$$$ READ IN A CARD
16      100  READ(NTIW,105,END=500) (ID(J),J=1,4),(ATS(I),I=1,6)
17      105  FORMAT(4A4,3X,6F10,3)
      C      AN END CARD
18           IF (ID(1).EQ.IEND) GO TO 550
      C      NORMALIZE
19           CALL NORM (ATS,ATN,24,00,6,T(1),ATS(8),ATN(8),IER)
      C      CALL FE2+ AND FE3+
20           A=ATN(6)
21           ATN(6)=8,00-ATN(4)-ATN(5)
22           ATN(7)=A-ATN(6)
      C      PRODUCE MOLE PROP
23           DO 110 I=1,7
24      110  ATW(I)=ATN(I)*PM(I)
      C      NORMALIZE
25           CALL NORM (ATW,WTPN,100,0,7,T(2),ATW(8),WTPN(8),IER)
      C      CALC OXIDES
26           OXIDE (8)=0
27           DO 115 I=1,7
28           OXIDE (I)=WTPN(I)*AN(I)
29      115  OXIDE(8)=OXIDE(8)+OXIDE(I)
      C      WRITE IT OUT
30           WRITE(NTOUT,117) (ID(L),L=1,4)
31      117  FORMAT('1PROBE-LEMATIC',30X,'SAMPLE '4A4)
32           WRITE (NTOUT,120)((NA(J,I),J=1,3),ATS(I),ATN(I),ATW(I)
     $,WTPN(I),OXIDE(I),I=1,8)
33      120  FORMAT ( '0'//                ' ION  OXIDE  ',4X,'INPUT',5X,'NORM'
     $,5X,'WT. PROP',4X,'OXIDE',5X,'ELEMENT'/47X,'WT. PCT.',3X,'WT. PCT.
     $'/6(/1X,3A4,4F10.4,'%',F10.4,'%')/1X,3A4,5X,F3.2,2X,3F10.4,'%',F10
     $.4,'%'/13X,52(1H-)//1X,3A4,4F10.4,'%',F10.4,'%')
      C      FACTORS
34           WRITE(NTOUT,125) T(1),T(2)
35      125  FORMAT ('0INPUT NORMALIZATION FACTOR=',F10.4/' OXIDE NORMALIZATION
     $ FACTOR=',F10.4)
```

```
      C     RATIOS
   36       ATS(1)=OXIDE(1)
   37       ATS(2)=OXIDE(2)
   38       ATS(3)=OXIDE(4)
   39       ATS(4)=OXIDE(6)
   40       ATS(5)=OXIDE(7)
   41       CALL NORM(ATS,ATN,100,0,5,SEMP,ATS(6),ATN(6),IER)
   42       T(1)=ATN(4)+(ATN(5))
   43       T(2)=T(1)+ATN(3)
   44       T(3)=ATN(2)/T(1)
   45       T(4)=OXIDE(5)/OXIDE(2)
   46       T(5)=ATN(3)/(ATN(3)+ATN(4))
   47       TEMP=ATN(1)+ATN(2)
   48       T(6)=ATN(2)/TEMP
   49       T(7)=ATN(5)/(TEMP+ATN(5))
   50       T(8)=WTPN(7)/WTPN(6)
   51       T(9)=ATN(4)/(ATN(3)+ATN(4))
   52       IF(ATN(1).GT.0.001) GO TO 128
   53       T(10)=1000000
   54       GO TO 129
   55  128  T(10)=ATN(2)/ATN(1)
   56  129  T(11)=ATN(3)/ATN(4)
      C     WRITE IT OUT
   57       WRITE(NTOUT,130) (ATS(I),ATN(I),I=1,6),SEMP,(T(J),J=1,11)
   58  130  FORMAT('0DATA FOR GRAPH'/15(1H=)//12X,' ELEMENT WT, PCT,'/
     $                              '  ION ',6X,'NOT NORM  ',3X,'NORM'//' AL
     $3+',4X,2F10.4,/' CR3+',4X,2F10.4,/' MG2+',4X,2F10.4/' FE2+',4X,
     $2F10.4/' FE3+',4X,2F10.4/10X,20(1H-)//' SUMS',4X,2F10.4//
     $' NORMALIZATION FACTOR= ',F10.4/
     $/,1X,'(FE3+ + FE2+)                ',F10.4
     $/,1X,'(FE3+ + FE2+ + MG2+)         ',F10.4
     $/,1X,'CR3+/(FE3+ + FE2+)           ',F10.4
     $/,1X,'NI2+/CR3+                    ',F10.4
     $/,1X,'MG2+/(MG2+ + FE2+)           ',F10.4
     $/,1X,'CR3+/(CR3+ + AL3+)           ',F10.4
     $/1X,'FE3+/(CR3+ + AL3+ + FE3+)',F9.4
     $/,1X,'FE203/FEO                    ',F10.4
     $/,1X,'FE2+/(MG2+ + FE2+)           ',F10.4
     $/,1X,'CR3+/AL3+                    ',F10.4
     $/,1X,'MG2+/FE2+                    ',F10.4)
      C     DO ANOTHER DATA POINT
   59       GO TO 100
      C     EOF
   60  500  WRITE(NTOUT,505)
   61  505  FORMAT('1*************** ERROR - NO END CARD'/'0*****  END OF PROBE
     $-LEMATIC ?  *****')
   62       GO TO 600
   63  550  WRITE(NTOUT,555)
   64  555  FORMAT('1*****  END OF PROBE-LEMATIC ?  *****')
   65  600  CONTINUE
   66       STOP
   67       END


   68       SUBROUTINE NORM (AV,AN,V,NO,F,S1,S2,IER)
   69       DIMENSION AV(8),AN(8)
      C     SET SUMS & ERROR FLAG
   70       S1=0.0
   71       S2=0.0
   72       IER=0
      C     SUM UP IN NORM
   73       DO 10 I=1,NO
   74  10   S1=S1+AV(I)
      C     CALC FACTOR
   75       IF (ABS(S1).LT.0.0001) GO TO 30
   76       F=V/S1
      C     RESCALE
   77  15   DO 20 I=1,NO
   78       AN(I)=AV(I)*F
   79  20   S2=S2+AN(I)
   80       RETURN
      C     AN ERROR
   81  30   IER=1
   82       F=1.0
   83       GO TO 15
   84       END


      $DATA
```

APPENDIX V

ELECTRON MICROPROBE ANALYSES

Tables of electron microprobe analyses of chrome spinels for which variation diagrams have been constructed but no individual analyses presented in the text.

The chromite core of the zoned spinels is indicated by a double line.The analyses between these lines may be averaged in the last column.

TABLE I W269(1) FIG.IV.1

	0	1	2	3	4	5	6	7	8	9	10	11	12	13	14
Al_2O_3	00.15	00.00	00.01	00.05	00.03	00.08	1.12	9.25	14.94	15.18	15.71	15.87	15.50	14.42	3.03
Cr_2O_3	2.93	3.87	6.37	9.85	15.07	28.65	45.91	47.24	48.27	48.53	48.55	48.28	48.21	48.04	45.84
TiO_2	00.14	00.24	00.23	00.28	00.44	00.78	00.48	00.21	00.34	00.30	00.21	00.23	00.29	00.32	00.50
MgO	00.69	1.24	2.13	2.02	2.95	4.88	5.87	9.89	11.23	11.31	11.31	11.20	11.06	10.33	6.45
NiO	00.61	00.56	00.69	00.60	00.54	00.45	00.18	00.06	00.02	00.00	00.00	00.01	00.04	00.00	00.17
FeO	29.46	28.65	27.19	27.52	26.23	23.57	22.75	18.21	17.26	17.20	17.30	17.49	17.60	18.57	22.23
Fe_2O_3	66.02	65.44	63.38	59.69	54.74	41.58	23.68	15.14	7.90	7.47	6.92	6.92	7.29	8.33	21.78

	15	16	17	18	19	20	21	22	8to13
Al_2O_3	00.72	00.20	00.06	00.02	00.00	00.05	00.00	00.00	15.27
Cr_2O_3	44.98	41.60	14.87	8.55	5.20	4.02	2.44	1.99	48.32
TiO_2	00.51	00.73	00.42	00.30	00.17	00.11	00.19	00.10	00.29
MgO	5.38	5.01	3.15	1.71	1.51	00.85	00.42	00.53	11.07
NiO	00.18	00.30	00.47	00.65	00.68	00.59	00.58	00.56	00.01
FeO	23.43	23.73	25.97	27.92	28.14	29.23	29.86	29.70	17.57
Fe_2O_3	24.81	28.42	55.05	60.84	64.31	65.15	66.51	67.11	7.47

TABLE II W269(2) FIG.IV.2

	0	1	2	3	4	5	6	7	8	9	10	11	13	14
Al_2O_3	00.11	00.00	00.03	00.00	00.01	00.02	00.03	00.11	00.06	00.04	00.03	00.00	00.02	00.06
Cr_2O_3	2.07	2.93	3.91	4.86	7.78	10.98	16.99	29.36	23.78	13.59	9.38	6.23	2.78	2.36
TiO_2	00.00	00.00	00.00	00.00	00.00	00.06	00.02	00.20	00.15	00.20	00.08	00.14	00.09	00.07
MgO	00.80	00.29	00.56	2.65	2.26	2.63	3.43	4.64	4.00	3.07	2.85	2.22	1.36	00.93
NiO	1.20	1.30	1.14	1.38	1.22	1.20	00.97	00.67	00.89	00.93	1.10	1.47	1.07	00.94
FeO	28.69	29.33	29.12	25.69	26.48	26.00	25.09	23.72	24.40	25.62	25.73	26.28	27.96	28.73
Fe_2O_3	67.13	66.12	65.23	65.42	62.24	59.11	53.47	41.30	46.72	56.54	60.83	63.67	66.74	66.90

TABLE III W91 FIG.IV.4

	1	2	3	4	5	6	8	9	10	11	12	13	14	15	16
Al_2O_3	00.23	00.27	00.32	00.45	00.70	1.22	15.32	16.14	15.95	16.48	16.22	15.90	16.12	3.96	1.35
Cr_2O_3	25.28	27.36	32.42	38.31	41.91	40.58	46.31	46.43	46.41	46.48	46.81	45.80	46.48	43.38	43.02
TiO_2	00.97	1.07	1.07	1.06	00.81	00.75	00.30	00.64	00.74	00.49	00.38	2.00	00.60	00.37	00.62
MgO	2.14	2.36	2.43	2.82	2.90	5.84	6.93	7.55	7.92	7.49	7.45	6.84	7.29	5.12	3.27
NiO	00.81	00.75	00.62	00.47	00.40	00.31	00.03	00.00	00.04	00.06	00.00	00.01	00.00	00.14	00.13
FeO	27.42	27.17	27.29	26.95	27.00	22.62	23.91	23.15	22.51	23.24	23.31	24.24	23.55	24.44	26.81
Fe_2O_3	43.15	41.00	35.84	29.93	26.28	28.68	7.21	6.09	6.43	5.75	5.83	5.22	5.96	22.60	24.79

	17	18	19	20	21	22	23	8to14
Al_2O_3	00.63	00.33	00.23	00.15	00.13	00.09	00.13	16.02
Cr_2O_3	41.34	34.35	26.36	20.83	17.78	15.47	13.36	46.41
TiO_2	00.79	1.06	1.08	00.99	00.83	00.65	00.57	00.69
MgO	2.98	2.38	1.85	1.54	1.45	1.22	1.26	7.36
NiO	00.42	00.54	00.72	00.88	00.98	1.03	00.97	00.02
FeO	26.83	27.48	27.98	28.20	28.17	28.43	28.40	23.41
Fe_2O_3	27.01	33.87	41.79	47.43	50.66	53.10	55.31	6.09

TABLE IV W84 Fig.IV.5

	0	1	2	3	4	5	6	7	8	9	10	11	12	0to3
Al_2O_3	13.41	13.42	13.59	13.69	6.63	2.51	1.26	00.40	00.19	00.09	00.04	00.00	00.00	13.53
Cr_2O_3	44.27	45.07	45.36	44.92	42.58	42.08	41.81	39.72	27.45	17.05	12.38	8.59	7.23	44.90
TiO_2	1.00	00.40	00.62	1.24	00.94	00.58	00.64	00.78	00.89	00.67	00.60	00.36	00.33	00.82
MgO	6.05	6.29	6.19	6.25	5.47	3.49	2.90	2.80	1.86	1.29	1.11	00.94	00.70	6.19
NiO	00.06	00.09	00.06	00.06	00.21	00.44	00.42	00.46	00.67	00.95	1.06	1.09	1.12	00.07
FeO	24.87	24.47	24.70	24.64	24.33	26.37	27.07	27.00	28.01	28.43	28.52	28.67	28.99	24.67
Fe_2O_3	10.33	10.25	9.48	9.20	19.84	24.53	25.90	28.84	40.94	51.52	56.30	60.35	61.63	9.82

TABLE V W89 FIG.IV.6

	S11	10	9	8	7	6	4	3	2	1S	0	N1	2	3	4
Al_2O_3	00.25	00.21	00.30	00.46	00.61	00.69	2.17	2.96	6.20	15.01	16.57	15.31	15.14	7.35	3.08
Cr_2O_3	21.67	22.88	28.39	34.37	42.75	42.98	41.46	45.07	46.27	48.45	48.50	45.92	45.17	42.41	41.44
TiO_2	00.95	1.09	1.18	1.40	1.22	00.90	00.71	00.70	00.65	00.49	00.25	00.19	00.16	00.48	00.66
MgO	1.83	1.87	2.04	2.44	2.68	2.90	3.94	3.51	3.47	4.22	6.92	7.14	6.89	4.02	3.31
NiO	00.94	00.83	1.00	00.65	00.48	00.42	00.35	00.37	00.31	00.09	00.00	00.06	00.06	00.24	00.33
FeO	27.71	27.77	27.45	27.32	27.27	27.00	25.71	26.55	27.28	28.01	24.22	23.55	23.89	26.65	26.85
Fe_2O_3	46.65	45.34	39.62	33.36	25.00	25.12	25.66	20.85	15.81	3.73	3.54	7.83	8.68	18.86	24.32

	4	5	6	7	8	9N	0to2N
Al_2O_3	3.08	1.75	00.78	00.40	00.18	00.17	15.43
Cr_2O_3	41.44	41.34	37.54	22.84	15.68	8.90	45.61
TiO_2	00.66	00.78	1.27	1.05	00.85	00.55	00.22
MgO	3.31	2.89	2.59	1.77	1.30	2.57	6.91
NiO	00.33	00.30	00.46	00.87	1.11	1.38	00.02
FeO	26.85	27.29	27.38	27.94	28.27	25.91	23.95
Fe_2O_3	24.32	25.65	29.98	45.14	56.62	60.51	7.86

TABLE VI W141

	0	1	2	3	4	5	6	7
Al_2O_3	00.39	00.05	00.07	00.07	00.10	00.08	00.05	00.03
Cr_2O_3	6.29	8.00	10.16	11.71	12.70	10.54	6.67	00.18
TiO_2	00.00	00.00	00.00	00.05	00.00	00.00	00.00	00.00
MgO	2.85	00.51	00.57	00.70	00.77	00.66	00.53	00.67
NiO	00.54	00.61	00.59	00.60	00.61	00.58	00.54	00.15
FeO	26.28	29.79	29.75	29.56	29.47	29.64	29.80	29.85
Fe_2O_3	63.65	61.04	58.86	57.29	56.35	58.51	62.41	69.11

TABLE VII W162

	0	1	2	3	4	5	6	7	8	9	10	11
Al_2O_3	00.07	00.06	00.05	00.08	00.06	00.04	00.10	00.09	00.05	00.07	00.12	00.07
Cr_2O_3	2.95	7.17	7.65	8.22	7.45	8.50	8.41	8.43	3.05	8.08	2.16	8.42
TiO_2	00.56	00.64	00.83	00.49	00.51	00.49	00.32	00.41	00.11	00.35	00.23	00.55
MgO	1.12	1.30	1.41	1.37	1.39	1.66	1.56	1.45	1.04	1.39	3.27	1.47
NiO	1.05	1.01	1.03	1.17	1.40	00.38	1.11	1.01	00.83	1.00	1.08	00.93
FeO	28.36	28.18	28.02	27.95	27.68	28.25	27.70	27.97	28.67	28.07	25.01	28.02
Fe_2O_3	65.89	61.63	61.01	60.72	61.51	60.68	60.80	60.64	66.24	61.04	68.13	60.53

TABLE VIII W264(1) FIG.IV.9

	1	2	3	4	5	6	7	8	9	10	11	13	14	15	16
Al_2O_3	00.04	00.03	00.50	2.30	15.80	17.35	17.48	17.74	17.43	16.94	16.56	10.39	2.02	00.57	00.00
Cr_2O_3	19.01	33.59	41.97	42.72	47.17	47.52	47.16	47.02	46.50	46.51	44.92	40.01	40.39	33.25	5.61
TiO_2	4.36	3.18	2.93	2.87	3.75	3.78	3.75	3.60	3.56	3.54	3.43	3.50	3.82	4.85	3.00
MgO	1.72	2.69	4.19	8.08	8.21	8.45	8.37	8.04	8.39	7.89	8.17	3.53	3.38	3.05	2.95
NiO	2.80	00.97	00.51	00.43	00.10	00.07	00.09	00.06	00.07	00.10	00.09	00.42	00.42	00.53	1.76
FeO	26.11	26.59	24.93	19.37	22.10	22.05	22.16	22.75	22.14	22.78	22.26	27.87	26.56	26.62	24.97
Fe_2O_3	45.96	32.95	24.97	24.24	2.93	00.78	00.98	00.80	1.92	2.25	4.57	14.28	23.41	31.15	61.71

TABLE IX W264(2)

	1	2	3	4	5	6	7	8	9	10	11	5,6,8	5to11
Al_2O_3	00.06	00.44	5.28	00.08	14.58	15.89	00.00	16.23	00.04	00.88	00.19	15.56	17.12
Cr_2O_3	16.68	44.80	7.75	6.79	47.52	47.21	2.04	47.67	00.06	9.00	32.95	47.47	46.97
TiO_2	1.34	00.52	00.25	00.12	00.17	00.25	00.23	00.27	00.26	00.12	00.78	00.23	3.66
MgO	2.58	5.70	3.36	5.19	11.13	11.87	2.57	11.86	1.52	2.42	4.89	11.62	8.22
NiO	7.50	00.57	2.08	2.02	00.20	00.15	1.99	00.14	4.69	4.95	1.99	00.16	00.08
FeO	20.07	22.50	24.95	21.20	17.15	16.31	25.19	16.41	24.15	22.80	22.14	16.62	22.33
Fe_2O_3	51.77	25.46	56.33	64.61	9.24	8.31	68.00	7.43	69.29	59.83	37.06	8.33	1.62

TABLE X W13 FIG.V.1

	0	1	2	3	4	5	6	7	8	9	10	11	0to7
Al_2O_3	24.56	24.56	24.24	24.10	24.19	23.95	24.09	24.57	00.00	00.00	00.00	00.00	24.27
Cr_2O_3	31.18	30.99	30.63	30.56	30.72	31.03	30.97	30.93	00.92	00.23	00.07	00.04	30.88
TiO_2	00.43	00.44	00.45	00.53	00.58	00.60	00.50	00.49	00.00	00.00	00.00	00.23	30.50
MgO	11.35	11.06	11.32	11.27	11.26	11.48	11.24	11.41	1.05	00.90	1.30	00.34	11.30
NiO	00.57	00.51	00.59	00.62	00.60	00.62	00.63	00.61	00.03	00.05	00.03	00.06	00.59
FeO	18.05	18.57	18.02	18.06	18.10	17.70	18.09	17.93	29.40	29.60	29.01	30.45	18.07
Fe_2O_3	13.86	13.87	14.75	14.88	14.55	14.61	14.49	14.05	68.59	69.22	69.59	68.87	14.38

TABLE XI GREAT DYKE

	0	1	2	3	4	5	6	7	8	9	10	11
Al_2O_3	12.72	12.81	13.19	13.21	13.35	13.47	13.49	13.59	13.71	13.82	13.90	00.00
Cr_2O_3	50.11	50.44	50.45	50.23	50.41	50.63	50.38	49.93	50.45	50.47	50.10	3.60
TiO_2	00.34	00.35	00.37	00.35	00.30	00.39	00.40	00.49	00.29	00.36	00.33	00.03
MgO	9.34	11.08	11.08	11.24	11.04	10.94	10.82	11.06	10.51	10.58	10.45	3.46
NiO	00.10	00.06	00.05	00.04	00.05	00.05	00.03	00.05	00.06	00.07	00.06	00.93
FeO	19.71	17.10	17.17	16.95	17.26	17.44	17.64	17.27	18.15	18.04	18.26	24.86
Fe_2O_3	7.67	8.17	7.69	7.99	7.59	7.08	7.22	7.60	6.85	6.65	6.91	67.12

APPENDIX VI

OTHER ANALYTICAL DATA

ROUTINE NI ASSAYS

Routine nickel (and copper) assays were made by Mr. H.E. MacRae, of Amax Exploration Inc., using a Varian Associates A-100 atomic absorption unit. All intersections of ultramafic, and some intersections of mafic rock were assayed.

A diamond impregnated disc grinds a small continuous fillet from the core and each sample obtained is estimated to total 3% of the complete footage sampled. All of the grind except that portion of +8 mesh grain size is retrieved and made to pass through a -100 mesh seive. The +8 mesh portion is not retained because it is believed to be composed of excess material plucked out by the grinding disc and therefore not a portion of the ground fillet. Each sample is subsequently homogenized prior to analysis.

The analytical procedure for <u>total nickel</u> (and copper) is as follows:-

1 gm sample weighed on analytical balance

+ 3 ml. 48% HF

+ 10 ml. 1/1 HCL

+ 5 ml. 70% HNO_3

+ 10 ml. Perchloric acid

Mixture heated for 45-75 minutes until perchloric acid begins to fume

Mixture cooled

+ 5 ml. demineralized water to redissolve salts - aided by warming

+ dilution to 200 ml.

Assay on A.A. unit for Ni and Cu

Calibration standard solutions (Fisher Stock) are prepared in a similar manner but mixtures are not heated.

Sulphide nickel is determined by using ammonium citrate as a chelating agent followed by hydrogen peroxide leach to selectively dissolve the sulphide phases. The analytical procedure is as follows:-

1 gm. sample weighed on analytical balance
+ 80 ml. Ammonium citrate 10% solution
+ 40 ml. reagent grade H_2O_2
Mixture homogenized on blender 30 minutes
Mixture stands overnight
Heat mixture gently ½ hour
Mixture filtered and washed twice
+ 10 ml. 1/1 HCL
Dilution to 200 ml.
Assay for Ni on A.A. unit

Calibration standard solutions (Fisher Stock) are prepared similarly but not heated.

Research on the various sulphide-leach techniques has been carried out by Amax Exploration Inc, the technique outlined above, was the most precise and reproduceable, although not all sulphide dissolved before incipient attack began on some non-sulphide phases. The figure obtained for sulphide nickel is believed to be very close to the real content.

WHOLE ROCK ANALYSES

The sample is crushed, and split, approximately 100 gms. being

retained for analysis. Si, Al, Fe, Ca, Mg, K, Na, Cr, Ti, P, V, Co, Ni, Cu, Mn, and Zn are determined by atomic absorption spectrophotometry. Dissolution for analyses involves a lithium metaborate fusion for determination of Si, Ti and Cr and for most other elements an HF digestion followed by HNO_3 treatment to quantitatively dissolve the remaining metallic elements for analyses. Sulphide nickel was leached with an ammonium citrate-hydrogen peroxide solution.

The values of $-H_2O$, LOI, total sulphur and total carbon, and an estimation of $+H_2O$ are obtained as follows:

A tared crucible is filled with a 1-gram sample and heated for $1\frac{1}{2}$ hours at 110°C, cooled in a dessicator and weighed. Weight loss is calculated to percent and recorded as percent $-H_2O$. The crucible and sample are placed in a resistance furnace and heated to 1100°C and held at this temperature for one hour, cooled and weighed. Weight loss is calculated to percent and recorded as LOI. This value represents carbon, CO_2, sulphur, and $+H_2O$ and fluorine. In this combustion reaction, some of the sulphur is trapped by reactive metal ions as sulphates, necessitating a sulphur determination on the LOI residue, calculation of oxygen tied up with the retained sulphur, and a correction of the LOI value reported. The corrected LOI value minus the total sulphur, fluorine and carbon contents is an approximation of the $+H_2O$ value.

Total sulphur is determined by the Leco carbon-sulphur instrument. A weighed sample is placed in a special (carbon and sulphur free) single use crucible, covered with metallic iron and tin (both carbon and sulphur free), and combusted in the sulphur

induction furnace in a stream of oxygen at a temperature "well in excess of 3000°F". The SO_2 is trapped and titrated with a standard KIO_3 solution. Reproducibility is ± .02% up to 2.00% sulphur and ± .2% from 2.00% to 20.00% sulphur.

The total carbon content is determined with the second induction furnace on the unit in a completely different combustion train. A second sample is weighed out. Iron and tin metals are added, and the sample is burned in a stream of oxygen. All gases are passed through a sulphur trap to remove SO_2 and through a catalyst furnace to convert any CO to CO_2. The gases are volumetrically trapped, measured, and CO_2 is absorbed in a KOH solution. The residual gas is remeasured and the difference is the amount of CO_2 contained in the combustion gases. Corrections are made for temperature and pressure, and the results are reported as total carbon. Adequate detection limits and precision for total carbon determinations have not yet been achieved.

The determination of FeO is a partitioning technique, due to the ease with which iron changes from the ferrous to the ferric state. For the determination, a small amount (0.5 grams) of sample is decomposed in a platinum crucible by boiling with $HF-H_2SO_4$. The resulting sample solution is then "spiked" with a fixed amount of ferrous ammonium sulphate solution and titrated with a standard dichromate solution with diphenylamine sulphonic acid as the indicator. The F-, 0.25 grams of sample is fused in a nickel crucible with NaOH. Water and a small amount of H_2SO_4 is then added to the fused sample and an ammonium citrate buffer is added to the resulting solution. The F- content is then determined with a specific ion electrode.